HOT WHITE DWARFS IN DETACHED BINARIES FROM THE ROSAT WFC ALL SKY SURVEY

Thesis submitted for the degree of
Doctor of Philosophy
at the University of Leicester.

by

Matthew R. Burleigh
X-ray Astronomy Group
Department of Physics and Astronomy
University of Leicester

7th February 1997

Declaration

I hearby declare that no part of this thesis has been previously submitted to this or any other University as part of the requirement for a higher degree. The work described herein was conducted by the undersigned except for contributions from colleagues as acknowledged in the text.

Matthew R. Burleigh,
7th February 1997

HOT WHITE DWARFS IN DETACHED BINARIES FROM THE ROSAT WFC ALL SKY SURVEY

Matthew R. Burleigh

ABSTRACT

White dwarfs in unresolved pairs with normal stars (spectral type K or earlier) are invisible at optical wavelengths, due to the close proximity of the much more luminous main sequence companion. ROSAT has provided evidence for the existence of a growing sample of these hidden white dwarfs through the detection of EUV and soft X-ray emission. For companions of spectral type $\sim$A5 or earlier, the white dwarf can be spectroscopically identified at far-ultraviolet wavelengths by IUE. Eleven such systems had previously been found in this way from ROSAT, EUVE and IUE observations. A search for fainter, less obvious examples of these binaries is presented, and five new systems have been discovered.

Three new close, pre-CV WD+dM binaries have also been found in the ROSAT WFC survey. Intriguingly, all three degenerates are rare mixed hydrogen/helium atmosphere DAO white dwarfs. The EUVE spectrum of one of these new systems, RE J0720$-$318, is analysed in detail. In particular, it is found that, while the optical spectrum can only be reproduced with a homogeneously mixed atmosphere, the EUVE spectrum can only be matched by a layered model, implying that the underlying structure of the white dwarf is stratified. The hydrogen layer mass of $3\times10^{-14}\,M_{\odot}$ is the lowest measured for any white dwarf from EUVE spectra. In addition, an unprecedented HeI/HI ratio of $\sim$1 is detected for the absorbing column along the line of sight, implying a hydrogen ionisation fraction of $>$90%, if all this material resides in the local interstellar medium. It is suggested that most of the helium lies in the vicinity of the star, possibly in the form of a circumbinary disk left over from the common envelope phase. These results have important implications for our understanding of the evolutionary status of DAO white dwarfs in particular, and for post-common envelope systems in general.

A catalogue of all the detached white dwarf binaries found in the ROSAT survey is presented, with an analysis of the white dwarf mass distribution. Compared with optically selected samples, a significant excess of hot, massive objects is detected. This excess probably arises from the slower cooling rates of massive ($>0.9\,M_{\odot}$) white dwarfs in comparison to normal mass ($\approx0.6\,M_{\odot}$) stars.

Publications

Barstow, M.A., Holberg, J.B., Marsh, M.C., Tweedy, R.W., Burleigh, M.R., Fleming, T.A., Koester, D., Penny, A.J., Sansom, A.E., 1994, *Mon. Not. R. ast. Soc.,* **271**, 175
"RE 1738+665, the hottest DA white dwarf detected by ROSAT"

Barstow, M.A., Burleigh, M.R., Fleming, T.A., Holberg, J.B., Koester, D., Marsh, M.C., Rosen, S.R., Rutten, R.G.M., Sakai, S., Tweedy, R.W. & Wegner, G., 1995, *Mon. Not. R. ast. Soc.,* **272**, 531
"The orbital period of the pre-cataclysmic binary RE 2013+400 and a study of the atmosphere of the DAO white dwarf primary"

Burleigh, M.R. & Barstow, M.A., 1995, In: *White Dwarfs*, eds., Koester, D. & Werner, K., Springer-Verlag, **318**
"Constraints on DAO white dwarf composition from the ROSAT EUV survey"

Marsh, M.C., Barstow, M.A., Holberg, J.B., O'Donoghue, D., Buckley, D.A., Fleming, T.A., Koester, D. & Burleigh, M.R., 1995, In: *White Dwarfs*, eds., Koester, D. & Werner, K., Springer-Verlag, **328**
"An EUV selected sample of DA white dwarfs"

Barstow, M.A., O'Donoghue, D., Kilkenny, D., Burleigh, M.R. & Fleming, T.A., 1995, *Mon. Not. R. ast. Soc.,* **273**, 711
"RE0720-318: A pre-cataclysmic binary system with a DAO white dwarf primary"

Barstow, M.A., Jordan, S., O'Donoghue, D., Burleigh, M.R., Napiwotzki, R. & Harrop-Allin, M.K., 1995, *Mon. Not. R. ast. Soc.,* **277**, 971
"RE J0317−853: The hottest known highly magnetic DA white dwarf"

Jeffries, R.D., Burleigh, M.R. & Robb, R.M., 1996, *Astr. & Astrophys. Letts.*, **305**, L45
"Is 2RE J0357+283 the most coronally active star in the Galaxy?"

Burleigh, M.R., Barstow, M.A. & Dobbie, P.D., 1997, *Astr. & Astrophys. Letts.*, **317**, L27
"The close DAO+dM binary RE J0720−318: a stratified white dwarf with a thin H layer and a possible circumbinary disk"

Marsh, M.C., Barstow, M.A., Buckley, D.A., Burleigh, M.R., Holberg, J.B., Koester, D., Penny, A.J. & Sansom, A.E., 1997, *Mon. Not. R. ast. Soc.,* **286**, 369
"An EUV selected sample of DA white dwarfs from the ROSAT all-sky survey. I: Optically derived stellar parameters"

Marsh, M.C., Barstow, M.A., Buckley, D.A., Burleigh, M.R., Holberg, J.B., Koester, D., Penny, A.J. & Sansom, A.E., 1997, *Mon. Not. R. ast. Soc.,* **287**, 705
"An EUV selected sample of DA white dwarfs from the ROSAT all-sky survey. II: EUV and soft X-ray properties"

Burleigh, M.R., Barstow, M.A. & Fleming, T.A., 1997, *Mon. Not. R. ast. Soc.,* **287**, 381
"A search for hidden white dwarfs in the ROSAT EUV survey"

Burleigh, M.R. & Barstow, M.A., 1997, In: *White Dwarfs*, eds., Isern, J., Hernanz, M. & Garcia-Berro, E., Kluwer, **329**
"Hot white dwarfs in non-interacting binary systems from the ROSAT EUV survey"

Burleigh, M.R., Barstow, M.A. & Holberg, J.B., 1997, *Mon. Not. R. ast. Soc.,* **in preparation**
"A search for hidden white dwarfs in the ROSAT EUV survey II: Discovery of a distant DA+F5V−G0V binary system in a direction of low density neutral hydrogen"

To my parents

Thank you

Acknowledgements

My introduction to the field of white dwarfs came in the summer of 1992 when, as an undergraduate student earning a few pounds to pay off my overdraft, I found myself helping my future supervisor Martin Barstow to organise a conference on the subject. That week, I spent most of the time operating a video camera to record each post-talk discussion. I didn't realise that two years later I would be attending the next white dwarf conference in Kiel, Germany, as a delegate, and that many of the astronomers I had been serving coffee to would later become my friends and colleagues. In the autumn of 1993, when I came back to Leicester to start a PhD with the X-ray astronomy group, Martin took me to one side and asked if I would be happy to work for him. I have never regretted saying yes. Martin has been as good a supervisor as I could have asked for. He has introduced me to a subject that I find fascinating, and hope to pursue for many years to come. He has always been willing to make time for me, to teach me and discuss our field with me, and, although I must have tried his patience on many occasions, he has never turned me away. From him I have learnt not only how to do good science, but how best to express and communicate results. Thank you for your support and confidence, Martin, and I hope that I shall be able to work with you on many future projects.

Through my subject I have met many bright, and brilliant scientists and characters from around the world. Special thanks to Jay Holberg for his hospitality during the week I spent with him and his family in Tucson, and for many enlightening discussions; to Rob Jeffries for always providing answers to my naive email questions; to Darragh O'Donoghue, Dave Buckley and Dave Kilkenny for teaching me about optical astronomy and letting me come to Cape Town, surely one of the most beautiful cities in the world; to Stefan Jordan and Rex Saffer for drinking me under the table in Kiel and Blanes; to Richard Monier and Constance la Dous for their hospitality at IUE Vilspa.

Throughout my PhD I have never been afraid to take advantage of the PPARC funds available for travel to conferences, meetings and observing runs around the world. Thanks to all the friends I have made in Cape Town (Hi Margie!), Blanes , Sydney and Los Angeles, for taking me out, pouring beer down my throat and forcing me to eat enormous steaks.

Of course, this overly-sentimental acknowledgements section would not be complete without mentioning my colleagues at Leicester. Thank you Jon, for knowing how to go out and have fun, Tim for being a fellow real-ale lover and suffering the lows of English cricket with me, Paul for Table Mountain and that Spanish resort, Gareth for being eternally optimistic about Wales's prospects, Dennis for being cool, Richard, Steve, Graham and Big Dave for endless conversations down the pub, and also to John, Keith, Ian, Jezza, Geoff, Geoff, Sarah, Helen, Simon, Ben and Matt (keep striving Marshy, we're all behind you). Thanks to Merv, Chris and the University Cricket Club for great matches and even better celebrations. And thank you Bev, for putting up with my moods and stress. Soon it'll be your turn.

Finally, my thanks to PPARC for supporting me throughout my PhD, and to the XRA Astronomy Group and the Department of Physics and Astronomy for giving me the opportunity in the first place. I fully intend to be in this career for a long time.

OVERVIEW

This thesis is devoted to the study of hot white dwarf stars in detached binary systems, found in the ROSAT Wide Field Camera (WFC) all sky survey of the Extreme Ultraviolet (EUV). I do not include white dwarfs in Cataclysmic Variable (CV) systems, since their evolution and composition has been severely affected by interactions with the companion star.

The vast majority of the >2000 known white dwarfs are single, isolated objects. This is largely a selection effect, since white dwarfs have generally been found in proper motion and blue colour surveys, and it is difficult to detect a low luminosity white dwarf in an unresolved binary system with a much brighter main sequence star like our own Sun. Perhaps the most famous white dwarf is Sirius B, a faint companion to the brightest star in the night sky. Sirius B orbits its neighbour once every $\sim$50 years, yet the ease with which it can be seen in a moderately sized telescope is only due to the close proximity of the system to Earth (2.64 parsecs). If Sirius was significantly further away from us, it is likely that Sirius B would have remained unidentified until the launch of ROSAT in 1990. As it is believed that somewhere between 50% and 80% of all stars are in binary or multiple systems, we can reasonably assume that a similar fraction of all white dwarfs must also have companions. Finding many of these systems has until recently been virtually impossible. Their discovery will not only add to our knowledge of white dwarfs, but also to our whole understanding of binary and stellar evolution.

Hot white dwarfs (T>20,000K) are brightest in the EUV part of the electromagnetic spectrum, a region where ordinary main sequence stars like the Sun are much fainter. For the first time, the ROSAT WFC survey has provided evidence for the existence of a substantial number of otherwise invisible white dwarfs in Sirius-type detached, or non-interacting, binaries, through the detection of their EUV radiation. The search for these hidden stars is described in Chapter 3.

White dwarfs are also found in binaries with faint red dwarf companions. In these systems it is the red dwarf which can be difficult to identify optically. Sometimes the two stars are found to be orbiting each other with a period of just a few hours or days. They are so close together that they must have interacted with each other in the past, for example when the white dwarf was in its red giant phase of evolution. In the future, the pair will interact again, by mass transfer in a CV system. These pre-CV systems are vital to our understanding of binary evolution. A number of white dwarfs in pre-CV systems belong to the rare DAO class, having mixed hydrogen/helium atmospheres. The DAO white dwarfs in pre-CV systems, and their possible origins, are discussed in detail in Chapter 4. The entire ROSAT WFC white dwarf binary sample is then presented and discussed in Chapter 5, including an analysis of the mass distribution.

Contents

List of Figures

List of Tables

Chapter 1

White Dwarfs

1.1 Overview

White dwarfs are dying stars. They are the burnt out cores of suns that have long since exhausted their nuclear fuel. They are extremely dense, compact objects, packing a stellar mass into a volume the size of the Earth. Only the most massive ($>8M_{\odot}$) stars will end their lives violently, perishing in supernova explosions to leave neutron stars and black holes. The vast majority ($\sim$97%), like our own Sun, will fade away more quietly as white dwarfs, slowly cooling over billions of years until they are no longer detectable.

Studying these stellar corpses is of interest not only to the astronomer, but also to the physicist. The extreme conditions of density and gravity that exist on them, and the matter from which they are made, cannot be reproduced on Earth. White dwarfs are, therefore, important laboratories for testing our knowledge of the laws of physics. Since they represent the most dominate end point of stellar evolution, studying the structure, formation and composition of white dwarfs is vital to our understanding of stellar astrophysics. These ancient objects have the memory of their lifetime imprinted on them, and can reveal to us not only their own history but that of our galaxy and the Universe itself. By their very nature the coolest white dwarfs are also the oldest stars in the galaxy; thus they can tell us the age of the Milky Way.

In this chapter I will introduce white dwarf stars, the history of their discovery, their unusual internal and atmospheric structure, and how they are formed, evolve and are classified. The formation and evolution of white dwarfs in binary systems is covered separately in Chapter 2.

1.2 The Discovery of White Dwarfs

In 1834 the astronomer Friedrich Bessel noticed that the motion of the bright star Sirius through the sky was not uniform. Instead, it seemed to be wobbling either side of a straight path. By the time of his death in 1844 Bessel had become convinced that Sirius was a binary system. The companion was too faint to be seen directly in his telescope, but Bessel concluded that he had observed and measured its gravitational influence on Sirius. Measurements continued to be taken over the following decades, and it was realised that the wavy course Sirius appeared to be pursuing repeated itself every fifty years. This must have been the orbital period of the companion. Finally, in 1862, the American telescope maker Alvan Clarke saw the hitherto invisible companion in his new 20 inch telescope, the largest in the world at the time. It lay in almost the exact spot that Bessel had predicted.

It was not until early this century that a spectrum of Sirius B was obtained, by Walter Sydney Adams at Mount Wilson in California, from which the temperature could be determined. At the same time Edward C. Pickering observed a similar spectrum from 40 Eridani B, another faint star in a binary system. These spectra revealed a great enigma. Sirius B and 40 Eri B were far hotter, yet 1000 times less luminous, than their much brighter companions. In fact, they had the same luminosity as very cool, faint red dwarf stars. This was a real problem for astrophysicists, since hot stars were supposed to be much more luminous than cool ones of the same size. Figure 1.1 shows the position of white dwarfs in a Hertzsprung-Russell diagram, which relates the temperature of a star to its brightness. The white dwarfs occupy the low luminosity, high temperature region in the lower left hand corner, well away from the main sequence stars. The only explanation was that Sirius B and 40 Eri B were 100 times smaller than the Sun, but this then implied the interior densities were 5 or 6 orders of magnitude greater (about 1400 tonnes per cubic metre). In the early twentieth century there was no known physical laws to explain such densities and the existence of these strange, exotic stars.

The answer lay in one of the great successes of twentieth century physics. In 1926 Enrico Fermi and Paul Dirac developed the quantum statistical theory of an electron gas. Individual electrons in an atom will behave according to the laws of quantum mechanics. For example, they are only allowed to occupy particular discrete energy levels and spin in certain directions. In a material where the atoms are spaced closely together (e.g. a metal), the most weakly bound electrons

can move about freely and can be considered to behave like a gas. This 'gas' is responsible for the conduction of heat in a metal. Under conditions of extreme pressure the electrons are forced much closer to the nuclei of the atoms than in normal matter. The quantised structure of the atom's energy levels is then broken down, but there is a limit to how 'squashed' the electrons will become. If two electrons occupy states with the same energy the 'gas' is called degenerate. The Pauli Exclusion Principle says that no more than two electrons with the same spin direction can occupy the same quantum energy state. Once this occurs the electrons resist being compressed further, giving rise to a force called electron degeneracy pressure. Sir Ralph Fowler, also in 1926, showed that this pressure could support a solar mass white dwarf against gravitational collapse.

In 1931 a young Indian physicist called Subrahmanyan Chandrasekhar, on a voyage to England to continue his research, correctly combined quantum mechanics and relativity to derive the basic equations of white dwarf structure. He determined the first white dwarf mass-radius relationship, and predicted that the maximum mass that could be supported by electron degeneracy pressure against gravitational collapse was 1.4 times that of the Sun ($1.4\,M_{\odot}$). This is known as the Chandrasekhar Limit, and earned him the Nobel Prize for Physics in 1983.

Main sequence stars like the Sun shine by burning hydrogen and helium in their cores. In white dwarfs this nuclear fusion has ceased, and there is no internal source of energy. They shine by radiating the energy generated when they are formed. Starting out as extremely hot objects, this stored thermal energy is released from the atomic nuclei in the cores, and transported via highly efficient conductivity through the electron 'sea' to the surface. Over time, as more energy is released, the white dwarf cools. Leon Mestel first estimated the cooling times for white dwarfs, and realised that it takes billions of years for them to fade to invisibility (a state known as a 'black dwarf'). Cool white dwarfs, therefore, are the oldest stars in the universe, and by finding the coldest ones astronomers can determine the age of the galaxy.

Most of the properties of white dwarfs have been determined through theory rather than observation. Since these stars are so faint, measurements to determine parameters such as temperature and the strength of the surface gravity were based for a long time on their visual colours. In the last twenty years a revolution has occurred in observational astronomy. Improvements in the sensitivity of telescopes and detectors, the launching of satellites to study stars in previously inaccessible wavebands like X-rays and the ultraviolet (UV), vast improvements in computing

power, and refinements to the original theories of white dwarf structure and evolution have transformed our ability to study and understand these remarkable objects.

1.3 Basic Internal Structure and Cooling Processes

The basic internal structure of a white dwarf has been well understood since the work of Chandrasekhar (1939). White dwarfs consist of an electron degenerate core, which constitutes over 99.99% of its mass, surrounded by a thin non-degenerate atmosphere, between $60-100$km thick. The core is usually made of the products of helium burning (carbon and oxygen), since the majority of the progenitors of white dwarfs will have burned H and He during their lifetimes. The core is a plasma consisting of ions and degenerate electrons. The thermal pressure of the ions is negligible and it is the degenerate electrons which prevent the core collapsing under its own gravity. The pressure of the electrons is only weakly dependent on temperature, and so a white dwarf cools at a fairly constant radius throughout most of its life. Electron degeneracy is also responsible for the peculiar relationship between a white dwarf's mass and its radius: the more massive a white dwarf, the smaller it is. Degeneracy is also the reason why a white dwarf has a limiting mass above which it cannot exist, $1.4\,M_{\odot}$ (Chandrasekhar 1931).

In addition, degenerate electrons are excellent conductors of heat, and do not contribute to the reservoir of energy within the core because they cannot be cooled (they already occupy the lowest energy levels in the atom). It is the non-degenerate ions that supply the thermal energy that slowly leaks out to provide the star's luminosity. As the core cools, these ions evolve from a gas to a liquid, and finally, at between $4{,}000-10{,}000$K, they crystallize into a solid. Ultimately, the star disappears from sight as a cold, black dwarf.

The thin, non-degenerate envelope surrounding the core acts as an insulating blanket, controlling the cooling rate of the star. How rapidly the star loses thermal energy to space depends on the thermal structure and chemical composition of the atmosphere. It can also depend on the white dwarf's size: smaller, more massive, less luminous white dwarfs cool the slowest. The atmosphere of a white dwarf consists of mainly hydrogen and helium left over from when the star ejected its outer layers during its pre-white dwarf evolution. Initially, when the white dwarf is in the hottest part of the cooling sequence ($T>100{,}000$K), the dominant cooling process is

neutrino loss. At this stage, around twice as much energy is lost by this method than by normal radiation. However, by about T≈15,000K neutrino flux has fallen to about 1% of the total energy loss rate. Energy is also transported through the atmosphere by photon diffusion and convection, and released as electromagnetic radiation. This is the dominant cooling process for the stars observed by ROSAT (20,000<T<100,000K).

An average ($0.55\,M_{\odot}$) white dwarf will take ∼500,000 years to cool to 50,000K, and a further five billion years to cool to 5,000K. Figure 1.1 shows two cooling curves, for $0.6\,M_{\odot}$ and $1.0\,M_{\odot}$ DA white dwarfs, from Matt Wood's evolutionary models (Wood 1995, assuming CO-cores and thick H-layers, $10^{-4}\,M_{\odot}$). Note that the cooling rate of the more massive star significantly decreases in comparison to the lower mass object when it reaches T≈50,000K. The major uncertainties in the cooling theory surround the physics of the core crystallisation process, for example the initial C/O composition and the level of stratification (does the oxygen accumulate near the centre of the core?). Another source of uncertainty is the thickness of the helium layer which regulates the emergent heat flux. The thicker the layer, the younger the age. These uncertainties translate to a ∼1-2Gyr uncertainty in the age of the local galactic disk (Chabrier 1997).

1.4 White Dwarf Classification

Most stars are classified according to the particular characteristics of their optical spectra, and white dwarfs are no exception. Classification according to the presence or absence of distinguishing absorption lines due to elements like H, He, C, O, Ca, Mg, and Fe allows us to, generally, say something about the star's temperature, mass and evolutionary status. Schatzman (1958) first realised that the extreme gravitational field of a white dwarf will make most heavy elements sink quickly out of the thin atmosphere, leaving the lightest, H and He, floating at the surface. Thus most white dwarfs are classed as being either H-rich or He-dominated, and are devoid of heavier elements (although, as we will see later, studies in the UV and EUV have shown that some hot white dwarfs contain relatively large abundances of heavy elements in their photospheres).

The first attempts to classify white dwarfs were made by Kuiper (1941) and Luyten (1952). These schemes were based upon photographic spectra, and were introduced at a time when it was not realized that a fascinating diversity of spectral types existed among white dwarfs.

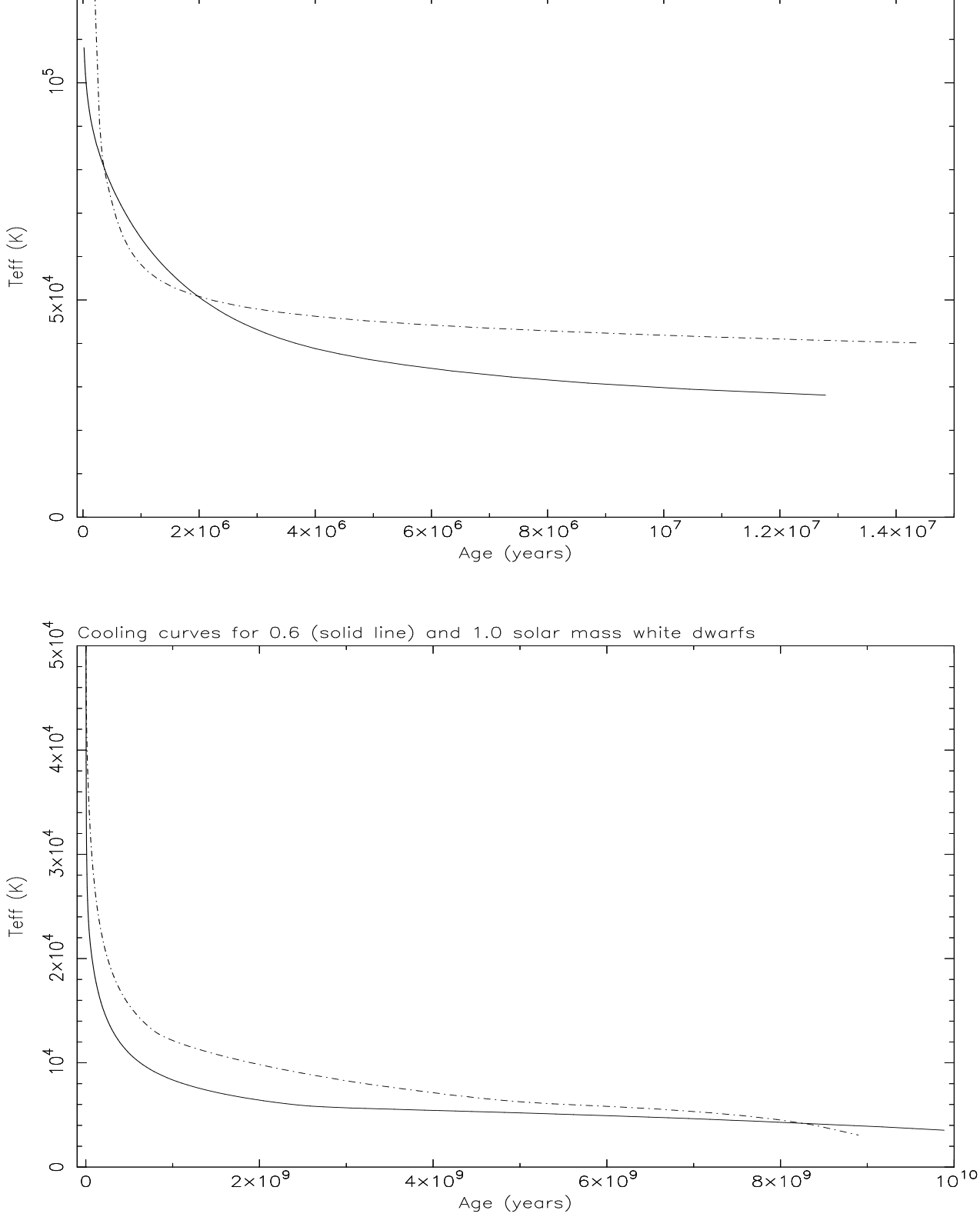

Figure 1.1: Cooling curves for $0.6\,M_\odot$ (solid line) and $1.0\,M_\odot$ (dashed line) DA white dwarfs, from Matt Wood's evolutionary models, assuming CO-cores and thick H-layers $>10^{-4}\,M_\odot$. Top: cooling curves for young ($<1.5\times10^7$years), hot (20,000<T<120,000K) white dwarfs. Bottom: cooling curves covering the whole of a white dwarf's lifetime (up to 10^{10} years).

Greenstein (1960) refined these early classifications into a system that was used for the next 20 years. All the spectral classes were prefixed with a capital D for degenerate. They were then classed according to their spectroscopic resemblance to main sequence stars (O to M). Thus, there were the hydrogen dominated DA white dwarfs, with optical spectra similar to main sequence A stars, and also objects belonging to groups such as DF, DG, DK and even DM. However, by the late 1970s and early 1980s, a large number of objects with hybrid spectra were being found, particularly with the advent of space-based ultraviolet astronomy (e.g. the International Ultraviolet Explorer satellite). It was realised that the number of subclasses and peculiar objects, coupled with an inability to distinguish between a cool star and a hot one, was beginning to make the system confusing and unworkable. Thus Sion *et al.* (1983) proposed and introduced a refined classification scheme which has now been universally adopted (Table 1.1).

The D prefix has been retained, but all white dwarfs are now classed with a second letter according to their dominant spectral feature (mainly in the optical region). The DA classification remains for H-rich stars with strong Balmer lines, and the DO and DB classes for He-rich objects with strong HeII and HeI features respectively. A third letter may be added for stars with hybrid spectra. Thus DAO white dwarfs display the strong Balmer lines seen in DAs, but they also have relatively strong HeII features as in the DOs. Similarly, DBA white dwarfs have weak H Balmer lines in addition to strong HeI features. DAZ, DOZ and DBZ white dwarfs all contain weak metal features in the optical or UV (e.g. CaII is usually present in DAZ stars), while magnetic stars are denoted by a capital P, and peculiar stars with an X.

Table 1.1: Primary White Dwarf Spectral Classifications

Class	Approx. Temperature Range (K)	Spectral Characteristics
H-rich		
DA	6,000−100,000	Balmer lines only, no He or metal features
DAO	>45,000	Balmer lines and weak HeII features
He-rich		
DO	45,000−100,000	Strong HeII lines, some HeI present
DB	12,000−30,000	HeI lines, no H or metals
DBA	12,000−30,000	HeI lines and weak Balmer lines present
Cool WDs		
DQ	6,000−12,000	C features (atomic or molecular)
DZ	<6,000	Metal lines only, no H or He
DC	<6,000	Featureless continuum (no lines deeper than 5%)

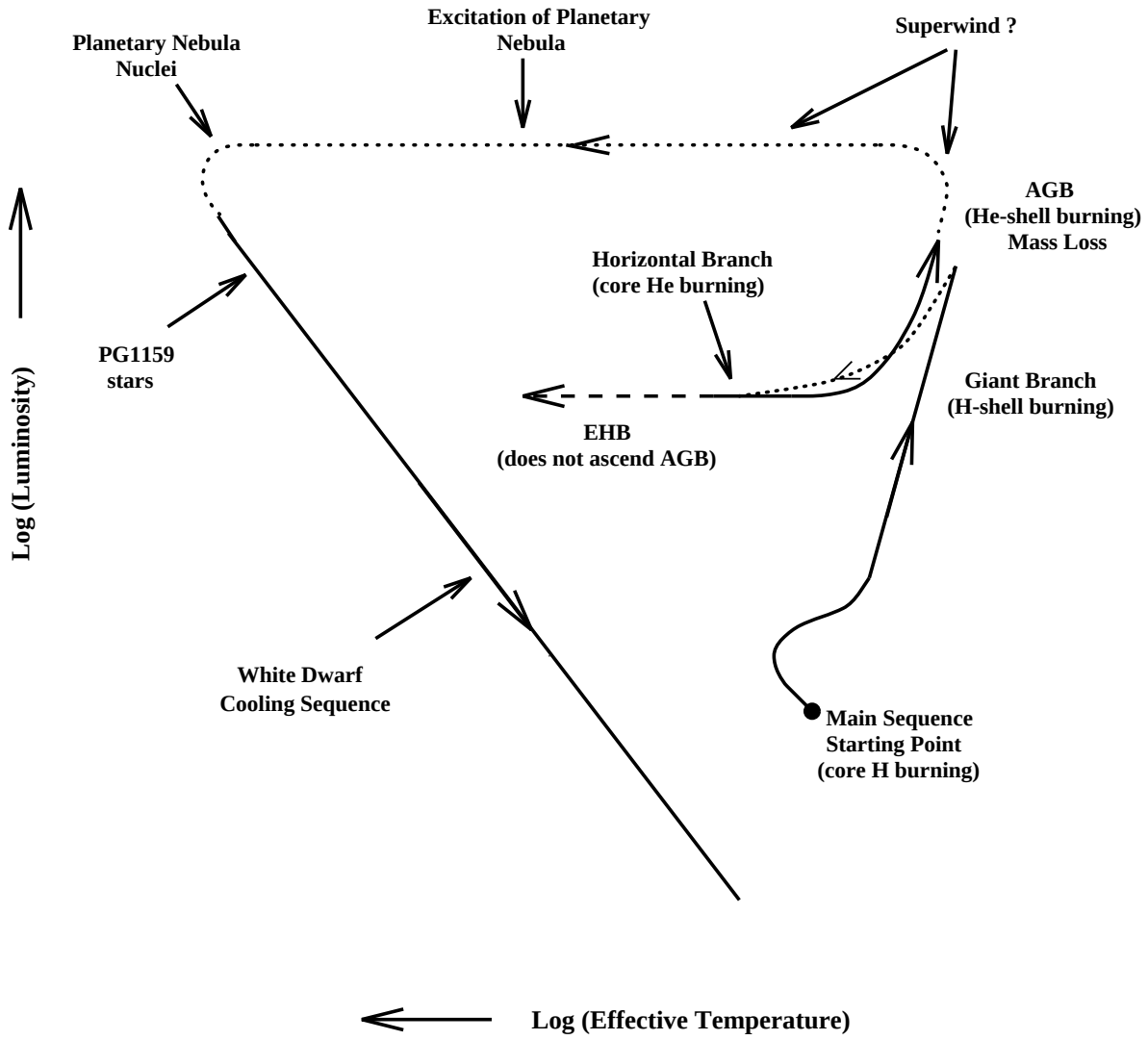

Figure 1.2: The Hertzsprung-Russell diagram, showing the evolutionary paths of stars from the main sequence to the white dwarf cooling sequence (reproduced from Marsh 1995a).

Sion *et al.* (1983) also introduced a temperature index, from 0 to 9, defined by $10\times\theta_{eff}$, where θ_{eff}=5040/T$_{eff}$, to distinguish between, say, a cool and a hot DA. These temperatures were originally determined from broad band colour measurements. Today, the optical spectra themselves are largely used to determine temperatures by comparing them with theoretical models, although the use of the temperature index in classification appears to have declined.

1.5 White Dwarf Formation

All stars with an initial mass $<8\,M_{\odot}$ are expected to end their lives as white dwarfs (Weidemann & Koester 1983). During most of its lifetime, the main source of energy for an ordinary star such as our own Sun is the fusion of hydrogen into helium in the stellar core. The gravitational contraction of the material in the core is counteracted by the radiation pressure propagating outwards from the burning hydrogen at the centre, preventing it from collapsing. The star steadily burns its hydrogen at an essentially constant radius, and this part of its lifespan is called the main sequence (MS) stage. Eventually, however, the hydrogen in the centre will be fully consumed, and, since there is no longer a source of energy to support it, the core will collapse (Schönberg & Chandrasekhar 1942).

The evolutionary path that will now be taken by a star like the Sun is illustrated in Figure 1.2 (a Hertzsprung-Russell diagram). Hydrogen burning starts in a shell around the core, and this provides $\sim$100 times the luminosity previously supplied. As a result, the star will expand by around a factor of $100-1000$, and the outer atmosphere will consequently become much less dense, cooling as it does so. The star is now a Red Giant.

The core, meanwhile, ceases to collapse once the temperature has become hot enough to initiate helium burning. It then expands, slowing the rate of core helium and shell hydrogen burning, and causing the atmosphere to rapidly shrink. The star now moves onto the horizontal branch.

In intermediate mass stars ($\sim 2-8\,M_{\odot}$), helium burning begins before the core has collapsed to a dense enough stage to be degenerate. However, in lower mass stars ($\sim 0.8-2\,M_{\odot}$), the core may already be in a partially degenerate state when helium ignition occurs. Pressure is only weakly dependent on temperature in degenerate material, and so the core does not expand at first. Instead, there is a runaway thermal effect called the helium flash, which only ends when the core temperature has risen sufficiently for it to expand and lift the degeneracy.

Eventually, the helium in the centre is also exhausted. The star then begins burning helium in a shell around a carbon/oxygen core, and its atmosphere expands again, moving it onto the Asymptotic Giant Branch. The highest mass stars may burn carbon in their cores, even oxygen and silicon, but eventually the red giant stage will come to an end. In a star like our Sun, this

will happen once the shell helium runs out. For reasons that are not well understood, thermally-driven radial pulsations begin to occur and the star becomes unstable. The outer atmosphere is then ejected, later to become a planetary nebula.

The modern view is that the atmosphere is removed by one or more types of stellar wind, although how these winds are driven is again unclear. Red giants appear to be able to support wind-driven mass loss rates of $\sim 10^{-6}\,M_{\odot}yr^{-1}$, but it has been estimated that a mass loss rate of at least $10^{-5}\,M_{\odot}yr^{-1}$ is needed to form the observed planetary nebula (Renzini & Voli 1981). These 'superwinds' may operate on a very short timescale of only ~1000 years (Iben & Renzini 1983).

Inside the ejecting atmosphere, the core contracts at constant luminosity, moving horizontally to the left on the H-R diagram, until it is halted by degeneracy pressure. As it contracts, the surface gravity increases by a factor $>10^4$ and the photospheric temperature increases from around 5,000K to >100,000K. Once the temperature reaches ~30,000K there is sufficient flux to ionize the ejected envelope, creating the familiar Planetary Nebula (PN), and the core is observable as a Planetary Nebula Nucleus (PNN), sometimes referred to as the Central Star of a Planetary Nebula (CSPN). The PN itself has a very short lifetime. Within ~100,000 years it dissipates into the surrounding space and is no longer visible. During this time, the central star itself may continue to burn any remaining hydrogen fuel in a shell around the hot core, but eventually even this is exhausted, and the PNN can finally be considered to be a hot white dwarf.

1.5.1 Subdwarfs and the extended horizontal branch

The majority of main sequence stars ($\sim 1-8\,M_{\odot}$) will follow the evolutionary path described above, but the lowest mass stars that are still capable of burning helium in their cores will follow a somewhat different course. These stars do not retain enough envelope mass to support a helium shell burning stage, and thus they cannot ascend the AGB. Instead, they contract at constant luminosity along the Extended Horizontal Branch (EHB) until degeneracy pressure halts their collapse and they become white dwarfs.

Stars on the EHB are known as subdwarfs. They either have hydrogen-rich atmospheres (sdB),

helium-rich (sdO) or a mixture of both (sdOB). Since they have lower surface gravities than white dwarfs (log g$\sim$5$-$6.5 as against $\sim$7$-$9), they have narrower Balmer lines in their spectra. sdBs are found with temperatures up to about 35,000K, but sdOs are found up to 100,000K. It is tempting to think that the sdOs may therefore be the direct progenitors of DO white dwarfs. However, Drilling & Schönberner (1985) showed that the birthrate of sdOs is significantly lower than for helium-rich PNN, suggesting that they contribute to only a fraction of these objects. Similarly, they showed that sdBs and sdOBs could only contribute to 2% of all DAs.

1.6 White Dwarf Evolution and the Cooling Sequence

Understanding the life cycle of white dwarf stars should be simple, since there is no internal source of energy and they simply cool into oblivion. However, the rich variety of white dwarfs that exists complicates any attempt to piece together a coherent explanation of their evolution as they cool. The atmospheres of white dwarfs are vastly different from those of stars like the Sun. A white dwarf photosphere is almost exclusively composed of hydrogen and helium, with only trace amounts of heavier elements evident in some stars (at a level of one part in 1000 or less), yet the relative abundances of these two main elements can differ vastly from object to object.

1.6.1 The primordial, two channel evolution theory

The majority of white dwarfs ($\sim$75%) are hydrogen-rich DAs. Among the hottest stars (T>40,000K), DAs outnumber the helium-rich DOs by a ratio of $\sim$7:1. For a long time, it was thought that this distinction pre-dated the white dwarf stage of a star's life, and that white dwarfs cooled through two distinct, separate channels - a hydrogen-rich cooling sequence originating from hydrogen-rich PNN, and a helium-rich sequence.

Supporting evidence for this picture was, however, very thin. There were several major problems. Firstly, hydrogen-rich and helium-rich PNN exist in almost equal numbers, and thus at some point helium-rich planetary central stars must be turning into hot hydrogen-rich white dwarfs to give the 7:1 DA to DO ratio. Furthermore, up until the ROSAT EUV survey, no DA white dwarf had been found with a temperature greater than 70,000K, and there was, therefore, no

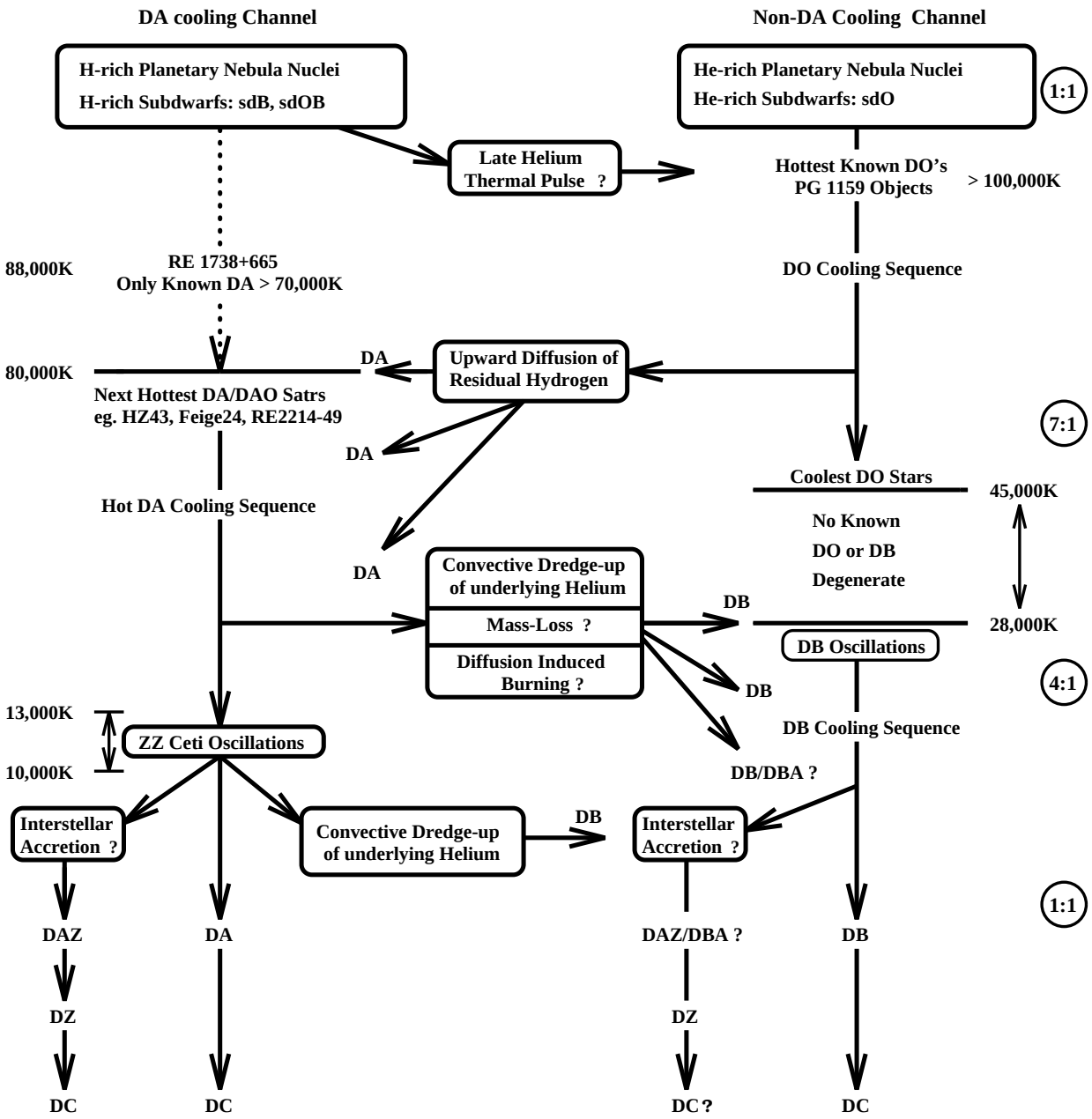

Figure 1.3: The white dwarf cooling sequence. The H-rich channel (DA) is on the left, the He-rich (non-DA) to the right. The circles to the right of the non-DA channel indicate the ratio of DA:non-DA stars at various points on the sequence (reproduced from Marsh 1995a).

observational evidence for a direct link between hot H-rich PNN and the DA cooling sequence. In contrast, there does exist a subclass of helium-rich DO white dwarfs with temperatures in excess of 100,000K - the PG1159 stars (named after the prototype, PG 1159−035). The hottest of these, H1504+65, has a temperature of ≈170,000K (Werner 1991). PG1159s also exhibit absorption lines of photospheric oxygen and carbon in their spectra. These features are commonly seen in helium-rich PNN, and indeed several PG1159s have been identified in the centre of a planetary nebula. Thus there exists strong observational evidence directly linking the helium-rich cooling chain to likely progenitor objects.

Further down the helium cooling sequence a peculiar gap exists between 45,000−28,000K, separating the DO white dwarfs from the DBs, in which no helium-rich star has ever been observed. After decades of searching and with around 2,000 white dwarfs known, this 'DB gap' must be considered to be real - the coolest DOs have temperatures around 45,000−50,000K (e.g. HD149499B, Napiwotzki *et al.* 1995, and HZ21, Sion 1986); the hottest known DBs are at ≈28,000K. Below 25,000K the ratio of DAs to DBs is found to be about 4:1, and below 10,000K the He-rich and H-rich white dwarfs exist in almost equal numbers.

Iben (1984) tried to explain these problems within the two channel scenario. Most white dwarfs will be H-rich with a thick H layer ($M_H \approx 10^{-4}\,M_\odot$), originating from H-rich PNN, unless the hot stellar remnant undergoes a late helium flash, burning helium in a shell around the core. If this occurs, a hot high velocity super-wind may develop, driving off the outer hydrogen layer. These stars will subsequently evolve along the He-rich sequence. They can turn into DAs further down the cooling chain by accreting hydrogen from the interstellar medium, and MacDonald & Vennes (1991) showed that this was certainly feasible. However, any weak (and undetectable) stellar wind could inhibit such accretion, and the accretion rates would have to be four magnitudes lower than expected to account for the presence of DOs as cool as 50,000K. In addition, Iben & Macdonald (1985) predicted that, in this scenario, DAs should exist as hot as 150,000K and cool at the same rate as DOs. The lack of DAs observed at temperatures as hot as this, together with the questions surrounding the accretion hypothesis, began to seriously undermine the two channel evolution theory.

1.6.2 Single channel evolution and the case for thin H layers

Challenges began to be mounted to the two channel evolution theory in the late 1980s. In particular, Fontaine & Wesemael (1987), and Vennes *et al.* (1988) proposed a single-channel evolutionary scheme for all white dwarfs. They postulated that there was really only one kind of white dwarf that went through a variety of changes as it cooled. In this scheme, all white dwarfs originate as helium-rich PNN. PG1159 stars may contain small amounts of hydrogen mixed up in their envelopes, and, as the star cools, this residual hydrogen diffuses up to the surface to form a thin H layer ($<10^{-7}\,M_{\odot}$). The star then takes on the appearance of a DA. This works for abundances as small as H/He=10^{-10}, and leads to a stratified atmospheric structure, with a thin H layer overlying a helium envelope. The amount of hydrogen left in an individual star after the ejection of the planetary nebula will vary, naturally leading to some hydrogen layers being thicker than others. The time taken to transform from a DO to a DA then simply depends on the star's surface gravity and the amount of hydrogen in its atmosphere. By 45,000K, all the DOs have transformed into DAs, giving the DB gap in the helium sequence.

The emergence of DB stars could be then explained by the onset of convection, mixing the He back into the atmosphere. Convection sets in when the temperature gradient becomes steep enough for convective instabilities to occur. Radiation is a less efficient process than convective transport, thus, if the gas becomes bouyant without getting rid of any energy radiatively, convection will become dominant. However, convective mixing of the atmosphere can only occur for white dwarfs with ultra-thin H layers, $M_H<10^{-15}\,M_{\odot}$. If a star has a hydrogen layer thicker than this it will remain a DA, and one would only expect to see DAs with H layers $>10^{-15}\,M_{\odot}$ below 28,000K. This explains the reduction in the DA:non-DA ratio from 7:1 above 45,000K to 4:1 below 30,000K. A further convection zone then develops at about 15,000K. This becomes strong enough that by 10,000K all DAs with H layer masses $<10^{-10}\,M_{\odot}$ will change into DBs, accounting for the further reduction in the DA:non-DA ratio to 1:1 below 10,000K.

This 'thin hydrogen layer' theory proved to be very attractive. It explained the DB gap, and it accounted for the absence of any DAs above 70,000K. The timescale for hydrogen to accumulate at the surface matches the cooling timescale of DO white dwarfs, and, furthermore, there exists above 45,000K a class of hybrid H/He stars called DAOs, whose optical spectra show HeII lines in addition to the Balmer series of H. These white dwarfs were the perfect candidates for objects

transferring from the helium cooling chain to the hydrogen sequence. Additional observational evidence to support the thin H layer scenario comes from the pulsating ZZ Ceti stars (DAV white dwarfs). The variability of these stars is caused by a non-radial oscillations dependent on the star's mass, temperature, radius and atmospheric structure. From modelling their power spectra, it is possible to deduce that the hydrogen layer mass cannot exceed $10^{-8}\,M_{\odot}$. Pulsating white dwarfs seem, therefore, to be consistent with the thin H layer theory.

1.6.3 Complications

There are, however, a number of problems with the single channel evolutionary scenario. For a start, theoretical calculations show that all DA white dwarfs should be born with thick hydrogen layers ($M_H > 10^{-4}\,M_{\odot}$), in order to account for the observed luminosity function (Iben & Tutukov 1984, Iben & Macdonald 1985, Koester & Schönberner 1986), although weak stellar winds could still feasibly produce thinner layers (Bruhweiler & Kondo 1986). Weak mass-loss in hot DAs has been inferred from the presence of blue shifted absorption components of highly ionised species (e.g. CIV) in far-UV spectra taken by IUE and HST (e.g. Holberg, Bruhweiler & Andersen 1995). However, a mass-loss rate $>10^{-14}\,M_{\odot}yr^{-1}$ is needed in order to overcome gravitational settling, and this would strip off a hydrogen layer as thin as $10^{-13}\,M_{\odot}$ almost immediately (Koester 1989a).

A much more serious challenge to the single channel hypothesis came with the discovery by ROSAT of a very hot DA, RE J1738+665 (Barstow *et al.* 1994b, T≈85−90,000K). Tweedy & Kwitter (1994) then discovered an old, dissipated planetary nebula associated with this star, linking it directly to the H-rich PNN. At the same time, a study of DAO stars by Bergeron *et al.* (1994) showed that most of these white dwarfs had homogeneously mixed atmospheres, and could not be transition objects between the two cooling sequences (if they were, they should have stratified atmospheres). In fact, most DAOs appear to be either the products of binary evolution, or descended directly from subdwarfs (see Chapter 4).

Two other sub-classes of white dwarf also need to be accounted for by the thin H layer theory. The first are DAB stars, hydrogen rich white dwarfs showing trace amounts of helium (in the form of HeI lines). It is tempting to think that these might be the first white dwarfs to be found with very thin H layers. However, it has proved difficult to reproduce the observed features in

these stars with stratified model atmospheres. The prototype, GD323 (T≈28,000K), can just about be matched with a hydrogen layer of $\sim 10^{-17}\,M_{\odot}$ (Koester, Liebert & Saffer 1994), but Wesemael *et al.* (1994) suggest that these objects might in fact be double degenerates consisting of a DA and a DB.

DBA white dwarfs, which have small hydrogen features in an otherwise helium-dominated optical spectrum, are generally found just below the 28,000K end of the DB gap. The hydrogen appears to be homogeneously mixed into the atmosphere with an abundance H/He$\approx 10^{-4}$. If DBAs are related to DBs, we may expect to see some trace amounts of hydrogen in high resolution spectra of all DBs. This hydrogen may have been mixed into the helium-dominated atmosphere after the star has crossed the DB gap, when the convection zone has become strong enough to stir up the thin surface H layer. However, Shipman *et al.* (1991) failed to find any hydrogen in a large sample of DBs. This could be because DBAs are accreting their hydrogen from the ISM (Aannestad & Sion 1985). There are, however, a number of arguments making accretion an unlikely hypothesis. The accretion rate needed to overcome gravitational settling is $\sim 10^{-16}\,M_{\odot}yr^{-1}$, and to achieve this the white dwarf would have to be in some sort of interstellar cloud. However, the typical time between encounters of such clouds is, at $\sim 5\times 10^{7}$yrs, longer than the cooling timescales of hot white dwarfs (Koester 1989a). The 'propeller mechanism' (Alcock & Illarionov 1980) may also prevent any accretion of hydrogen by a slowly rotating, weakly magnetic white dwarf, since it will be ionised, caught by the magnetic field lines and flung off by the centrifugal force. The discovery of a DA+DBA pair, L 151−81A/B (Oswalt, Hintzen & Luyten 1988) also argues against the accretion hypothesis, since the two stars have a common trajectory through space and therefore a common history of accretion. Perhaps the distinction between H-rich and H-poor white dwarfs is indeed made at birth.

The existence of the DB gap still strongly suggests, however, that the thin H layer theory is valid, at least for some stars. If DB stars evolve from DAs in the 30,000−45,000K gap, then there should be a population of DAs in this temperature region with ultra-thin hydrogen layers ($<10^{-15}\,M_{\odot}$). So far, no such star has ever been observed (Shipman 1997), and we do not know what fraction of DAs in this regime should possess thin H layers. Currently theorists are suggesting the number should be ∼20%. Below the gap, trace amounts of hydrogen have been found recently in HST GHRS UV spectra of the DB pulsator GD358 (T≈28,000K), at a level of H/He$\sim 10^{-7}$ (Provencal *et al.* 1996). This is so low, though, that it appears to rule out the

possibility that the star was *ever* a DA (if all this hydrogen was floating on the surface it would still look like a DB). A DAB star has also recently been found, at T≈36,000K, in the DB gap (HS0209+0832, Jordan *et al.* 1993). However, like GD358, this star cannot be matched by a stratified atmosphere, and thus the suspicion remains that this, like the other DABs, might be a double degenerate system.

Finally, searches for trace amounts of hydrogen in hot DOs and PG1159 stars have so far proved unsuccessful (Werner 1996), although the upper limits on the abundances are still relatively high. Further studies are needed to totally rule out the presence of hydrogen in these very hot stars.

1.6.4 Summary - the current picture

1) The majority (∼80%) of DA stars are evolving down a single channel from H-rich PNN, only mixing into the non-DA channel at very low temperatures with the onset of convection. The lack of very hot (T>80,000K) DAs so far observed may simply be because many of them are still embedded in their planetary nebulae. The hydrogen layer masses could be anywhere from $\sim 10^{-4}\,M_{\odot}$ to $\sim 10^{-15}\,M_{\odot}$.

(H-rich PNN)−(hot DA)−(cool DA)−(very cool DAs and non-DAs)

2) The non-DA channel is a much more confusing picture. No ultra-thin H layered DAs have been found in the DB gap, and the DB star GD358 does not contain enough hydrogen to have ever looked like a DA when it was in the gap. In addition, the DAO stars no longer appear to be transition objects between the two chains. Many unanswered questions remain about this sequence, but the DB gap appears in study after study to be real. Thus, the thin H layer theory may still prove to be the correct explanation for the non-DA cooling chain. To reiterate, a He-rich PNN is the descendant of a post-AGB star which lost its hydrogen layer during a late He-shell flash. A PG1159 star emerges from the planetary nebula, which changes into a hot DO as the carbon and oxygen sink out of sight. By 45,000K residual hydrogen has floated to the surface to give an ultra-thin H layered DA. At 30,000K, convection begins and the hydrogen is stirred back into the vastly more massive helium layer, giving first a DBA and then a DB star.

(post-AGB star)−(He-shell flash)−(He-rich PNN)−(PG1159 star)−(hot DO)−(ultra-thin H layered DA)−(DBA)−(DB)−(cool DQ, DC, DZ)

3) Other channels may exist, including one for the post-EHB objects (the subdwarfs), that may be related to the lowest mass DAOs, and another for those DAOs in close pre-CV binaries which may be accreting helium from the stellar wind of their companion (see Chapter 4). Interacting binary white dwarfs (those in CVs) may also provide yet another evolutionary track.

1.7 The White Dwarf Mass Distribution, Luminosity Function and Birth Rate

Although their main sequence progenitors can have a large range of masses from $\sim$0.5−8.0 $M_\odot$, white dwarf masses generally span a remarkably small range. Bergeron, Saffer & Liebert (1992) found, from a study of >100 DAs T>15,000K, that 80% had masses between 0.4 and 0.6 $M_\odot$. This narrow peak implies that the initial-to-final mass relation is very flat; i.e. in general, whatever the zero-age main sequence mass of their progenitor stars, white dwarfs will always have very similar masses. The exceptions occur at the low (M_{WD}<0.4 $M_\odot$) and high (M_{WD}>0.8 $M_\odot$) ends. A low mass cut off occurs because, with a finite age to the galaxy, the smallest stars will not have had time to evolve off the main sequence. White dwarfs with masses <0.4 $M_\odot$ can only have been formed through binary interactions, during which the progenitor stars lose mass. High mass stars may be formed from high mass progenitors. Various authors (e.g. Liebert & Bergeron 1995) have noted that a high mass peak may exist around 0.9 $M_\odot$. D'Antona & Mazzitelli (1995) attempted to explain this secondary peak in terms of white dwarfs descended from population I stars with initial masses >4.5 $M_\odot$. In this picture, the progenitor of, for example, Sirius B (M$\approx$1.05 $M_\odot$) is a 6.5−7 $M_\odot$ giant. An alternative source of massive white dwarfs are the ultimate end products of binary evolution - merged double degenerates. This may explain the existence of the most massive white dwarf ever found, RE J0317−853 (Barstow *et al.* 1995b, 1.35 $M_\odot$). This highly magnetic object is the the most rapidly rotating isolated white dwarf known, spinning with a period of $\sim$12 minutes. The spin up and high mass may be the result of a merger of two lower mass white dwarfs, whose combined mass was not enough to push the star over the Chandrasekhar limit (coalescing white dwarfs with a total mass >1.4 $M_\odot$ maybe a cause of some Type I supernovae). The possible origins of high mass white dwarfs are

discussed in more detail in Chapter 5.

The white dwarf luminosity function of an open stellar cluster, a globular cluster, or the local stellar disk, will have a sharp truncation at a luminosity determined by the time since the first stars in the cluster ended their lives on the AGB. Measurements of the white dwarf luminosity function can, therefore, provide a method of measuring a cluster age or putting a lower limit on the age of the Galaxy and the Universe, since the cooling time of a white dwarf is very much greater than its progenitor's main sequence lifetime. Calculating white dwarf ages is based on relatively well understood physics and is independent of stellar evolution theories. Currently, the age of the local galactic disk is put at around $10 \pm 2 \times 10^9$ years. The error comes largely from a lack of knowledge about how the core crystalises, the phase separation of the carbon and oxygen in the core during crystallisation, and the influence of trace amounts of heavier elements. Measurements of the white dwarf luminosity function may also potentially reveal past eras of unusually high or low star formation.

Currently, due to selection effects in optical surveys, the majority of known white dwarfs are isolated stars (see Chapter 3 for a further discussion of this problem). Fleming, Liebert & Green (1986) found that this led them to measure a white dwarf birth rate in the local galactic disk some $60\% - 75\%$ lower than expected. After correcting for the unseen fraction in binaries, Fleming, Liebert & Green (1986) found that the local white dwarf mass density ($0.006\,\mathrm{M}_\odot \mathrm{pc}^{-3}$) is not enough for white dwarfs to account for the missing mass in the local disk.

1.8 Soft X-ray and EUV Observations of Hot White Dwarfs

The temperature, gravity and mass of a white dwarf can be found from modelling the star's optical spectrum. However, only lines of hydrogen, helium and occasionally carbon are seen at these wavelengths in white dwarfs. In contrast, large numbers of important lines are found in the far ultraviolet (far-UV, $1000 - 2000$Å), extreme ultraviolet (EUV, $100 - 1000$Å) and soft X-ray ($10 - 100$Å) regions. In addition, the hottest and youngest white dwarfs radiate the majority of their energy at these wavelengths. This radiation is blocked and absorbed by the Earth's atmosphere, and, therefore, far-UV, EUV and X-ray detectors have to be placed in space, on board orbiting satellites. A major motivation for these space-based observatories has been the

study of the hot end of the white dwarf cooling sequence in order to build a detailed picture of their changing photospheric composition as they cool, and to try to understand the nature of the white dwarf evolutionary sequences.

1.8.1 Early results

Until the early-1970s it was assumed that interstellar space was filled with hydrogen gas that would be opaque to EUV radiation. However, in 1974 Cruddace *et al.* (1974) first predicted that if the local interstellar medium (LISM) consisted of non-uniform, low density material, then it should be possible to observe astrophysical sources of EUV and soft X-ray radiation over relatively large distances. That year, a small EUV telescope was flown aboard the US-Soviet Apollo-Soyoz mission and four EUV sources were discovered, including the hot white dwarfs HZ43 (Lampton *et al.* 1976) and Feige 24 (Margon *et al.* 1976). For a while it was thought that this flux could only come from a hot corona, but Shipman (1976) showed that instead it was originating from deep inside the white dwarf's atmosphere. This was because the outer layers of a hot DA will be highly ionised, and so they will be essentially transparant to emergent EUV and soft X-ray radiation. Thus observations in these wavelength regions should allow us to examine how a white dwarf's atmospheric composition changes with increasing depth.

Rocket-born observations of the hot DA HZ43 (Margon *et al.* 1976, Lampton *et al.* 1976 and Holberg *et al.* 1980) showed that its atmosphere, like Sirus B, was consistent with a pure H composition. However, broadband photometric observations by the Einstein (1978-1980) and EXOSAT (1983-1986) satellites provided the first evidence that there was an additional source of opacity in the atmospheres of many hot DAs. At first, it was assumed that the cause was helium, homogeneously mixed into the atmosphere with an abundance He/H$\geq 10^{-6}$. Kahn *et al.* (1984) suggested that this helium was either being accreted from the interstellar medium, or it was being levitated within the photosphere by radiation pressure. Petre, Shipman & Canizares (1986) found that the amount of opacity appeared to increase with increasing temperature. This was to be expected if DO white dwarfs are transforming into DAs with thin H layers, and favoured selective radiative levitation as the only mechanism to give such a correlation with temperature. Although the photometric data were being modelled with homogeneously mixed atmospheric structures, Jordan *et al.* (1987) reminded us that, due to the high gravitational field, a stratified

structure should be the more physically realistic configuration. Koester (1989b) subsequently discovered that the EXOSAT photometric count rates could be equally well matched with a stratified model. The photometric data, therefore, could not distinguish between a stratified and a homogeneous atmospheric structure.

These models all made the assumption that helium is the only significant opacity source in the EUV/X-ray region of the photosphere. This was not neccesarily true. Early results from IUE had revealed the presence of lines from highly ionised states of C, N and Si in high resolution far-UV data, for example in the hot DA Feige 24 (Wesemael, Henry & Shipman 1984). Then Vennes *et al.* (1988) showed that the amount of helium that could actually be supported by radiative levitation in a white dwarf atmosphere was too small by a factor of 2 to account for the observed levels of opacity in many stars. Finally, three white dwarfs (Sirius B, HZ43 and Feige 24) were observed spectroscopically by EXOSAT around the important HeII Lyman absorption series near 228Å, providing the first opportunity to attempt to directly detect any helium present in their atmospheres.

No helium was found in all three stars but, whereas the spectra of Sirius B and HZ43 could be matched by pure H models, there was a considerable discrepancy between the model predictions and the observed data for Feige 24. Given the evidence of the far-UV data, the most plausible explanation for the flux deficit was the presence of trace heavy element pollutants. Indeed, a model containing C, N, O, Ne, Si, Ar and Ca could reproduce the EUV spectral shape well, although no individual features could be identified (Vennes *et al.* 1989).

Feige 24 itself lies in a close binary system, and may have interacted with its red dwarf companion in the past. Thus it was not clear whether it was representative of the majority of white dwarfs, or whether in fact the archetypal star was the pure hydrogen DA HZ43. Before the launch of ROSAT in 1990 the general consesus was that the majority of hydrogen-rich white dwarfs were like HZ43, although Feige 24 was not necessarily unique.

1.8.2 The EUV and X-ray emission of hot white dwarfs

Hot white dwarfs are predominantly composed of H and/or He, and their spectral shape and energy distribution is dependent on the atmospheric structure and temperature gradient, together

with the relative abundances and absorption characteristics of the two main constituents.

The EUV absorption cross-section per He atom is many orders of magnitude greater then the optical cross-section (see Figure 2.1, Marsh 1995a). In other words, helium is very opaque to EUV radiation. This means that He-rich white dwarfs show very little emission in the EUV compared to the optical. However, as the temperature increases more atoms are ionised into excited states, and consequently the difference between the EUV and optical cross-sections decreases. Even so, Barstow (1989) found that a DO white dwarf would have to have a temperature in excess of 60,000K to be detected by the ROSAT WFC through a hydrogen column of 10^{19} atoms cm^{-2}. In the final analysis, only $\sim$10 hot DOs and PG1159 stars were detected in the survey.

In stark contrast, the limiting temperature for detecting a DA is substantially lower than for He-rich white dwarfs, since the absorption cross-section at EUV wavelengths is relatively similar to the optical cross-section (Marsh 1995a). For a column of 10^{19} atoms cm^{-2}, Barstow (1989) found that a DA would be detected at just 20,000K. Based on this, Barstow (1989) predicted upwards of 1000 DAs would be found by ROSAT. Crucially, however, this analysis was made assuming pure H compositions, and in the absence of any other source of opacity.

A white dwarf will appear optically like a H-rich DA even if it has a significant amount of He hidden deeper in its atmosphere, which could significantly affect the emergent EUV flux. This point is demonstrated in Figure 1.4, which shows four model spectra for a stratified white dwarf, T=30,000K and log g=8.0, but with varying hydrogen layer masses. It is clear from the diagram that at this particular temperature and gravity, if the hydrogen layer was as thin as a few $\times 10^{-14}\,M_{\odot}$, then the underlying helium envelope would be visible in EUV spectra in the form of the lyman series of absorption lines converging on 228Å. Thus it was hoped that the ROSAT and EUVE missions would be able to find very thin layered DA white dwarfs and prove that at least some DAs were descended from the helium-rich cooling sequence.

The EXOSAT and high resolution IUE observations of Feige 24 (discussed above) had revealed the presence of trace amounts of elements heavier than He suspended in the white dwarf's photosphere, acting as additional absorbers of emergent EUV and soft X-ray radiation. The amount of any one element that can be supported this high up in the atmosphere for any length of time depends critically on the balance between gravitational settling and any possible support

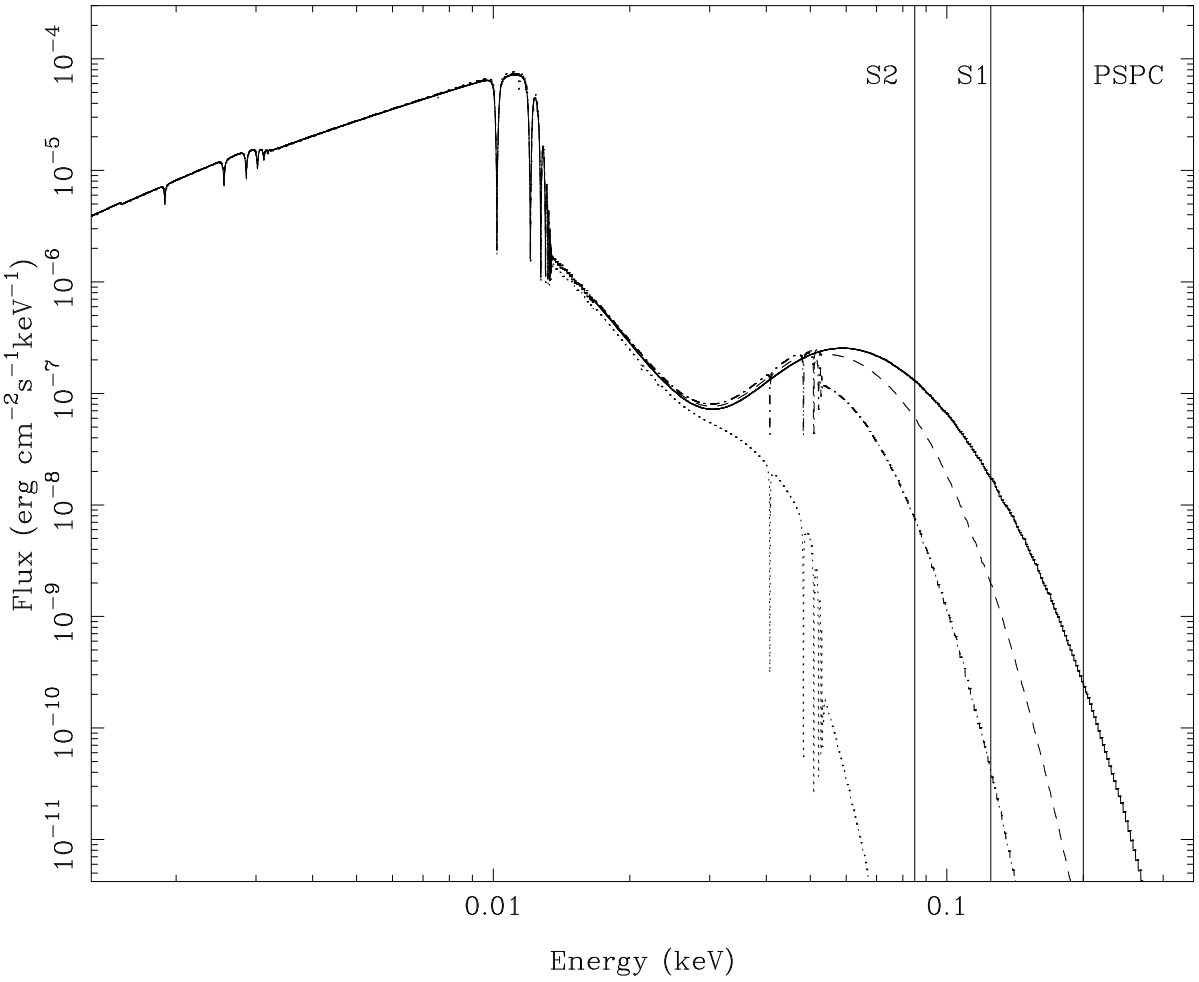

Figure 1.4: Four model white dwarf spectra for a 30,000K DA white dwarf, log g=8.0, with a stratified atmosphere and a varying hydrogen layer mass M_H. Solid line - $M_H=7.32\times10^{-13}$ (effectively a pure hydrogen photosphere), dashed line - $M_H=3.21\times10^{-14}$, dash/dot line - $M_H=9.16\times10^{-15}$, dotted line - $M_H=2.89\times10^{-15}$. Superimposed on the diagram are the mean ROSAT filter band energies. The PSPC value is for the soft (0.1−0.4keV) band only. (reproduced from Marsh 1995a).

mechanisms, e.g. accretion, stellar winds, and, most importantly, radiative levitation. Detailed calculations by many authors (e.g. Morvan, Vauclair & Vauclair 1986, Chayer, Fontaine & Wesemael 1989, Chayer *et al.* 1995) have shown that significant quantities of these elements (e.g. C, N, O, Si, Fe and Ni) may be levitated over a long period by radiation pressure through bound-bound transitions at the surface of hot white dwarfs. It was found that the line spectra of these elements can generally absorb enough momentum from the radiation field of sufficiently hot white dwarfs to counteract gravitational settling, although the surface gravity still dictates the observed abundances (Chayer, Fontaine & Wesemael 1995). The elements in question have many transitions in the EUV region, and thus there was the distinct hope and possibility that they would be identified in EUV spectra.

1.8.3 The ROSAT WFC survey

ROSAT was launched on June 1st 1990 from Cape Canaveral on board a Delta II rocket. It was placed into a circular low earth orbit at an altitude of 580km with a period of 96 minutes. ROSAT carried two instruments: a German X-ray telescope and a British EUV telescope, the Wide Field Camera (WFC, Sims *et al.* 1990). In the first six months of operation, the WFC carried out the first survey of the entire sky in EUV and X-ray radiation. A technical description of the satellite and the WFC experiment can be found in the Appendix.

The all-sky survey began on 31st July 1990 and continued until the 25th January 1991. The spacecraft was rotated on its axis once per orbit so that the telescopes were pointing away from the Earth at all times, and full sky coverage could be achieved. The spacecraft effectively traced out great circles on the sky, with each circle passing through the ecliptic poles. To maintain the required orientation of the solar panels to the Sun, the scan path was advanced by $\sim 1^{\circ}$ per day, and thus the whole sky was covered in about 6 months. The longest exposures were at the ecliptic poles, since the exposure was a function of ecliptic latitude. The detectors were switched off for approximately 25% of each day to protect them as the satellite passed through regions of high particle background, such as the South Atlantic Anomaly and the Auroral Zones. Although there was a drop in the sensitivity of the detectors during the survey, it was found that the decline was steady and could be modelled by a simple function, so that corrections to the count rates could be easily applied (Willingale 1997). Unfortunately, the spacecraft suffered an

attitude control systems failure on 25th January 1991 during which the telescopes were pointed at the Earth and Sun. This resulted in permanent damage to the S2a filter and the PSPC, although by this time only $\sim$10% of the survey remained incomplete. These missing patches were scheduled to be filled in February 1997, during a series of pointed observations.

During the data reduction process, the PSPC images were divided into strips of ecliptic longitude, and those of the WFC into $2^\circ \times 2^\circ$ maps. These were searched for point sources using an automated detection searching algorithm, NIPS (Page 1990). For the white dwarfs, the PSPC soft band (0.1$-$0.28keV) count rates were determined by Fleming *et al.* (1996). In total, 383 EUV sources were found in the original WFC survey, and these were published as the Bright Source Catalogue (Pounds *et al.* 1993). Later, the survey data was reprocessed with improved methods for source detection, lower detection thresholds, better background screening and better rejection of poor aspect periods, to give the 2RE Catalogue (Pye *et al.* 1995). This new catalogue contains 479 sources.

Tentative identifications were originally made by comparing the positions of detected sources with astronomical catalogues of known objects. In this way, 44 white dwarfs were identified from the catalogue of McCook & Sion (1987). Optical identification campaigns were then mounted to find counterparts for the unidentified sources, led by Mason *et al.* (1995). Around 180 of the original BSC sources and about 75 of the new 2RE sources are associated with active stars. Hot white dwarfs account for the majority of the remaining sources (>120 have now been identified). Other classes of EUV emitting objects found in the survey include Active Galactic Nucleii (AGN), Cataclysmic Variables (CVs) and supernova remnants.

A similar survey was carried out by NASA's Extreme Ultraviolet Explorer (EUVE) between 24th July 1992 and 21 January 1993 (for a technical description, see Appendix). 410 sources were listed in the First EUVE source Catalog (Bowyer *et al.* 1994), and, in a similar fashion to the WFC survey, the EUVE data was later reprocessed to produce the Second EUVE Source Catalog (Bowyer *et al.* 1996) containing 727 sources. Again, the majority of the detections are associated with active stars, with hot white dwarfs being the second most numerous class of astronomical object seen.

1.8.4 Major results from ROSAT and EUVE

Prior to the ROSAT survey, only ∼20 hot white dwarfs had been detected photometrically in the EUV and soft X-rays by EXOSAT and Einstein, and only a dozen had been observed in high dispersion by IUE to look for heavy elements. ROSAT greatly increased the number of known EUV-bright white dwarfs to >120 objects, although this was still only ∼10% or less than the number predicted by pre-launch estimates (e.g. Barstow 1989). Where were the missing stars?

Comparing the X-ray and EUV detections with optically selected samples of white dwarfs provides a clue to the reason for their non-detection. Between 20,000−40,000K almost 100% of previously known DA white dwarfs are detected. However, above 40,000K the fraction of known stars actually detected falls with increasing temperature. If the fluxes predicted for the detected white dwarfs, assuming they had pure H atmospheres, is compared with the actual fluxes, we find another clue. Below 40,000K, the observed fluxes closely match the predictions. Above 40,000K, the observed luminosities depart strongly from the predictions of a pure H envelope, with the discrepancy becoming larger for higher temperatures.

The first major study of the ROSAT white dwarfs was undertaken by Barstow *et al.* (1993c), who analysed the EUV data for 30 well known DAs. They modelled the ROSAT fluxes with H+He atmospheres, and found that in many cases the presence of helium alone was not enough to account for the observed levels of opacity above 40,000K. Indeed, where helium could account for the flux deficit, the predicted optical and UV HeII line strengths were far greater than the observed levels. Thus, the authors concluded that trace amounts of elements heavier then He must be present to provide the additional EUV opacity.

This conclusion was strengthened by a full analysis of 89 ROSAT-detected white dwarfs, including many of the new discoveries, by Marsh *et al.* (1997b). These authors found that above 55,000K, all the DAs showed some evidence for heavy element opacity, although there were still a handful of stars between 40,000−55,000K which resembled the pure H white dwarf HZ43.

As was noted earlier, high resolution IUE far-UV spectra of a number of hot DA white dwarfs taken prior to the ROSAT mission had already revealed the presence of elements such as C, N and Si in the stellar photospheres. New IUE observations of some of the ROSAT discoveries (e.g.

RE J0623−37 and RE J2214−49, Holberg *et al.* 1993) and of Feige 24 and G191−B2B (Vennes *et al.* 1992) revealed the presence of iron in these stars photospheres, and later co-addition of several spectra to improve the signal-to-noise also revealed the presence of significant quantites of Ni in these same stars (e.g. Holberg *et al.* 1994). Interestingly, the current radiative levitation theories predict that iron can be supported in a white dwarf's photosphere at temperatures of 55,000K and greater (Chayer, Fontaine & Wesemael 1995), the same temperature regime in which all the ROSAT white dwarfs display evidence of heavy element contamination.

Since then, many of these hot DAs have been observed spectroscopically with EUVE. Even before that satellite's launch, Wilkinson, Green & Cash (1992) had used a rocket-borne experiment to provide the first tentative evidence for iron transitions in the EUV spectrum of G191−B2B. The EUVE spectrum of this star has, however, proved very difficult to model. Several million transitions of FeV and FeVI must be included in model calculations to provide the necessary line blanketing before a reasonable match to the observed data can be achieved (Lanz *et al.* 1997). However, the abundances of iron and the other heavy elements found in these white dwarfs are far in excess of the predictions of radiative levitation theory. Accretion from the interstellar medium may be an explanation in some cases, although the most likely mechanism appears to be mass loss via a stellar wind. It is easy to see that a weak wind, driven by radiation pressure, could lead to a further differentiation of a star's atmospheric composition. Winds are seen in the central stars of planetary nebula, but these have much lower gravities than true white dwarfs. In a white dwarf, mass loss is still a very poorly understood process.

Observational evidence for weak stellar winds in hot white dwarfs has come from high resolution IUE observations of the EUV-bright helium-rich DO RE J0503−289, the only example of this class of white dwarf to be discovered by ROSAT. The blueward assymetry of the HeII 1640Å line in this star's spectrum indicates the presence of a wind with a terminal velocity of $\sim$600kms^{-1}.

What ROSAT and EUVE have not been able to do is to provide any evidence for the existence of very thin H layered DA white dwarfs ($M_H < 10^{-15}\,M_\odot$), which might be descended from the helium cooling sequence. Indeed, from the ROSAT photometric fluxes alone it has not been possible to establish whether these stars have homogeneous or stratified atmospheres, since good fits are obtained in many cases with both structures. None of the DAs observed spectroscopically by EUVE have been found with hydrogen layer masses $<10^{-14}\,M_\odot$. However, if the ultra-thin H

layered DAs do exist, they may have such thin hydrogen layers that they are simply not bright enough at EUV wavelengths to be seen at all. This is evident in Figure 1.4. The EUV flux of a DA with a thin H layer of just a few$\times 10^{-15}$ $M_{\odot}$ is absorbed by the underlying helium before it is ever emitted at the stellar surface, and the star is invisible to ROSAT and EUVE.

One of the most important discoveries in the ROSAT survey was a very hot (T$\approx$90,000K) DA white dwarf, RE J1738+665, which provides a direct link between H-rich planetary nebula central stars and the DA cooling sequence (Barstow *et al.* 1994b). The discovery of a dissipated, tenuous old planetary nebula near to this star (Tweedy & Kwitter 1994) strengthened the conclusion that the majority of DA white dwarfs were indeed directly descended from H-dominated planetary nucleii. Another important individual discovery in the survey was RE J0317$-$853, at 1.35 $M_{\odot}$ the most massive white dwarf ever found (Barstow *et al.* 1995b). This star possesses the second largest magnetic field ever detected in an isolated white dwarf ($\sim$340MG), and is rapidly rotating with a period of $\sim$ 12 minutes. One other magnetic white dwarf was also discovered by ROSAT, RE J0616$-$649, which, at V=18.4, is also the faintest white dwarf to be detected in the EUV surveys.

Hot white dwarfs are extremely good probes of the interstellar medium, since the column densities of HI, HeI and HeII can be determined directly from their EUV absorption signatures in the white dwarf spectra. Thus, from soft X-ray and EUV observations, it is possible to map out the approximate distribution of hydrogen and helium in the local 'bubble'. It has been known for some time that the solar system sits inside a bubble of low density gas, which may have been swept out by one or more supernova explosions in the last few million years (e.g. Bruhweiler 1995). From the ROSAT photometric EUV fluxes of hot white dwarfs and active stars, Diamond, Jewell & Ponman (1995) and Warwick *et al.* (1993) produced the first really detailed maps of the distribution of hydrogen within the local bubble. However, these early studies had to make the simplifying assumption that the ratio of neutral helium (HeI) to hydrogen was equal to the cosmic ratio He/H=0.1, and that the amount of singly ionized HeII was negligible. Spectroscopic observations of hot white dwarfs with EUVE have shown that many lines of sight are much more complex than this, and that He is substantially more ionized than previously thought (Dupuis *et al.* 1995, Barstow *et al.* 1997).

The first WFC source to be found (RE J1629+780, the 'Meaty' source, Cooke *et al.* 1992)

turned out to be a previously unknown, relatively close DA+dMe binary, the first of a growing number of white dwarf binaries to be discovered by ROSAT. A number of known white dwarfs in binaries were also detected in the survey. These range from wide, resolved pairs like Sirius, to close pre-Cataclysmic Variable (pre-CV) systems like V471 Tauri (DA+K2V, Nelson & Young 1970) and Feige 24 (DA+dM). Five new pre-CV systems have now been discovered by ROSAT (see Chapter 2). The white dwarfs in three of these binaries have proved to belong to the extremely rare hybrid DAO class, which show helium in their optical spectra in addition to hydrogen. These systems are discussed in Chapter 4. ROSAT has also been vitally important in detecting optically hidden hot white dwarfs in unresolved pairs with much brighter main sequence companions (spectral type K or earlier). These stars are, and may always be, invisible at optical wavelengths and can only be detected in the EUV, where the cooler companions are much fainter. Only a handful of these kinds of systems were known prior to the survey. Since the majority of catalogued white dwarfs are isolated stars, the discovery of a significant number of these systems greatly improves our knowledge of not only the white dwarf population as a whole, but of binary evolution and interaction. The story of a search for these hidden white dwarfs is detailed in Chapter 3, and in Chapter 5 the properties of the entire ROSAT detached binary white dwarf sample are discussed.

Chapter 2

The Formation and Evolution of White Dwarf Binaries

2.1 Overview

Theory and observations suggest over half of all stars lie in binary or multiple systems. However, since most of the ~2000 known white dwarfs are isolated stars, it is these which dominate our knowledge of the white dwarf luminosity function, birthrate and space density (Fleming, Liebert & Green 1986). Observations of white dwarfs in binaries are, therefore, vital to our understanding of the entire white dwarf population. The evolutionary paths taken by white dwarfs in binary systems may, in some cases, be very different to the isolated stars. Observing binary white dwarfs allows us to compare and contrast the isolated and binary populations, and look for evidence of past interactions. For example, has the mass and past evolution of the white dwarf been affected by previous episodes of mass transfer, and has the companion star been affected in any way? Finding binary systems with a white dwarf component is also vital for testing theories of Common Envelope evolution, and for studying angular momentum loss mechanisms such as gravitational wave emission, and magnetic stellar wind braking.

In this chapter I will discuss the evolution of white dwarf binaries in more detail, explaining why only ~2% of main sequence binaries are able to evolve into CVs within the age of the Universe. In later chapters I will discuss my observations of pre-CV systems, and of the other wide WD+MS binaries detected by ROSAT and observed with IUE and EUVE. The evolution of these wider systems will also be discussed here.

2.2 Introduction

Close, detached binary systems consisting of a white dwarf (WD) and a normal late type star are formed from originally rather wide main sequence (MS) binaries, and may be the progenitors of Cataclysmic Variables (CVs). Paczynski (1976) first suggested that these systems must have undergone a phase of common envelope (CE) evolution when the white dwarf precursor, a red giant, fills its Roche Lobe and begins to transfer mass to its less massive companion. This interaction is unstable - the secondary cannot cope with the speed and amount of matter flowing from its evolving companion, and it is soon engulfed by the primary's envelope. On a very short timescale, angular momentum is lost from the system as the secondary star spirals-in towards the core of the red giant. The orbital energy is then used to expel the giant's envelope, leaving behind, in a very close orbit, the hot core (soon to become a white dwarf) and the almost unaffected low mass main sequence secondary. This is the pre-cataclysmic binary. Immediately after the CE phase, the system begins to lose orbital angular momentum by magnetic stellar wind braking and gravitational wave emission, and the two stars start to move closer together. The main sequence secondary may also expand through its own evolution, eventually filling its Roche Lobe and interacting with the white dwarf via mass transfer. This is the semi-detached CV configuration.

Observations of close but detached WD+MS binaries can be potentially used to study the widely quoted angular momentum (a.m.) loss mechanism, magnetic stellar wind braking, that is thought to occur in interacting CVs. Here, the stellar wind attaches itself to open magnetic field lines until very far away from the star (the Alfren radius), and thus angular momentum is lost from the star via the wind. Tidal effects lock the star's spin to the orbital period of the binary, and so angular momentum can be lost from the entire system. In pre-CV systems there is no mass transfer to complicate this effect, and so it can be studied in detail. Orbital a.m. losses cause the systems to evolve to shorter periods, and the magnitude of the loss will determine how long a system will stay in a certain period interval. The shorter the orbital period, the greater the effect of magnetic braking and the closer the two stars become. By observing the period distribution of these systems, and having some knowledge of the formation rate, it may be possible to reconstruct the angular momentum loss rate.

Studying close WD+MS systems also allows us to test estimates of the formation rates of double

degenerate binaries and their potential role as progenitors of Type 1 supernovae, since double degenerates must at some point pass through the evolutionary phase being discussed here.

EUV-bright pre-CVs are particularly important since, because the white dwarf is so young, they must be in an orbital state almost identical to that in which they were left immediately after the CE phase. They are far enough apart that the effects of magnetic braking will not be noticeable until the white dwarf has cooled, and so they could provide important tests of our admittedly weak understanding of CE evolution.

2.3 Common Envelope Evolution

It is well known that over half of all stars lie in binaries. Studies of binary separation (*e.g.* Popova, Tutukov & Yungelson 1982) have shown that, since single stars will evolve to a radius of $\sim 10^{14}$cm on the giant branch, then $\sim 50\%$ of all binaries will interact in some way before the primary ejects its outer layers to form a planetary nebula (PN) (de Kool 1990). The question is, which binaries are likely to start unstable mass transfer and form a CE, and what fraction are likely to survive the process and emerge as a close binary system?

White dwarf binaries will form from main-sequence pairs if the more massive primary can become a white dwarf within the age of the Galaxy but avoid turning supernova (and so forming a neutron star) through being too massive. The upper mass limit for the primary is generally agreed to be $8.0\,M_\odot$. The lower mass limit will depend, of course, on the assumed age of the Galaxy (and the Universe). Broadly speaking, the star would have to be $\sim 1.0\,M_\odot$ or larger. In this section I draw heavily on the work of de Kool (1990) who, in studying CE evolution, puts these zero-age limits at $0.7<M_p/M_\odot<8.0$, and also from deKool & Ritter (1993), who assumed $0.95<M_p/M_\odot<8.0$.

The type of interaction in the main-sequence binary is divided into three classes (for a more detailed description, see *e.g.* de Kool 1990, de Kool 1992, deKool & Ritter 1993, Iben & Livio 1993). Mode I mass transfer starts when the donor star is still on the main-sequence and has a radiative envelope. The mass transfer is stable, *i.e.* the secondary can happily accept the amount and rate of matter being given to it. If the evolutionary timescale of the mass gaining star becomes shorter than the original donor (*i.e.* it has become the more massive star),

a contact binary will be formed (*e.g.* W Ursae Majoris). This type of interaction is poorly understood but is unlikely to lead to the formation of a pre-CV (de Kool 1992). If the original primary's evolutionary timescale remains the shorter, then mode II mass transfer can begin. These systems cannot form a CV, however, because studies have shown that the secondary in all cases will be too massive to initiate stable mass transfer to the WD. They can, though, continue their evolution to become double degenerate systems (deKool & Ritter 1993).

Mode II mass transfer starts when the primary is on its first ascent of the giant branch, *i.e.* before helium ignition, and before it has developed a deep convective envelope. The mass transfer will be stable, in the sense that no CE is formed, because the envelope of the donor star is radiative and will shrink in response to mass loss. This type of mass transfer is also conservative because all of the envelope mass of the primary is transferred to the secondary. Binaries of this type can continue their evolution to become WD+MS pairs with periods $\sim$10 days and with fairly massive ($1\,M_\odot$) main sequence companions (deKool & Ritter 1993). The primary core will be non-degenerate immediately after mass transfer. If this He-core is less massive than $0.35\,M_\odot$ it cannot ignite the helium and will collapse to become a He white dwarf. A core greater than $0.35\,M_\odot$will become a helium burning star before evolving into a CO-core white dwarf [1]. The only possibility for the formation of a CE in mode II mass transfer is if the mass ratio is extreme ($q = M_2/M_1 < 0.25$). In this case the Roche Lobe of the primary will shrink faster than its radius, the mass transfer will rapidly become unstable, and a CE phase will occur. However, in these extreme mass ratio cases de Kool (1992) shows that there is not enough energy available to eject the CE, and the two cores will coalesce. Thus a pre-CV binary cannot be formed from mode II mass transfer.

The most common type of mass transfer, mode III, occurs when the primary is on either the giant branch or the AGB, and has a deep convective envelope. This time, the star will expand in response to mass loss, and the mass transfer will become unstable. A common envelope will form, during which the secondary star spirals in towards the core of the primary (see below). In some cases this will lead to a complete merger of the two stars. Binaries which survive will typically have short orbital periods and a low mass secondary, and these are the progenitors of CVs.

[1] $0.35\,M_\odot$ is the rather conservative CO-core mass limit adopted by deKool & Ritter (1993). Bergeron *et al.* (1994), for example, suggest that all white dwarfs below $0.48\,M_\odot$ must have He-cores, and generally speaking most authors adopt a CO-core white dwarf lower mass limit of $0.45-0.5\,M_\odot$.

As the main sequence star spirals-in towards the giant core, gravitational energy is gained by the decrease in separation. The system cannot survive as a binary if the separation is reduced to the point at which the companion fills its Roche lobe. However, if enough orbital energy is gained to eject the envelope then a close binary will emerge. Energy is dumped into the low density giant envelope because of friction between it, the giant core and the secondary, leading to a large loss of mass and angular momentum from the system.

Even then there are more criteria to be fulfilled in order for the close binary to become a CV. It must be able to evolve into a semi-detached state by losing angular momentum within the age of the Galaxy, and before the secondary begins to evolve off the main sequence. The mass transfer rate must also be stable when the white dwarf binary becomes semi-detatched. For this to be possible the zero-age main sequence mass ratio $q = M_p/M_2$ must have been large, typically > 3.5 (Politano 1996). The close WD+MS mass ratio $q = M_1/M_2$ must be > 0.8 if $M_2 > 0.65\,\mathrm{M}_\odot$ and > 1.6 if $M_2 < 0.65\,\mathrm{M}_\odot$ (King *et al.* 1994).

Figure 2.1 illustrates these possible binary evolutionary paths. Most theoretical studies (*e.g.* de Kool 1992, deKool & Ritter 1993) show that $\sim 50\%$ of all zero age main sequence binaries (in the assumed primary mass range) are too wide to ever interact. Around 4% will become contact binaries while still on the main sequence, $\sim 5\%$ will undergo stable mode II mass transfer, and $\sim 40\%$ will fill their Roche lobes, initiate unstable mass transfer and undergo CE evolution. Typically about 11% of the initial binaries will survive the CE phase, 5% will be close enough to turn on mass transfer within the age of the Galaxy, but only 2% will be in a stable enough configuration to become a CV.

The actual numbers depend on the assumptions and input parameters of the theoretical models. In particular, a value must be assumed for the common envelope ejection efficiency parameter α. This number states how efficiently the gravitational energy gained during the spiral-in phase is being used to eject the CE. Studies show it must lie somewhere between 0.3 and 1.0. de Kool (1992) shows that if $\alpha = 1.0$ then about 40% of binaries entering the CE phase will survive, but only 20% if $\alpha = 0.3$. Unfortunately there is no direct observational evidence for CE evolution since it is very rapid (between a few and 10^3 years).

The best evidence is the existence of double cores of planetary nebula, consisting of a hot central

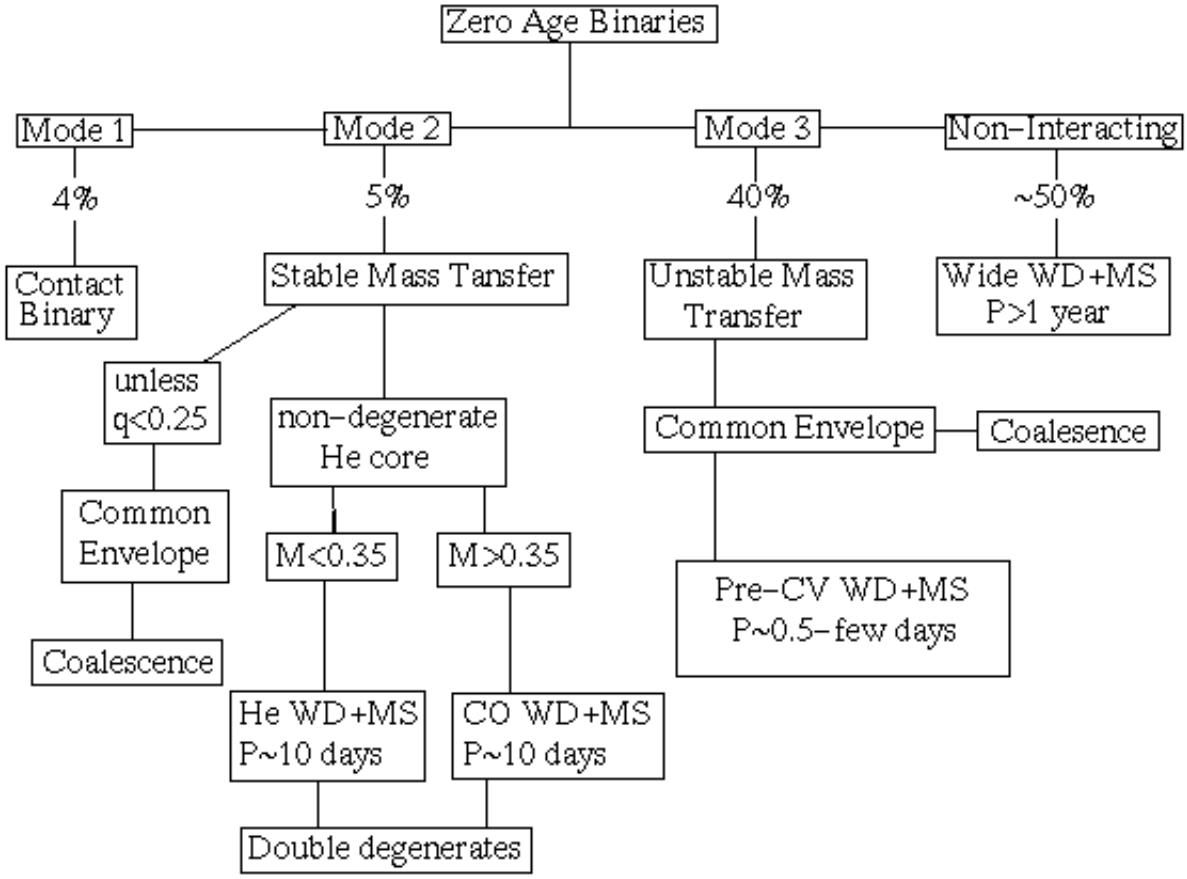

Figure 2.1: A simplified overview of the various evolutionary paths for binary stars to a detached WD+MS configuration.

star and a main sequence companion. The ejected envelope of the giant will form a planetary nebula around the binary with a lifetime of $\sim 10^5$yrs. The hot, collapsing giant core may appear as a subdwarf star, with a luminosity similar to that of the pre-CE giant. The more massive cores will join the white dwarf cooling sequence before the PN has dispersed. Less massive cores can appear as subdwarfs for some time, longer than the dispersal time of the PN. Those with very low masses may not even become hot enough to be subdwarfs until the PN has gone. Eventually, though, the PN will have dispersed and the system will be visible as a long lifetime WD+MS binary.

Table 2.1: WD+MS Pre-CV Candidates

System	Type	P (d)	$M_1(M_\odot)$	$M_2(M_\odot)$	EUV?	Refs.
IK Peg	DA+A8V	21.72	1.1±0.1	1.7	Y	1
Feige 24	DA+dM1−2	4.2316	0.47±0.03	0.30±0.04	Y	2
KW Aur C	DA+F4V	2.99	0.55	1.3	Y	3
RE J0720−31	DAO+dM4−5	1.201	0.55±0.03	0.25±0.5	Y	4
RE J1016−05	DAO+dM1−3	0.7893	0.57±0.03	?	Y	5
RE J2013+40	DAO+dM1−4	0.7059	0.60±0.12	0.3±0.1	Y	6
EG UMa	DA+dM4−5	0.66765	0.38±0.07	0.26±0.04		7
PG 1026+002	DA+dM4−5	0.597	0.68±0.23	0.22±0.05		8
HZ9	DA+dM5	0.56433	0.51±0.10	0.28±0.04		7
V471 Tau	DA+K2V	0.521183	0.71±0.02	0.73±0.03	Y	7
PG1413+015	DAO+dM3−5	0.344331	0.51±0.04	0.10		9
RR Cae	DA+dM	0.30371	0.43±0.09	?		10
PG0308+096	DA+dM5	0.284309	0.40±0.11	0.18±0.05		8
GD245	DA+dM3−5	0.17366	0.48±0.02	0.22±0.02		11
NN Ser	DAO+dM5−6	0.13008	0.57±0.04	0.12±0.02		12
GD448	DA+dM5	0.103042	0.44±0.03	0.09±0.01		13

Refs.: 1] Wonnacott, Kellett & Stickland (1993) 2] Vennes & Thorstensen (1994a) 3] Webbink *et al.* (1992) 4] Barstow *et al.* (1995c) 5] Thorstensen, Vennes & Bowyer (1996) 6] Barstow *et al.* (1995a) 7] King *et al.* (1994) 8] Saffer *et al.* (1993) 9] Fulbright *et al.* (1993) 10] Bragaglia, Renzini & Bergeron (1995) 11] Schmidt *et al.* (1995) 12] Catalan *et al.* (1994) 13] Marsh & Duck (1996)

2.4 Known pre-CV Systems

There are now almost 40 pre-cataclysmic variable binary systems known (Ritter 1996). These consist of double cores of planetary nebulae (DCPN, a hot central star plus a MS companion), hot subdwarf+MS binaries with and without PN, and close WD+MS pairs. To this number could be added seven close double degenerate WD binaries which may undergo some kind of mass transfer before coalescing, or becoming a Type I supernova. Most have orbital periods less than one day.

In Table 2.1 I have listed the 16 known pre-CV WD+MS binaries with well determined periods. I have indicated on the list whether the system is an EUV source. The majority are red dwarf/white dwarf (DA+dM) pairs, although three (V471 Tau, IK Peg, KW Aur C, all ROSAT WFC sources) have secondaries with earlier spectral types. Indeed IK Peg (HR8210, Wonnacott, Kellett & Stickland 1993) is an A star/massive ($1.1\,M_\odot$) WD binary with a relatively long

period of 21.72 days, and therefore of particular interest since it is currently the only system of this type known. Another WFC WD/A star binary, β Cratoris (Fleming *et al.* 1991), may have an orbital period of <20 days, although more detailed radial velocity measurements are needed to confirm this. V471 Tau is a well known eclipsing binary, sometimes called the 'prototype' pre-CV, and KW Aur C (HD33959C, Hodgkin *et al.* 1993) was also discovered as a result of the WFC survey.

In addition to the previously known Feige 24 (Vennes & Thorstensen 1994a), three new red dwarf/white dwarf binaries were detected by the WFC: RE J0720−318 (Barstow *et al.* 1995c, Vennes & Thorstensen 1994b), RE J1016−053 (Tweedy *et al.* 1993, Thorstensen, Vennes & Bowyer 1996) and RE J2013+400 (Barstow *et al.* 1995a, Thorstensen, Vennes & Shambrouk 1994). Intriguingly, all three are hybrid DAO white dwarfs displaying a weak HeII feature in their spectra at 4686Å. Indeed, Vennes & Thorstensen (1994a) report a transient 4686Å feature in their spectra of Feige 24, so this star too might be better classed as a DAO. A more detailed investigation and discussion of these white dwarfs will be conducted later in this thesis (see Chapter 4).

One close DA+dM EUV binary missing from the list is RE J1629+780, the first source detected by the ROSAT WFC (the "meaty" source). The period of this system is not well defined, and there is some debate (*e.g.* Catalan *et al.* 1995, Sion *et al.* 1995) whether this pair are close enough to form a CV within an acceptable timescale. Binaries like this are often optically identified from variable emission cores in the H Balmer absorption lines of the white dwarf spectrum. The emission features are due to radiation from the white dwarf being reprocessed and emitted by the surface of the red dwarf. However, in the case of RE J1629+780 there is evidence that the red dwarf itself is active. If all the emission features are due to reprocessing then the orbital period is <3.4 days and the system can be considered a pre-CV. However, if the red dwarf is indeed active then the period is longer, somewhere between 4 and 6.5 days.

The other pre-CV WD+MS binaries on the list are not detected in EUV surveys. The references given in Table 2.1 are the sources for the parameters quoted. One often cited WD+MS pre-CV, BE UMa, *e.g.* by deKool & Ritter (1993) and King *et al.* (1994), has recently been shown to be an sdOB+MS pre-CV (Wood, Robinson & Zang 1995). Searches continue for more of these astrophysically important systems, for example Schultz, Zuckerman & Becklin (1996)

have measured radial velocities for 21 WD+dM binaries and conclude that the system KPD 2145+408 is highly likely to be a pre-CV. However, they do not give a period and so I have omitted it from Table 2.1.

2.5 Summary

The vast majority ($\sim$ 90%, deKool & Ritter 1993) of white dwarf binaries will be too wide to ever interact, but their study allows us to place constraints on on binary evolution models (*e.g.* deKool & Ritter 1993). In particular, studying the closer, possibly pre-CV systems which make up only $\sim$ 2% of all the WD binaries, allows us to test our understanding of common envelope evolution, and to investigate angular momentum loss mechanisms like magnetic stellar wind braking. Since selection effects have mitigated against finding white dwarfs in unresolved binaries in optical surveys to date, their detection will also add greatly to our knowledge of the general white dwarf population.

Chapter 3

A Search for Hidden White Dwarfs with ROSAT and IUE

3.1 Overview

The ROSAT WFC survey has provided evidence for the existence of a previously unidentified sample of hot white dwarfs in non-interacting binary systems, through the detection of EUV and soft X-ray emission. These stars are invisible at optical wavelengths due to their close proximity to much more luminous main sequence companions (spectral type K or earlier). However, for companions of spectral type ~A5 or later the white dwarfs are easily visible at far-UV wavelengths, and can be identified in spectra taken by IUE. Eleven hidden white dwarf binary systems have previously been found in this way from ROSAT, EUVE and IUE observations (e.g. Barstow *et al.* 1994a). In this chapter I announce the discovery of five more such pairs, through programmes in recent episodes of IUE. I also discuss a number of targets observed where no white dwarf companion was found. Some of these stars are chromospherically and coronally active. Finally, I re-analyse the data for three previously reported hidden WD+MS binaries. New insights to the HD18131 (Vennes *et al.* 1995) and RE J1925−566 (Barstow *et al.* 1994a) systems are provided by the addition of the ROSAT PSPC X-ray fluxes, which were not available to the original discoverers. In addition, I show that the white dwarf in the HD27483 system, which was indentified independently from the ROSAT survey (Böhm-Vitense 1993), is contributing to the EUV flux detected from its active F star companions. Including HD27483, 17 optically hidden WD+MS binaries have now been discovered through the EUV surveys.

3.2 Introduction

The extreme ultraviolet (EUV) surveys of the ROSAT Wide Field Camera (WFC, Pounds *et al.* 1993, Pye *et al.* 1995) and the Extreme Ultraviolet Explorer (EUVE, Bowyer *et al.* 1994, Malina *et al.* 1994, Bowyer *et al.* 1996) have found a substantial number of hot white dwarfs (≈ 120). The majority of these are single isolated stars, but about 30 are now known to lie in detached binary systems. Some have been found, from optical observations, to be in pairs with faint red dwarf companions (e.g. RE J1629+780, Cooke *et al.* 1992). A few are in resolved wide binaries (e.g. HD74389B, Liebert, Bergeron & Saffer 1990). However, non-interacting unresolved pairs with companions earlier than M-type have remained very difficult to identify.

In optical surveys, white dwarfs have been identified on the basis of colour information (e.g. Green, Schmidt & Liebert 1986), and there is thus a selection effect against the detection of those in unresolved binaries. Any companion star of type K or earlier will completely dominate the optical spectrum of the white dwarf (see Figure 3.1, BD+27°1888, WD+A8V). For example, Sirius B would be optically undetectable were it not for the close proximity of the system to Earth (2.64pc), allowing it to be resolved from Sirius A.

Several unresolved systems have been discovered serendipitously. The white dwarf in the well-studied system V471 Tauri was found as a result of an eclipse by its K2V companion (Nelson & Young 1970). A number of others have been found by chance in ultraviolet (UV) spectra taken by the International Ultraviolet Explorer (IUE). For example, the white dwarf companion to HD27483 (Böhm-Vitense 1993, also an EUV source, see later in this chapter) was discovered as part of an IUE study of Hyades F stars by Böhm-Vitense (1995). Others detected in a similar fashion include ζ Cap (Böhm-Vitense 1980), 56 Peg (Schindler *et al.* 1982) and 4 o^1 Ori (Johnson & Ake 1986). In 1989, Shipman & Geczi (1989) conducted a systematic survey of the then existing IUE archive for white dwarf companions to G, K and M stars, but found no further examples. Recently, Landsman, Simon & Bergeron (1996) have detected, using IUE, two white dwarf companions to F stars showing an excess of ultraviolet radiation in the TD-1 sky survey (Thompson *et al.* 1978). The white dwarf in the 56 Persei system (F4V) is, at T=16,400K, too cool to be seen with the WFC. The white dwarf companion to HR3643 is hot (29,000<T<36,000), but it is not detected by either EUVE or ROSAT. This is probably because of a high interstellar hydrogen column ($\sim 2\times10^{20}\mathrm{cm}^{-2}$) to this star.

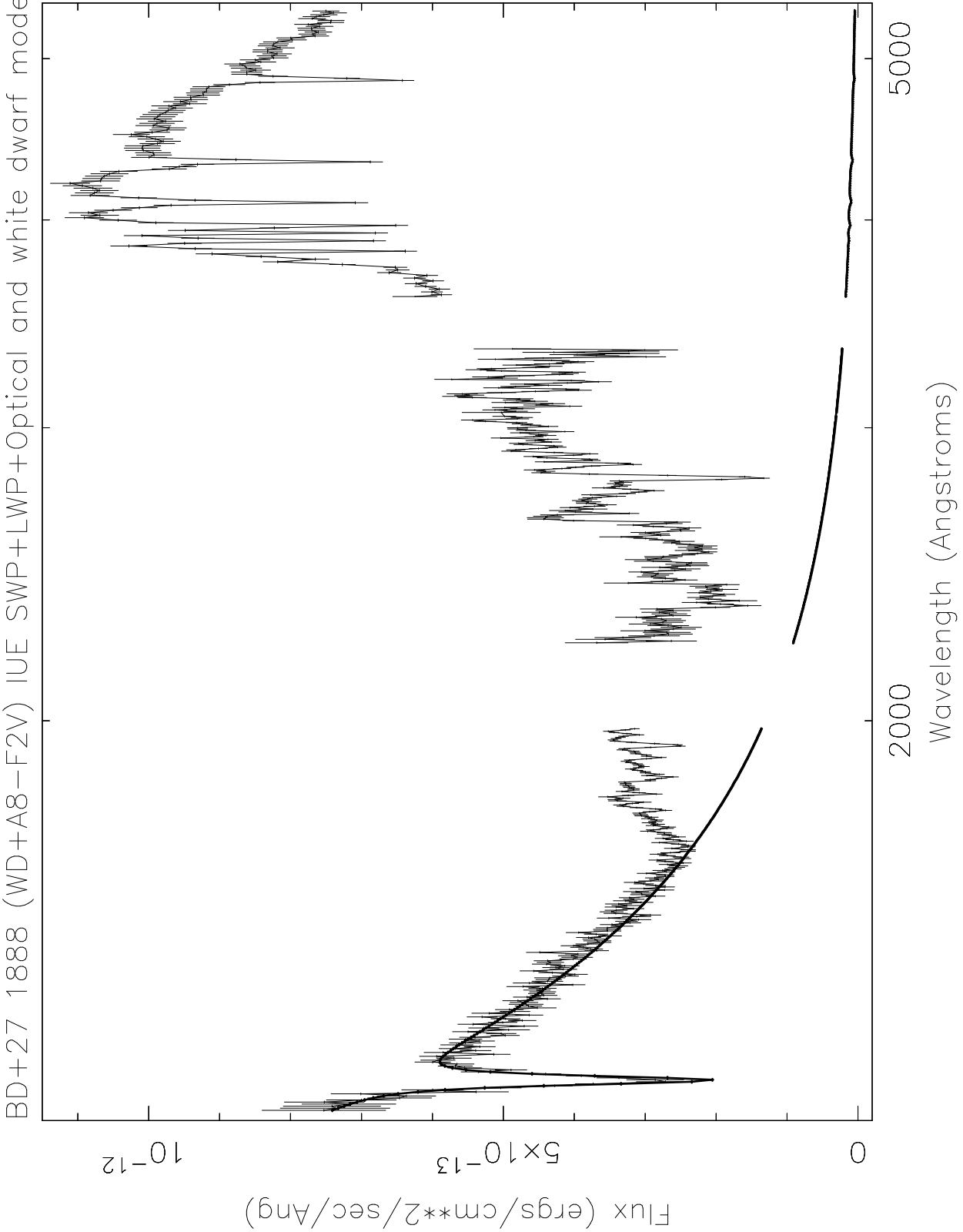

Figure 3.1: IUE SWP and LWP spectra of BD+27°1888 (WD+A8V), displayed together with an optical spectrum of the main sequence star V≈9.1). The white dwarf (V≈14.8) can be seen emerging from the glare of its companion shortwards of ∼1600Å. A white dwarf model for T=34,000K and log g=7.25 is also included (solid line). This diagram clearly illustrates that the white dwarfs in these binaries are undetectable at optical wavelengths and can only be seen in the far-UV.

ROSAT and EUVE have now provided us with evidence for the existence of many more of these hidden hot white dwarfs through the detection of EUV and soft X-ray emission. Follow-up observations in the UV with IUE have enabled detection of unresolved white dwarfs in systems with a companion later than spectral type ∼A5. The initial discovery of companions to β Crateris (A2IV, Fleming *et al.* 1991) and HD33959C (KW Aur C, F4V, Hodgkin *et al.* 1993) was followed by seven others, all discussed in Barstow *et al.* (1994a): BD+08°102 (K1-3V, also Kellett *et al.* 1995), HR1608 (K0IV, also Landsman, Simon & Bergeron 1993), HR8210 (IK Peg, A8m, also Landsman, Simon & Bergeron 1993, Wonnacott, Kellett & Stickland 1993, Barstow, Holberg & Koester 1994a), HD15638 (F3-6V, also Landsman, Simon & Bergeron 1993, Barstow, Holberg & Koester 1994a), HD217411 (G5), HD223816 (F5-G0), and RE J1925−566 (G2-8). Since then Vennes *et al.* (1995) have reported a DA companion to the active K0IV star HD18131 through its detection as an EUVE/WFC source, and Christian *et al.* (1996) have discovered yet another DA+G star binary, MS 0354.6−3650, which is also an EUVE source (although it does not appear in the ROSAT WFC catalogues). This work has clearly demonstrated that there is an as yet unexplored population of white dwarfs with companions earlier than type M.

Most of these white dwarfs are all relatively bright EUV sources (with the exceptions of BD+08°102 and MS 0354.6−3650), with distinctive spectral signatures. Typically, the S2/S1 count rate ratios are >2. For example HD33959C has a count rate of $2.628 s^{-1}$ in the WFC S2 filter, and $1.172 s^{-1}$ in S1. Comparisons with known white dwarfs detected by the WFC (e.g. GD659 $2.193 s^{-1}$ in S2, $0.722 s^{-1}$ in S1) left little doubt that these sources were indeed white dwarfs. The observations with IUE merely confirmed the identifications.

About 120 of the 383 sources in the original Bright Source Catalogue (BSC, Pounds *et al.* 1993) have been associated with hot white dwarfs, and a larger number (∼ 180) with active late type stars. However, from a cursory glance at the original BSC, it is clear that some of these late type stars were not previously known to be chromospherically active. Indeed, follow-up optical studies (e.g. Mason *et al.* 1995, Mullis & Bopp 1994) failed to find any evidence of activity at all in a few cases. It is also obvious from the WFC catalogues that there are many faint hot white dwarfs with low count rates, and with EUV colours that are not particularly distinctive. These stars may lie in relatively high column directions that affect the S2/S1 ratio and, from the count rates alone, it is difficult to immediately distinguish them from an active star. Furthermore, some of the primaries in the binaries already discovered are also active (e.g. HD18131, BD+08°102 and

RE J1925−566). Determining which EUV source is due to an active star and which is due to a white dwarf is clearly, in some cases, not an easy task. Given all these factors, the search was continued with IUE for further, less obvious white dwarfs hidden in non-interacting binaries. Since the first of these IUE programmes, the 2nd ROSAT WFC catalogue (Pye *et al.* 1995) has been published. This utilises improved source detection methods and contains 120 new sources as well as updating the BSC identifications. There is thus a pool of new, fainter and less obvious candidates requiring observation.

This chapter discusses the results of the latest searches with IUE. I have identified five more hot white dwarfs in non-interacting binary systems with main sequence stars earlier than type M have been identified. In addition, I show that the independently discovered white dwarf companion to HD27483 (Böhm-Vitense 1993) is also an EUV source. Including this system, the total number of such binaries discovered as a result of the EUV surveys currently stands at seventeen.

3.3 Observations

3.3.1 Detection of the sources in the ROSAT and EUVE surveys

The EUV and X-ray count rates for all the sources discussed in this chapter are given in Table 3.1. The WFC count rates are taken from the 2RE Catalogue (Pye *et al.* 1995), and these are equivalent, on axis 'at-launch' values. The revised 2RE catalogue is discussed in more detail in Chapter 1. The PSPC count rates for all the white dwarfs detected in the X-ray survey, including the binaries discussed here, are given in Fleming *et al.* (1996). The PSPC count rates for the active stars (i.e. the non-detections of white dwarf binaries) were obtained either by private communication from Tom Fleming (Steward Observatory, University of Arizona) or more recently, since its publication, from the on-line ROSAT All-Sky Survey Bright Source Catalogue (via the World Wide Web [1]), maintained by the Max Planck Institute in Germany (Voges *et al.* 1997).

Some of the sources were also detected by EUVE in its all-sky survey (Bowyer *et al.* 1994, Malina *et al.* 1994). The quoted EUVE count rates in Table 3.1 are taken mainly from the Second EUVE

[1] http://www.rosat.mpe-garching.mpg.de/survey/rass-bsc/cat.html

Table 3.1: ROSAT WFC/PSPC and EUVE count rates ($1000s^{-1}$)

		WFC		PSPC		EUVE	
ROSAT No.	Name‡	S1	S2	(0.1-0.4keV)	(0.4-2.4keV)	100Å	200Å
WD+MS Binaries							
RE J0024−74	HD2133	14±5	32±9	46±11	no det.	no det.	no det.
RE J0254−05	HD18131	65±13	127±21	262±36	52±16	137±14	44±12
	no det.						
RE J0420+13[1]	HD27483	15±4	27†	78±14	33±9	no det.	no det.
RE J0500−36[2]		20±5	47±8	no det.	no det.	21±6	no det.
RE J1024+26	BD+27°1888	33±5	19±7	212±24	no det.	46±10	no det.
RE J1027+32		15±4	23±7	52±17	no det.	40*	no det.
RE J1925−56		710±38	697±40	5987±307	no det.	890±26	no det.
Non-WD Systems							
2RE J0014+69	AG+68 14	no det.	36±10	no det.	no det.	no det.	no det.
2RE J0222+50	BD+49°646	14±3	17±5	258±20	195±18	no det.	no det.
2RE J0232−02		15†	45±11	no det.	no det.	no det.	no det.
RE J0312−44	CD−44 1025	25±6	27±6	693±47	575±41	36±7	no det.
RE J0402−00	HR1249	34±6	41±7	785±50	739±48	50±12	no det.
2RE J0530−19	SAO150508	8±3	16±5	159±18	195±20	no det.	no det.
2RE J0534−15	HD36869	8±3	19±5	221±22	217±22	no det.	no det.
2RE J0544−22	Gl 216	7±3	22±5	261±23	82±13	no det.	no det.
RE J0613−23	HR2225	18±3	35±9	517±30	256±21	no det.	no det.
RE J0637−61	HR2468	34±3	32±4	1389±38	919±31	47±4	9±4
2RE J0640−03	HD295290	9±3	32±8	304±28	281±27	no det.	no det.
RE J0650−00	BD−00°1462	13±3	26†	196±28	134±22	no det.	no det.
2RE J0710+45	HD54402	8±3	26±7	no det.	no det.	no det.	no det.
2RE J0813−07	SAO135659	14±6	55±16	207±35	195±34	no det.	no det.
RE J0823−25[3]		52±7	83±9	175±24	no det.	28±11	no det.
2RE J1212+77	HR4646	13†	18±5	157±42	114±36	no det.	no det.
RE J1809+29	HD166435	26±4	51±13	307±21	197±17	25±7	no det.

‡ In some cases there is no evidence that the named counterparts of the non-detections are active and/or the true EUV sources (see section 3.6.3)
No error given in Bowyer *et al.* (1996)
† upper limit
1] ROSAT WFC Bright Source Catalogue detection only (Pounds *et al.* 1993)
2] Detected in the First EUVE Source Catalog only (Bowyer *et al.* 1994)
3] HD70907 and a V≈11 companion were both observed as possible counterparts to this source

Source Catalog (Bowyer *et al.* 1996), which includes an improved all-sky detection method offering better detection sensitivity and reliability. The exception is RE J0500−362, which is only listed in the First EUVE Source Catalog (Bowyer *et al.* 1994) and the EUVE Bright Source List (Malina *et al.* 1994). The quoted count rate is taken from Bowyer *et al.* (1994).

The naming convention I have adopted is as follows: ROSAT sources are given an 'RE' number

if they appear in the original Bright Source Catalogue (Pounds *et al.* 1993), but sources that were only detected in the revised Pye *et al.* (1995) survey are allocated a '2RE' designation.

3.3.2 Selection and identification of white dwarfs in unresolved binaries

The hot white dwarfs detected in the ROSAT EUV and X-ray all-sky surveys typically have very soft spectra compared to normal stars, particularly when the hydrogen column is low. The ratio of the WFC survey S2 to S1 count rates can sometimes exceed a factor 2. Additionally, no photons will be detected from a white dwarf above the 0.28 keV carbon K_α edge of the ROSAT PSPC. All other objects generally have spectra extending to higher energies.

White dwarfs with red dwarf companions are easily identified from their composite optical spectra, but for binaries with companions of spectral type K or earlier the white dwarf cannot be discerned from an optical observation (see Figure 3.1). However, it is possible to distinguish between the two stars in a far-UV spectrum obtained with the IUE short wavelength (SWP) camera. Thus, initially, the stars we chose to observe with IUE were selected by the similarity of their EUV colours and luminosities to known isolated white dwarfs in the WFC survey, after the elimination of field white dwarfs in chance alignments with late-type stars, and known EUV active stars. Nine non-interacting binaries were discovered in this way and discussed by Barstow *et al.* (1994a).

However, only ~50% of isolated DAs, where the interstellar absorption is relatively low, have these characteristics. Typically the first of these systems to be identified were among the brightest EUV sources, but most isolated white dwarfs are detected at low signal-to-noise ratio (SNR) and are indistinguishable from coronal sources from EUV data alone. Clearly, these binaries represent only part of the possible population.

Only the most active late-type stars are detected as EUV sources. Any that are weakly active must be very nearby to be seen. Thus RE J1027+323 and BD+27°1888 were included on the original IUE target list precisely because they were not known to be active. During the EUV source optical identification programme (Mason *et al.* 1995) observations were made of possible non-degenerate counterparts to see whether they were sufficiently active, as indicated by the strength of CaII H and K and Hα emission cores, to be the EUV sources. For example, HD2133

was listed in the WFC Bright Source Catalogue as active, but Mason *et al.* (1995) found no evidence of activity and thus the most likely explanation for the EUV flux was a hidden white dwarf companion. Similarly, no evidence of activity was seen in HR2468, BD-00°1462, RE J0500−362 or RE J1027+323. In separate observations, Mullis & Bopp (1994) found that HD166435 exhibits no measurable emission in the core of Hα, and could not conclude that it was chromospherically active. In an entirely different programme, RE J0357+283 was observed by Jeffries, Burleigh & Robb (1996) with the LWP camera on IUE (LWP26441) in an attempt to detect chromospheric MgII H and K emission. An excess of flux blueward of 2800Å was discovered which, the authors suspected, was probably due to a hot white dwarf companion. An SWP spectrum was needed to conclusively prove the white dwarf's existence.

In 1995, the publication of the 2nd ROSAT WFC catalogue (Pye *et al.* 1995) provided a pool of ≈120 new EUV sources from which to select potential hidden white dwarfs. In a separate programme undertaken by myself and various colleagues worldwide, a number of the unidentified 2RE fields were observed optically to try to determine the counterpart. In some cases, for example RE J0500−362, 2RE J0222+503 and 2RE J0232−025, only one star was visible in the field. As these stars (10<V<15) were unlikely to be active enough to be detectable by the WFC, a hidden white dwarf was a reasonable explanation for the EUV radiation, and thus they were added to our target list.

3.3.3 UV spectroscopy

A log of all the UV observations of these objects is given in Tables 3.2 and 3.3. RE J0357+283 was added to the programme and observed in August 1995 to confirm the presence of the white dwarf predicted by Jeffries, Burleigh & Robb (1996). Observations of HD18131 were originally reported by Vennes *et al.* (1995). The white dwarf companion to HD27483 was accidentally discovered in October 1992 by Böhm-Vitense (1993), independently of the ROSAT survey. RE J0500−362 was first observed in a short half hour exposure in November 1995, and a faint white dwarf was detected. A further 8 hour exposure was therefore obtained a month later. The programme was cut short in February 1996 when a gyro failed on IUE, limiting the satellite to observe only objects for which a bright (V<8) guide star was available. Unfortunately, this was not the case for any of our remaining targets.

Table 3.2: Log of IUE observations of the WD+MS binaries

Name	SWP No.	LWP No.	Date	Exp. (s)	Observer	notes
HD2133	55659		1995/234	1800	Burleigh	
	56231		1995/329	2700	SO	newsips
		31757	1995/329	600	SO	newsips
HD18131	52151		1994/266	5500	Vennes	mildly saturated
	52158		1994/267	2000	Byrne	
RE J0357+283	55660		1995/234	3780	Burleigh	
		26441	1993/265	1500	Jeffries	
HD27483	45940		1992/273	2100	Böhm-Vitense	
RE J0500−362	56217		1995/323	1800	SO	newsips
	56338		1995/358	29400	SO	new., 159DN
		31729	1995/323	1800	SO	newsips
BD+27°1888	49779		1994/006	4000	Burleigh	2× over-exposed
	49780		1994/006	1200	Burleigh	
	56261		1995/336	1200	SO	newsips
		31785	1995/336	300	SO	newsips
RE J1027+322	49778		1994/006	1200	Burleigh	
	49793		1994/008	11100	Burleigh	
	54501		1995/115	7500	Burleigh	newsips
RE J1925−566	49048		1993/303	900	Marsh	

SO= Service Observation
159DN=159DN problem (see text)

Two spectra, SWP56333 (RE J0500−362) and LWP31726 (HD295290) were affected by the so-called '159DN anomaly'. A number of pixels, for an as yet unknown reason, were assigned the flux value 159DN when they should in fact have had a higher number. However, on close inspection it was found that only a small fraction of the data was contaminated and the science was not affected by this problem (Andernach, private communication).

3.3.4 Optical spectroscopy

Optical spectroscopy of RE J1027+323, HD18131, HD27483, and RE J0357+283 is reported by Genova *et al.* (1995), Vennes *et al.* (1995), Böhm-Vitense (1993), and Jeffries, Burleigh & Robb (1996) respectively, and their results are quoted here. BD+27°1888 was observed in August 1995 by Tom Fleming with the Steward Observatory 2.3m telescope on Kitt Peak, Arizona (Figure 3.1). I observed RE J0500−362 in April 1996 with the 1.9m telescope at SAAO, South Africa

Table 3.3: Log of IUE observations of the non-WD systems

Name	IUE SWP No.	LWP No.	Date	Exp. (s)	Observer	notes
AG+68 14	52807		1994/319	1800	Burleigh	
2RE J0222+50	56333		1995/358	1800	SO	newsips
2RE J0232−02	56272		1995/340	1800	SO	newsips
		31800	1995/340	1800	SO	newsips
CD−44 1025	56046		1995/274	900	Burleigh	newsips
	56047		1995/274	900	SO	newsips
		31570	1995/274	35	SO	newsips
HR1249	49792		1994/008	2400	Burleigh	
SAO150508	56195		1995/317	1800	SO	newsips
		31700	1995/317	1200	SO	newsips
HD36869	56196		1995/317	1800	SO	newsips
		31701	1995/317	360	SO	newsips
Gl216	56194		1995/317	1800	SO	newsips
		31699	1995/317	120	SO	newsips
HR2225	56206		1995/319	1800	SO	newsips
		31715	1995/319	60	SO	newsips
HR2468	52802		1994/318	1800	Burleigh	
HD295290	56211		1995/322	1800	SO	newsips
		31726	1995/322	1200	SO	new., 159DN
BD−00°1462	38355		1990/072	5400	Simon	
	52801		1994/318	1800	Burleigh	
HD54402	56193		1995/317	1800	SO	newsips
		31698	1995/317	300	SO	newsips
SAO135659	56273		1995/340	1800	SO	newsips
		31801	1995/340	1200	SO	newsips
HD70907	56344		1995/359	1800	SO	newsips
		31836	1995/359	300	SO	newsips
RE J0823−25[1]	56266		1995/338	1800	SO	newsips
		31796	1995/338	300	SO	newsips
HR4646	56393		1996/009	100	SO	newsips
HD166435	55658		1995/264	3600	Burleigh	

SO= Service Observation
1] V≈11 companion to HD70907
159DN=159DN problem (see text)

(Figure 3.3). These data have been used to help identify the spectral type of the normal star in each system. There is no available optical data for HD2133. Table 3.4 lists the parameters of the normal (main sequence and evolved) stars in the white dwarf binaries. In most cases, the distances have been calculated from the spectral types. The distances to HD18131, RE

J0357+28 and HD27483 are taken from the quoted references in the table.

Table 3.5 lists some of the properties of the stars observed where no white dwarf was detected. Optical observations from a variety of authors are summarized in section 3.6.3.

Table 3.4: Physical parameters of the normal stars in the binaries

RE No.	Cat. Name	SpT	V	d est. (pc)	references
RE J0024−74	HD2133	F8V	9.7	146	SIMBAD
RE J0254−05	HD18131	K0IV	7.32	67	Vennes *et al.* (1995)
RE J0357+28		K2V	11.7	>107	Jeffries *et al.* (1996)
RE J0420+13	HD27483	F6V	6.17	47.6	Böhm-Vitense (1993)
RE J0500−36		F5-G0	13.7	800−1150	SIMBAD
RE J1024+26	BD+27°1888	A8V-F2V	9.1	185−218	SIMBAD
RE J1027+32		G0V-G4V	13.0	380−550	Genova *et al.* (1995)
RE J1925−56		G2-G8	10.6	95−160	Barstow *et al.* (1994a)

Table 3.5: Physical parameters of the stars observed where no white dwarf was detected

RE No.	Cat. Name	Spectral type	V magnitude	references
2RE J0014+69	AG+68 14	F8	10.3	SIMBAD
2RE J0222+50	BD+49°646	?	10.1	SIMBAD
2RE J0232−02		K	14.8	SIMBAD
RE J0312−44	CD−44 1025	F3V+A8V	5.93	SIMBAD
RE J0402−00	HR1249	F6V	5.38	SIMBAD
2RE J0530−19	SAO150508	G5V	9.0	SIMBAD
2RE J0534−15	HD36869	G2V	8.0	SIMBAD
2RE J0544−22	Gl216B	K2V	6.15	SIMBAD
RE J0613−23	HR2225	G5V	6.39	SIMBAD
RE J0637−61	HR2468	G1.5V	6.18	SIMBAD
2RE J0640−03	HD295290	G0	9.1	SIMBAD
RE J0650−00	BD−00°1462	F2V	5.77	SIMBAD
2RE J0710+45	HD54402	K0	7.7	SIMBAD
2RE J0813−07	SAO135659	K0	8.8	SIMBAD
RE J0823−25	HD70907	F3IV/V	8.8	SIMBAD
		late	11	Mason *et al.* (1995)
2RE J1212+77	HR4646	A5m	5.14	SIMBAD
RE J1809+29	HD166435	G0	6.84	SIMBAD

3.4 Data Reduction

The majority of the far-UV spectra were obtained at IUE Vilspa. The standard IUESIPS extraction was used in the Starlink program *IUEDR* (Rees *et al.* 1994), with the addition of the following: a white dwarf based absolute calibration including an effective area correction (Finley 1993), and a correction for the degradation of the detector with time (Bohlin & Grillmair 1988). Garhart (1992) used more recent IUE images to confirm that the degradation of the SWP camera sensitivity remained linear with time.

In 1995 first Goddard, and then from October 1995 Vilspa, began using the NEWSIPS calibration which incorporates these corrections. The NEWSIPS calibrated data is indicated in Tables 3.2 and 3.3. Multiple exposures were obtained for HD2133, RE J1027+322, BD+27°1888 and the 'non-detection' CD−44 1025, and co-added before analysis by weighting each data set according to the relative exposure times.

3.5 Analysis

3.5.1 White dwarf model atmospheres

The spectra of all H-rich DAs contain strong absorption lines due to the transitions of a single electron between the energy levels. The Balmer lines lie in the optical region, but in IUE far-UV spectra only the single Lyman α line is covered. The strengths of the lines depends on the number density of atoms in which the electron is in the energy level from which the particular absorption line transition occurs, and this in turn depends on the temperature and density of the gas. The lines can be broadened by the doppler effect, due to the motion of the gas, and by the extreme pressure, and sometimes by other effects such as a magnetic field. The Balmer lines become weaker at higher temperatures, because more of the hydrogen becomes highly ionized, and broader at higher gravities, because of the increased pressure. At cooler temperatures the Balmer lines vanish (e.g. in DC and DZ white dwarfs, see Table 1.1), because in this regime there are few collisions of sufficient energy to promote the electrons to the n=2 level, from which the Balmer series arises. By comparing model spectra with the shape of the observed lines, it becomes possible to determine the star's temperature and surface gravity.

Two or more lines are required to give a unique, unambiguous solution, and each additional line reduces the uncertainties in the measured parameters, since the T and log g determine the relative populations of atoms with electrons in different levels, and hence the shapes and relative strengths of the Balmer lines themselves.

In this chapter, the observed UV data are compared with synthetic spectra for grids of fully line blanketed LTE (local thermodynamic equilibrium) homogeneously mixed model atmospheres (Table 5.6), spanning a temperature range from 20,000K to 100,000K and log g=7.0 to 9.0, supplied by Detlev Koester (e.g. Koester 1991). Alternative stratified structures are also available, covering the same temperature and gravity range. These assume plane parellel geometry with a thin H layer overlying a helium atmosphere, also under LTE conditions. The models are assumed to be pure H.

In LTE, Saha-Boltzmann statistics are used to describe the populations of the different energy levels in the atoms. Departures from LTE only occur if the effect of the radiation field becomes important; for example, in the outer layers of a star's atmosphere. Here, the occupation numbers are determined mainly by the radiative rates, and the state of the material is only weakly coupled to local conditions (e.g. temperature and density). The excitation and ionisation state of the gas is strongly influenced by the radiation field, and full statistical equilibrium calculations must be done to accuratly describe the atmosphere. In white dwarfs, however, the density is so high that departures from LTE only become significant at high temperatures ($T>10^5$K, Barstow 1990). The white dwarfs in the ROSAT sample are all in the range where errors due to LTE will be very small, although in high resolution optical spectra non-LTE (NLTE) emission cores are sometimes seen in the H_α absorption line.

It is not entirely clear which structure is the more appropriate for hot H-rich (DA) white dwarfs (e.g. see discussion in Marsh 1995a, and chapter 1). Evry Schatzmann proposed as long ago as 1958 that the high surface gravities of hot white dwarfs would cause heavy elements to quickly sink out of the photosphere, leaving a hydrogen layer at the surface (Schatzman 1958). Analysis of a number of stars since then lends support to the stratified hypothesis. For example, if the soft X-ray spectrum of the hot DA G191−B2B is modelled with a homogeneous atmosphere, then a significant HeII line is predicted to lie in the optical region at 4686Å, and this just isn't seen (Koester 1991). The single channel evolution hypothesis also requires that DA white dwarfs

have stratified atmospheres, with a thin (10^{-15} $M_\odot$<M_H<10^{-8} $M_\odot$) H layer overlying a helium envelope. On the other hand, Bergeron *et al.* (1994) has shown that the hybrid H/He DAO white dwarfs can only be modelled with homogeneous atmospheres (see Chapter 4).

3.5.2 White dwarf binaries - UV data

The IUE data can be used to estimate the temperature and gravity of the white dwarf by fitting the observed Lyman α profile and the uncontaminated UV continuum to the synthetic white dwarf spectra described above. Since, in this analysis, both the stratified and homogeneous models are assumed to be in the limit of zero He/H or large H layer mass M_H, they give essentially the same results. Therefore, only the results for the homogeneous structures have been reproduced here (Table 5.7) so that, in a later analysis of the ROSAT data points (section 3.5.3, below), the helium content of each star could be estimated (Table 3.8). Obviously in binary systems like these, there is no possibility of fitting the Balmer line profiles in the optical region for measurement of T and log g. Unfortunately, the Lyman α information alone can give somewhat ambiguous results (two or more absorption lines need to be fitted simultaneously to give an unambiguous determination of T and log g, see Chapter 1). For example, fitting the IUE SWP spectrum of the almost pure H hot white dwarf HZ43 yields T=57,500K for log g=8.5, whereas fitting the Balmer lines gives a lower T and log g of 49,000±2000K and 7.7±0.2 (Napiwotzki *et al.* 1993).

The spectral fitting is conducted with the programme XSPEC (Schafer *et al.* 1991). XSPEC works by folding a predicted model spectrum through an instrument response function, and comparing it with the observed data (the count spectrum). A chi-squared statistic is calculated for the fit between the data and the model, and this is then minimised by adjusting the free model parameters in incremental steps until the best representation of the count spectrum is achieved. A mathematical description of this technique is given by Lampton, Margon & Bowyer (1976).

In this analysis, I fit the Lyman α profile and the region of the UV continuum which is uncontaminated by the primary star. Grids of models are determined for each star by stepping through values of log g, and finding the best fit temperature and normalisation $[(R_\star/d)^2]$ at each point. Although the slope of the continuum is related to the temperature of the star, it contains

no information about the surface gravity. By fixing log g in the fit we are thus constraining the width of Lyman α, and reducing the errors in the temperature determination.

Only in BD+27°1888 and HD27483 is there significant contamination from the companion in the SWP spectrum (Figures 3.4 and 3.8). For BD+27°1888, comparison with stars of similar spectral type (A8V-F2V) from the IUE archive shows that the flux is significantly greater than that of the white dwarf at $\approx$ 1800Å but is effectively zero at 1500Å. Thus for BD+27°1888 the UV continuum up to 1500Å is fitted. Similarly, the UV continuum of HD27483 (F6V companion) is modelled up to 1600Å. There might also be a small amount of contamination in the SWP from the primary in HD2133 (Figure 3.2). From an IUE LWP spectrum (LWP31757) the spectral type of this star appears to be closest to F7V−F8V. Comparison with example spectra from the IUE archive shows that there will be a contribution from a companion of this type of a few % of the white dwarf flux at 1800Å, but none at 1600Å. Therefore, the UV continuum up to 1600Å is utilised.

In the IUESIPS data sets, the Lyman α profile is sometimes significantly contaminated by geocoronal radiation, and only the outer wings can be used. This geocoronal line is removed during the calibration process in the NEWSIPS data sets. However, there are significant differences in the fits to BD+27°1888 from the NEWSIPS and the IUESIPS data. This problem is discussed in more detail later.

There is no need to take into account any interstellar component in the fits to the Lyman α profile, because for low columns this will be negligible, and for columns of a few $\times 10^{19}$ the contribution is still lower than the typical uncertainties in the observed fluxes (between $\approx$ 5−10%). For columns greater than a few $\times$ 10^{19} the white dwarf is unlikely to be detected in EUV surveys.

The errors on the flux values are derived using the general scatter from a smooth curve passing through the SWP spectrum, since our own calibrations, unlike the NEWSIPS data, do not have an absolute error calculated for each individual data point. When the two differently calibrated data sets have been merged together, the absolute errors on the NEWSIPS data can be used to estimate the error on the co-added data. Typically, the flux errors are of the order 5-10%.

Once a best model fit to the data has been achieved, it is possible to estimate the uncertainty

in the temperature by considering the variation in χ^2 as this parameter is stepped in small increments away from the best fit value. The other free parameter (the normalisation) is allowed to vary so that the new value of χ^2 is a minimum. Lampton, Margon & Bowyer (1976) showed that for a best fit model with p free parameters and a minimum chi squared ${\chi^2}_m$, then if the parameter is to be known to a confidence C it must lie within a region of parameter space bounded by $\chi^2={\chi^2}_m+\delta\chi^2$. The values of $\delta\chi^2$ for different values of p and C are given in Table 3.6. Thus, in practice, once a confidence level has been defined, each free parameter is incremented in turn and a fit made until the value of χ^2 increases by the relevant value of $\delta\chi^2$ given in Table 3.6. This is taken to be the error range for that parameter, and can be visualised as a process of finding the edges of a confidence region. If the confidence region for a model with two free parameters x and y is plotted on a graph, it is characteristically shaped like an ellipse with the best fit values at the centre. To know the parameters to the specified confidence level, they must lie within the ellipse.

The appropriate value of $\delta\chi^2$ depends on the number of 'interesting' parameters, or in other words the number of variables in the model which can significantly affect the quality of the fit. In this case there are two 'interesting' unknown parameters, the temperature and the normalisation $[(R_\star/d)^2]$. Thus, for a 90% confidence limit, the required value of $\delta\chi^2$ was 4.61 (see Table 3.6).

Table 3.6: $\delta\chi^2$ as a function of confidence level and degrees of freedom

Confidence C	p=1	p=2	p=3	p=4	p=5	p=6
68.3% (1.00σ)	1.00	2.30	3.53	4.72	5.89	7.04
90.0% (1.60σ)	2.71	4.61	6.25	7.78	9.24	10.6
99.0% (2.60σ)	6.63	9.21	11.3	13.3	15.1	16.8
99.7% (3.00σ)	9.00	11.8	14.2	16.3	18.2	20.1

The radii and masses were calculated using the evolutionary models of Wood (1995) for carbon core white dwarfs with thick ($10^{-4}\,M_\odot$) H layers, in the range $0.4-1.2\,M_\odot$. Where necessary the models were extrapolated below the $0.4\,M_\odot$ grid limit. However, it should be noted that, in reality, stars with masses lower than $\approx 0.4\,M_\odot$ would have helium cores, and in addition they could not have formed as a result of single star evolution alone.

The calculated radii are used to estimate the distance from the normalisation parameter $[(R_\star/d)^2]$.

The distances to the primaries in each case are estimated from their spectral type and V magnitude, and given in Table 3.5. The V magnitude of each white dwarf is estimated from the model flux at 5500Å. These results are all given in Table 3.7.

3.5.3 White dwarf binaries - ROSAT data

Once the temperature and gravity of each star has been determined, the ROSAT EUV and soft X-ray fluxes can give an indication of the level of photospheric opacity in the white dwarf, by comparing them with predicted values for a pure H atmosphere (e.g. Barstow *et al.* 1993c). The ROSAT data is fitted independently from the IUE data since contamination from elements heavier than H and He only has a significant effect at EUV and soft X-ray wavelengths. The data from the two WFC filters is fitted simultaneously with the integrated count rate in the $0.1-0.28$keV PSPC band, within which all white dwarf soft X-ray flux is expected to lie. It is possible that some EUV and X-ray emission might originate from the main sequence star in these binaries, and so the PSPC count rates at energies above 0.4keV are noted in Table 3.1 as an indication of an active companion.

The errors on the ROSAT count rates in Table 3.1 are 1σ statistical values. Systematic errors associated with the absolute photometric calibration of the instrument are also taken into account. The largest errors arise from the uncertainty in the reference standards used. These were proportional counters, whose quantum efficiency can be theoretically calculated. These give a 1σ error of 10%, which is added in quadrature to the statistical error on the count rate before analysis.

Once again, the set of fully line blanketed homogeneous LTE H+He models, computed by Koester (1991), is fitted to the ROSAT data. The models assume a homogeneous distribution of H+He, under LTE conditions, in the range $-8<\log \mathrm{He/H}<-3$. Homogeneous models have been chosen for this analysis of optically hidden white dwarfs in order to give an indication of the helium content of each star.

A number of variables can determine the predicted EUV/X-ray fluxes in the model - T, log g, $[(R_\star/d)^2]$, He/H ratio and HI, HeI and HeII columns. The ROSAT fluxes depend only weakly on log g, but can depend strongly on T, column density and the He/H ratio. Marsh (1995a)

shows that the fluxes increase sharply from 20,000−30,000K, and then linearly up to 100,000K. Interstellar matter can heavily attenuate the EUV flux. The S2 band is affected the most, due to the energy dependence of the photometric cross section of the interstellar medium below the Lyman limit. An HI column of only 10^{18} atoms cm^{-2} can reduce the S2 flux by 10%. A column of 10^{19} atoms cm^{-2} more than halves the S2 count rate. In homogeneous models, the presence of helium affects the S2 band the most, due to the HeII absorption edge at 228Å increasing in strength with increasing He abundance. However, it should be remembered that the presence of heavy elements at temperatures >40,000K can also severely affect the emergent EUV and, in particular, soft X-ray fluxes.

A valid chi-squared analysis of the fit to the ROSAT data points requires the number of degrees of freedom, ν (number of data points minus number of free parameters), to be greater than or equal to one. Since only three independent data points are modelled, other information is needed to specify some of the parameters. Therefore, the T, log g and $[(R_\star/d)^2]$, determined from the fit to the UV data are used and frozen during the fit. This time, however, the He/H ratio is allowed to vary. The reasonable assumption is made that the local ISM is not highly ionised (therefore, there is negligible HeII absorption) and that the HeI/H ratio is cosmic. Thus the HI column can be estimated, using the standard WABS (Wisconsin Absorber) model in XSPEC (Morrison & McCammon 1993).

In using this technique the χ^2 minimum is often ill-defined. In this study, I consider a good fit to the data to correspond to the probability that a particular value of the reduced χ^2 ($\chi_r{}^2=\chi^2/\nu$) can occur by chance to be 0.1 or greater (i.e. 90% confidence), and a bad fit 0.01 or less (99% confidence). The fits in between may not be very good, but cannot be ruled out with high confidence. For ν=1, as in this analysis, then a good fit requires $\chi_r{}^2$ to be less than 2.71, but until the value of $\chi_r{}^2$ exceeds 6.63 a model cannot be excluded with any certainty. Therefore, all model fits to the ROSAT data for which $\chi_r{}^2$ is less than 6.63 are noted. Table 3.8 gives the HI column densities and He/H ratios for the homogeneous fits to the ROSAT data.

Table 3.7: Temperatures and gravities for the white dwarfs from homogeneous model fits

Binary	log g	Temp K	90% error K	Mass $M_\odot$	Radius $R_\odot$	d $_{wd}$ (pc)	Estimated V
New discoveries							
HD2133	7.0	24,490	24,160-24,870	0.37	0.032	234	15.4
	7.5	26,420	26,100-26,810	0.42	0.019	165	15.6
	7.75	26,780	26,510-27,270	0.52	0.016	139	15.6
	8.0	28,260	27,910-28,630	0.65	0.013	132	15.7
	8.25	**28,700**	**28,350-29,050**	**0.79**	**0.011**	**112**	**15.7**
	8.5	29,900	29,560-30,400	0.95	0.009	100	15.8
	9.0	31,650	31,240-32,260	1.20	0.006	68	15.9
RE J0357+28	7.0	27,330	27,050-27,640	0.37	0.032	185	14.6
	7.5	29,460	29,130-29,820	0.43	0.019	130	14.8
	7.9	**30,960**	**30,620-31,410**	**0.60**	**0.014**	**105**	**14.9**
	8.0	31,340	30,940-31,760	0.65	0.013	100	14.9
	8.5	33,430	32,950-33,950	0.95	0.009	75	14.9
	9.0	35,840	35,240-36,540	1.20	0.005	51	15.0
RE J0500−36	7.0	37,800	33,800-41,200	0.38	0.032	1080	17.8
	7.5	**42,000**	**36,400-45,700**	**0.47**	**0.020**	**740**	**17.9**
	8.0	45,000	40,500-50,500	0.68	0.014	530	17.9
	8.5	50,500	45,400-57,700	0.97	0.009	390	18.0
	9.0	60,500	51,900-67,500	1.21	0.006	270	18.1
BD+27°1888	7.0	33,180	32,340-34,380	0.38	0.032	242	14.8
	7.25	**34,130**	**33,330-35,780**	**0.39**	**0.025**	**193**	**14.8**
	7.5	35,370	34,530-37,300	0.45	0.020	162	14.9
	8.0	38,420	37,330-40,870	0.67	0.014	120	14.9
	8.5	42,470	41,050-45,690	0.96	0.009	89	15.0
	9.0	47,640	45,800-51,790	1.21	0.005	61	15.1
RE J1027+32	7.0	30,560	29,560-32,600	0.37	0.032	589	16.9
	7.25	32,265	30,760-33,500	0.39	0.025	487	16.9
	7.5	**32,440**	**31,570-34,450**	**0.44**	**0.020**	**388**	**16.9**
	8.0	34,000	33,400-36,460	0.66	0.013	288	17.0
	8.5	37,020	35,620-38,650	0.96	0.009	216	17.1
	9.0	39,240	37,910-41,380	1.20	0.005	144	17.2
Previous discoveries							
HD18131	7.0	26,440	26,170-26,740	0.37	0.032	126	13.9
	7.5	29,290	28,650-29,640	0.43	0.019	93	14.1
	8.0	**31,130**	**30,750-31,540**	**0.65**	**0.013**	**72**	**14.2**
	8.5	32,980	32,530-33,470	0.95	0.009	53	14.2
	9.0	35,050	34,500-35,640	1.20	0.005	36	14.3
HD27483	7.0	20,000	upper limit	0.37	0.032	128	14.4
	7.5	20,000	upper limit	0.40	0.019	74	14.4
	8.0	21,210	21,040-21,380	0.63	0.013	60	14.5
	8.5	**22,000**	**21,960-22,040**	**0.94**	**0.009**	**45**	**14.6**
	9.0	24,280	24,110-24,470	1.20	0.006	35	14.9
RE J1925−56	7.0	29,590	29,030-30,870	0.37	0.032	172	14.3
	7.25	**30,820**	**30,240-31,800**	**0.39**	**0.025**	**141**	**14.4**
	7.5	31,675	31,040-32,640	0.44	0.020	118	14.4
	8.0	33,500	32,770-34,500	0.65	0.013	88	14.5
	8.5	35,400	34,570-36,490	0.95	0.009	64	14.5
	9.0	37,700	36,720-38,790	1.20	0.006	43	14.6

Bold type indicates the WD model that best agrees with the distance estimate to the normal star companion

Table 3.8: He/H ratios and column densities from homogeneous models

Name	log g	T	He/H	HI column	$\chi_r{}^2$	Comment
New discoveries						
HD2133	7.0	24,490	-	-	19.2	No Fit
	7.5	26,420	1×10^{-8}	0.0	2.71	
	7.75	26,780	1.35×10^{-7}	0.0	0.79	
	8.0	28,260	1.29×10^{-5}	1.58×10^{18}	0.54	
	8.25	**28,700**	$\mathbf{3.00\times10^{-5}}$	**0.0**	**0.63**	
	8.5	29,900	5.89×10^{-5}	0.0	1.56	
	9.0	31,460	-	-	8.44	No Fit
RE J0357+283	7.0	27,330	-	-	22.9	No Fit
	7.5	29,460	-	-	11.4	No Fit
	7.9	**30,960**	$\mathbf{6.67\times10^{-5}}$	$\mathbf{2.10\times10^{19}}$	**4.27**	
	8.0	31,340	6.90×10^{-5}	2.27×10^{19}	3.16	
	8.5	33,430	7.33×10^{-5}	1.92×10^{19}	2.08	
	9.0	35,840	6.91×10^{-5}	1.02×10^{19}	2.42	
RE J0500−362	7.0	37,800	1×10^{-8}	5.55×10^{18}	1.88	
	7.5	**42,000**	$\mathbf{1.78\times10^{-5}}$	$\mathbf{1.09\times10^{19}}$	**1.14**	
	8.0	45,000	5.37×10^{-5}	1.23×10^{19}	1.24	
	8.5	50,500	6.92×10^{-4}	0.0	0.29	
	9.0	60,500	5.62×10^{-3}	0.0	4.82	
BD+27°1888	7.0	33,180	-	-	17.5	No Fit
	7.25	**34,130**	$\mathbf{9.8\times10^{-7}}$	$\mathbf{3.31\times10^{19}}$	**3.28**	
	7.5	35,370	1×10^{-8}	4.79×10^{19}	3.87	
	8.0	38,420	1×10^{-8}	7.25×10^{19}	6.27	
	8.5	42,470	-	-	22.7	No Fit
	9.0	47,640	-	-	31.0	No Fit
RE J1027+323	7.0	30,560	1.0×10^{-8}	2.86×10^{18}	5.85	
	7.25	32,265	9.55×10^{-7}	8.24×10^{18}	3.31	
	7.5	**32,440**	$\mathbf{4.78\times10^{-7}}$	$\mathbf{1.05\times10^{19}}$	**2.38**	
	8.0	34,000	1.0×10^{-8}	1.66×10^{19}	1.25	
	8.5	37,020	2.51×10^{-4}	0.0	2.04	
	9.0	39,240	5.75×10^{-4}	0.0	3.24	
Previous discoveries						
HD18131	7.0	26,440	-	-	17.0	No Fit
	7.5	29,290	1×10^{-8}	1.17×10^{19}	1.61	
	8.0	**31,130**	$\mathbf{3.63\times10^{-5}}$	$\mathbf{7.20\times10^{18}}$	**1.17**	
	8.5	32,980	2.29×10^{-4}	0.0	3.64	
	9.0	35,050	4.90×10^{-3}	0.0	2.31	
HD27483	7.0	20,000	-	-	46.4	No Fit
	7.5	20,000	-	-	24.8	No Fit
	8.0	21,210	-	-	144.0	No Fit
	8.5	**22,000**	**-**	**-**	**25.44**	**No Fit**
	9.0	24,280	-	-	43.9	No Fit
RE J1925−566	7.0	29,590	-	-	162	No Fit
	7.25	**30,820**	**-**	**-**	**134**	**No Fit**
	7.5	31,675	-	-	118	No Fit
	8.0	33,500	-	-	96	No Fit
	8.5	35,400	-	-	80	No Fit
	9.0	37,700	-	-	60	No Fit

Bold type indicates the WD model that best agrees with the distance estimate to the normal star companion

3.5.4 Non-detections and active stars

Emission features (e.g. CIV 1549Å and CII 1335Å) were detected in the IUE SWP spectra of a number of targets where no white dwarf was seen. Emission lines were also observed in the cores of the MgII 2798Å lines of a number of stars in IUE LWP spectra. A search through the recent literature showed that other observers had also detected evidence for activity in these stars at optical wavelengths. The UV, EUV and soft X-ray data for these stars is analysed here.

The line fluxes of the emission features were measured using a simple Gaussian profile, fitted to each line, after the continuum has first been subtracted (the continuum flux is represented by a low degree polynomial). The measured line fluxes have been compared with those of two known active stars, HD39587(χ^1 Ori, G0V) and HD126660(θ Boo, F7V), also detected by the ROSAT WFC. Low resolution SWP spectra for these stars exist in the IUE archive, and the line fluxes (Table 3.9) have been published by Ayres et al. (1995).

Estimates of the ratio L_{EUV}/L_{bol} have also been made as an indicator of the level of activity. The method outlined by Jeffries (1995) has been followed here. The S2 count rate is converted into a flux (f_{EUV}) in the 0.1−0.28 keV PSPC band using a uniform conversion rate of 1.5×10^{-10} erg cm^{-2} count^{-1}, assuming an effective coronal temperature of (5-10)$\times10^6$K. The bolometric luminosity m_{bol} of each star is determined using the bolometric corrections given in Allen (1964). L_{EUV}/L_{bol} can then be calculated using equation (1) of Jeffries (1995). These ratios are valid assuming neutral hydrogen column densities less than $\sim10^{19}$cm^{-2}. As all four active stars lie within a few tens of parsecs of the Sun, this is a reasonable assumption.

Some of the active stars (e.g. CD−44 1025, HR1249, HR2468 and BD−00°1462) were also detected by the PSPC in both the soft (S, 0.1−0.4keV) and hard (H, 0.4−2.4keV) bands. Therefore, L_x and L_x/L_{bol} have also been calculated from the total PSPC count rate, using the hardness ratio (H−S/H+S) and the flux conversion factor given by Fleming *et al.* (1995). I have also calculated L_x/L_{bol} for the companion star in the WD binary HD18131, which was detected in the PSPC hard band where no flux is expected from the WD. A flux conversion factor for the hard band alone is also given by Fleming *et al.* (1995).

The L_{EUV}/L_{bol} and L_x/L_{bol} ratios are presented in Table 3.10, with estimates of L_{EUV} and L_x.

Table 3.9: Line fluxes for the active stars with emission features observed in IUE SWP spectra

Name	CII* 1335Å	SiIV* 1397Å	CIV* 1549Å	HeII* 1640Å
HD39587^{+}	4.02±0.12	4.01± 0.14	5.15±0.14	2.50±0.11
HD126660^{+}	6.21±0.5	4.74±0.34	10.4±0.62	2.91±0.5
CD−44 1025	-	-	4.40±0.67	1.35±0.40
HR1249	1.83±0.24	3.67±0.43	4.11±0.35	0.75±0.21
HR2468	1.26±0.22	-	2.89±0.4	1.26±0.29
BD−00°1462	-	-	1.82±0.34	-

* $\times 10^{-13}$ ergs/cm^2/sec
$^{+}$ comparison star (see text)
† possible feature

Table 3.10: EUV and X-ray luminosities for the probable and confirmed active stars

Name	d(pc)	L_{EUV} $\times 10^{29}$ ergs	L_{EUV}/L_{bol} $\times 10^{-5}$	L_x $\times 10^{29}$ ergs	L_x/L_{bol} $\times 10^{-5}$
HD39587^{+}	11	0.8	1.2	1.9	3.0
HD126660^{+}	12	0.9	0.8	2.9	2.8
CD−44 1025(F3V)	37	6.6	3.8	16.7	9.6
CD−44 1025(A8V)	51	12.6	3.5	31.7	8.8
HR1249	23	3.9	3.5	7.9	7.1
SAO150508	59	10.0	36.1	1.3	47.1
Gl216A	8	0.3	0.4	0.2	0.2
Gl216B	8	0.3	2.8	0.2	1.6
HR2225	18	2.0	7.1	2.0	7.0
HR2468	23	3.0	5.5	10.9	19.7
HD295290	95	51.8	82.2	51.5	81.7
BD−00°1462	36	6.0†	3.1†	3.8	2.0
SAO135659	34	11.4	91.6	4.5	3.8

* $\times 10^{-13}$ ergs/cm^2/sec
$^{+}$ comparison star (see text)
† upper limits

3.6 Discussion

3.6.1 White dwarf binaries - new discoveries

HD2133

HD2133 (Figure 3.2) is listed as a V=9.7 F7V star in the SIMBAD database. If these parameters are correct, it lies at a distance of $\approx$ 160 parsecs. If the white dwarf is associated with HD2133, then the best fit T and log g from the UV data are 26,420$\pm$500K and 7.50 respectively (see Table 3.7). However, a fit to the ROSAT data points with these parameters yields a negligible column. In fact in this direction (l=305°, b=-43°) and for a distance of $\approx$ 160 parsecs, a HI column density of $\sim 10^{19} \mathrm{cm}^{-2}$ should be expected (Diamond, Jewell & Ponman 1995).

In the absence of optical data, an IUE LWP spectrum (LWP31757) of the main sequence star can be used to estimate its spectral type by comparing it with standard F stars in the IUE archives. Unfortunately, no match could be found in the database. Therefore, the quoted V magnitude of this star maybe inaccurate. HD2133 would appear to be closest in flux level and spectral shape to an F8V. However, a good match to an F8V standard can only be achieved if V$\approx$9.2. This would place the star $\sim$115pc away.

At that distance, the best fit pure-H white dwarf model is log g=8.25, T$\approx$28,700K and M=0.79M$_\odot$. A corresponding fit to the ROSAT data (Table 3.8) gives an essentially pure H atmospheric composition, but there is still a negligible hydrogen column density. Clearly, accurate optical spectroscopy and photometry is needed to better constrain the parameters of this system.

RE J0357+283

Jeffries, Burleigh & Robb (1996) concluded that the rapidly rotating K2 dwarf star located at the centre of the ROSAT source RE J0357+283 error box would have to be the most active star in the galaxy to account for all the EUV and soft X-ray flux detected by the WFC. Instead, the authors predicted that a hidden white dwarf was responsible for the EUV emission and they estimated, from the faint excess short wavelength flux in an IUE LWP spectrum, that any degenerate companion must have a temperature between 30,000$-$40,000K, log g=7.5$-$8.0, and

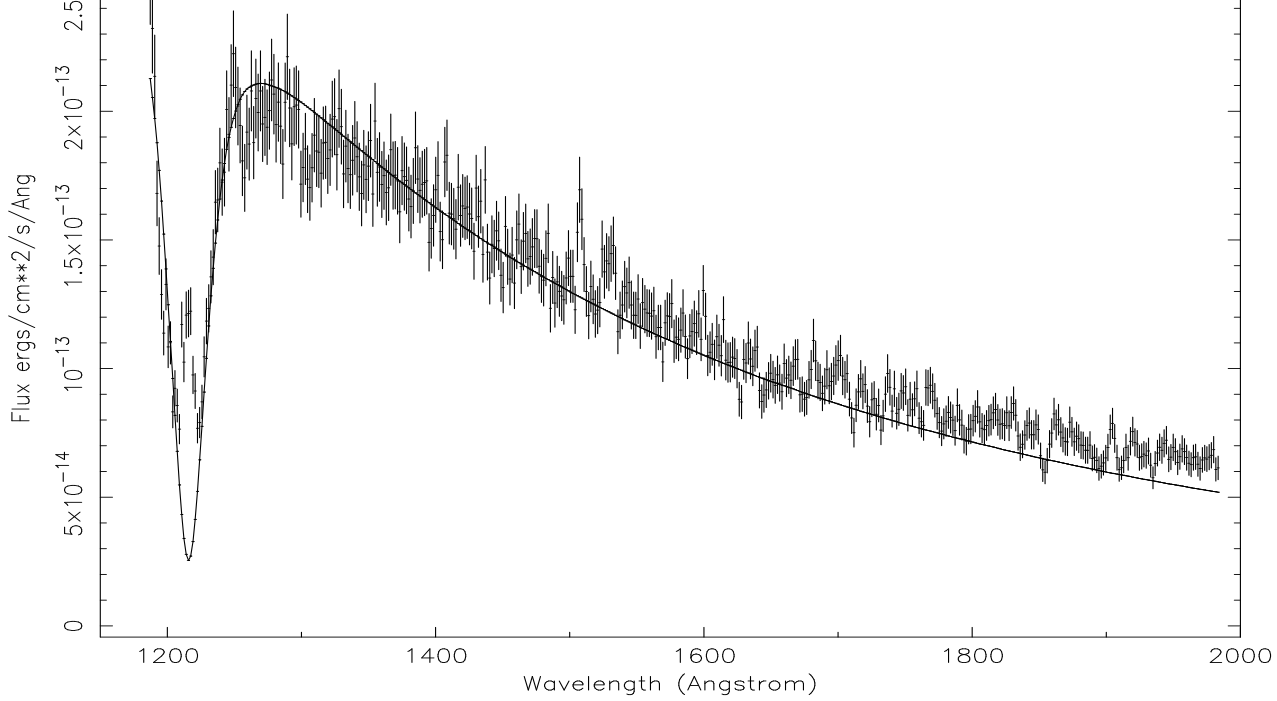

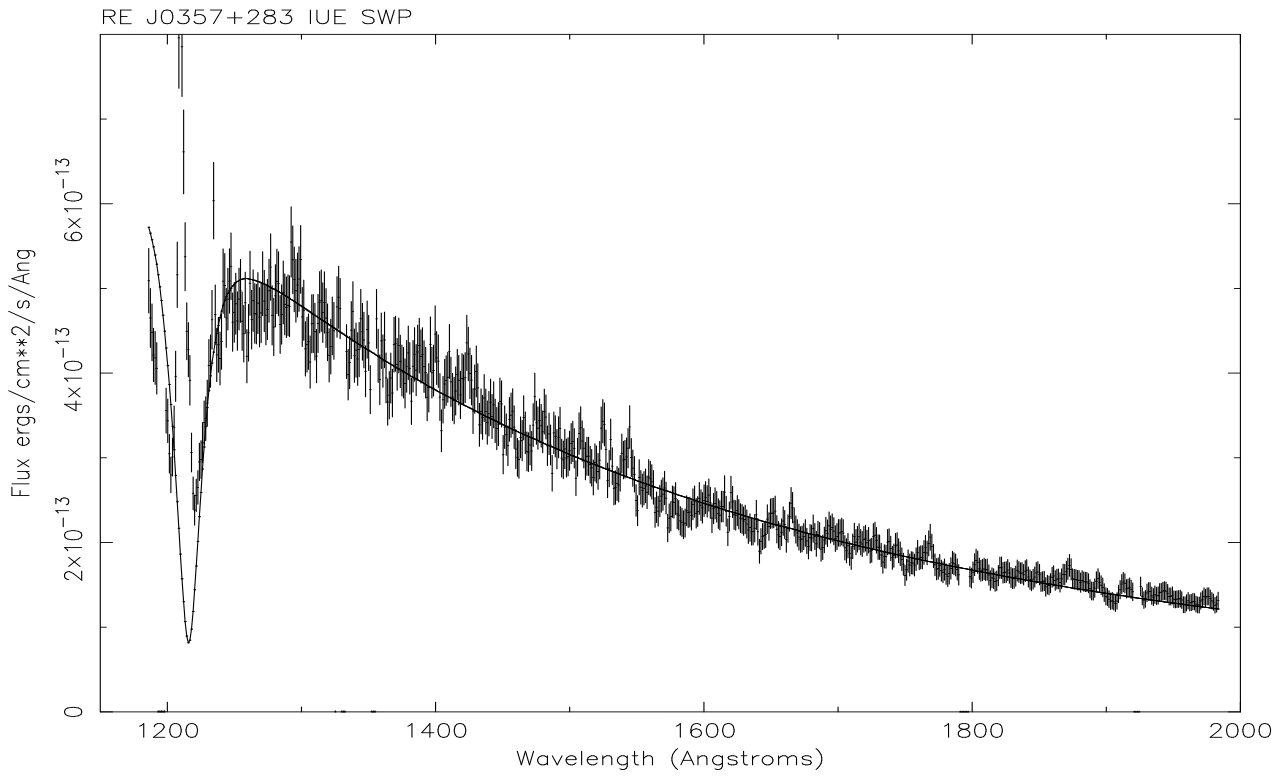

Figure 3.2: Top: Co-added low resolution IUE SWP spectrum of HD2133 (SWP55659+SWP56231) compared to a predicted pure H white dwarf spectrum for log g=8.25 and T=28,700K. Note that there is a small contribution to the flux at the long wavelength end from the F7V-F8V companion. Bottom: Low resolution IUE SWP spectrum of RE J0357+283 (SWP55660), compared to a predicted pure H white dwarf spectrum for log g=7.9 and T=30,960K.

the H column density N_H=(2-6)$\times 10^{19}$, assuming the distance to the system to be 107pc.

An IUE SWP spectrum, obtained in August 1995, confirms this identification (Figure 3.2). If the white dwarf is associated with the K dwarf, then a fit to the UV data for log g=7.9 gives approximately the minimum distance allowed. Fits at higher gravities give distances inconsistent with that of the late-type star. At log g=7.9, the temperature of the white dwarf T=30,960K, and mass=0.6$M_\odot$. Fitting the ROSAT data with these parameters gives N_H=2.1$\times 10^{19}$cm^{-2}, and the He/H ratio $\approx 10^{-8}$. The atmosphere of this star can then be considered to be effectively pure H. The ROSAT data cannot be matched for log g<7.9. This source is not detected in the PSPC hard band, and Jeffries, Burleigh & Robb (1996) argue that the vast majority of the soft X-ray counts must be coming from the white dwarf and cannot be due to the K2V star, which shows no evidence of chromospheric Mg II emission in the IUE LWP spectrum.

This is the second white dwarf/rapidly rotating cool-star wide binary to be discovered. The other, BD+08°102 (RE J0044+093, Barstow *et al.* 1994a, Kellett *et al.* 1995), consists of a K1−3V star with a spin period of ∼10 hrs, and a white dwarf T≈28,700K, log g=8.4 and mass≈0.91$M_\odot$ (distance to the system is about 55pc). The K2V primary in RE J0357+283 has an even faster rotation period of 8.76 hrs. Both Jeffries, Burleigh & Robb (1996) and Kellett *et al.* (1995) find that the binary periods of these two systems are likely to be measured in months or years, so it is unlikely that there was ever common envelope evolution to spin-up the cool stars, as is thought to have happened in the 12.5hr 'pre-CV' K2V/hot white dwarf binary V471 Tau (Nelson & Young 1970). Jeffries & Stevens (1996) provide an alternative model to explain the spin-up in long-period binaries. They show that a significant amount of material and angular momentum can be accreted from the slow, massive wind of an AGB star in a detatched system. In this model final binary separations of up to ∼100AU are allowed. The K2V component of RE J0357+283 also appears to be the first dwarf Barium star to be identified, and as such may be a direct progenitor of the Barium giants. Jeffries & Smalley (1996) have recently reported an excess of barium in the star's spectrum, and a possible excess of carbon. Barium stars, and related objects such as Carbon stars and CH stars, show significant overabundances of certain elements in their spectra, e.g. an overabundance of s-process elements like barium and strontium in Barium giants, and likewise an overabundance of carbon in Carbon stars. It is now believed, and there is much observational evidence to support this theory (e.g. McClure & Wordsworth 1990, McClure 1997, Han *et al.* 1995), that all these objects have low

mass companions, specifically white dwarfs (e.g. Böhm-Vitense 1980). It is thought that the overabundance of these elements is due to accretion from the wind of the white dwarf progenitor. The discovery of the nature of RE J0357+283 now provides strong observational evidence to support this theory.

Interestingly, BD+08°102 is a hard X-ray source (0.201 counts sec^{-1} in the 0.4−2.4keV PSPC band), but RE J0357+283 is not detected at these energies. The columns to the two stars are fairly similar (a few$\times 10^{19}$ atoms cm^{-2}), and so, scaling from the V magnitudes, RE J0357+283 should only be about a factor 4 fainter than BD+08°102 (V=10.16). Yet the 3σ upper limit to the PSPC hard band count rate for RE J0357+283 is just 0.029 counts sec^{-1}, around a factor 2 too low. Given its rapid rotation rate, it is unclear at this stage why RE J0357+283 is not a hard X-ray source.

RE J0500−362

The field of this EUV source was surveyed by Mason *et al.* (1995) during the WFC optical identification programme. No evidence of activity was found in the cores of Ca II H & K in the spectrum of a ∼13th magnitude star located at the centre of the source error box. Various stars were also examined outside the error box, but none proved to be the EUV source. The field was examined again in 1995 by Jay Holberg (private communication) with the 2.3m Steward Observatory telescope on Kitt Peak, as part of a programme to attempt to identify unknown sources in the ROSAT WFC 2RE catalogue (Pye *et al.* 1995). Again, no plausible EUV source was found, but it was suggested that the central star in the error box may be hiding a hot white dwarf companion. Therefore, the star was added to the IUE target list for observations during 1995/96.

A preliminary half hour low resolution exposure (SWP56217) was obtained with IUE in November 1995. This revealed a weak, noisy spectrum of what was undoubtedly an ∼18th magnitude hot white dwarf. A follow-up spectrum, with an 8 hour exposure to achieve the required signal-to-noise, was taken in December 1995 (SWP56338, Figure 3.3).

Figure 3.3 (lower) shows an optical spectrum of the primary, obtained at the 1.9m telescope at SAAO in April 1996. The spectrum is of poor quality, and very noisy, as there was cloud

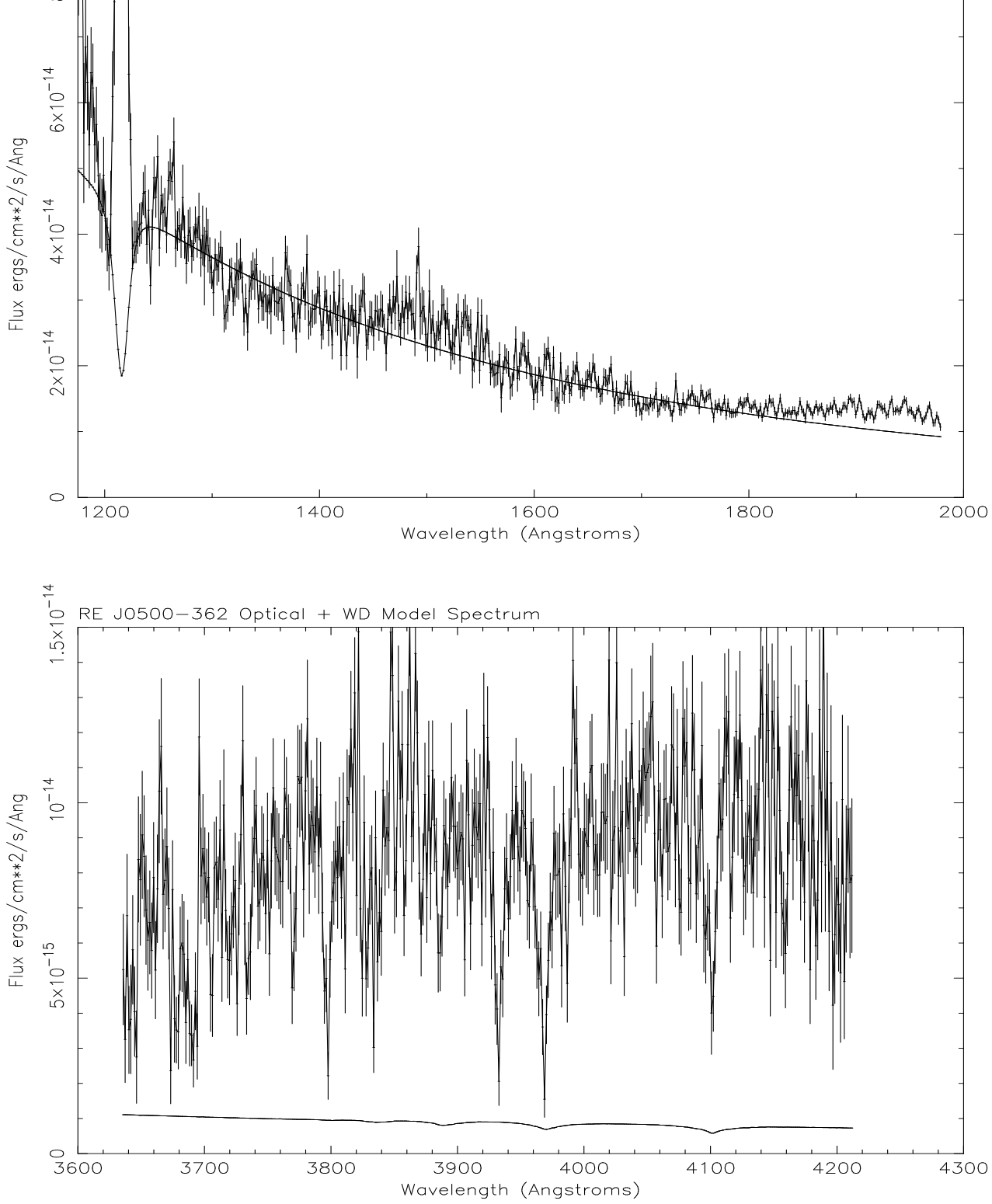

Figure 3.3: Top: Low resolution IUE SWP spectrum of RE J0500−362 (SWP56338) compared to a predicted pure H white dwarf spectrum for log g=7.5 and T=42,000K. Note that there may be a small contribution to the flux at the long wavelength end from the late F companion. Bottom: Optical spectrum of RE J0500−362 (V=13.7, late F), obtained on the 1.9m at SAAO in April 1996, compared to the same white dwarf model spectrum (same T, log g and normalisation) as above.

during the observation. However, from the relative strengths of the Ca II H (3934Å) and the Hϵ (3970Å) lines, this most resembles a late F star. This conclusion is strengthened when the IUE LWP spectrum (LWP31729) is compared to spectra in the IUE Spectral Atlas (Wu *et al.* 1991). Again, the data are very noisy, but most closely match stars in the range F5V−G0V. There also appears to be a slight excess of flux in the IUE SWP spectrum, at wavelengths >1850Å, above the level of the white dwarf model atmosphere. If the excess is real then it must attributable to the primary. As mid-late G and all K stars do not contribute to this region of the spectrum, this also indicates that the companion is probably a late F. Taking the Guide Star Catalogue magnitude of V=13.7, the system lies between 790 (G0V) and 1150 (F5V) parsecs away.

A model fit to the IUE spectrum at log g=7.0 gives T=37,800K and M=0.39 $M_{\odot}$, corresponding to a distance of 1080 parsecs. If the system is closer, then the temperature and gravity are higher. At 740 parsecs away, log g=7.5, T=42,000K and M=0.47 $M_{\odot}$.

There is no soft X-ray emission from this source. The S1 data point cannot be fitted at log g=7.0, but there is a good fit at log g=7.5, giving a hydrogen column density N_H=1.1×10^{19} atoms cm^{-2}. At 740 parsecs distance, this translates into a volume density of only 0.0048 atoms cm^{-3}, well below the average local volume density (0.007 atoms cm^{-3}). Notably, the system (galactic co-ordinates l=239.6°, b=−37.2°) lies in a similar direction to the known exceptionally low column direction towards β CMa (l=226°, b=−14°, Welsh 1991), and in particular to two other ROSAT-discovered hot white dwarfs, RE J0457−281 and RE J0503−289 (l=229.3°, b=36.2°, Barstow *et al.* 1993b).

At V=17.9, this is one of the faintest white dwarfs to be detected in the ROSAT WFC survey. The faintest, RE J0616−649 (V=18.4), is a rare magnetic DA, but there are very few other hot white dwarfs detected fainter than 17th magnitude.

BD+27°1888

The white dwarf companion to BD+27°1888 was discovered with IUE (SWP49780) in January 1994. Initial studies of the white dwarf utilised this spectrum because SWP49779, obtained at the same time, was overexposed in places by as much as a factor of 2. Unfortunately, the hydrogen Lyman α absorption line in SWP49780 has been heavily filled in by geocoronal

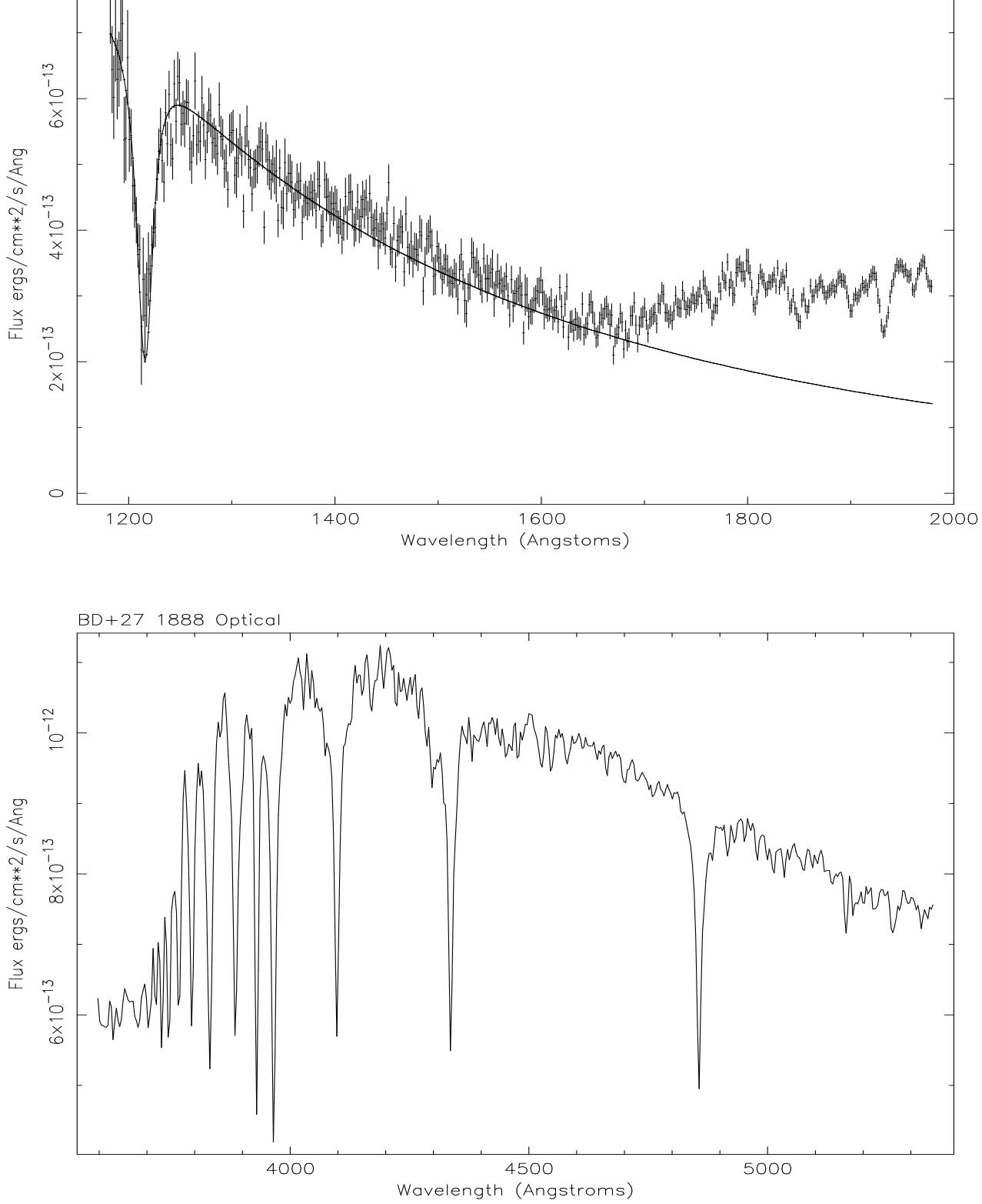

Figure 3.4: Top: Low resolution IUE SWP spectrum of BD+27°1888 (SWP56261) compared to a predicted pure H white dwarf spectrum for log g=7.25 and T=34,130K. Note the contribution to the flux longwards of ∼1600Å from the A8V−F2V companion. Bottom: Optical spectrum of BD+27°1888 (V≈9.1, A8V−F2V), obtained in August 1995 by Tom Fleming with the Steward Observatory 2.3m at Kitt Peak.

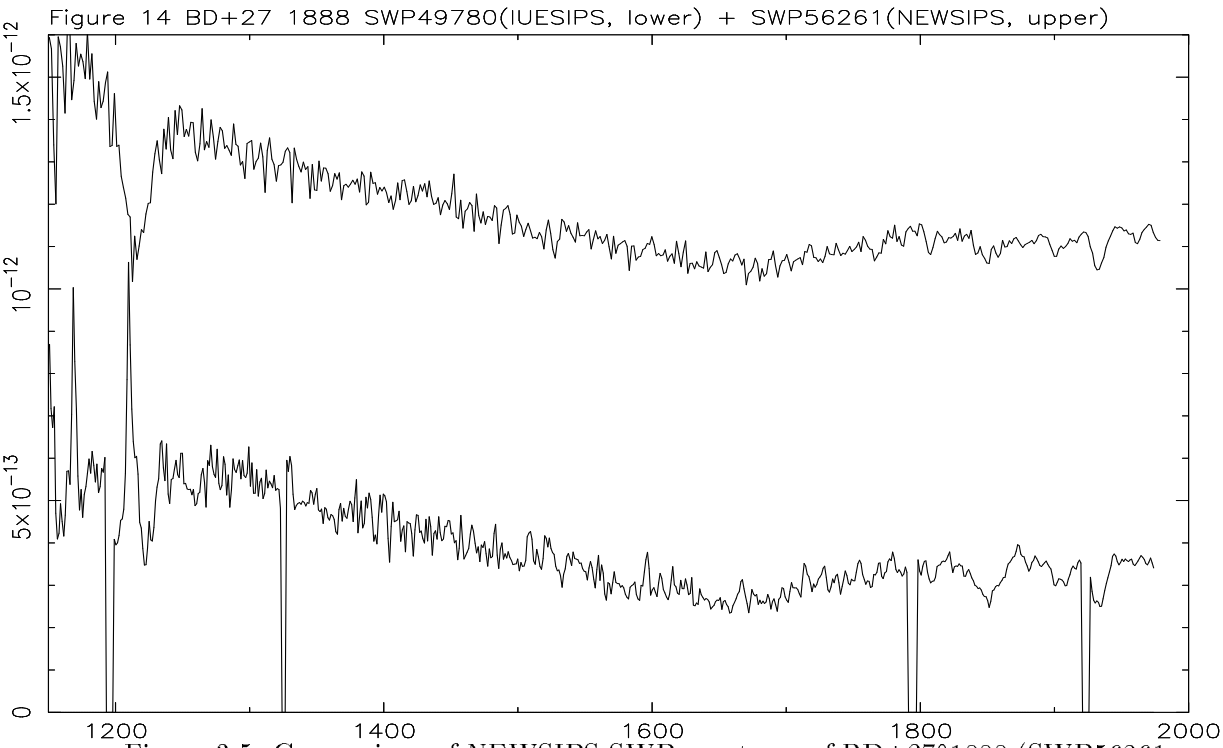

Figure 3.5: Comparison of NEWSIPS SWP spectrum of BD+27°1888 (SWP56261, upper) with the older IUESIPS-extracted SWP49780 (lower). The flux levels are arbitrary. Note the presence of a strong geocoronal Lyman α emission line in SWP49780.

emission, and in addition there is a reseau mark (giving a zero reading across several channels) on one wing, making modelling extremely difficult, so the star was reobserved in the SWP and LWP cameras in November 1995. These two more recent spectra, SWP56261 (Figure 3.4) and LWP31785 (Figure 3.6), were both extracted with the NEWSIPS calibration. In the SWP this largely removes the contamination from the geocoronal Lyman α line, and thus the hydrogen absorption line can be fitted more accurately. In addition there are no zero points due to reseau marks, and the NEWSIPS calibration also provides an absolute error for each individual data point. Figure 3.5 compares the NEWSIPS extracted spectrum with the earlier one, and clearly in the NEWSIPS spectrum there are many more uncontaminated data points to fit in the crucial Lyman α region. From fitting the NEWSIPS data alone, the temperature is found to be higher for each value of log g by ~6000K at the lower end of the gravity range and by ~10,000K at the upper end. Table 3.11 compares the fitted temperatures for both spectra, stepping up through log g.

The differences in the fits between the two spectra are most likely due to the poor quality of

Table 3.11: BD+27°1888: Comparison between the temperatures derived from fitting SWP49780 and SWP56261 (NEWSIPS)

	SWP49780		SWP56261	
log g	Temp	90% Range	Temp	90% Range
7.0	27,620	26,760-29,140	33,180	32,340-34,380
7.5	30,400	29,220-31,470	35,370	34,530-37,300
8.0	31,980	31,000-33,480	38,420	37,330-40,870
8.5	34,390	33,080-35,865	42,470	41,050-45,690
9.0	37,180	35,615-38,740	47,640	45,800-51,790

the SWP49780 spectrum, in which it is necessary to remove, before modelling, a large number of the most vital data points in the Lyman α region. Therefore, rather than attempt to co-add the spectra, only the NEWSIPS calibrated spectrum has been used. The results in Table 3.7 are all derived from this data set.

There is some discrepency between the V magnitude given for the main sequence star in the SIMBAD database (9.6) and the Guide Star Catalogue (GSC, 9.08). Therefore, the V magnitude has been estimated from the optical spectrum (Figure 3.4, lower), and agrees with the GSC value of ≈ 9.1. Unfortunately, there was cloud during the optical observation and so the absolute flux values of the spectrum are not totally reliable. A spectral classification of A8V-F2V is adopted for the primary from this optical spectrum, by comparing it visually with spectra in the atlas of Jacoby, Hunter & Christian (1984), although SIMBAD lists it as a G5. However, it is clear from Figure 3.4 that there is considerable flux from this star in the IUE SWP spectrum, where a G5 would not be seen. The LWP spectrum (LWP31785) can be matched to stars of known spectral type in the IUE database to try to get a better constraint on the classification. From this method the star appears to be closest in shape and flux to an A8V (Figure 3.6). From a quick glance through an atlas of optical spectra (e.g. Jacoby, Hunter & Christian 1984) it is immediately apparant that the differences in spectral shape between late A type stars and early Fs is very subtle. However, Figure 3.6 shows that at UV wavelengths the difference in flux level from one subclass to the next is substantial. In Figure 3.6 the LWP spectrum is compared with examples of F2V and A8V spectra from the archive, each scaled for the differences in V magnitude, and BD+27°1888 most closely resembles an A8V.

If the primary is in the range of spectral types A8-F2V and assuming V=9.1, it lies between 185-

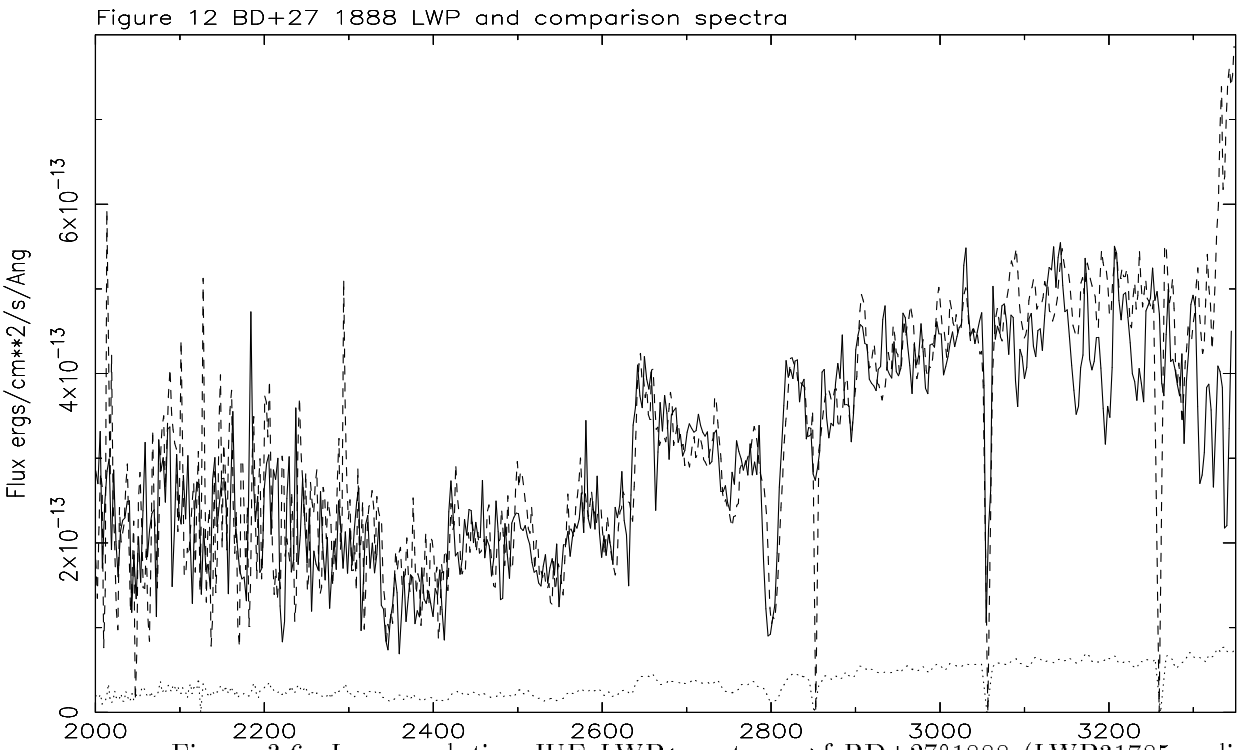

Figure 3.6: Low resolution IUE LWP spectrum of BD+27°1888 (LWP31785, solid line) and comparison spectra - HD28910 (LWP27455, A8V, dashed line) and HD29875 (LWP20865, F2V, dotted line), scaled for differences in magnitude (assuming V=9.1 for BD+27°1888).

218 parsecs away. The closest model fit is for a white dwarf at about that distance is T=34,000K, log g=7.25, and M=0.39$M_{\odot}$. This mass estimate is surprisingly low, given that if this is a true binary then the white dwarf must have evolved from a progenitor more massive than an A8V, and would suggest that the star has lost mass in the past, possibly during a common envelope stage. However, it is easy to over-interpret these results, particularly given the difficulties in fitting IUE data unambiguously and the large error in log g ($\pm$0.25). Fitting the ROSAT data with these parameters gives a pure H atmosphere and a column of 3.3×10^{19}cm^{-2}. The entire spectrum of BD+27°1888, from the far-UV to the optical, was displayed earlier in this chapter in Figure 3.1.

RE J1027+322

The discovery of this WD+MS binary was first reported by Genova *et al.* (1995). The authors studied the entire field of the ROSAT/EUVE source, and concluded that although it was more likely that the white dwarf was the sole source of the EUV flux, there may be a contribution

from a QSO in the field. Genova *et al.* (1995) used only a single spectrum, SWP49778, originally obtained by myself at the IUE ground station at Vilspa, Madrid, in January 1994. Subsequently, two further exposures were obtained (SWP49793 and SWP54501) and co-added together with SWP49778 to give the results presented here. This higher signal-to-noise data allows better constraints to be put on the white dwarf parameters. An intense emission feature is seen in SWP49778 at 1700Å, but there are no known strong emission features at this wavelength. Genova *et al.* (1995) consider that it may well be spurious, and it is not seen in either SWP49793, taken $\approx$ 48hrs later, or in SWP54501. This emission feature is almost certainly due to a cosmic ray hit on the detector plate.

Genova *et al.* (1995) estimate the spectral type of the main sequence star to be G2($\pm$2)V, and that it lies at a distance of 380$-$550pc. If the white dwarf is indeed associated with this star, then, from a fit to the IUE data, it must have a surface gravity log g of 7.0$-$7.5 and a temperature of around 30$-$33,000K. However, a good fit to the ROSAT data can only be achieved at log g=7.5 or higher, although fits at log g=7.0 and 7.25 cannot be completely excluded. At log g=7.5, T=32,440K, M=0.44M$_\odot$, the column density N_H=1.05$\times$10^{19}cm^{-2}, and the atmosphere can be assumed to be essentially pure H.

3.6.2 Previously discovered white dwarf binaries

HD18131

Vennes *et al.* (1995) first reported the discovery of this binary, classifying HD18131 as K0IV, and concluded that together with the white dwarf it forms a physical pair at a distance of 70$-$90pc. Based on the IUE and EUVE data sets, Vennes *et al.* (1995) give the white dwarf parameters as T$\approx$30,000K and log g$\approx$7.5, and the interstellar column density as $\sim$10^{19}cm^{-2}. However, the PSPC count rates were not available to Vennes *et al.* (1995), so they have been included here (Table 3.1). The same technique has been adopted for analysing the IUE and ROSAT data as in the other binaries in this chapter. Vennes *et al.* (1995) give the spectral type of the companion as K0IV.

At a distance of 70pc, the best fit white dwarf parameters (from the IUE data) are T=31,130K, log g=8.0 and mass=0.65M$_\odot$ (see Table 3.7), giving an age for the white dwarf of $\sim$10 mil-

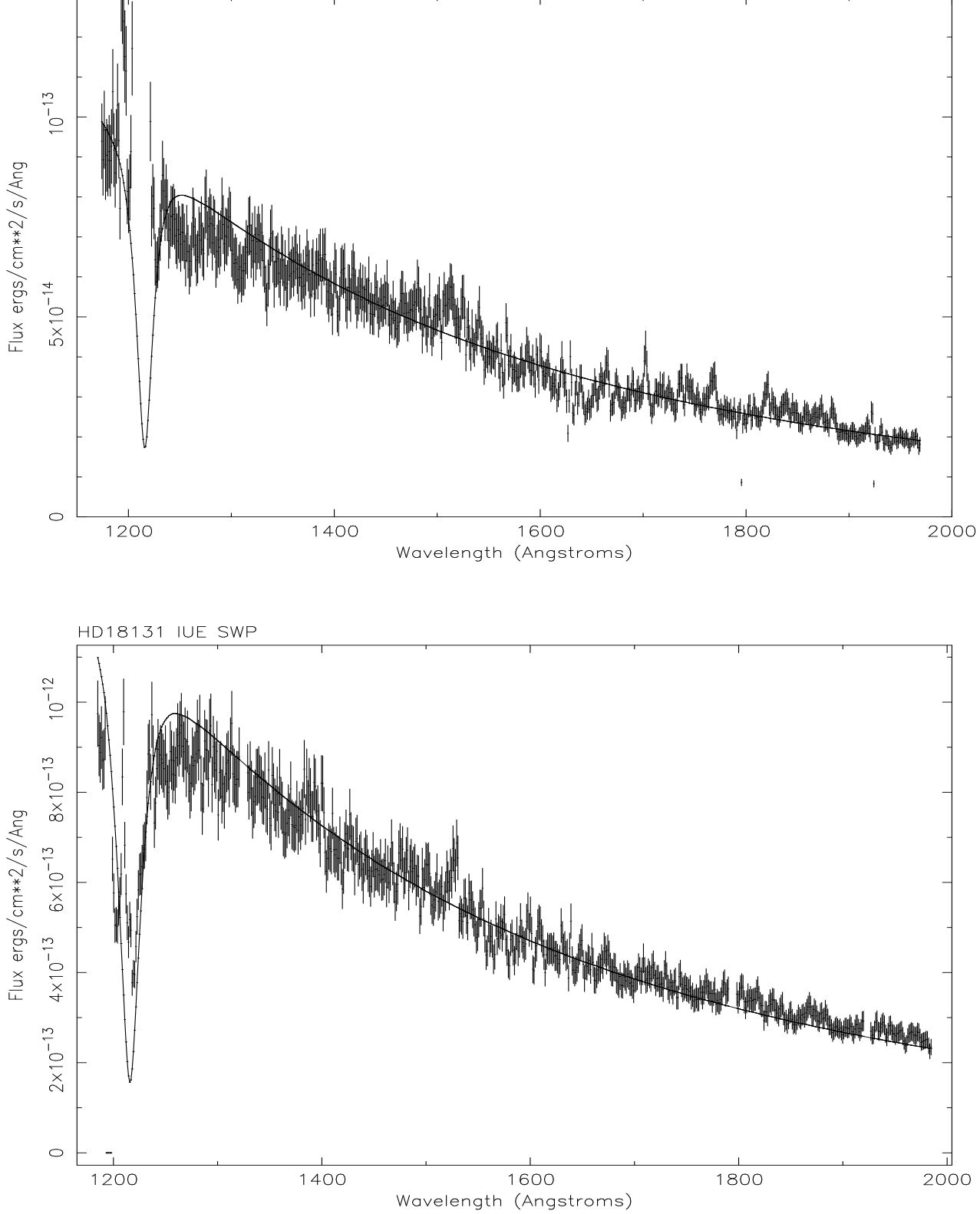

Figure 3.7: Top: Low resolution IUE LWP spectrum of RE J1027+322 (SWP49778+SWP49730) compared to a predicted pure H white dwarf spectrum for log g=7.5 and T=32,440K. Bottom: Low resolution IUE LWP spectrum of RE J1027+322 (SWP52158) compared to a predicted pure H white dwarf spectrum for log g=8.0 and T=31,130K.

lion years. If the pair were further away at a distance of ~90pc, log g=7.5, T=29,290K and mass=0.43$M_{\odot}$, and the white dwarf is slightly younger at 7 million years. However, for log g $\geq$8.0 the temperatures given in Table 3.7 are considerably lower than those measured by Vennes *et al.* (1995) (e.g. for log g=9.0 we find T≈35,000K but Vennes *et al.* (1995) give T≈44,000K). These differences merely reflect the problems in deriving atmospheric parameters for white dwarfs from IUE data alone. The Lyman α absorption line in the SWP spectrum of HD18131 is partly filled-in by geocornal emission (see Figure 3.7, lower) and, as discussed previously (e.g. for BD+27°1888), this can influence the values of the parameters measured by fitting this line. In addition, a careful comparison at the short wavelength end of the spectrum between Vennes *et al.* (1995)'s calibration and our own shows that there is a small difference of ~10% in the flux level at 1300Å. This may be attributable to the different method used by Vennes *et al.* (1995) to correct for the temporal degradation in detector sensitivity. They utilised an archival spectrum of the hot DA G191−B2B, a method that involves assuming appropriate atmospheric parameters for that star, whereas the correction of Bohlin and Grillmair (1988) has been used here.

Only the PSPC lower band count rate (262±36 counts/ks) is included in the analysis of the ROSAT data set, assuming initially that just the white dwarf is responsible for this flux. Good fits can only be achieved for log g=7.5 and 8.0 (see Table 3.8). At log g=8.0, the He/H ratio is $\approx 4\times10^{-5}$ (i.e. virtually pure hydrogen) and the interstellar hydrogen column is 7.2×10^{18}cm^{-2}, in agreement with Vennes *et al.* (1995). This is the only binary in the sample in this paper that has a detection in the 0.4−2.4keV hard band of the PSPC (52±16 counts/ks). Since no flux from the white dwarf is expected in this band, this soft X-ray flux must be coming from the evolved K0 companion, confirming Vennes *et al.* (1995) 's conclusion that the star is active. Although no CaII H & K emission cores were seen in the optical spectrum of HD18131, the IUE LWP spectrum reveals Mg II emission. From the hard band count rate alone, the L_x/L_{bol} ratio is 1.4×10^{-5}, and the X-ray luminosity $L_x\approx3\times10^{29}$erg s^{-1} (assuming d=70pc).

Could there be a contribution from the late type star to the PSPC soft band flux? For example the white dwarf in the binary system HD217411 (Barstow *et al.* 1994a) has a roughly similar best fit temperature (≈35,600K) and gravity (log g=8.2) to HD18131. The hard band count rate for this source is also similar (56±15 counts/ks), but there is a higher soft band rate (442±38 counts/ks). The authors found they could not fit the ROSAT data with the parameters

determined from a fit to the IUE data. They concluded that the G5 companion in this sytem is probably coronally active and contaminating the soft PSPC band.

In HD18131 the soft band flux can be fitted well without needing to account for a contribution from the primary. However, if the reasonable assumption is made that there is as much flux from the K0 subgiant below the carbon edge as there is above, then by subtracting this contribution ($\sim$50 counts/ksec), it is found that the ROSAT data points can only be matched for log g>8.0. This would set an upper limit distance to the system of $\sim$70 parsecs.

HD27483

The Hyades system HD27483 consists of two F6V stars orbiting each other with a period of 3.05 days. Although it was detected as an EUV source during the ROSAT WFC all sky survey in 1990, the hot white dwarf in the HD27483 system was identified independently and serendipitously by Böhm-Vitense (1993) during an IUE SWP observation as part of a survey of Hyades F stars. Böhm-Vitense (1993) derived atmospheric parameters for the white dwarf of 23000$\pm$1000K and M=0.6 $M_{\odot}$. Unfortunately, the author utilised the out-dated, unblanketed models of Wesemael *et al.* (1980) (which do not depend on log g) to fit the far-UV spectrum at just two points.

The ROSAT WFC source RE J0420+138 was listed in the original Bright Source Catalogue (Pounds *et al.* 1993), with a count rate of 15.0$\pm$4.0 counts 1000s^{-1} (it was not detected in S2), but was not subsequently detected in the reprocessed 2RE survey (Pye *et al.* 1995). The significance of the S1 detection in the 2RE survey was 4.2; sources had to exceed a significance of 5.5 in a combination of both bands to be included in the catalogue. Even so, at 23,000K it is not obvious that the white dwarf is contributing anything to this small EUV flux. Therefore, I extracted the SWP spectrum (SWP45940) from the IUE archive and analysed it in an identical fashion to the other white dwarfs in this chapter, in order to determine whether the white dwarf was indeed an EUV source, and should be included in the sample of ROSAT white dwarf binaries.

The spectrum (Figure 3.8) has not been reprocessed with NEWSIPS. There is significant contamination at the long wavelength end from the two F6V star companions, but this falls to zero by 1600Å. Therefore, the continuum flux was fitted up to this point. Since this system lies

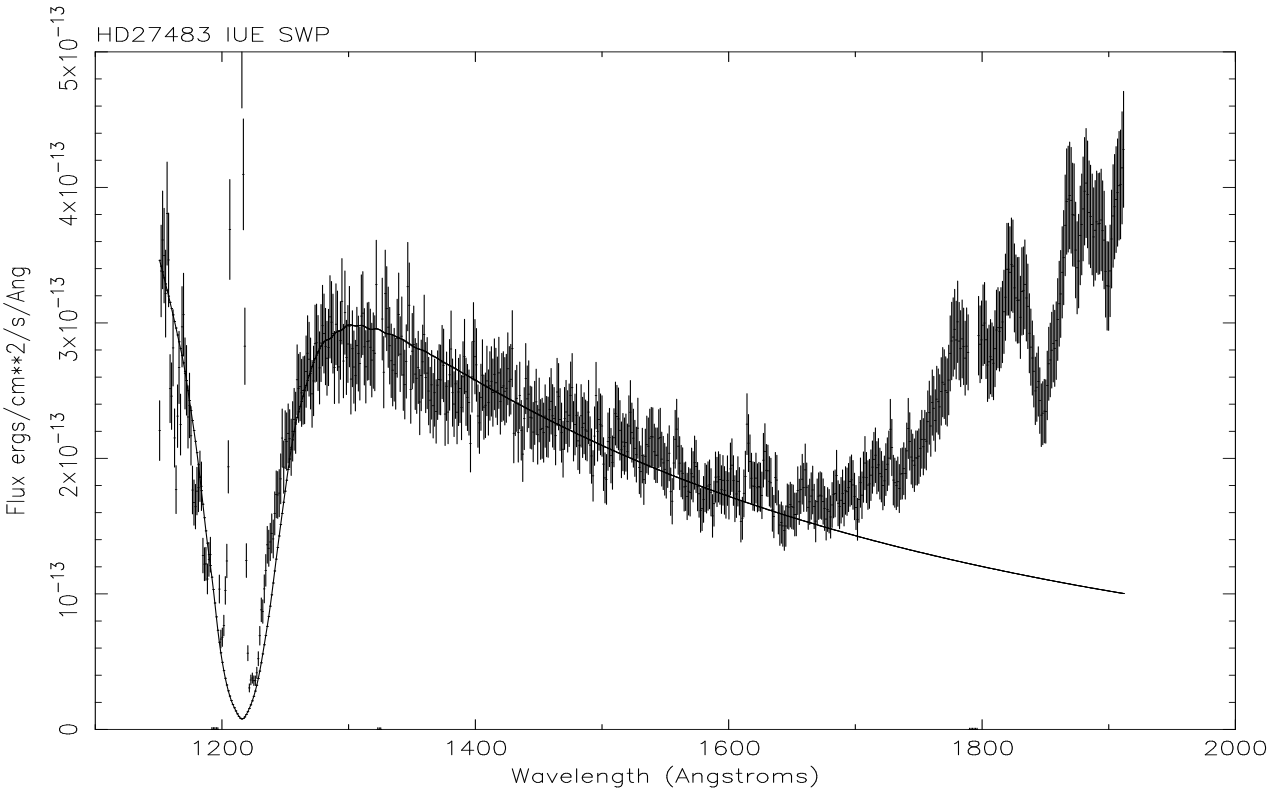

Figure 3.8: Low resolution IUE SWP spectrum of HD27483 (SWP45940) compared to a predicted pure H white dwarf spectrum for log g=8.5 and T=22,000K. Note the presence of the F6V companion longwards of ∼1600Å.

in the Hyades cluster, its distance is well constrained, and Böhm-Vitense (1993)'s estimate of 47.6 parsecs is adopted here. At that distance, the best fit model is T=22,000K, log g=8.5 and M=0.94 $M_{\odot}$. The white dwarf age is 2.35×10^{7} years, in comparison with the known age of the Hyades cluster, 7×10^{8} years (Böhm-Vitense 1993). The white dwarf progenitor must have been 6.765×10^{8} years old when it expelled its envelope.

The WFC source is coincident with a ROSAT PSPC X-ray source, with a total count rate of 1306 ± 198 counts ks^{-1}, including a detection in the upper band. This indicates that at least one of the two F6V companion stars must be active. The ROSAT data points cannot be matched with any of the white dwarf models. As no heavy element contamination is expected in this cool temperature regime, the active star must be contributing to the EUV flux, and it is even possible that there is no flux at all from the white dwarf at these wavelengths. The contribution of the white dwarf to the S1 count rate can, however, be estimated. Another hot WD+MS binary, V471

Tauri (Nelson & Young 1970), is detected by ROSAT in the Hyades cluster. From modelling the WFC count rates, after subtracting the contribution from the active K2V companion, Marsh *et al.* (1997b) find the H column density to this system is 8.52×10^{18} atoms cm^{-2}. Adopting the same column density to HD27483, assuming a pure H atmosphere, and using the parameters derived from the log g=8.5 model, the white dwarf is found to contribute 5.3 counts ks^{-1} to the S1 flux, and can be regarded as a real EUV source.

RE J1925−566

This binary was originally studied by Barstow *et al.* (1994a). The soft X-ray count rate (5.987±0.307 counts s^{-1}) was not available to the authors at the time, and so the system is re-analysed here.

The spectral type of the primary is not well determined. Comparisons of a spectrum taken with the 1.9m telescope at SAAO in April 1996 (Figure 3.9, lower) with stars in the catalogue of Jacoby, Hunter & Christian (1984) constrain it to be between G2−G8. Assuming it is a main sequence star leads to a distance estimate of 95−160 parsecs.

Two of the model fits to the white dwarf (Figure 3.9, upper) give distances within the range for the primary (at log g=7.5 and 7.25, Table 7). Interestingly, both models result in a low mass for the white dwarf ($0.44\,M_\odot$ and $0.39\,M_\odot$ respectively), suggesting that it may have lost mass in the past.

The ROSAT data points cannot be matched with either of these white dwarf models, or with any other higher gravity fits. Barstow *et al.* (1994a) found that, for any given model, the observed S1 count rate was always higher than expected. This result is confirmed here, and, in addition, the observed soft X-ray count rate is also always higher than predicted. This suggets that the companion star must be intrinsically active and contributing significantly to the ROSAT count rates. Although the system is barely detected in the PSPC upper band, there are large emission reversals in the cores of the Ca II H & K lines in the optical spectrum (Figure 3.9, lower), confirming that the primary is indeed active.

Extrapolating the IUE model fits into the EUV region shows that at most the white dwarf

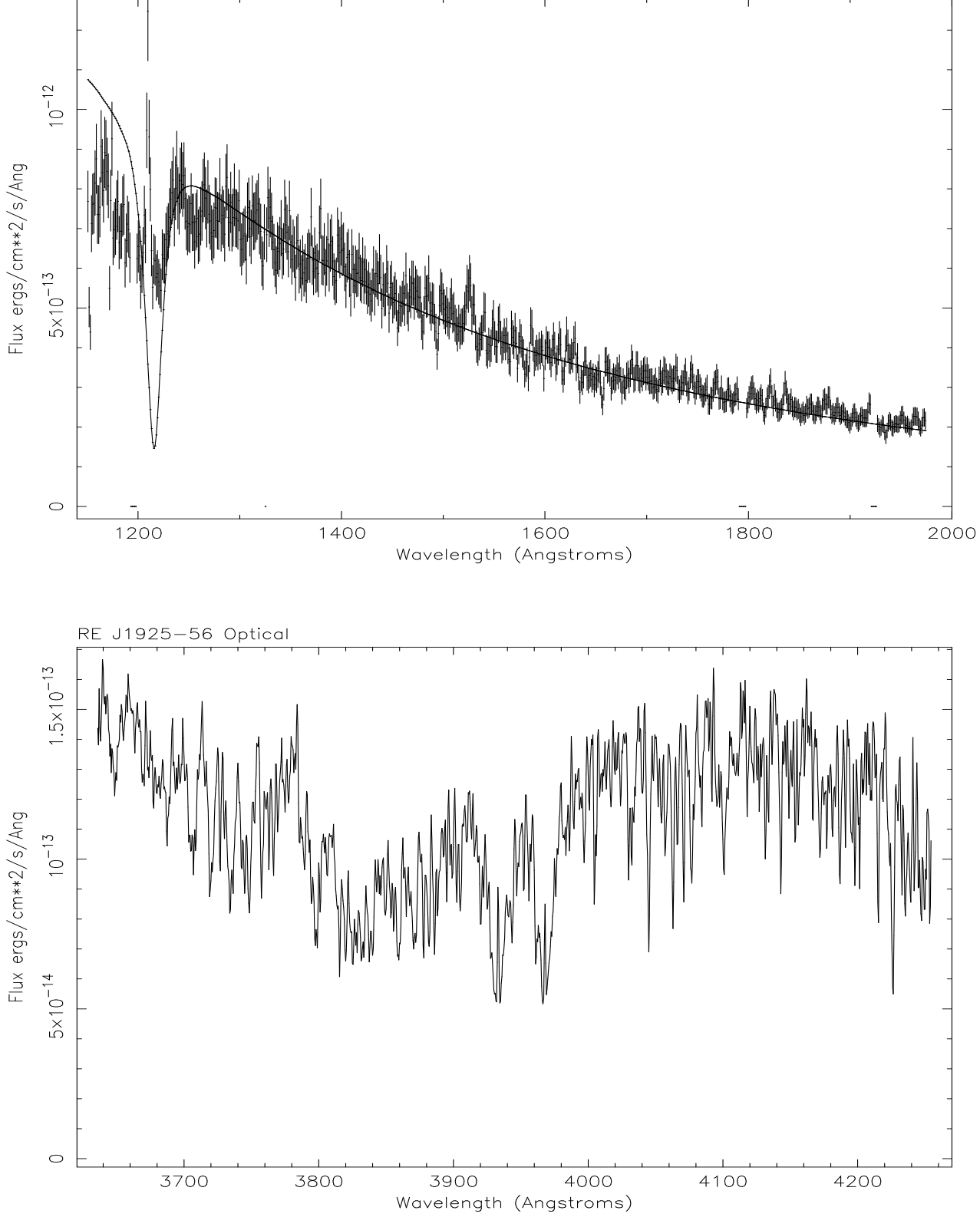

Figure 3.9: Top: Low resolution IUE SWP spectrum of RE J1925−566 (SWP49048) compared to a predicted pure H white dwarf spectrum for log g=7.25 and T=30,820K. Bottom: Co-added optical spectrum of RE J1925−566 (G2-8) taken in April 1996 on the 1.9m at SAAO. Note the emission cores in Ca II H & K.

contributes only 20% of the observed S1 flux in both the log g=7.5 and log g=8.0 models, and only 10% to the PSPC soft band count rate. If we assume, then, that 90% of the X-ray flux originates from the companion, we can estimate its X-ray luminosity. Using the method of Fleming *et al.* (1995) described earlier (section 3.5.4), the X-ray flux from the G star is 1.7×10^{-11} ergs/sec. Assuming the star is a dwarf, then I derive an X-ray luminosity $L_x=1.8\times10^{31}$ for a G2V spectral type, and $L_x=5.2\times10^{31}$ if the companion is a G8V. The corresponding L_x/L_{bol} ratios are 1.1×10^{-2} and 1.0×10^{-2} respectively. This would make the star spectacularly active! In fact, the widely held belief is that coronal emission saturates at a level of $L_x/L_{bol}\approx10^{-3}$.

In RE J0357+283 (see earlier this section) a similar problem existed initially, in that the observed EUV and soft X-ray fluxes seemed to indicate that the star must be the most coronally active object in the Galaxy. In that case, a hot white dwarf companion was later found to account for virtually all the observed EUV and soft X-ray flux. In the RE J1925−566 system, however, the hot white dwarf companion is not bright enough or hot enough, whichever model fit to the IUE data is chosen to be correct, to account for 90% of the X-ray flux. This leaves us with a problem: either this is by far and away the most active star ever seen, or another solution needs to be found. Perhaps there is another object in the field contributing to the ROSAT count rates, or perhaps the system is much closer than currently suspected (which would decrease the intrinsic X-ray luminosity of the companion). It should be emphasised that the G star companion has yet to be studied in sufficient detail for it to be assigned a reliable spectral and luminosity classification, and thus further observations and studies of this remarkable system are urgently required.

3.6.3 Non-detections

AG+68 14

This V=10.3 star, listed in SIMBAD as an F8, was observed as the potential counterpart to the 2RE EUV source 0014+691. It was selected as a possible white dwarf binary on the basis that it is a very soft EUV source. No flux was observed above the background in the UV spectrum (SWP52807), except at the very long wavelength end where a small contribution could be expected from a late F star. There is, therefore, no hot white dwarf companion to this star, and in the absence of any emission features in the far UV, and the non-detection of the source by the PSPC, it is probably not active. The field of this star needs re-examining in the optical to find the true EUV source.

BD+49°646 (2RE J0222+50)

BD+49°646 was chosen as a possible white dwarf binary since, at V=10.1, it is unlikely to be active enough to be detected in the EUV. The unclassified star was only observed by the SWP camera (SWP56333), and there was no flux visible above the background. If BD+49°646 is a G or K star, then clearly it would not be detect it in this waveband anyway. No emission features are visible in the UV spectrum, but the EUV source is coincident with a ROSAT PSPC hard X-ray source, and the possibility remains that BD+49°646 is an active star. At the very least, it must be observed in the optical at high resolution around Ca II H & K to search for any other evidence of activity.

2RE J0232−02

As with the WD+MS binary RE J0500−362 (discussed above), the field of this WFC source was originally observed in 1995 by Jay Holberg (private communication) with the 2.3m Steward Observatory telescope at Kitt Peak. Jay suggested that, in the absence of any plausible EUV source, then the 15th magnitude G-type central star in the error box may be hiding a hot white dwarf companion. The far-UV spectra obtained with IUE (SWP56272 and LWP31800) were very noisy and showed no evidence for a hot white dwarf. There was some flux above the

background longwards of ∼2700Å in the LWP spectrum, which may have been due to a G star, but it is possible that the target was missed altogether, and this flux was due to scattered solar light which effects the LWP camera sporadically. At V=14.8 this star is not itself bright enough to be the source of the EUV flux, and the ROSAT field needs re-examining.

CD−44 1025

This star is a PSPC X-ray source with a detection in the hard band (575±41 cs^{-1}). Early references (e.g. Malaroda 1973) claim it is a spectroscopic binary (F3V+A8V). The 2RE catalogue lists it as an F7III. Mason *et al.* (1995) observed the star during the WFC identification programme. They saw a CaII H 3933Å chromospheric emission line with an equivalent width ≈0.1Å, and noted that this emission core is variable in strength. They only class the star as an F type.

Two SWP spectra (SWP56046 and SWP56047) were taken consecutively in October 1995 with 15 minute exposures and co-added to improve the signal/noise (Figure 3.10, lower). Emission lines of CIV 1549Å and HeII 1640Å are visible; measurements of these lines are presented in Table 3.9, where they are compared with similar lines in low resolution IUE SWP spectra of HD126660 (F7V) and HD39587 (G0V), two known active stars in the WFC catalogue (RE J1425+515 and RE J0554+201).

In an attempt to obtain a better spectral classification, the IUE LWP spectrum (LWP31570) was matched to stars of known spectral type in the IUE archives. Figure 3.10 (upper) shows that at these UV wavelengths the star is closest in flux level and shape to an A8V. However, below ∼2800Å the flux levels are not quite matched and this could be an indication that this is indeed a binary. Measurements of the EUV and X-ray luminosities are given in Table 3.10, assuming the spectral type to be (a) F3V and (b) A8V.

HR1249

Until its discovery as an EUV source in the WFC survey, HR1249 (RE J0402−001) was not known to be active. However, it is detected in the 0.4−2.4keV band of the PSPC, and further evidence of activity was observed optically by Mason *et al.* (1995) during the WFC source

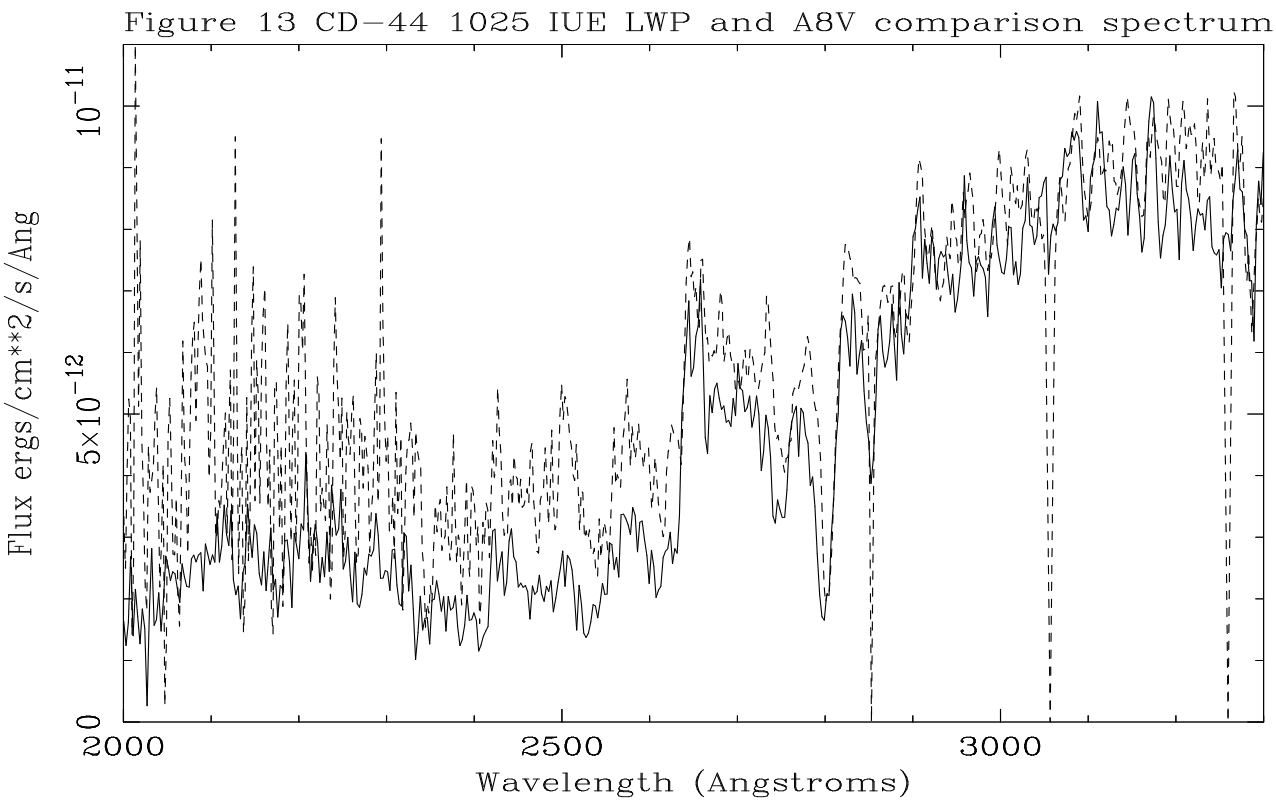

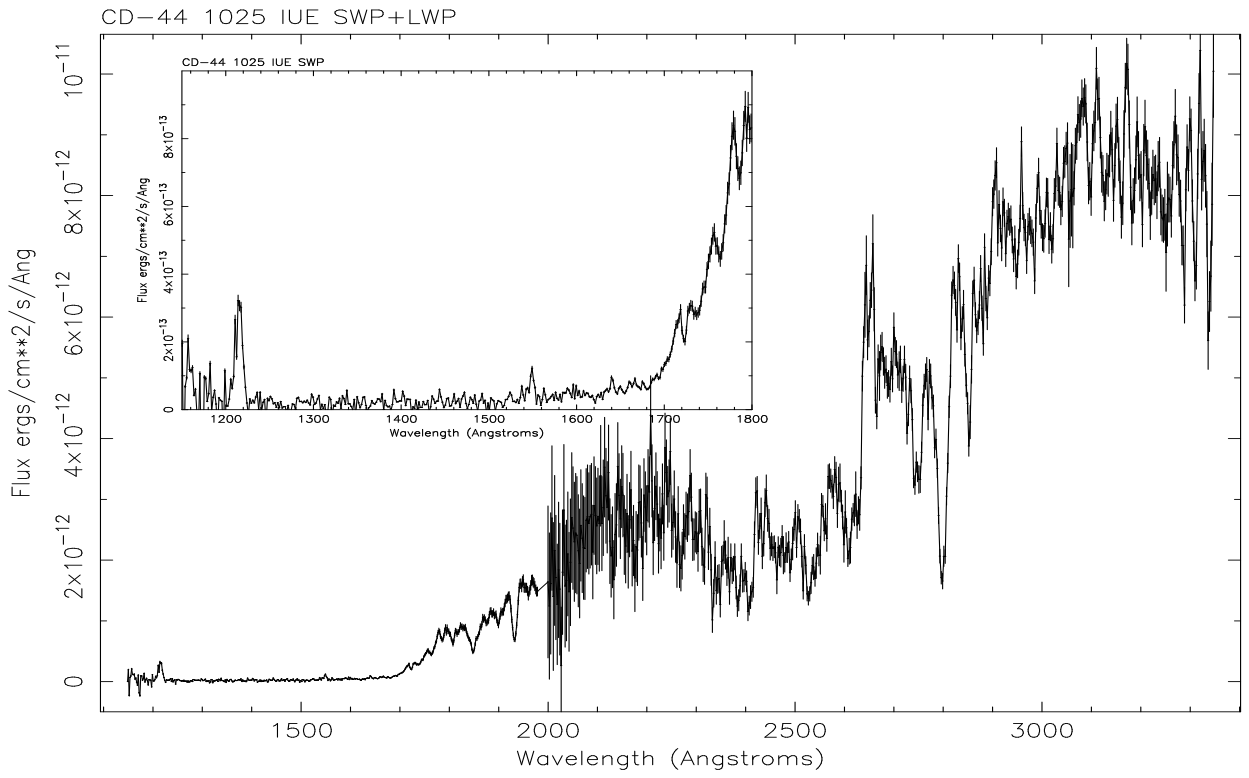

Figure 3.10: Top: IUE LWP spectrum of CD−44 1025 (LWP31570, solid line) compared to HD28910 (LWP27455, A8V, dashed line), scaled for difference in magnitude. Bottom: Low resolution IUE spectrum of CD−44 1025 (A8V−F3V, co-added SWP56406+SWP56407 and LWP31570.) Inset, the co-added SWP spectrum showing more clearly the CIV 1549Å emission feature.

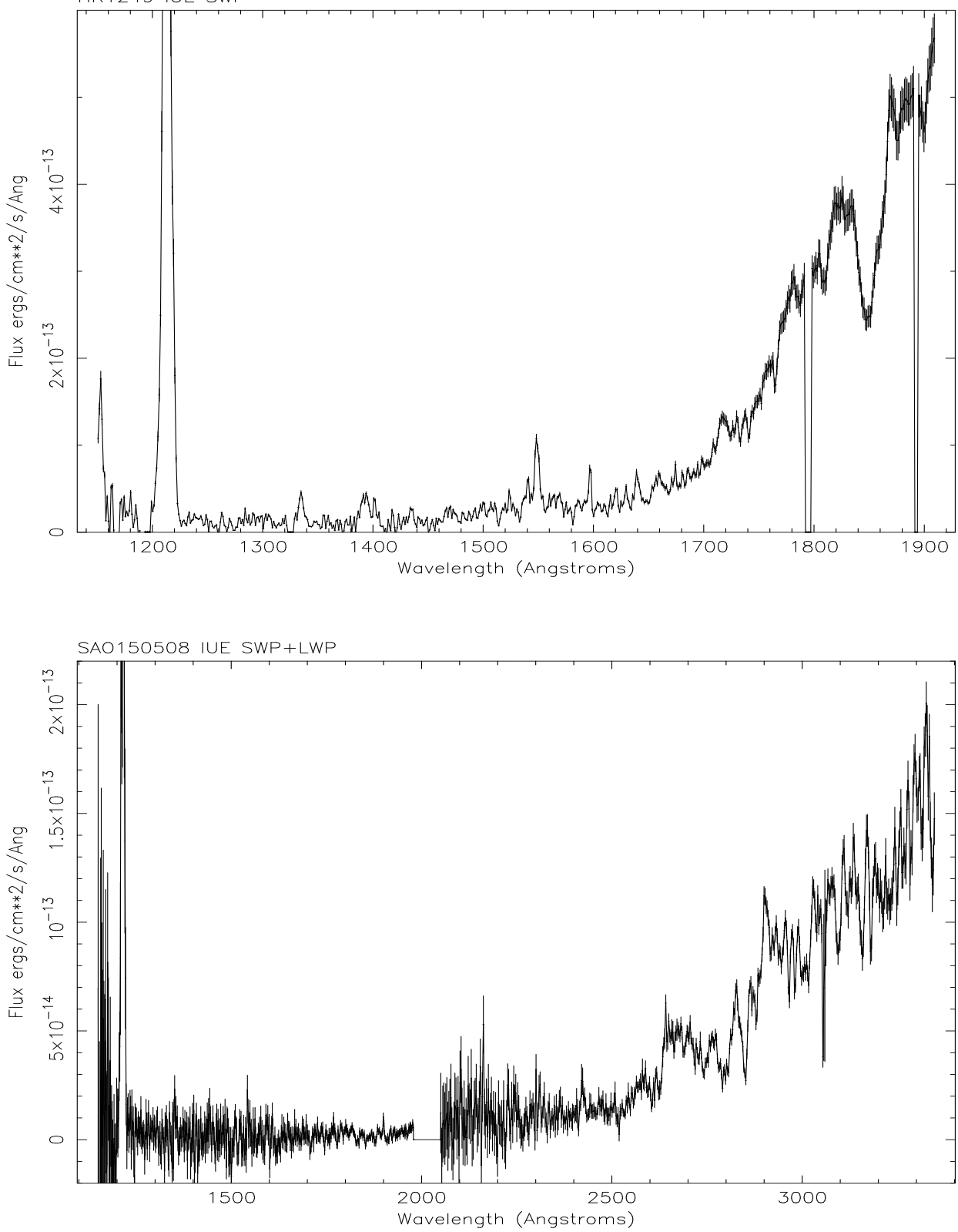

Figure 3.11: Top: Low resolution IUE SWP spectrum of HR1249 (F6V, SWP49792). Emission lines of CII 1335Å, SiIV 1397Å, CIV 1549Å and HeII 1640Å are visible. Bottom: IUE spectrum of SAO150508 (SWP56195+LWP31700).

identification programme. They observed and measured the equivalent width of the CaII H 3393Å emission core=0.01Å. However, they note that they saw this weak emission on only one occasion. The star has also been studied by Jeffries & Jewell (1993) who classify it as F6V.

Figure 3.11 (upper) shows SWP49792, and clearly there is no white dwarf present. However, chromospheric and transition region emission lines of CIV, SiIV, CII and HeII are visible. Measurements of these lines are presented in Table 3.9, and measurements of the X-ray and EUV luminosities are given in Table 3.10. Comparing with the known active star WFC sources HD39587 and HD126660 indicates that HR1249 is almost certainly the source of the EUV radiation.

SAO150508

Prior to the publication of the 2RE catalogue (Pye *et al.* (1995)), the 9th magnitude F6V star SAO150508 was not known to be active. There are no published optical observations. The IUE spectra (SWP 56195 and LWP31700, Figure 3.11, lower) show no evidence for a hot white dwarf companion. However, close examination of the LWP spectrum shows a possible small emission core in the MgII 2798Å line. No emission features are visible in the short wavelength region. SAO150508 is also coincident with a ROSAT PSPC X-ray source. Measurements of the X-ray and EUV luminosities, assuming SAO150508 is the the true source of the EUV and X-ray flux, are presented in Table 3.10.

HD36869

There is no evidence in the literature that the 8th magnitude G2V star HD36869 is active. The IUE spectra (SWP56169 and LWP 31701, Figure 3.12, upper) also show no evidence for activity. The star is coincident with a ROSAT PSPC source, and further observations are required in the optical to determine if this star could be the counterpart of the ROSAT detection.

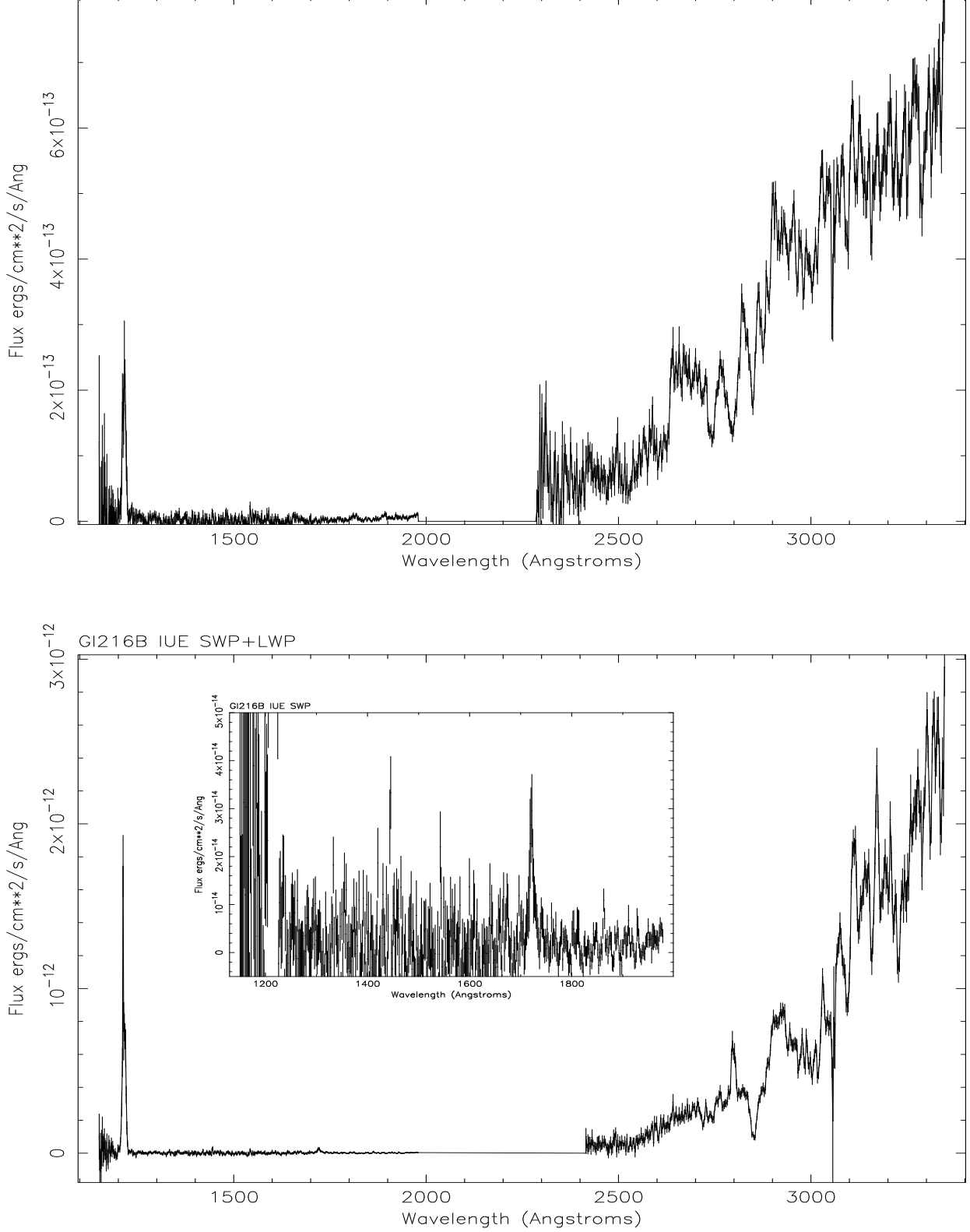

Figure 3.12: Top: Low resolution IUE spectrum of HD36869 (G2V, SWP56169+LWP31701). There is no evidence of activity. Bottom: Low resolution IUE spectrum of Gl216B (K2V, SWP56194+LWP31699). Mg II 2798Å is visible in emission. The feature at ~1720Å (inset) is probably due to a cosmic ray hit.

Gl216B

Gl216B (K2V) is part of a nearby (≈8 parsecs) triple system, and was chosen as a candidate white dwarf binary system on the basis of the S2/S1 count rate ratio. The IUE spectra (SWP56194 & LWP31699) show no evidence for a hot white dwarf. However, Mg II 2798Å is visible in emission (with a line flux of $2.8\pm1.0\times10^{-12}$ ergs cm^{-2} s^{-1} above the continuum). The emission feature in the SWP spectrum at ∼1720Å is probably spurious, since it does not coincide with any commonly seen line. From observations made in the optical, de Strobel *et al.* (1989) concluded that this is a young, active star. If it is the only source of the EUV flux, then I determine $L_{EUV}/L_{bol}=2.78\times10^{-5}$. Schmitt *et al.* (1990) observed the entire Gl216 system in an Einstein HRI pointing, and found that the nearby F7V star Gl216A was 8 times brighter in X-rays than Gl216B. Thus Hodgkin & Pye (1990) concluded that all of the EUV radiation in fact comes from Gl216A. Measurements of the X-ray and EUV luminosities are given in Table 3.10 assuming a) all the flux comes from Gl216A and b) all the flux comes from Gl216B.

HR2225 (HD43162)

This G5V star was not known to be active prior to the ROSAT survey, but since then it has been studied in detail by Jeffries & Jewell (1993). It is also an X-ray source, and measurements of the X-ray and EUV luminosities are given in Table 3.10. No obvious emission features are visible in the IUE LWP and SWP spectra (Figure 3.13, upper; the feature longwards of 1800Å in the SWP spectrum is almost certainly spurious, as there is no commonly seen line at this wavelength).

HR2468 (HD48189)

This star (alternatively HD48189) was not well studied prior to the WFC survey, and not known to be magnetically active. Jeffries & Jewell (1993) find it is a double star, and class the two components as G0V and K3V respectively. SIMBAD lists a combined spectral type of G1.5V. The EUV source (RE J0637−613) has proved to be a young lithium-rich object, and Jeffries (1995) measures the equivalent width of the LiI 6708Å line =133mÅ.

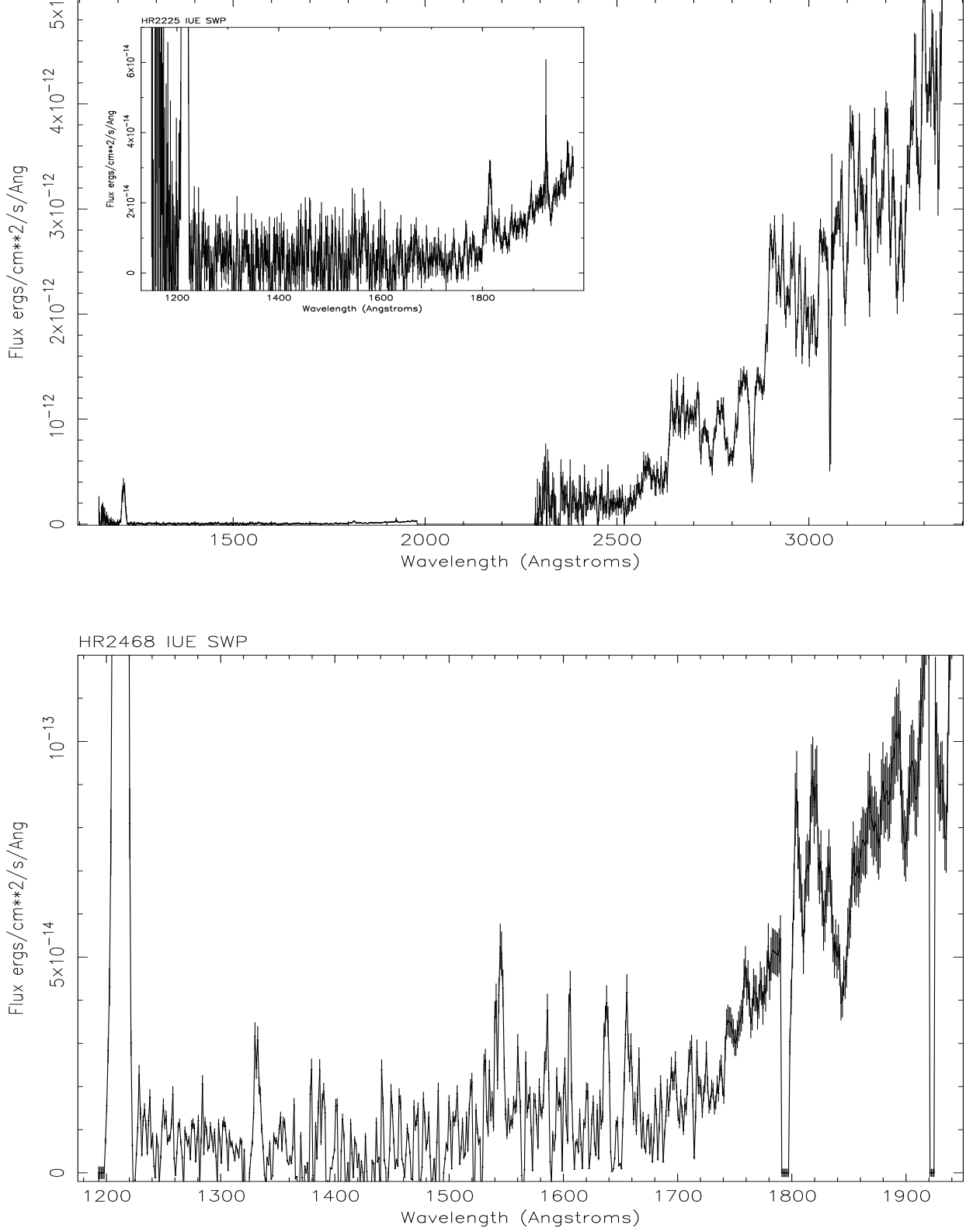

Figure 3.13: Top: Low resolution IUE spectrum of HR2225 (G5V, SWP56206+LWP31715). The emission feature at ∼1800Å is probably spurious. Bottom: Low resolution IUE SWP spectrum of HR2468 (G1.5V, SWP52802). Emission lines of CII 1335Å, CIV 1549Å and possibly HeII 1640Å are visible.

The IUE SWP spectrum (Figure 3.13, lower, SWP52802) shows no evidence for a white dwarf companion, but there are CIV 1550Å, CII 1335Å and HeII 1640Å emission lines visible. Measurements of these lines are presented in Table 3.9. Measurements of the EUV and X-ray luminosities in Table 3.10 are made assuming a G1.5V spectral classification.

HD295290

There are no references in the literature to this being an active star. However, Mg II is clearly seen in emission at 2800Å in the IUE LWP spectrum (Figure 3.14, top), and there is a suggestion of CIV in emission at 1550Å in the short wavelength region. Measurements of the X-ray and EUV luminosities are given in Table 3.10 assuming the G0V classification given by SIMBAD.

BD−00°1462

This star was observed three times as part of the WFC optical identification programme of Mason *et al.* (1995), although the authors failed to find emission cores in either Ca H&K or Hα, with an upper limit to the equivalent width of 0.05Å. A previously known active F2V star, BD-00°1462 has been well studied in the far UV and optical (e.g. Oranje & Zwaan 1985, Simon & Landsman 1991, Andersson & Edvardsson 1994) and is very likely the optical counterpart to RE J0650−003. In the far-UV, emission cores are seen in the MgII H & K lines in high resolution LWP spectra. We obtained one low resolution SWP spectrum, SWP52801, although earlier spectra exist in the archive. Figure 3.15 shows the best of these, SWP8200, with an inset of SWP52801 showing an emission feature at ≈1540Å. This may be spurious, as it is a little too far from CIV 1549Å. There is clearly no white dwarf. This star is also an X-ray source (see Table 3.1).

HD54402

No references are given in the literature to this being an active star. There is clearly no white dwarf visible in the IUE SWP spectrum, and the emission line at ∼1800Å is probably spurious, perhaps due to a cosmic ray hit. The EUV source is not coincident with an X-ray source. The star needs to be examined optically to search for any evidence of chromospheric activity.

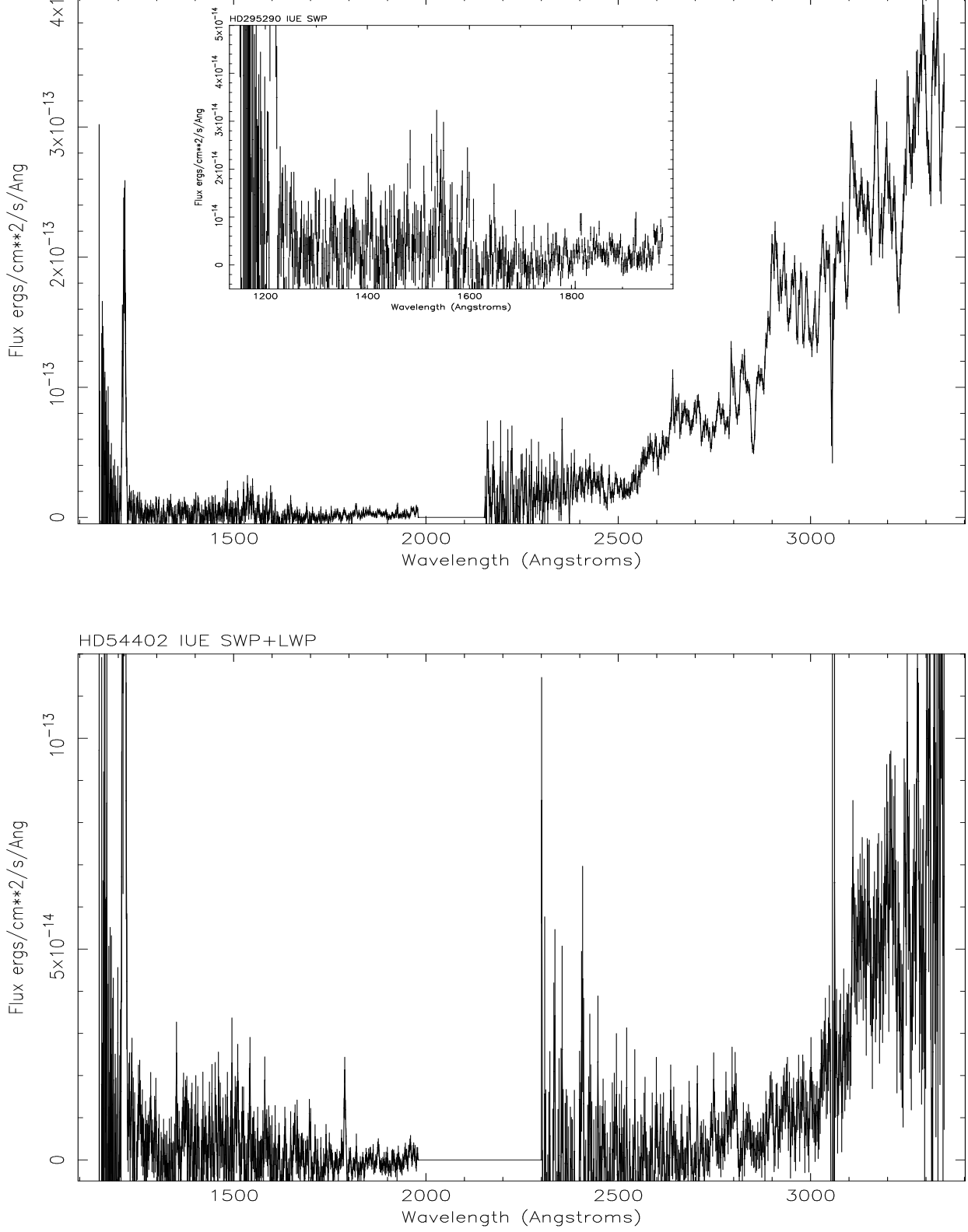

Figure 3.14: Top: Low resolution IUE spectrum of HD295290 (G0V, SWP56211+LWP31726). MgII is clearly seen in emission at 2798Å. CIV 1549Å emission is suggested in the SWP spectrum (inset). Bottom: Low resolution IUE spectrum of HD54402 (K0, SWP56193+LWP31698). The feature at ∼1800Å is probably due to a cosmic ray hit.

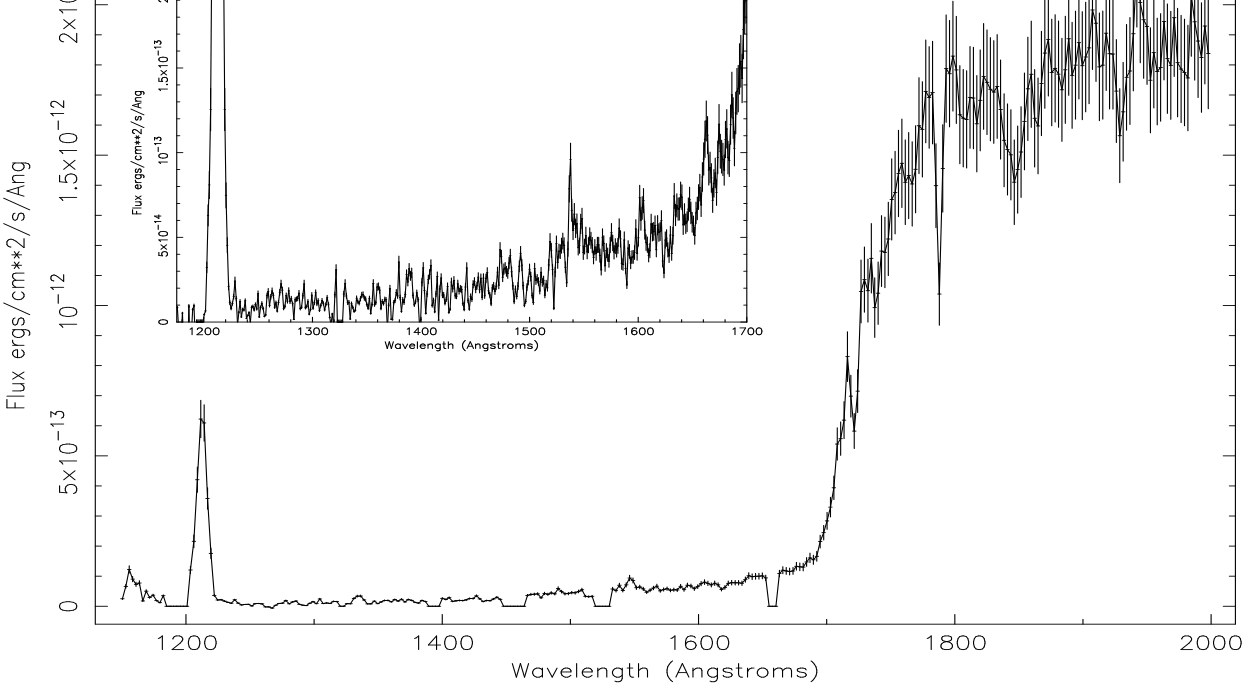

Figure 3.15: Low resolution IUE SWP spectrum of BD−00°1462 (F2V, SWP8200)). The inset (SWP52801) shows a possible emission feature near 1549Å.

SAO135659

Again, this star was not known to be active prior to the ROSAT survey. The IUE LWP spectrum (Figure 3.16, top) reveals Mg II in emission at 2800Å. Measurements of the EUV and X-ray luminosities (this star is also a PSPC source) are given in Table 3.10.

RE J0823−252/HD70907

The soft X-ray and EUV photometric properties of this ROSAT source are characteristic of a hot white dwarf, and, therefore, it was selected as a potential hidden white dwarf binary. The S2/S1 count rate ratio =1.6,and there is no detection in the PSPC upper band, making this a relatively soft source. The V=8.8 star in centre of the field, HD70907 (F3IV/V), was observed in both the IUE SWP and LWP cameras (Figure 3.16, lower). There is no evidence for a white dwarf companion or emission features indicative of an active star. A V≈11 companion was also observed and again there was no evidence for a white dwarf, although, in the absence of any flux in the LWP camera that could be attributed to a stellar source, it seems likely that that the target may have been missed altogether. Mason *et al.* (1995) report that this companion object is indeed active, although they give no indication of the size of any emission features seen in the

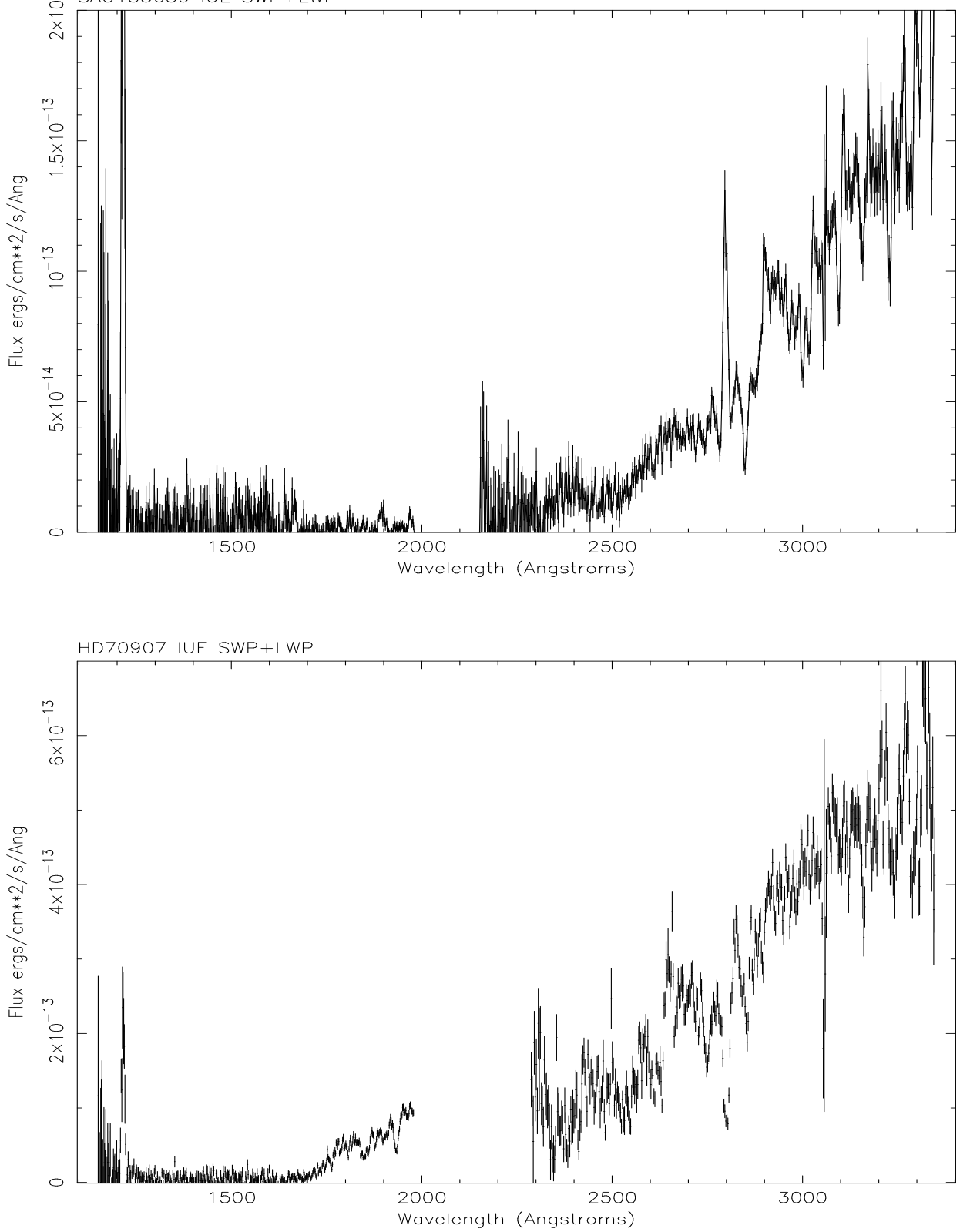

Figure 3.16: Top: Low resolution IUE spectrum of SAO135659 (SWP56273+LWP31801). MgII is visible in emission at 2798Å. Bottom: Low resolution IUE spectrum of HD70907 (SWP56344+LWP31836). There is no evidence for activity.

optical. They also do not give a spectral type for this star, and thus I have not been able to determine the EUV and X-ray luminosities. Whether this star is active enough to be the true EUV source remains unclear, and further observations are necessary. A hidden hot white dwarf companion cannot be completely ruled out.

HR4646

Until recently it was assumed that A stars did not possess convective chromospheres and hot coronae (Simon & Landsman 1997). It is, therefore, highly unusual to detect an A star in EUV or X-ray surveys (Fleming *et al.* 1991). Observations by the Einstein and EXOSAT observatories failed to find any convincing detections other than the nearby quadrupal A star system Castor (Pallavicini *et al.* 1990). Thus HR4646, an Am star coincident with ROSAT WFC 2RE and PSPC sources, was selected as a potential hidden white dwarf binary. In fact, the IUE SWP spectrum (Figure 3.17, top) shows no evidence for a hot white dwarf companion. Could HR4646 itself be the ROSAT source?

Magnetic line Am stars are A or early F stars to which no unique spectral type can be assigned (Margoni, Munari & Stagni 1992). They are difficult to study without high quality spectra. They have metallic lines as in early F stars, strong hydrogen lines as in late A type stars, and very weak Ca I 4427Å and CaII K 3968Å lines as in early A type stars. Abt & Morrell (1995) find HR4646 looks like a combination of an A4 (from the Ca II K line), an F2 (from the H Balmer lines) and an F3 (from the metallic lines). Am stars do not possess significant magnetic fields and they are slow rotators, although Abt & Morrell (1995) find v sin i=78km s^{-1} for HR4646. This suggests, therefore, that HR4646 is not going to be particularly active. Interestingly, Am stars almost always appear to lie in close binary systems (Abt 1961). Margoni, Munari & Stagni (1992) find that HR4646 is a spectroscopic binary with a period of 1.27 days.

There is no spectroscopic evidence for activity in the SWP spectrum of HR4646, but, as the star is a confirmed spectroscopic binary, it is plausible that an unseen late-type companion is also active and responsible for the EUV radiation. Further study of this system is required.

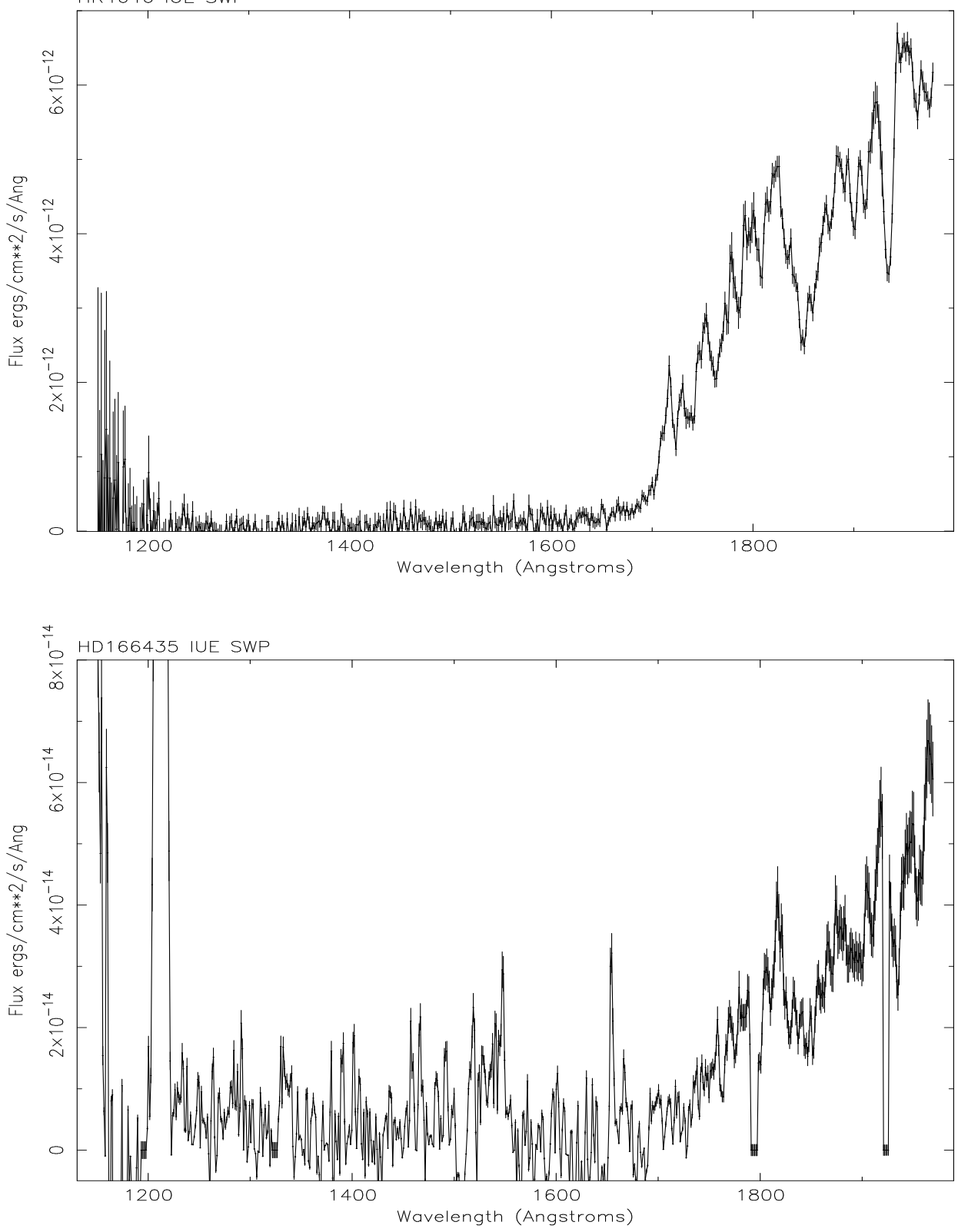

Figure 3.17: Top: Low resolution IUE SWP spectrum of HR4646 (A5m, SWP56393). Bottom: Low resolution IUE SWP spectrum of HD166435 (SWP55658). There is a suggestion of CIV 1549Å, CII 1335Å and HeII 1640Å in emission.

HD166435

Observations of this star in the optical have revealed little evidence of activity, hence it was selected as a likely candidate for an unresolved white dwarf binary. The star is classified in SIMBAD as G0. Observations by Mason *et al.* (1995) showed it to be, at most, mildly active. They measured an equivalent width of the CaII H 3393Å emission line of 0.07Å, but detected no emission core in Hα. Mullis & Bopp (1994) also concluded that there was insufficient evidence to prove that this star is chromospherically active. They found no emission core in Hα, and only a small core in CaII 8542Å which they were not convinced was real.

HD166435 was observed in low resolution with the IUE SWP camera in August 1995 (Figure 3.17, SWP55658). There is clearly no white dwarf companion, and no obvious emission features, although there is a hint of a CIV 1549Å emission feature rising above the background noise with a peak flux of $\sim 3\times10^{-14}$ ergs cm^{-2} sec^{-1}.

Interestingly, the WFC source is coincident with a PSPC source including a 0.4−2.4keV hard band detection. A white dwarf can be excluded as the origin of this hard band radiation, which suggests that HD166435 may indeed be coronally active. If we assume the source is HD166435, then the X-ray luminosity of this star $L_x=9.3\times10^{29}$, $L_x/L_{bol}=1.5\times10^{-4}$, and $L_{EUV}/L_{bol}=1.6\times10^{-4}$. Comparing with the other stars in Table 3.10, this would make HD166435 a reasonably active object. Further high resolution optical spectroscopy of this object is obviously required in order to unambiguously determine whether it is actually active, and the field of this source may also need re-examining.

3.7 Summary

Five more white dwarfs in unresolved, non-interacting binary systems with normal stellar companions have been discovered in the ROSAT WFC survey. This brings the total number found through the EUV surveys to seventeen (including the independently identified HD27483, Böhm-Vitense 1993, and MS 0354.6−3650, Christian *et al.* 1996, which was only seen by EUVE). These invisible white dwarfs could never have been observed optically, and only a handful of such systems have previously been discovered (usually by accident). Thus, although between 50−80% of all stars are thought to lie in binary systems, the majority of known white dwarfs are isolated stars (most of the currently known white dwarfs in binaries have a cool red dwarf companion). ROSAT and EUVE have, therefore, provided us with a powerful tool for discovering many more of these optically hidden white dwarfs.

The demise of IUE means that this particular method of searching for these important systems is no longer available. Although HST can observe the same wavelength region, it is of course much harder to obtain the observing time required for such a study. It is likely, therefore, that very few further examples will be discovered in the near future. However, the searches with IUE have been fairly exhaustive. For example, in the final episode (1995/96), thirteen targets were observed but only one new white dwarf binary was discovered (RE J0500−36).

Follow-up work to this study now needs to be undertaken. In particular, it is important to determine whether these systems are wide or close, possibly pre-CV binaries. To this end, observing time has been requested with WFPC2 on HST to attempt to resolve some of the pairs, while studies are also been undertaken to look for radial velocity variations in some of the main sequence stars. Detailed studies of the companions may also reveal evidence of past interactions, further examples of the WIRR-ing stars (Jeffries & Stevens 1996), and stars with possible abundance anomalies, that may be the progenitors of the Barium and Carbon giants.

Table 3.12: Summary of results: Best fit models for the white dwarfs[1]

Name	System	T	log g	M	D(WD)	V	HI column
				M⊙	pc		atoms cm^{-2}
New discoveries							
HD2133	DA+F8V	28,700	8.25	0.79	115	15.7	0.0
RE J0357+283	DA+K2V	30,960	7.9	0.60	105	14.9	2.1×10^{19}
RE J0500−362	DA+late F	42,000	7.5	0.47	740	17.9	1.1×10^{19}
BD+27°1888	DA+A8V−F2V	34,130	7.25	0.39	193	14.8	3.3×10^{19}
RE J1027+323	DA+G0V−G4V	32,440	7.5	0.44	388	16.9	1.05×10^{19}
Previous discoveries							
HD18131	DA+K0IV	31,130	8.0	0.65	72	14.2	7.2×10^{18}
HD27483	DA+F6V	22,000	8.5	0.94	45	14.6	8.5×10^{18}
RE J1925−566	DA+G2−G8	32,265	7.25	0.39	141	14.4	unknown

[1] Matching the estimated distance to the companion

Table 3.13: Summary of results: Stars observed where no white dwarf was detected

ROSAT source	Name	SpT	V	Active?	Far-UV Emission Lines	comment
2RE J0014+69	AG+68 14	F8	10.3	N	None	SWP only
2RE J0222+50	BD+49°646	?	10.1	N	None	SWP only, no flux
2RE J0232−02		K	14.8	N	None	Target missed?
RE J0312−44	CD−44 1025	F3V+A8V	5.93	Y	CIV, HeII	
RE J0404−00	HR1249	F6V	5.38	Y	CII, SiIV, CIV, HeII	
2RE J0530−19	SAO150508	G5V	9.0	Y	MgII	
2RE J0534−15	HD36869	G2V	8.0	N		
2RE J0544−22	Gl216B	K2V	6.15	Y	MgII	Gl216A is EUV source
RE J0613−23	HR2225	G5V	6.39	Y		
RE J0637−61	HR2468	G1.5V	6.18	Y	CII, CIV, HeII	
2RE J0640−03	HD295290	G0	9.1	Y	MgII, CIV?	
RE J0650−00	BD−00°1462	F2V	5.77	Y	MgII, CIV?	
2RE J0710+45	HD54402	K0	7.7	N		
2RE J0813−07	SAO135659	K0	8.8	Y	MgII	
RE J0823−25	HD70907	F3IV/V	8.8	N		
		late	11	Y		Target missed
2RE J1212+77	HR4646	A5m	5.14	N		
RE J1809+29	HD166435	G0	6.84	Y?	CII?, CIV?, HeII?	

Chapter 4

DAO White Dwarfs in the ROSAT WFC Survey

4.1 Overview

DAO white dwarfs are a peculiar class of degenerate objects whose evolution is not well understood. It appears that they are a rather inhomogeneous collection of objects with a variety of different origins. Only three DAOs were detected by the ROSAT WFC, and, notably, all three lie in close, post-Common Envelope (post-CE) pre-Cataclysmic Variable (pre-CV) binaries. This chapter explores the origin and evolutionary status of these three objects, how this relates to their binary nature, and what this might tell us about DAO stars in general. In particular, an extraordinary spectrum from the Extreme Ultraviolet Explorer (EUVE) of one of these systems, RE J0720−318, is studied in detail.

4.2 Introduction

DAO white dwarfs have hybrid spectra showing both hydrogen and helium lines, in particular a weak HeII feature in the optical region at 4686Å, and they are rare, comprising less than 1% of all white dwarfs. They have effective temperatures in the range 50,000-70,000K, and typical abundances N(He)/N(H)$\sim 10^{-2}$.

The first comprehensive photospheric analysis of DAO white dwarfs, the protoype of which is HZ34, was undertaken by Wesemael, Green & Liebert (1985), and the sample was enlarged through studies by Holberg (1987) and Holberg *et al.* (1989). Wesemael, Green & Liebert (1985) showed that atmospheric parameters such as temperature, gravity and helium abundance could be determined assuming simple homogeneously mixed H+He compositions.

Originally, observational evidence suggested that the majority of white dwarfs may have evolved from helium-rich PG1159 stars (Fontaine & Wesemael 1987). Helium-rich and hydrogen-rich central stars of planetary nebula (CSPN) are equally common, yet further down the cooling sequence hydrogen-rich DA stars outnumber helium-rich DOs by a factor 7:1. Thus, it appeared likely that a fraction of DA stars may have evolved from hot helium-rich objects by gravitational settling of helium and the upward diffusion of hydrogen in the atmosphere to form a stratified envelope with an overlying hydrogen layer. The absence of any known DAs above 70,000K, and the gap in the helium cooling sequence between 30,000-45,000K supported this idea. Helium-rich objects were then expected to reappear as DBs at 30,000K, due to the convective mixing of the He layer back up into the atmosphere. DAOs were thus interpreted as white dwarfs undergoing metamorphosis from helium-rich types to hydrogen dominated stars. Vennes *et al.* (1988) demonstrated that if this interpretation was correct, chemically stratified configurations are the only viable explanation for the presence of helium in DAO stars.

However, recent work has seriously undermined this theory. Firstly, a very hot (90,000K) DA white dwarf was found by ROSAT (RE1738+665, Barstow *et al.* 1994b), which can be viewed as a 'missing link' between hydrogen-rich CSPN and DA stars, eliminating the need to invoke evolution through the helium channel first. In addition, Bergeron *et al.* (1994) undertook a detailed spectroscopic analysis of a large sample of DAOs to test the predictions of homogeneous and stratified models with observed line profiles. Unexpectedly, they proved that, in almost all

cases, *homogeneous* compositions provide excellent fits to the observed HeII 4686Å absorption line, while stratified models predict line profiles which are too broad and shallow. They went on to propose five subclasses of DAOs (see Table 4.1), representing a rather disparate collection of objects with a variety of origins.

The largest of the Bergeron *et al.* (1994) DAO subclasses comprises six stars with masses too low ($M<0.48M_{\odot}$) for them to be the result of post-AGB evolution (see Table 4.1). Instead, the authors argue that these stars are the direct descendents of hot B and OB subwarfs (those containing hydrogen), having evolved directly from the Extended Horizontal Branch (EHB). It has been accepted since the early 1970s that subdwarfs will eventually evolve into white dwarfs, although the details are not well understood (Dorman, Rood & O'Connell 1993). It is believed that after helium exhaustion these stars cannot ascend the Asymptotic Giant Branch (AGB) as they have not retained enough hydrogen envelope mass to support a thermally pulsing stage. Instead, they contract at constant luminosity due to the release of gravitational energy until degeneracy pressure halts the collapse and they become white dwarfs. The birth rate of this subsample of DAOs is consistent with estimates of the birth rate of low mass post-EHB stars. Furthermore, both Bergeron *et al.* (1994) and Tweedy & Napiwotzki (1994) find evidence for an old planetary nebula associated with one of these low mass DAOs, GD561. This implies that mass ejection in the form of a planetary nebula is not only associated with post-AGB stars, and that mass loss could explain the presence of helium in these stars. Indeed, Dreizler *et al.* (1995) argue that mass loss is occuring from the newly discovered isolated DAO HS2115+1143, which does not possess a detectable PN.

Analysis by Napiwotzki *et al.* (1993) shows that most DAO CSPN have gravities $\log g \leq 7.0$, while those classified DA have $\log g \sim 7.5$. The high gravity objects, being more luminous, may lose mass more easily than the low gravity stars where significant helium enhancement may occur in the photospheres. Alternatively, the high-gravity CSPN may have thicker hydrogen envelopes, and thus the helium is buried deeper in the star where it is undetectable in optical spectra, but can be seen in hot low mass DAO central stars. Indeed, Bergeron *et al.* (1994) conclude that, if one assumes that a moderate helium abundance is present in the atmospheres of DA stars, then all hot, low surface gravity, single hydrogen-rich white dwarfs are necessarily DAOs. Post-EHB DAOs may, therefore, offer a third evolutionary sequence for white dwarfs, in addition to the post-AGB helium-rich and hydrogen-rich cooling chains.

Table 4.1: A catalogue of DAO white dwarfs, listed by subclasses

Name	V	T_eff (K)	log g	log H/He	PN?	ref.
post-EHB						
HZ34	15.66	79900	6.61	1.33	N	Bergeron *et al.* (1994)
						Tweedy & Kwitter (1994)
GD 561[a]	14.52	65300	6.71	2.40	Y	Bergeron *et al.* (1994)
						Tweedy & Napiwotzki (1994)
PG0834+501	15.82	60400	7.11	2.18	N	Bergeron *et al.* (1994)
TON 353	16.71	66100	7.11	2.88	N	Bergeron *et al.* (1994)
PG0134+181	17.14	56400	7.4	2.98	N	Bergeron *et al.* (1994)
post-AGB						
LS V +46 21	12.4	77300	7.31	2.06	Y	Bergeron *et al.* (1994)
						Tweedy & Napiwotzki (1992)
TON 320	15.82	68800	7.68	2.74	Y	Bergeron *et al.* (1994)
						Tweedy & Kwitter (1994)
LB2	15.62	65700	7.67	2.51	N	Bergeron *et al.* (1994)
						Tweedy & Kwitter (1994)
DAO+dM						
PG1413+015	17.09	48100	7.69	2.57	N	Bergeron *et al.* (1994)
						Fulbright *et al.* (1993)
RE J1016−053	14.15	56400	7.74	3.26	N	Tweedy *et al.* (1993)
						Jomaron *et al.* (1993)
RE J2013+400	14.60	47800	7.69	2.62	N	Barstow *et al.* (1995a)
RE J0720−318	14.87	56360	7.64	3.56	N	Barstow *et al.* (1995c)
						Vennes & Thorstensen (1994b)
						Vennes & Thorstensen (1996)
NN Ser[b]	16	55000	8.0	no data	N	Catalan *et al.* (1995)
Stratified						
PG1305−017	16.23	44400	7.76	M_H=9.5e-15	N	Bergeron *et al.* (1994)
Variable						
PG1210+533[c]	14.07	44800	7.89	2.08	N	Bergeron *et al.* (1994)
Double Degenerate						
Feige 55	13.57	58300	7.15	2.92	N	Holberg *et al.* (1995)
						Tweedy & Kwitter (1994)
Massive WD						
GD50	14.04	42400	9.00	3.60	N	Vennes, Bowyer & Dupuis (1996)
Unclassified						
PG 0950+139	16.02	70000	7.5	no fit	Y	Liebert *et al.* (1989)
HS2115+1148[d]	16.5	67000	6.9	2.8	N	Dreizler *et al.* (1995)
PG0231+051	16.10	no data			N	Heber, Dreizler & Hagen (1996)
HS0505+0112[e]	14.9(B)	no data			N	Heber, Dreizler & Hagen (1996)
HS1136+6646[f]	13.9(B)	no data			N	Heber, Dreizler & Hagen (1996)
HS2033+0327	16.3(B)	no data			N	Heber, Dreizler & Hagen (1996)

Notes: a) From age considerations Tweedy & Napiwotzki (1994) suggest GD561 is in fact a double degenerate (see text). b) The parameters given by Catalan *et al.* (1995) were determined using a pure H, stratified model and must be taken as rough estimates only. c) Recent observations by Jay Holberg suggest PG1210+533 may be a member of a binary system (private communication). d) Plotting the newly discovered low mass DAO HS2115 on Figures 5.1 and 5.1 suggests it should be classified as a post-EHB object. e) HS0505+0112 displays prominent CIV absorption in its optical spectrum. f) HS1136+6646 is a spectroscopic binary with possibly a late K companion

Table 4.2: Other DAO Stars, all CSPN

Name	V	T_{eff} (K)	log g	log H/He	PN?	ref.
Sh 2-68	16.6	74000	6.75	1.0	Y	Napiwotzki & Schonberner (1995)
						Napiwotzki (1995)
NGC7293	13.4	107000	7.00	1.30	Y	Napiwotzki & Schonberner (1995)
						Napiwotzki (1995)
NGC6853	14.2	99000	6.75	1.0	Y	Napiwotzki & Schonberner (1995)
						Napiwotzki (1995)
Abell 74	17.0	no data			Y	Napiwotzki & Schonberner (1995)
Sh 2-188	17.7	no data			Y	Napiwotzki & Schonberner (1995)
HDW3	17.2	no data			Y	Napiwotzki & Schonberner (1995)
PW 1	15.7	no data			Y	Napiwotzki & Schonberner (1995)
Abell 7	15.6	109000	6.75	1.0	Y	Napiwotzki & Schonberner (1995)
						Napiwotzki (1995)
Abell 31	15.6	92000	6.30	1.0	Y	Napiwotzki & Schonberner (1995)
						Napiwotzki (1995)
Abell 39	-	118000	6.50	1.0	Y	Napiwotzki (1995)
						Heber, Dreizler & Hagen (1996)

More recently, an unexpected discovery has provided us with an alternative explanation for the origin of low mass DAOs. Holberg *et al.* (1995) found, from high resolution IUE spectra, that the 'post-EHB' DAO Feige 55 is in fact a close double degenerate (DD) binary. Feige 55 must, therefore, have undergone mass transfer and at least one stage of common envelope evolution. In addition, Tweedy & Napiwotzki (1994) argue that another 'post-EHB' DAO, GD 561 must also be a double degenerate. As has been discussed above, this is the only low mass DAO that has a planetary nebula (PN) associated with it, giving an upper age limit of $<10^6$ years. Assuming single star evolution, though, would give a cooling age of $\sim 10^7$ years. The discrepancy can be explained if GD 561 is a member of a close binary system, and, like Feige 55, has lost mass as a result of mass transfer and common envelope evolution. It is currently believed that planetary nebula are only formed by post-AGB objects more massive than $0.5 M_{\odot}$, and so the existence of a post-EHB star with a PN is a challenge to stellar evolution theory. This problem would be removed if it could be shown that GD 561 is a close DD, and the composite spectrum is giving a misleadingly low gravity.

It can be argued, therefore, that all low mass DAOs, and indeed all low mass white dwarfs, are the result of binary interaction. For example, Marsh (1995b) and Marsh, Dhillon & Duck (1995) have surveyed many of the low mass DA stars found in the sample of Bergeron, Saffer & Liebert (1992) and found compelling evidence for a double degenerate nature in 6 out of 8 cases. This is impressive comfirmation that such low mass white dwarfs are the result of binary evolution.

However, the existence of a double-degenerate among the low mass DAO stars does not necessarily invalidate the Bergeron *et al.* (1994) post-EHB scenario. Figure 4.1, reproduced from Bergeron *et al.* (1994), shows, by considering the relation between T_{eff} and log g, that while Feige 55, GD561 and PG0834 lie some distance from theoretical post-EHB evolutionary tracks, HZ34, PG0134 and Ton 353 may still be consistent with a post-EHB origin.

Four other subclasses of DAO were identified by Bergeron *et al.* (1994) (see Tables 4.1/4.2). Three stars have masses entirely consistent with post-AGB evolution (see Figures 4.1 and 4.2). Indeed, two of these are associated with PN. Two stars are peculiar and belong to their own subclasses. PG 1210+533 cannot be modelled with either a stratified or homogeneous structure, and has a variable spectrum which may be the result of surface abundance inhomogeneities, although recent observations suggest that this too may be a binary system comprising a white dwarf plus a faint, low mass companion (Holberg, private communication). PG 1305−017 *can* be fitted with a layered atmosphere and could be the one star in the Bergeron sample representing a transitional object from a DO to a DA. The fifth class of DAOs identified by Bergeron et al. (1994) are those lying in close binary systems with red dwarf companions. These stars have typical masses for white dwarfs and are also consistent with post-AGB evolution (see Figure 4.2). Five of these systems are now known (see also Table 2.1): NN Ser, PG 1413+015, RE J1016−053, RE J2013+400, and RE J0720−318. The last three were all discovered in the ROSAT WFC survey.

Figure 4.1: T_{eff}−log g diagram, reproduced from Bergeron *et al.* (1994), for the DAO stars in their sample. Also displayed are Matt Wood's cooling sequences for carbon core white dwarfs with hydrogen layer mass M_H=0 (dashed curves), and a sequence with a thick hydrogen layer (M_H=10^{-4}, solid line).

Figure 4.2: T_{eff}−log g diagram, also reproduced from Bergeron *et al.* (1994), showing the location of the 'post-AGB' and 'post-EHB' DAO white dwarfs. Also shown are post-EHB cooling sequences of Dorman, Rood & O'Connell (1993) (solid lines, starting at upper right) and various post-AGB (dashed curves) and carbon core (thick H layer) white dwarf cooling tracks (solid lines, bottom right).

4.3 Constraints on DAO White Dwarf Composition from the ROSAT WFC Survey

4.3.1 Introduction

The failure to find all but a handful of DAO white dwarfs with the ROSAT WFC prompted a detailed investigation into their non-detection. Between 1000-2000 white dwarfs were expected to be seen in the survey from pre-launch estmates. However, only around 120 were found in the end. Barstow *et al.* (1993c) first showed that trace elements heavier than helium in the atmospheres of hot DA stars prevented many of them from being detected by blocking the EUV flux, although helium may still contribute to the opacity. Similarly, Bergeron *et al.* (1994) hypothesised that heavy elements in the atmospheres of DAO white dwarfs could also account for their non-detection by ROSAT. Using the sample of Bergeron *et al.* (1994) as a basis, this hypothesis is tested to try to explain why the only DAOs actually detected by ROSAT all lie in binaries.

4.3.2 Sample

Table 4.3 shows the DAO stars in the sample, with temperature, log gravity and chemical abundance log He/H taken from Bergeron *et al.* (1994). Only one star, PG1305−017, can be interpreted with a stratified atmosphere. PG1210+533 appears on both lists because it is not well fitted by either kind of model. The parameters of RE J0720−318 were taken from Barstow *et al.* (1995c).

4.3.3 Method

Images were selected from the ROSAT WFC survey and the background examined at the positions of each star. The images have been reprocessed to improve signal to noise, and with improved attitude and background rejection. The number of counts in a source box of radius three arcmin was measured, together with the background counts in an annulus around the source box. A Baysian statistical technique was used to determine the three sigma upper limit on the source counts at the position of each DAO white dwarf in the sample.

Table 4.3: DAO Sample Stars and Atmospheric Parameters

A) Homogeneous models							
Name	Teff (K)	log g	log He/H	Name	Teff (K)	log g	log He/H
LS V +46 21	77300	7.31	-2.06	PG0134+181	56400	7.40	-2.98
Ton 320	68800	7.68	-2.74	RE J1016−053	56400	7.74	-3.26
Ton 353	66100	7.11	-2.88	RE J0720−318	56360	7.64	-3.56
LB2	65700	7.67	-2.51	PG1413+015	48100	7.69	-2.57
GD 561	65300	6.71	-2.40	RE J2013+400	47800	7.69	-2.62
PG0834+501	60400	7.11	-2.18	PG1210+533	44800	7.89	-2.08
Feige 55	58300	7.15	-2.92				
B) Stratified models							
Name	Teff (K)	log g	log q_H	Name	Teff (K)	log g	log q_H
PG1210+533	46600	7.91	-15.98	PG1305−017	44400	7.76	-15.98

The parameters in Table 4.3 were applied to homogeneous and stratified models, supplied by Detlev Koester (and described in Chapter 3), to predict the count rate for each star as a function of interstellar hydrogen column density. The V magnitude was used to normalise each model spectrum. The normalisation parameter, a measure of $(R/D)^2$, was used with Matt Wood's evolutionary code (which gives mass and radius for a given T and log g) to estimate the distance to each star. Hence the column density to each star could be obtained using the published work of Paresce (1984) and Frisch & York (1983).

4.3.4 Results

Comparing the predicted count rates with observed count rates and upper limits allows us to draw several conclusions.

The non-detection of five stars (PG0834+501, PG0134+181, PG1413+015, PG1210+533 and Ton 353), can be accounted for purely in terms of absorption by interstellar hydrogen gas. For example, Figure 4.3 shows the predicted count rates for the S1 and S2 filters for PG1413+015 as a function of column density. The straight horizontal lines are the upper limits on the count rates for the two filters. From the Frisch and York maps the estimated column density to this star (at a distance of 490 parsecs) is greater than 10^{20}. Clearly the predicted count rates (1.5×10^{-4} counts/sec in S1 and 3×10^{-6} counts/sec in S2) are much lower than the upper limits (8×10^{-3}

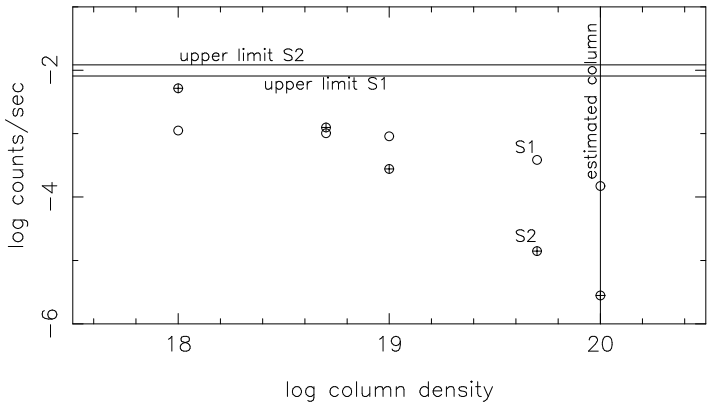

Figure 4.3: PG1413+015: Model predicted count rates for the S1 and S2 filters plotted as a function of interstellar column density

counts/sec in S1 and 12.1×10^{-3} counts/sec in S2). Thus this star's non-detection is simply accounted for by absorption.

The non-detection of the stratified star PG1305−017 can be easily explained because it has a very thin hydrogen layer; the EUV flux is blocked by the underlying helium. However, the non-detection of five stars (LS V+46 21, Ton 320, LB2, GD 561, Feige 55), cannot be accounted for by column density alone, or by their helium content. A good example is LB2. Figure 4.4 shows the predicted count rates for this star in the S1 and S2 filters as a function of column density. The straight horizontal lines are the upper limits on the count rates for the two filters. The Frisch and York maps give an estimated column density to this star (at a distance of approximately 300 parsecs) of less than 5×10^{18}. Paresce (1984) gives the column density as 2×10^{19} or less. Either way it is clear from the diagram that column density cannot account for the non-detection of this star, since the predicted count rates are far in excess of the upper limits. Instead, the suggestion is that heavy elements, in addition to helium, are providing the opacity to block the EUV flux.

4.3.5 Discussion

Although the non-detection of some DAO white dwarfs in the EUV by ROSAT can simply be accounted for by interstellar absorption, the non-detection of most of the brightest, nearest DAOs can only be accounted for by heavy element opacity. This confirms the hypothesis suggested earlier by Bergeron *et al.* (1994). However, it should be noted that statistically we should not

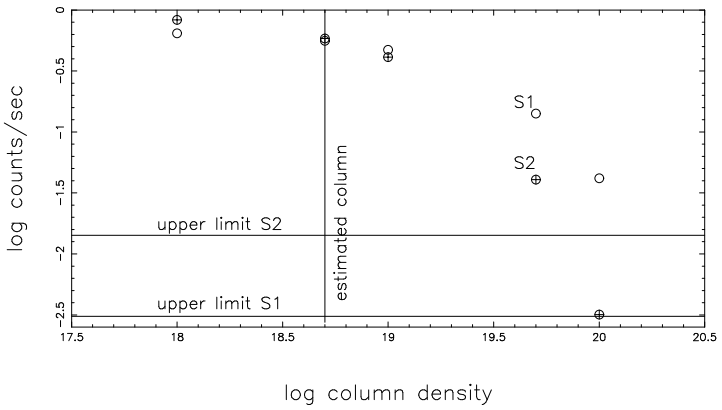

Figure 4.4: LB2: Model predicted count rates for the S1 and S2 filters plotted as a function of interstellar column density

Table 4.4: The DAO sample stars: reasons for non-detection by ROSAT

Name	V	T_eff	log g	d(pc)	N_H	sub-class	reason
PG0134+181	17.14	56400	7.4	710	$>10^{20}$	post-EHB	interstellar absorption
PG0834+501	15.82	60400	7.11	520	$>10^{20}$	post-EHB	interstellar absorption
Ton 353	16.71	66100	7.11	840	$>10^{20}$	post-EHB	interstellar absorption
GD 561	14.52	65300	6.71	330	$>10^{20}$	post-EHB/DD?	heavy elements
Feige 55	13.57	58300	7.15	170	10^{20}	DD	heavy elements
PG1413+015	17.09	48100	7.69	490	$>10^{20}$	DAO+dM	interstellar absorption
PG1210+533	14.07	44800	7.89	100	$5x10^{19}$	binary?	interstellar absorption
LS V +46 21	12.4	77300	7.31	110	10^{20}	post-AGB	heavy elements
Ton 320	15.82	68800	7.68	350	$>10^{20}$	post-AGB	heavy elements
LB2	15.62	65700	7.67	310	$<5x10^{18}$	post-AGB	heavy elements
PG1305−017	16.23	44400	7.76	250	$>10^{20}$	stratified	thin H layer

necessarily expect to see any more DAOs in the EUV than the three that have already been detected. Overall, DAOs constitute around only 1% of all known white dwarfs, but they already constitute 2.5% of the ROSAT sample.

Table 4.4 summarises the results of this study. The DAOs have been listed according to their subclassification. Of the 'post-EHB' stars, only GD 561 shows any evidence for heavy element contamination. This is an interesting observation, given that GD 561 may be a double degenerate like Feige 55, whose non-detection can also only be accounted for by heavy element opacity. As mentioned earlier, if GD 561's spectrum is in fact a composite of two closely separated white dwarfs, then the temperature and surface gravity measurements may be erroneous, seriously effecting this analysis (and the same might be true for Feige 55). On the other hand, this may

not be a significant result. Most of the 'post-EHB' stars are faint (V<16) and distant (>500pc). There is no reason to suppose that 'post-EHB' stars should be deficient in elements heavier than He compared to hot (T>60,000K) post-AGB CO white dwarfs of average mass such as G191−B2B (Lanz *et al.* 1997), and if they were closer they may well have shown evidence for photospheric contamination.

All the 'post-AGB' stars show strong evidence for heavy elements, but the non-detection of the close DAO+dM binary PG1413+015 and the possible binary PG1210+533, both consistent with post-AGB evolution, can be accounted for by interstellar absorption. Again, are these results significant, and is it telling us anything about the three systems seen by ROSAT?

With the exception of the 'post-EHB' Ton 353, the non-detection of all the DAOs T>60,000K cannot be accounted for by interstellar absorption. Ton 353 is very faint (V≈17) and distant (d=840pc) and its non-detection is not really a surprise. On the other hand, the post-AGB LB2, for example, is much closer and lies in a low column direction (<5x10^{18}cm^{-2}) where it should have been seen. Indeed, there are several hydrogen-rich DAs, for example RE J1738+61 (Barstow *et al.* 1994b), detected by ROSAT at temperatures greater than 60,000K. It may be that the DAOs in this temperature range are in general not detected either because of the mixture of helium and heavier elements, or because the presence of helium and a different atmospheric structure allows more heavy elements to be supported.

It should be noted that for the higher temperature (T>56,000K) DAOs, especially those associated with planetary nebula, a self consistent fit cannot be achieved for all the Balmer lines simultaneously (Napiwotzki & Schönberner 1993). This is believed to be caused by the presence of additional opacity due to heavy elements, and not helium alone. In fact, the problem is seen in all the DAOs studied by Bergeron *et al.* (1994), except those in close WD+dM binaries, PG1210+533 and PG1305−017. The strong evidence presented here for heavy elements in some of these stars supports this solution for this Balmer line problem. It has been argued earlier in this chapter that mass loss may account for the presence of helium in hot DAOs. This mass loss could also strongly affect the metallic content of the DAO atmospheres. Indeed, significant quantities of heavy elements have been detected in the IUE echelle spectra of LS V+46 21 (Tweedy & Napiwotzki 1992) and Feige 55 (Holberg *et al.* 1995).

Recently, Barstow *et al.* (1997) have shown from analysis of EUVE spectra of white dwarfs that the presence of heavy elements does not in fact become significant until temperatures of at least 50,000K. The ROSAT DAOs, plus PG1413+015 and PG1210+533, are all below T≈55,000K, and thus we would not necessarily expect to see much heavy element contamination. In addition, none of these stars suffer from the Balmer line problem discussed above, and, since they are the product of binary interaction, the metal abundances in these objects may be significantly different from the post-EHB and isolated post-AGB objects. No heavy elements are seen in the high resolution IUE spectrum of PG1210+533 (Holberg 1996), and, although CIV is seen in the far-UV spectrum of RE J1016−053 (Figure 4.6) and possibly in RE J2013+400 (Figure 4.7), this is probably circumstellar. Indeed later in this chapter it is shown that the EUVE spectrum of RE J0720−318 can be matched with a simple H+He structure.

This study has helped to strengthen the suggestion that the three ROSAT DAOs, which all lie in close binary systems with dM companions, belong to a separate, distinctive subclass, in which the atmospheres are not significantly enhanced with heavy elements, and the helium originates from a different source to the isolated post-AGB and post-EHB objects. The other confirmed member of this subclass, PG1413+015 was not detected because it is faint and its EUV flux is absorbed in the interstellar medium. Until the nature of PG1210+533 has been unambiguosly determined, it is difficult to say anything definitive about this star.

4.4 The ROSAT DAOs

RE J1016−053, RE J2013+400 and RE J0720−318 were identified as DAOs from their optical spectra as part of observations to follow-up ROSAT EUV sources. As well as the distinctive HeII absorption feature at 4686Å, narrow emission lines were also observed in the cores of the Balmer absorption dips, the signature of a close binary system (Figure 4.5). This emission arises as EUV radiation from the white dwarf illuminates the face of the red dwarf, photoionizing H and He atoms in the star's photosphere. Recombination follows, giving rise to HI, HeI and HeII emission features in the optical region. The emission lines vary in strength and velocity as the pair orbit each other, and in general this enables the binary period to be determined.

In fact, a fourth DAO has now been identified in the ROSAT WFC and EUVE surveys. Photospheric helium (HeII) has recently been found in the EUVE spectrum of GD50, a massive ($\approx$1.2M$_\odot$), isolated white dwarf, which maybe the result of a stellar merger (Vennes, Bowyer & Dupuis 1996). If this is the case, angular momentum may have been conserved in the merging process. Indeed, Vennes, Bowyer & Dupuis (1996) find evidence for large rotational velocities in the line profiles, indicating that the helium may be being dredged up from deeper layers into the EUV-emitting region of the photosphere by large circulation currents. The DAO classification of GD50, which shows no evidence of a HeII line at 4686Å in its optical spectrum, further confuses the evolutionary picture of these white dwarfs, and it must be considered as another, separate, DAO subclass.

GD50 will not be discussed further in this chapter, since it is clearly a peculiar, unique object, and does not display HeII in its optical spectrum (though this may be due to line broadening at high gravity and large rotational velocity). The rest of this section is devoted to discussing what is already known about the three ROSAT DAO+dM binaries in the literature.

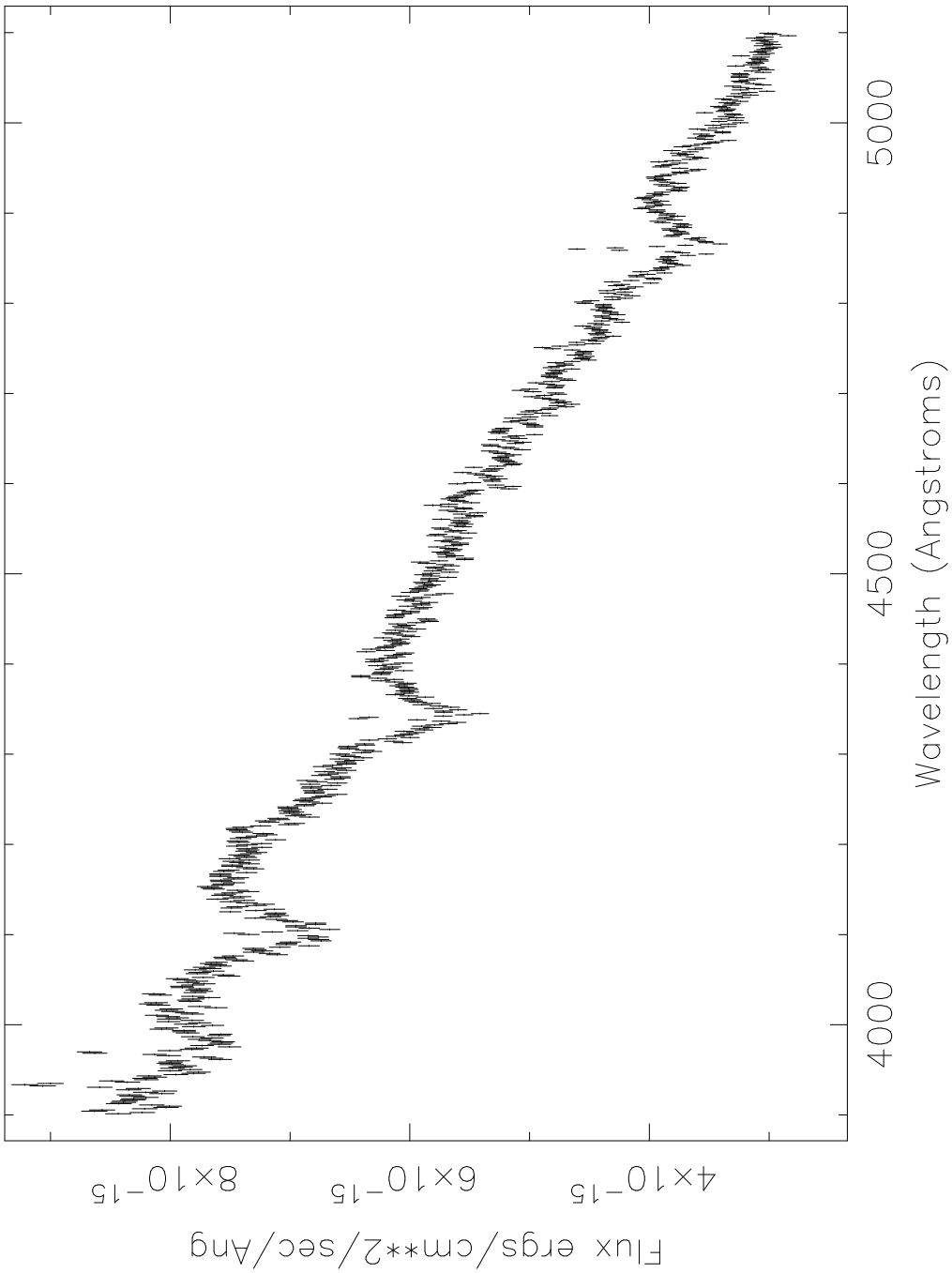

Figure 4.5: Optical spectrum of RE J0720−318, showing the distinctive emission lines in the cores of the H Balmer absorption dips. These are due to EUV radiation from the white dwarf being reprocessed and re-emitted at optical wavelengths by the red dwarf. Note also the HeII absorption feature at 4686Å which characterises all DAO white dwarfs.

4.4.1 RE J1016−053

The binary nature of RE J1016−053, and the classification of the white dwarf as a DAO, was first discussed by Tweedy *et al.* (1993) and Jomaron *et al.* (1993). Using a homogeneous model fit, Tweedy *et al.* (1993) found the temperature of the white dwarf to be 55800±1000K, log g=7.81±0.07, He/H=3x10^{-4}, and M=0.57M$_{\odot}$.

Tweedy *et al.* (1993) also reported a weak HeII feature at 1640Å in the low resolution IUE SWP spectrum of RE J1016−053. In addition, they found an unexpectedly strong CIV absorption feature at 1549Å. I have extracted four low resolution IUE spectra of this object that now exist in the archive (SWP44748, SWP44749, SWP49831 and SWP49884) , all reprocessed with the NEWSIPS calibration (see Chapter 3), and co-added them (Figure 4.6) to improve the signal-to-noise. The CIV 1549Å feature is clearly visible, although the reality of the HeII 1640Å feature is a little harder to demonstrate.

The most detailed analysis of the system to date has been undertaken by Thorstensen, Vennes & Bowyer (1996). From extensive optical spectroscopy they find the orbital period of the system to be 0.78929±0.00003 days. The inclination of the system is at least 40° and probably higher when the likely masses of the two components are taken into account. Thorstensen, Vennes & Bowyer (1996) estimate the red dwarf spectral type to be dM1.5±2, by comparing the optical spectrum between 5700−6700Å (where the red dwarf is visibly contaminating the white dwarf) with a collection of scaled, flux calibrated M dwarf spectra (Boeshaar 1976). They recognise, however, that this spectral type estimate may only be an upper limit if there is substantial heating of the continuum and line-forming region of the red dwarf's photosphere by EUV radiation from the white dwarf. The authors also obtained high resolution far-UV spectra with IUE, and matched the HeII 1640Å absorption line with an abundance He/H=2x10^{-3}, considerably in excess of the abundance determined from fitting the optical spectrum. If the carbon is photospheric in origin, the abundance is at least C/H=1x10^{-4}.

The most likely origin of the helium in RE J1016−053 is accretion from the stellar wind of the red dwarf companion (Tweedy *et al.* 1993, Jomaron *et al.* 1993, Thorstensen, Vennes & Bowyer 1996). However, the discrepancy between the optically measured helium abundance and that determined from the high resolution IUE data is intriguing. One explanation might be that the

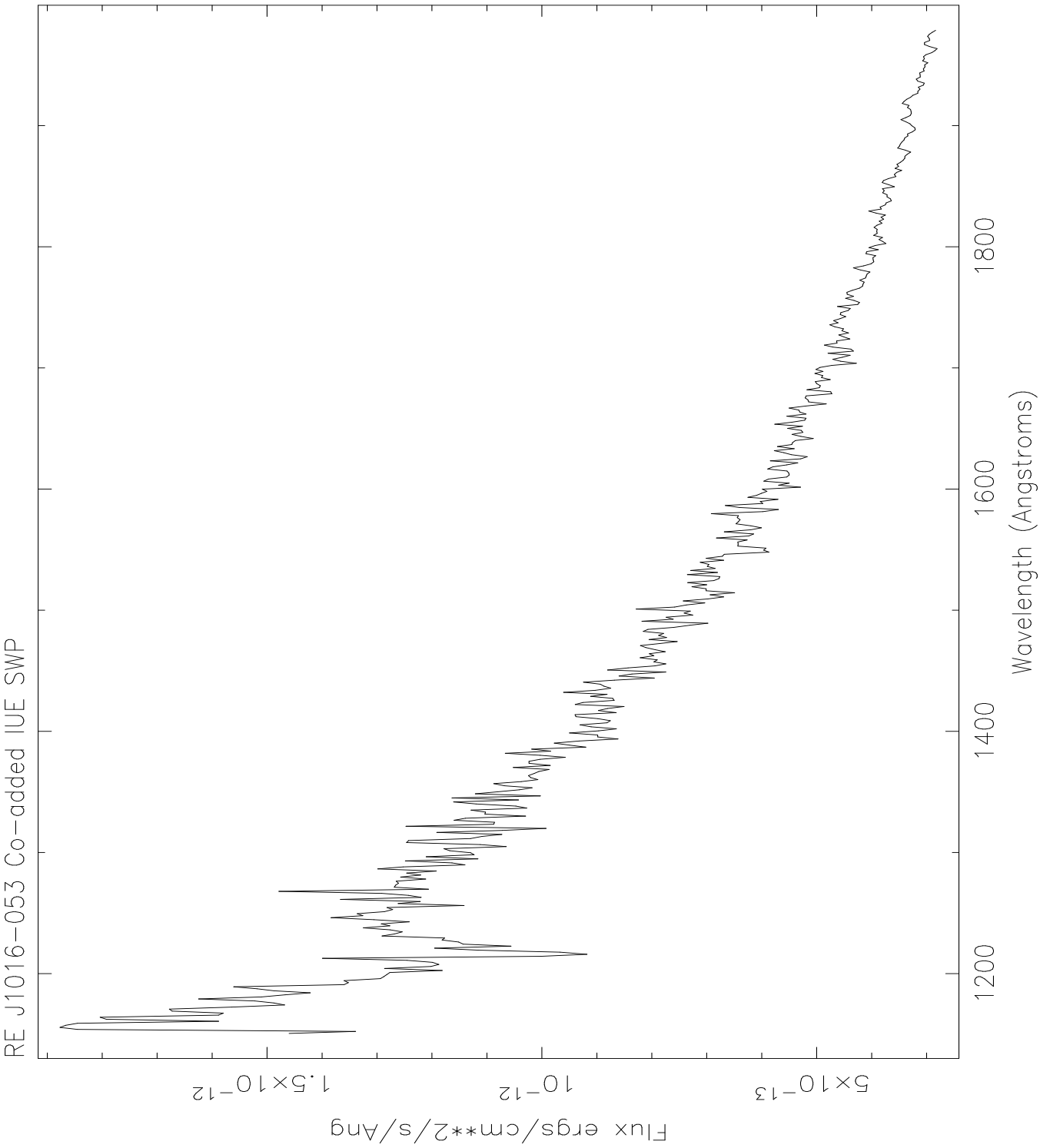

Figure 4.6: Co-added low resolution IUE SWP spectrum of RE J1016−053, showing the CIV absorption feature at 1549Å. Note the lack of a HeII absorption feature at 1640Å, although Tweedy *et al.* (1993) claimed the existence of such a line in two IUE spectra (SWP44748 and SWP44749).

optical HeII 4686Å absorption line is filled in by the emission component, giving an erroneously low abundance measurement when compared to the far-UV measurement. Alternatively, if the helium is being accreted, the accretion may be episodic. Thorstensen, Vennes & Bowyer (1996) note that the HeII 4686Å absorption dip varies in antiphase to the emission, suggesting the helium is indeed photospheric in origin. The unusually large carbon abundance indicates, however, that this is more likely to be circumstellar in origin, since if it was photospheric then the star would almost certainly be undetectable in the EUV.

4.4.2 RE J2013+400

This second EUV-bright DAO+dM system was first identified by the Leicester white dwarf group in 1992 (Barstow *et al.* 1993a). The binary period is estimated from radial velocity variations at 0.71 days, and, like the majority of DAOs, the optical spectrum of the white dwarf can only be matched by a homogeneous model. Bergeron *et al.* (1994) give the photospheric parameters as T=47,800±2400K, log g=7.69±0.16 and He/H=2.4x10^{-3}. However, the co-added low resolution IUE spectrum (Figure 4.7, SWP46427+SWP54498) shows no evidence of a HeII absorption feature at 1640Å. Barstow *et al.* (1995a) claim a detection of CIV 1549Å in SWP46427, although this is not obvious in SWP54498 or the co-added spectrum (the star is too faint to be observed in high resolution with IUE). Furthermore, the EUV/soft X-ray data from ROSAT requires the helium abundance to be a factor 1-2 lower in the deeper photospheric layers than at the surface. This strengthens the conclusion from RE J1016−053 that the helium in these stars is being accreted onto the surface of the white dwarf from the wind of the dM companion.

4.4.3 RE J0720−318

RE J0720−318 became the third DAO+dM system to be discovered by the ROSAT WFC and EUVE when it was independently identified optically by Vennes & Thorstensen (1994b) and Barstow *et al.* (1995c). The spectroscopically determined parameters, T=53,630±1000K, log g=7.64±0.1, He/H=2.75x10^{-4} and M=0.57M$_{\odot}$ confirm that, like RE J2013+400 and RE J1016−053, the white dwarf is the product of post-AGB evolution (Barstow *et al.* 1995c). A later, more detailed study by Vennes & Thorstensen (1996) places the binary period at 1.26245±0.00004 days.

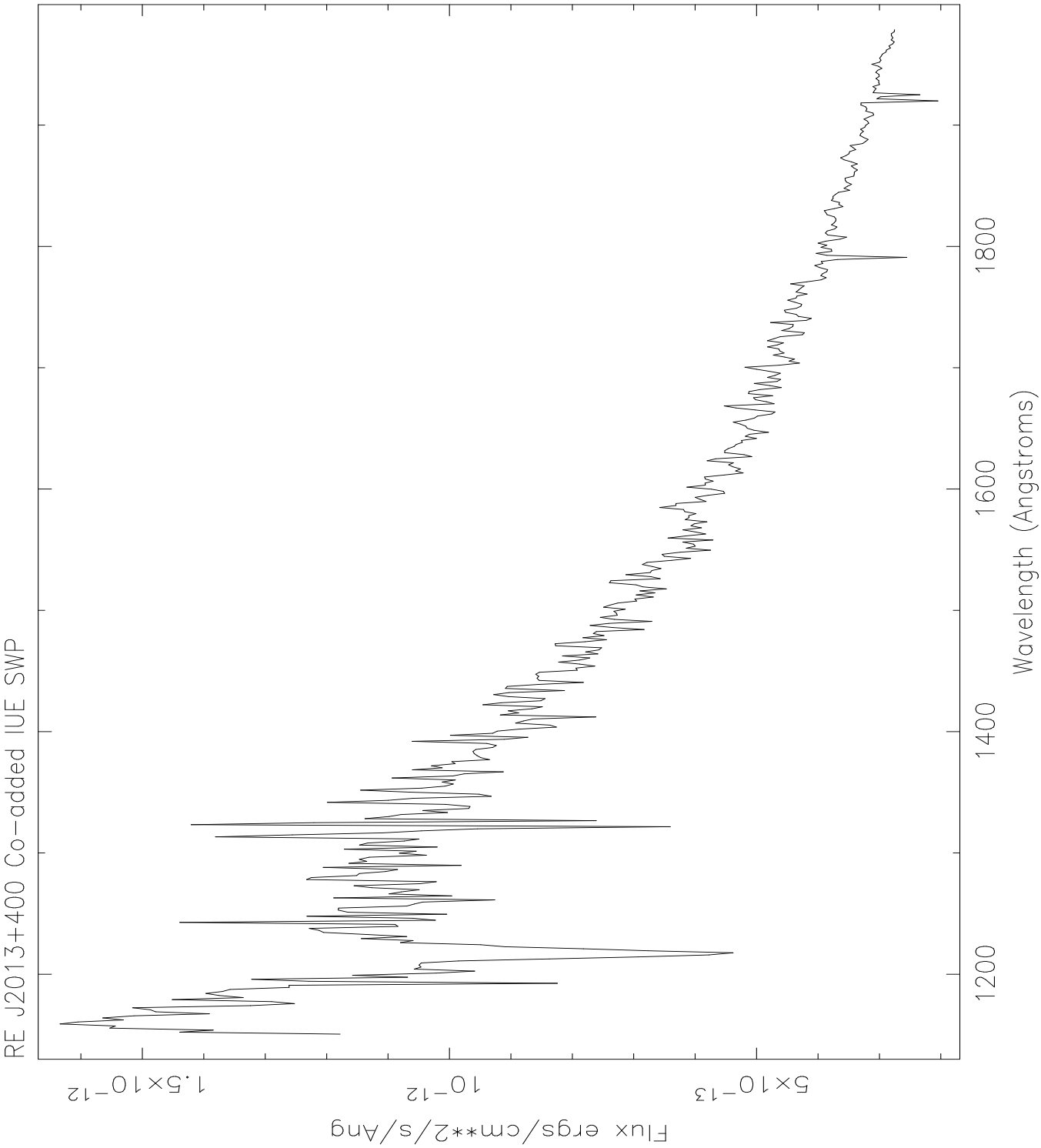

Figure 4.7: Co-added low resolution IUE SWP spectrum of RE J2013+400. There is no evidence for CIV 1549Å or HeII 1640Å in this spectrum.

As with RE J1016−053 and RE J2013+400, the simple homogeneous H+He model fits to the optical data cannot be reconciled with the ROSAT data points. All three stars display significant EUV opacity, and while in RE J2013+400 this may well be interstellar, in the other two stars Barstow *et al.* (1995c) conclude that this is probably due to elements heavier than He.

4.5 A Far-UV and EUV Study of RE J0720−318

4.5.1 Observations and Data Reduction

EUVE

RE J0720−318 was observed by EUVE in 'dither' mode between 1995 December 16-20, and was detected in all three wavebands with exposure times of 122,459s (SW, 70−190Å), 121,067s (MW, 140−380Å) and 112,861s (LW, 280−760Å). The average spectral resolutions in each band are 0.5Å (SW), 1Å (MW) and 2Å LW respectively, although these vary by about a factor ≈2. A more detailed description of the satellite and the instruments can be found in the Appendix.

Systematic variations in the EUVE detector efficiency, with an amplitude of up to ±20% with respect to the average, originally limited the signal-to-noise that could be achieved to ≈5. However, since 1993 the satellite has operated in 'dither' mode, which consists of a series of pointings slightly offset in different directions from the nominal source position, and was employed for this observation of RE J0720−318. By using this mode to average out flat field variations, a substantial fraction of the fixed pattern noise can be removed. This technique has improved the S/N of the dithered spectrum of HZ43 by around a factor 4 (Dupuis *et al.* 1995, Barstow, Holberg & Koester 1995). A more detailed description of the 'dither' mode and the causes of the systematic variations in the detector quantum efficiency is given by Dupuis *et al.* (1995).

Dupuis *et al.* (1995) also found that the 2nd, 3rd and 4th order spectral responses, which all overlap in the LW spectrometer, had been over-estimated pre-flight. This is an important instrumental effect to take into account, since near the HeI 504Å edge (which is very strong and astrophysically important in RE J0720−318, Figure 4.9) a substantial contribution by 2nd and 3rd orders is expected. Dupuis *et al.* (1995) find that a correction needs to be applied to each order, and they divide the 2nd order by a factor 1.4, 3rd by 1.2 and 4th by 1.1. These corrections have been included in the instrumental effective areas used in the analysis presented here.

The spectra have been extracted from the images using the EUV package in IRAF and other standard IRAF procedures, because the nominal extraction provided to guest observers neglects

the presence of a curvature in the spectrum on the detector plate, and also fails to account for substantial deviations from the plate centre. The observation was split into two exposures (e.g. exposure times of 116164s+6296s in SW), and needed to be aligned and co-added in IRAF before extraction. A 20 pixel wide aperture defined the source spectrum, with 50 pixel wide strips either side of this used to estimate the background contribution. As discussed above, the count rate errors in a source as bright as this are dominated by pixel to pixel variations in the detector efficiency. Therefore, to take account of any remaining residual fixed pattern noise in this dithered observation, a 5% systematic has been quadratically added to the statistical errors on the data (Barstow, Holberg & Koester 1995).

Two bright spots were seen on the SW detector plate image. These could not have been cosmic ray hits since the dithering had spread them out into a characteristic pattern. It transpired that these were due to previously unknown but recurring, variable intensity hot spots, and that one fell on the spectrum itself at about 114Å (EUVE Newsletter, Feb. 1996). This area has been ignored during the subsequent modelling and analysis.

IUE

Two low resolution IUE SWP spectra (SWP54496 and SWP54497, exposure = 40 minutes each) were obtained at the IUE ground station at Vilspa, Spain on 1995 April 24. These have been extracted and calibrated with the NEWSIPS processing, which gives an absolute error for each data point, and then co-added to improve the overall signal-to-noise (Figure 4.8). A full description of the IUE satellite is given in the Appendix. The NEWSIPS extraction and calibration process is discussed in Chapter 3.

ROSAT PSPC

We have also included the ROSAT PSPC soft band (0.1-0.4keV) X-ray count rate (0.455 counts/sec) in our analysis (Fleming *et al.* 1996). Significantly, RE J0720−318 was not detected in the PSPC hard (0.4-2.4keV) band. We can assume, therefore, that the vast majority of the EUV and soft X-ray flux comes from the white dwarf alone, and that the red dwarf companion is not active.

4.5.2 Spectral Analysis

A set of fully line blanketed stratified and homogeneous H+He models, computed by Koester (1991) (see also Chapter 3), has been fitted to the far-UV and EUV data, using the XSPEC spectral fitting programme. The stratified model assumes plane parallel geometry with a thin H layer overlying a helium atmosphere, under LTE conditions. The H layer mass spans in the approximate range $10^{-16}\,M_{\odot}>M_H>10^{-11}\,M_{\odot}$. The second model structure assumes a homogeneous distribution of H+He, also under LTE conditions, lying in the range $-8>\log\,He/H>-2$. The spectral fitting technique has been described in detail for the modelling of IUE and ROSAT data in Chapter 3, but it is worth reiterating here to emphasise the approach for the analysis of EUVE spectra, paying particular attention to how the errors are estimated for the measured parameters.

XSPEC works by folding the predicted spectrum through an instrument response function and then comparing it with the observed count spectrum using a χ^2 statistic. Due to the difficulty in finding suitable order separation filters in the EUV, there is considerable overlap of the spectral orders in EUVE data, and it is not possible to provide a flux calibration for the instrument simply by dividing the counts by the effective area function. The folding operation in XSPEC calculates the count spectra for each order of an individual grating, and then co-adds them to model the effective spectrometer response. When a good fit has been achieved, a fluxed spectrum is produced by deconvolution of the data and instrument response with reference to the model. The instrument response function is in the EUVE reference calibration data archive, which is supplied with Guest Observer data. It takes into account the overlapping orders, including the Dupuis *et al.* (1995) corrections described previously, and the variation with wavelength of the spectral resolution.

Once a best model fit to the data has been achieved, it is possible to estimate the uncertainty in any parameter by considering the variation in χ^2 as the parameter value is stepped in small increments away from the best fit value. All the other parameters are allowed to vary so that the new value of χ^2 is a minimum for the fixed value of the parameter in question. This technique was pioneered by Lampton, Margon & Bowyer (1976), who showed that for a best fit model with p free parameters and a minimum chi squared ${\chi^2}_m$, then if the parameter is to be known to a confidence C it must lie within a region of parameter space bounded by $\chi^2={\chi^2}_m+\delta\chi^2$. The

values of $\delta\chi^2$ for different values of p and C are given in Table 3.6. Thus, in practice, once a confidence level has been defined, each free parameter is incremented in turn and a fit made until the value of χ^2 increases by the relevant value of $\delta\chi^2$ given in Table 3.6. This is taken to be the error range for that parameter, and can be visualised as a process of finding the edges of a confidence region. If the confidence region for a model with two free parameters x and y is plotted on a graph, it is charcteristically shaped like an ellipse with the best fit values at the centre. To know the parameters to the specified confidence level, they must lie within the ellipse.

The appropriate value of $\delta\chi^2$ depends on the number of 'interesting' parameters, or in other words the number of variables in the model which can significantly effect the quality of the fit. For the EUVE spectrum analysed here, the combined H+He synthetic spectra and ISM models are specified by a number of independent parameters including effective temperature, log surface gravity, helium abundance (or H layer mass in a stratified model), a distance/radius related normalisation constant, HI column density, HeI column density and HeII column density. However, the temperature and gravity were already known from Balmer line fits to the optical data, and were only allowed to vary within their 90% limits (see Table 4.5). In addition, the V magnitude (V=14.87$\pm$0.04), calculated by Barstow *et al.* (1995c) to account for the contribution by the red dwarf companion, was used as a normalisation point. Hence, only four parameters were completely unknown, and so for an estimate of the 1σ error on each of these the required value of $\delta\chi^2$ was 5.9.

Table 4.5: Optically derived parameters for RE J0720−318, from Barstow *et al.* (1995c). The 90% limits were used to constrain the fit to the EUVE data.

Parameter	Value	90% limits
Temperature (K)	53,630	52,400−54,525
log gravity	7.64	7.54−7.74
log He/H	-3.56	-3.43 to -3.70

4.5.3 Results

Far-UV data

The co-added low resolution IUE SWP spectrum (Figure 4.8) clearly shows no evidence for even weak HeII absorption at 1640Å or any other heavy element features. This is in contrast to far-UV spectra of the similar system RE J1016−053 (Figure 4.6), which displays absorption lines of CIV 1549Å and possibly HeII 1640Å. Barstow *et al.* (1995a) also report CIV in the IUE SWP spectrum of RE J2013+400, although the feature is not obvious in Figure 4.7. No HeII 1640Å absorption line is seen in RE J2013+400, although the corresponding upper limit to the helium content, log He/H=-2.5, is entirely consistent with the optical data.

For RE J0720−318, assuming a homogeneous model structure and fitting the optically derived T and log g, the helium content implied from a fit to the optical data (log He/H=-3.56) can easily be hidden within the general scatter of the data points around 1640Å in the IUE spectrum. Indeed, a helium line would only be visible above the noise for log He/H>-2.5.

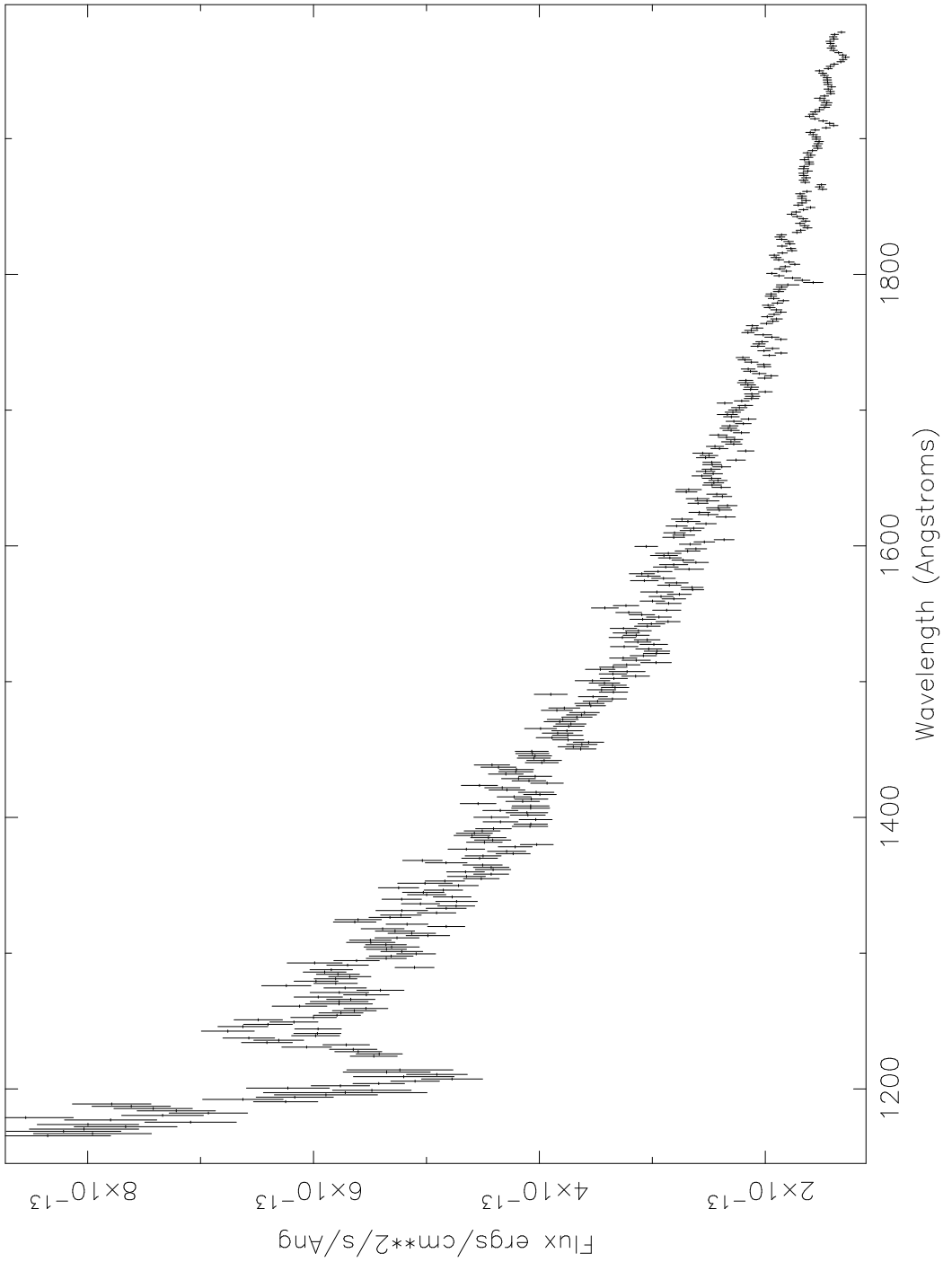

Figure 4.8: Co-added IUE SWP Spectrum of RE J0720−318. Note the absence of any weak HeII absorption feature at 1640Å

The EUVE spectrum

The entire EUVE spectrum is shown in Figures 4.9 and 4.10. The most striking feature is the saturated HeI absorption edge at 504Å, dominating the long wavelength spectrum. No similar feature has been seen in any other EUVE spectra of white dwarfs (e.g. Dupuis *et al.* 1995, Barstow *et al.* 1997).

Figure 4.9 shows the best fit using a homogeneous model. Although the HeI 504Å edge is well matched, the model flux cuts off before the predicted HeII edge at 228Å. The general shape of the short wavelength continuum is reproduced by the model, but the peak is redshifted by Z=0.511, which is not physically realistic. The photospheric helium abundance, log He/H=-3.43, is the upper limit of the 90% range derived from the fit to the optical data. In addition, the model predicts a negligible interstellar HeII column density and, therefore, the HeII absorption lines converging on 228Å must be photospheric in origin. However, in this model they are much deeper than the observed features. The 228Å edge can be better matched by assuming smaller photospheric helium abundances (log He/H<-4.0), but in these cases the model over-predicts the short wavelength flux. Larger helium abundances (e.g. log He/H=-2.90) provide worse matches to the 228Å edge, and cannot reproduce the short wavelength continuum.

The best fit stratified model is shown in Figure 4.10. All the major features are accurately reproduced, in particular the HeII series of absorption dips converging on the edge at 228Å, the edge itself, the 206Å HeI auto-ionisation feature, the short waveband continuum, and the HeI 504Å edge. The interstellar H and He column densities and hydrogen layer mass M_H derived from this best fit model are listed in Table 4.6. Removing the interstellar HeII from the model reveals that the HeII absorption lines must be due to photospheric helium, and the edge itself is produced by cooler, inter- or circumstellar material (see Figure 4.11).

Table 4.6: Interstellar H and He column densities and H layer mass derived from the best fit stratified model

Parameter	Value	1σ limits
nHI	2.30×10^{18}	$2.25-2.36\times10^{18}$
nHeI	1.44×10^{18}	$1.41-1.47\times10^{18}$
nHeII	9.78×10^{17}	$8.58-10.03\times10^{17}$
M_H	$3.07\times10^{-14}M_\odot$	$2.93-3.21\times10^{-14}M_\odot$

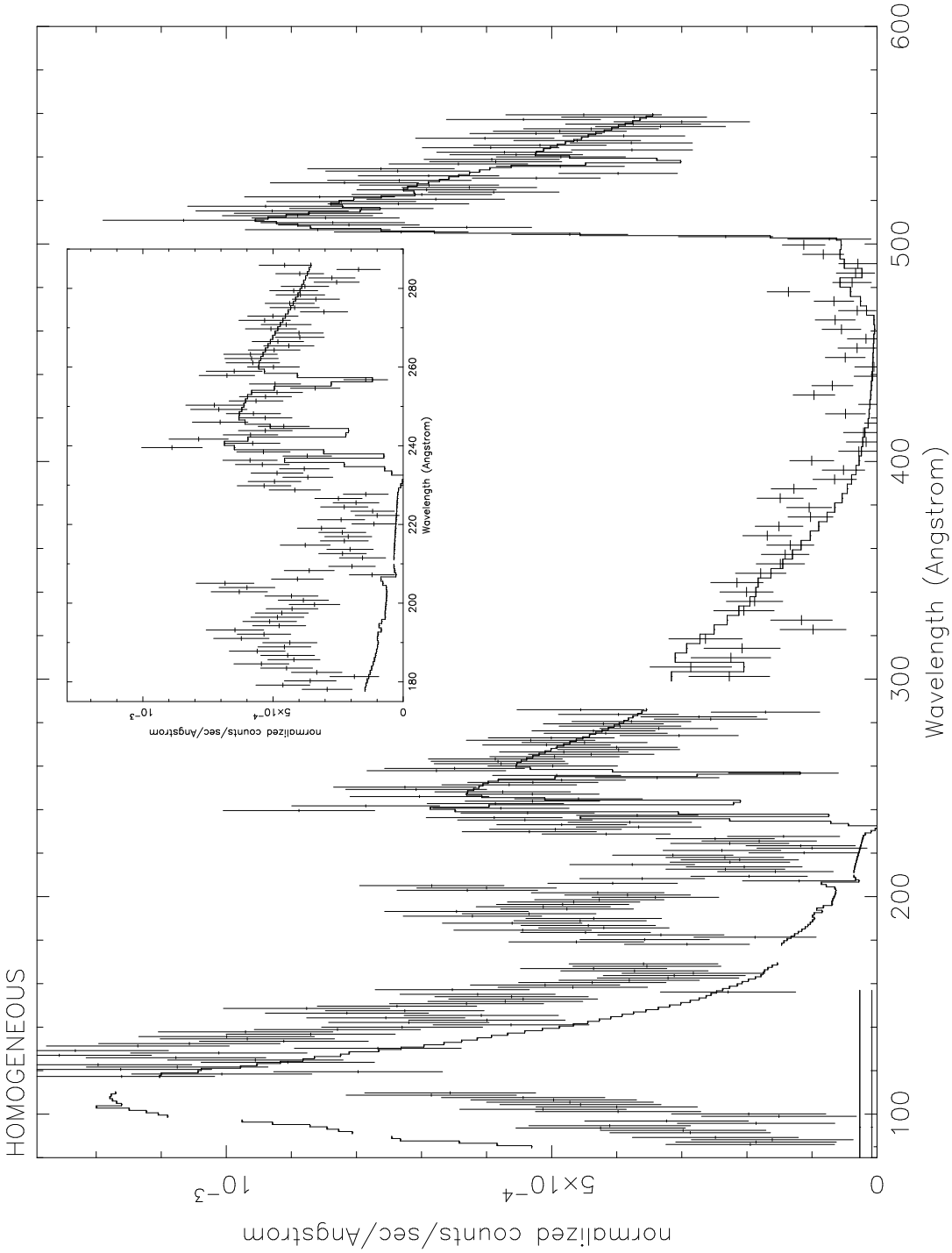

Figure 4.9: EUVE spectrum of RE J0720−318 with the best fit homogeneous model. Inset: the medium waveband spectrum and fit.

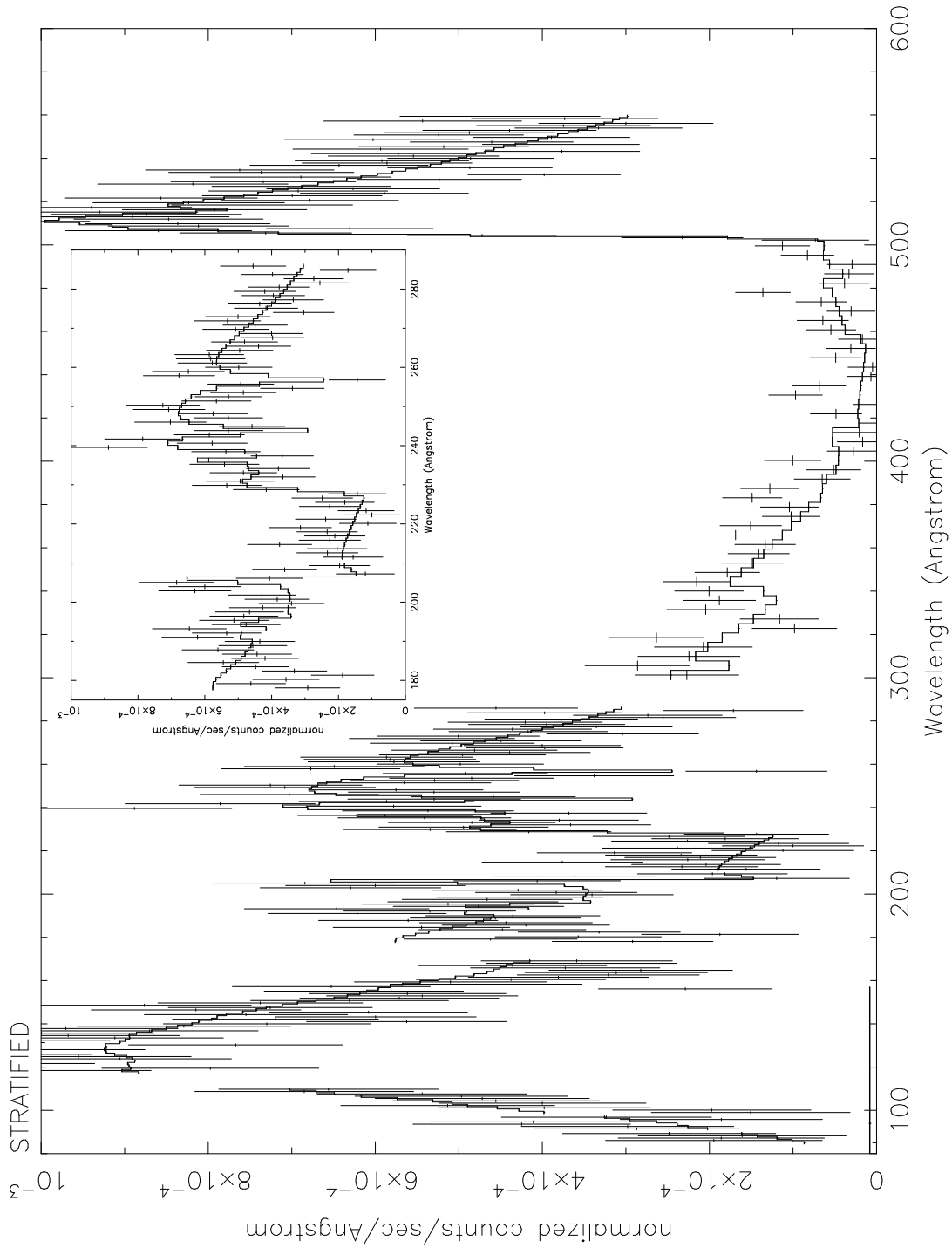

Figure 4.10: EUVE spectrum of RE J0720−318 with the best fit stratified model. Inset: Best fit to the medium waveband.

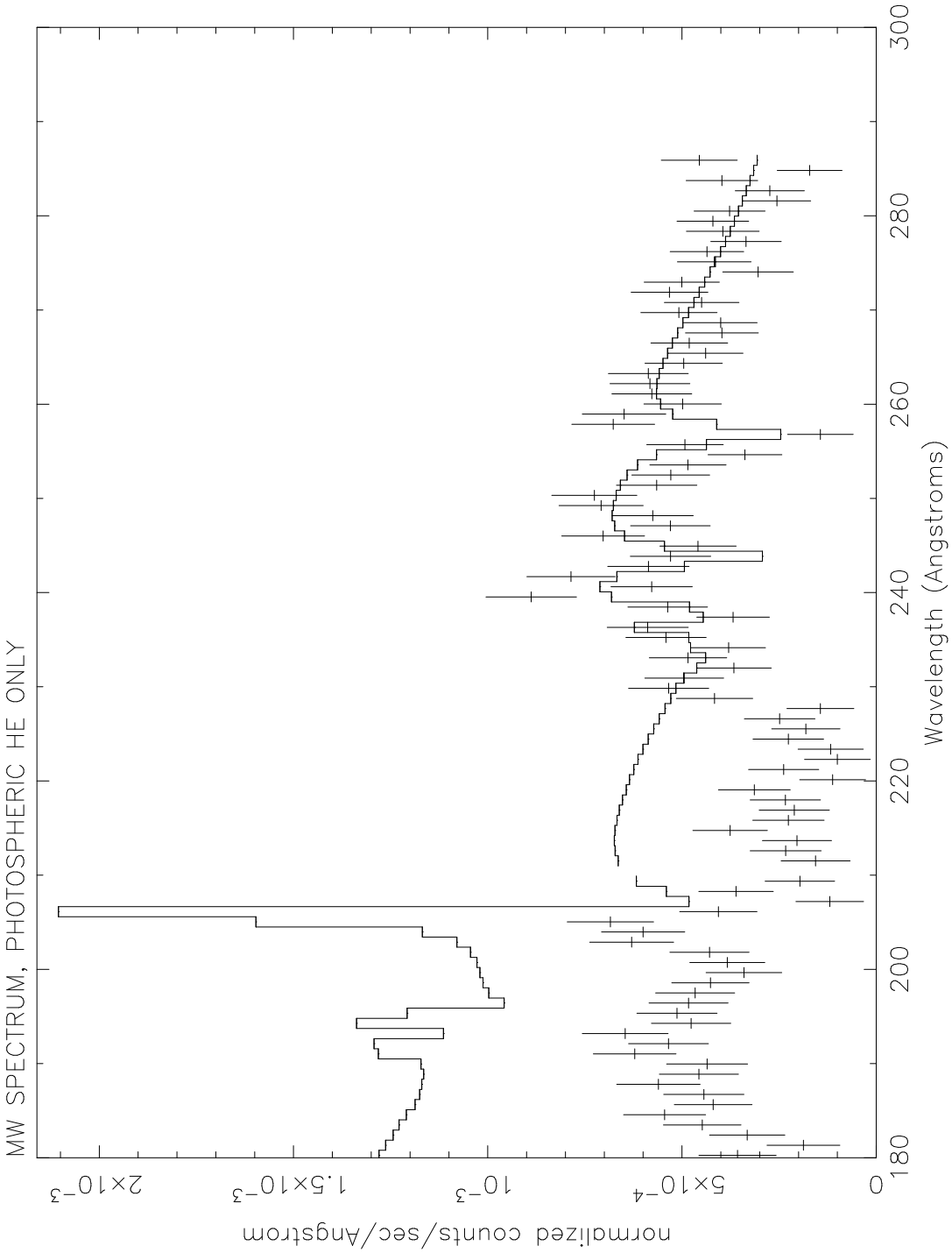

Figure 4.11: EUVE medium waveband spectrum of RE J0720−318, showing the model fit with photospheric helium only (i.e. N_{HeII}=0). The HeII absorption lines converging on 228Å are reproduced, but the edge itself is not matched.

4.5.4 Discussion

The EUVE spectrum of RE J0720−318 has yielded three important results. Firstly, in contrast to the optical spectrum, which can only be matched with a mixed H+He model structure, the EUV spectrum can only be reproduced by a stratified atmosphere. Secondly, the white dwarf has an unexpectedly thin H layer, $3\times10^{-14}M_{\odot}$. Finally, there appears, compared with HI, to be an unusually high line-of-sight helium column density to the system (see Table 4.6). If it is assumed to be interstellar, the implied hydrogen ionization fraction, given a cosmic He/H ratio, is 90%, and the helium ionization fraction is 40%. The failure to model the EUVE spectrum with a homogeneous atmosphere confirms the result of Barstow *et al.* (1995c), who could not match the ROSAT WFC and PSPC data points with a mixed H/He structure. These authors also failed to fit the ROSAT data with a stratified model. However, the EUVE spectrum reveals line of sight absorbing material with a HeI/HI ratio far removed from the canonical (cosmic) value of 0.1 originally assumed, and an additional HeII component not previously taken into account.

The EUV and soft X-ray data can be matched by a stratified model, although this model cannot reproduce the HeII 4686Å feature in the optical region. This has important implications for our understanding of the white dwarf's structure and evolution, and for the binary itself. Since the EUV radiation originates from hotter, deeper layers of the white dwarf atmosphere, the underlying structure of the star must be stratified. The helium present in the optical spectrum may reside on the surface of the white dwarf in a thin mixed layer. This would suggest that the helium is being accreted from the red dwarf companion via a stellar wind, and is not intrinsic to the white dwarf itself.

The hydrogen layer mass derived from the stratified fit is the lowest found for any white dwarf from EUVE spectra (Barstow *et al.* 1997). If this had been an isolated star it would probably have evolved into a normal DA, but as it is in a close binary system the thin H layer may well be the result of mass transfer between the two components during an earlier common envelope phase. Thereafter, it is possible for any moderate mass loss to bring some of the underlying helium to the surface, giving the optical HeII 4686Å line, although this does not rule out the possibility that helium is still being accreted from the companion's wind.

Do these results imply that all DAO white dwarfs might possess thin homogeneously mixed surface layers, and underneath they are stratified? Unfortunately, it is impossible to answer this question from optical spectroscopy alone, and the only DAOs that can be observed spectroscopically with EUVE are the three new binary stars (ignoring GD50). However, the hydrogen columns towards RE J1016−053 and RE J2013+400 are high enough to prevent their detection in the EUVE MW and LW spectrometers, and a similar analysis to that performed here for RE J0720−318 cannot be undertaken.

Analysis of the fit to the medium waveband spectrum, with the interstellar HeII component removed (Figure 4.11), clearly shows that while the HeII series coverging on 228Å is photospheric in origin, the edge itself must be due to cooler interstellar or possibly circumstellar material. The high densities and temperatures encountered in the photosphere means there are significant populations of atoms being excited from the ground state, giving rise to these broad absorption lines. The cool interstellar/circumstellar gas is not dense, and the ground states of the atoms are mostly populated. Any absorption lines resulting from this gas will therefore be very weak, and very narrow in comparison to the photospheric lines since there is a far weaker gravitational field acting. In practise, only the 304Å interstellar HeII line is prominent in EUVE spectra. The thin H layer covering this star therefore allows us to see into the photospheric He layer, which is not visible in a DA white dwarf with a thick H atmospheric structure.

Barstow *et al.* (1995c) noted that RE J0720−318 displays significant EUV opacity, and they concluded that this was probably due to elements heavier than He. Dupuis, Vennes & Bowyer (1997) have indeed shown that the EUVE spectrum of RE J0720−318 can be matched by a homogeneous model including trace amounts of heavy elements, e.g. C, N, O, Si, S and Fe, amounting to about 1/100th the metallicity of the Sun, and providing the necessary EUV opacity. However, the fact that the EUVE spectrum can be so easily matched by a simple stratified H+He model argues against significant heavy element contamination. Barstow *et al.* (1997) have shown that the EUVE spectra of some DA white dwarfs in this temperature regime, which also appeared to show evidence for heavy elements from the ROSAT data, can in fact be modelled with pure H structures. The opacity in these cases appears to be in the interstellar medium. Similarly, in this case, the high HeI and HeII columns can provide the required opacity, and the detection of photospheric HeII in the EUV region provides a strong argument in favour of the thin H layer model.

Table 4.7: Comparison of the ionization fractions of H and He in the interstellar medium, and the HeI/HI ratio, measured for RE J0720−318, compared with the highest fractions calculated from EUVE spectra of DA white dwarfs using stratified photospheric models (source Barstow *et al.* 1997)

Star	f_H		f_He		N_{HeI}/N_H
	Value	1σ limits	Value	1σ limits	
RE J0720−318	0.91	0.90−0.91	0.40	0.37−0.42	0.63
HZ43	0.22	0.08−0.33	0.39	0.30−0.47	0.08
GD659	0.25	0.00−0.55	0.39	0.28−0.52	0.08
RE J2156−546	0.35	0.05−0.48	0.41	0.32−0.50	0.09
RE J1032−535	0.53	0.44−0.60	0.32	0.29−0.36	0.15
RE J2324−547	0.79	0.71−0.83	0.48	0.44−0.53	0.25

The HeI/HI ratio of ∼1 is, by around a factor ten, the highest measured in any direction in the sky from EUVE data (Barstow *et al.* 1997). This is so high that, taken together with the implied ∼90% hydrogen ionization fraction (also the highest measured from EUVE data, Table 4.7), we must question whether the absorbing gas lies in the local interstellar medium between ourselves and RE J0720−318, or if in fact this gas lies in the vicinity of the binary system. Analysis of the EUVE spectrum of a nearby DA white dwarf only a few degrees away, RE J0723−277 (Dupuis, Vennes & Bowyer 1997), reveals a line-of-sight HeII column density to this star N_{HeII}=1.6x10^{17} atoms cm^2, and an implied H ionization fraction of only 66%, significantly different from those measured for RE J0720−318. This suggests that either the ionization state of the local interstellar medium can vary substantially over very small angular scales, or that the peculiar ionization fractions measured to RE J0720−318 are partly due to circumstellar material.

It is possible that most of the helium resides in the RE J0720−318 system itself, in the form of a circumbinary gas. Recent theoretical studies of CE evolution by Terman & Taam (1996) suggest that circumbinary disks are likely to form in post-CE systems. The spiral-in process decelerates so rapidly in the final stages of CE evolution that material in the immediate vicinity of the binary cores is not expected to be immediately ejected from the system (the timescale of orbital evolution increases, and so less energy is being deposited into the common envelope from its interaction with the two orbiting cores). Instead, this matter forms a disk in the orbital plane of the binary (since studies show that ejection of the CE mainly takes place in this direction). It should be noted that Barstow *et al.* (1995c) find evidence to suggest the orbital inclination

of the binary may be as high as 85° (the HI emission falls to zero at one phase, implying the illuminated face of the red dwarf is obscured, although the system is not eclipsing), and thus it is possible that we are seeing the system through an optically-thin disk. The presence of this disk may affect the orbital evolution of the detached pre-CV, as is known to occur in pre-main sequence stars, through tidal and resonant interaction between the binary and disk. Processes such as gravitational radiation and magnetic braking have often been discussed as mechanisms in the evolution of pre-CV binaries, but thus far the effect of a circumbinary disk has been generally overlooked. The possible detection of such a disk in a post-CE system therefore has profound implications for our understanding of the formation and evolution of close binaries.

Chapter 5

The ROSAT WFC White Dwarf Binary Sample

5.1 Overview

Thirty-two hot white dwarfs have now been identified in detached binary systems from the ROSAT WFC all-sky survey, representing around 25% of the white dwarfs discovered in the EUV. A catalogue of these systems is presented in this chapter, together with a short discussion of some of the binaries not analysed in detail earlier in this thesis, and an analysis of the sample as a whole. In particular, an excess of high mass objects is found in this sample, similar to that seen in the study of 89 mainly isolated WFC white dwarfs by Marsh *et al.* (1997a), in comparison to optical surveys of white dwarfs. However, no optical sample has ever covered the same temperature regime as the EUV surveys, and the high mass excess may be common to all surveys of hot white dwarfs. Finally, I consider whether there are more detached white dwarf binary systems still awaiting discovery in the EUV surveys.

5.2 A Catalogue of White Dwarfs in Detached Binaries in the ROSAT WFC Survey

A catalogue of the 32 hot white dwarfs from the ROSAT WFC survey that have now been discovered to lie in detached binary systems is presented in Table 5.1. The temperature, surface gravity, mass and V magnitude of the white dwarfs are given, as well as the spectral type and magnitude of the companion. Finally, references are included indicating from where the parameters given in the catalogue were mainly taken.

An unambiguous temperature and gravity cannot be determined for the optically-hidden white dwarfs from fitting the H Lyman α 1216Å line in the far-UV IUE spectra alone, as has been discussed already in Chapter 3. Therefore, the assumption is made that the white dwarf and the main sequence star do indeed form a physical pair. Hence, the parameters are for the model which gives the best match to the distance of the main sequence companion. Twelve stars in the catalogue, mainly WD+dM pairs, are also included in the analysis of 89 ROSAT WFC hot white dwarfs by Marsh *et al.* (1997a). With one exception (PG 0824+289, see discussion later) the temperatures and gravities of these stars were determined from fitting the H Balmer lines seen in optical spectra, and the Marsh *et al.* (1997a) results are reproduced in Table 5.1.

White dwarf masses can be determined from theoretical mass-radius relationships once the temperature and gravity are known. Until recently, the zero-temperature mass-radius relation of Hamada & Salpeter (1961) was widely employed. However, Koester & Schönberner (1986) showed that if the effects of temperature are not taken into account in hot white dwarfs, then the predicted radii and masses are lower than their true values. Therefore, in this thesis, I have utilised the models of Wood (1995) for carbon core white dwarfs in the range $0.4\,M_{\odot}-1.2\,M_{\odot}$, and incorporating thick H layers ($10^{-4}\,M_{\odot}$). It should be noted that the masses of some of the white dwarfs hidden in binaries with normal stars (those discussed by Barstow *et al.* (1994a)) have been recalculated using the Wood (1995) models, since these were orginally determined using earlier (Wood 1992) models which did not incorporate thick H layers and did not extend to $1.2\,M_{\odot}$.

5.2.1 Subclasses

The majority of the systems in this sample are unresolved, spectroscopic binaries, although a couple of resolved systems such as Sirius are included. However, Sirius B has an orbital period of ~50 years, and were it not for the fact that it lies so close to Earth (2.64pc) it would be unseen and undetectable in the optical. Very wide common proper motion binaries (CPMB) such as HZ43 and G191−B2B are excluded from this study.

Seventeen of the binaries (50%) consist of an unresolved hot white dwarf plus a normal (main sequence or slightly evolved) star which dominates the spectrum in the optical, rendering the white dwarf undetectable at these wavelengths. Only two of these systems, were known before the publication of the first WFC catalogue (Pounds *et al.* 1993). The Hyades system V471 Tauri (WD+K2V) was discovered because the two components are eclipsing (Nelson & Young 1970), while HD27483 was a serendipitous discovery in an IUE observation of its active Hyades F-star companion (Böhm-Vitense 1993). Thus, the vast majority of this sample of invisible white dwarfs would have remained unknown and unidentifiable without the EUV surveys.

Twelve white dwarfs are found to be in pairs with red dwarf companions. Some of these are easily identifiable from the presence of emission lines in the cores of the H Balmer absorption dips (e.g. Figure 5.1). These are usually indication of a close binary system, and originate from the nearby red dwarf. Soft X-ray and EUV radiation from the hot white dwarf is reprocessed in the atmosphere of the red dwarf and re-emitted at optical wavelengths to produce these distinctive emission features. The period of the binary can be determined from radial velocity measurements of these emission lines, which can also vary in intensity as the pair orbit each other and the emitting face of the red dwarf moves in and out of view. However, caution must be applied as in some cases the emission can be intrinsic to the M star itself, for example if it is magnetically active and/or rapidly rotating. Where emission lines are not seen, the presence of the late-type companion can be seen through contamination of the white dwarf's optical spectrum at longer wavelengths (e.g. Figure 5.4).

Seven of the binaries have been confirmed, from their orbital periods of less than a few days, to be pre-cataclysmic variable (pre-CV) systems. Four of these (Feige 24, RE J0720−318, RE J1016−053 and RE J2013+400) are WD+dM binaries. Intriguingly, all four hot white dwarfs

display evidence of helium in their atmospheres (see Chapter 4). The prototype pre-CV V471 Tau (DA+K2V, Nelson & Young 1970) is also detected by ROSAT. Interestingly, the other two systems, KW Aur C (WD+F4V, P=2.99 days) and IK Peg (WD+A8m, P=21.7 days), both contain main sequence stars more massive than those normally associated with CVs. Since many of the binaries have yet to be studied in detail (e.g. some of the WD+dM pairs), and their orbital periods have yet to be determined with any certainty, more of these systems may yet turn out to be pre-CVs.

Two binaries detected in the EUV have not been included in this catalogue. The white dwarf in AY Cet (RE J0116−02, WD+G5IIIe, Simon, Fekelj & Gibson 1985) is, at T=18,000K, too cool to be the source of the EUV flux. The central star of the planetary nebula (PN) IN Com (RE J1255+255) consists of a G5III star plus a very hot (T≈100,000K) pre-white dwarf. However, due to the presence of the PN, no reliable parameters have been determined for this star and thus it is cannot be included in the study of this sample.

5.2.2 Notes on individual systems

A brief summary is given below of some of the binaries not analysed earlier in this thesis. In particular, the evolutionary status of some of the WD+dM binaries for which no orbital periods have been determined is discussed. Optical observations of many of these systems were made by myself and colleagues as part of the follow-up study of the white dwarfs in the ROSAT WFC survey. The captions in Figures 5.1−5.4 indicate the source of each spectrum.

BD+08°102

The parameters of this hidden white dwarf are taken from Kellett *et al.* (1995); the system was also discussed extensively by Barstow *et al.* (1994a). The primary is an ultra-rapidly rotating early K star (period∼10 hours), is very magnetically active, and is the prototype of the newly proposed 'WIRRing' stars. Jeffries & Stevens (1996) argue that it may have been spun-up by accretion from the wind of the progenitor of the white dwarf, and could itself evolve into a Barium-giant star.

Table 5.1: A catalogue of white dwarfs in binaries in the ROSAT WFC survey

RE	Name	White Dwarf T	log g	M ($M_\odot$)	V_{wd}	Comp. SpT	V_{comp}	ref.
†RE J0024−74	HD2133	29,700	8.25	0.79	15.7	F7−8V	9.2	this thesis
†RE J0044+09	BD+08°102	28,700	8.5	0.91	14.5	K1−3V	10.16	Kellett et al. (1995)
RE J0134−16	GD984	44,850	7.96	0.66	13.96	M5V	?	Marsh et al. (1997)
RE J0148−25	GD1401	24,540	7.84	0.55	14.69	M4V	?	Marsh et al. (1997)
†RE J0228−61	HD15638	46,000	8.5	0.97	14.7	F3−6V	8.8	Barstow et al. (1994)
*RE J0235+03	Feige 24	62,950	7.53	0.54	12.56	M1.5V	14.7	Marsh et al. (1997)
†RE J0254−05	HD18131	31,130	8.0	0.65	12.5	K0IV	7.32	this thesis
*RE J0350+17	V471 Tau	34,200	8.80	1.12	13.65	K2V	9.7	Marsh et al. (1997)
†RE J0357+28		30,960	7.9	0.60	14.9	K2V	13.0	this thesis
†RE J0420+135	HD27483	22,000	8.5	0.94	14.6	F6V	6.17	this thesis
†RE J0459−10	HR1608	27,260	8.0	0.55	13.1	K0IV	5.38	Barstow et al. (1994)
†RE J0500−36		39,000	7.0	0.40	17.8	F5-G0V	13.7	this thesis
§RE J0534−02		28,680	7.99	0.64	16.20	dM	?	this thesis
†*RE J0515+32	KW Aur C	46,550	8.0	0.55	13.9	F4V	7.95	Barstow et al. (1994)
RE J0645−164	Sirius	24,700	8.65	1.03	8.35	A1V	-1.47	Marsh et al. (1997)
*RE J0720−31		53,630	7.64	0.55	14.87	M2V	16.66	Barstow et al. (1995B)
§RE J0827+28	PG 0824+289	36,000	8.0	0.66	14.79	dC	?	Wolff et al. (1995)
RE J0845+48	HD74389	41,000	7.85	0.56	15.0	A0V	7.4	Liebert et al. (1990)
*RE J1016−05		53,830	8.08	0.65	14.21	M1.5V	16.6	Marsh et al. (1997)
†RE J1014+26	BD+27°1888	34,130	7.25	0.39	14.8	A8−F2V	9.2	this thesis
†RE J1027+32		32,440	7.5	0.45	16.9	G0−4V	13.0	this thesis
§RE J1036+46	GD123	28,770	7.92	0.61	14.34	dM	?	Marsh et al. (1997)
§RE J1111−22	β Crt	36,500	7.5	0.45	13.9	A2III	4.48	Barstow et al. (1994)
RE J1126+18	PG 1123+189	55,640	7.62	0.55	14.13	dM	?	Marsh et al. (1997)
§RE J1426+50		26,290	8.00	0.64	14.00	dM2	?	this thesis
§RE J1629+78		42,500	7.6	0.47	13.0	M4−5V	?	Sion et al. (1995)
RE J1925−56		30,820	7.25	0.39	14.4	G2−8	10.6	this thesis
*RE J2013+40		47,800	7.69	0.57	14.6	M1−4V	?	Barstow et al. (1995A)
RE J2024+20		50,560	7.96	0.67	16.59	dM	?	Marsh et al. (1997)
†*RE J2126+19	IK Peg	34,540	8.95	1.19	14.4	A8m	6.07	Barstow et al. (1994)
†RE J2300−07	HD217411	35,600	8.2	0.68	14.7	G5	9.8	Barstow et al. (1994)
†RE J2353−70	HD223816	69,300	8.0	0.55	14.2	G0	9.9	Barstow et al. (1994)

† Hidden white dwarf

* Close pre-CV binary

§ Possible close binary

GD984

The white dwarf parameters are taken from Marsh *et al.* (1997a). The optical spectrum (Figure 5.1, top) reveals the presence of emission lines in the cores of the H_β 4861Å and H_γ 4341Å absorption dips. However, radial velocity measurements of this system by Schultz, Zuckerman & Becklin (1996) show that it is not likely to be close enough (P∼few days) to evolve into a CV within a Hubble time. Bues & Aslan (1995) give the spectral type of the red dwarf companion as dM5. They also report HeI (4471Å) and HeII (4686Å) absorption features in the optical spectrum of the hot white dwarf, in which case the star might be better classified as a DAO, but no such features are visible in Figure 5.1. Indeed, it is very unlikely for HeI to be detected in a 45,000K star.

GD1401

Again, the white dwarf parameters are taken from Marsh *et al.* (1997a). Bues & Aslan (1995) give the spectral type of the red dwarf companion as dM4. The absence of Balmer emission features in the optical spectrum (Figure 5.1, bottom) indicates that this is probably not a close binary system.

HD15638

The atmospheric parameters of this hidden white dwarf are taken from the analysis of the EUVE spectrum by Barstow, Holberg & Koester (1994b). The gravity is higher than derived in either of the discovery papers (Barstow *et al.* 1994a and Landsman, Simon & Bergeron 1993) from fitting the IUE spectrum alone. Similarly, the temperature is somewhat lower, and leads to a discrepancy between the distance calculated to the white dwarf and the distance to the primary. However, if heavy elements are present, (and they could be in sufficiently small quantities so as to yield no obvious spectral features), then the temperature would need to be higher and the discrepancy would disappear.

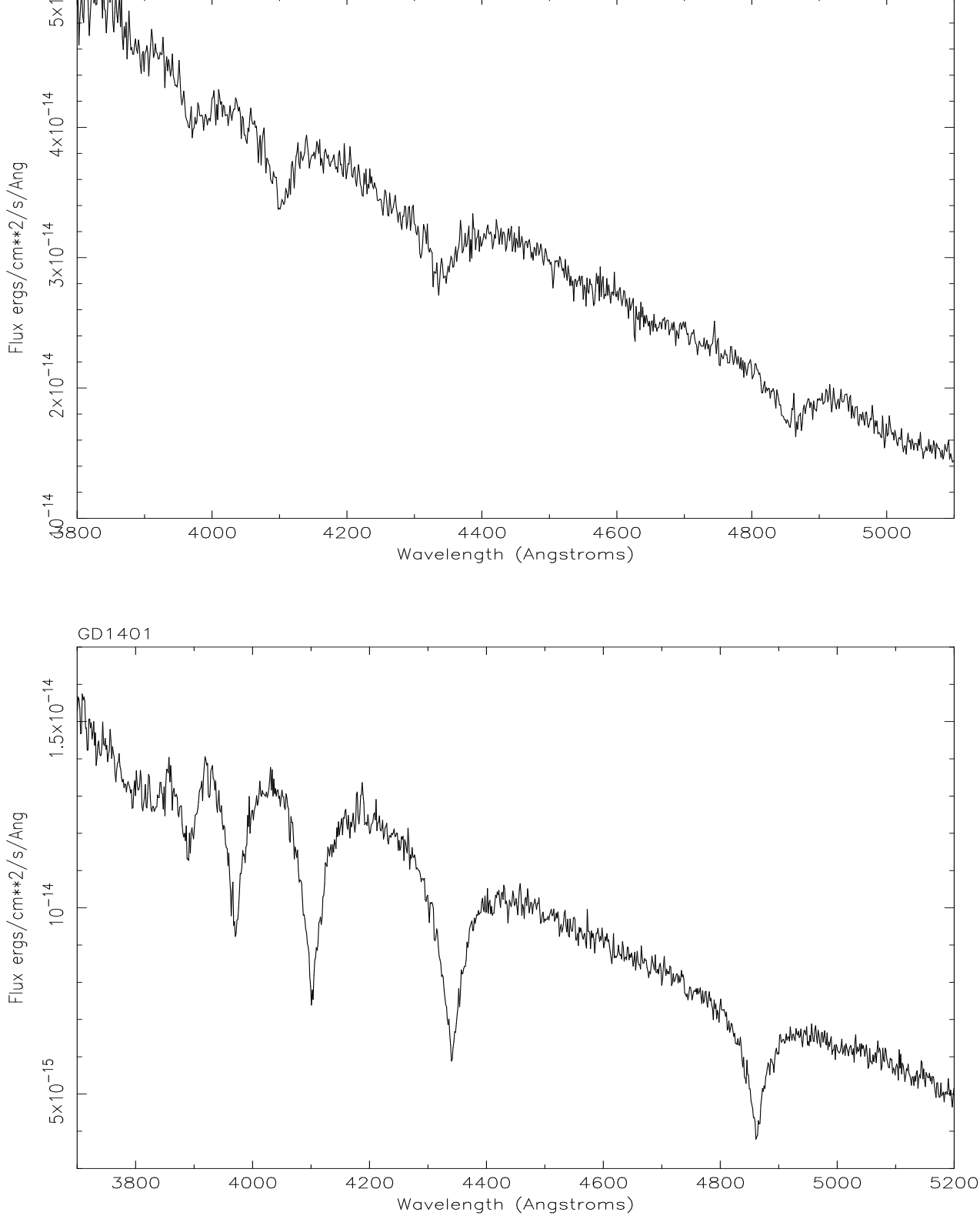

Figure 5.1: Top: Optical spectrum of GD984, obtained in September 1993 by Martin Barstow and Matthew Marsh with the 1.9m telescope at SAAO. Emission lines are present in the cores of H_β 4861Å and H_γ 4341Å. Bottom: GD1401, also observed from SAAO in September 1993. In contrast to GD984, no emission features are present.

Feige 24

The white dwarf parameters are taken from Marsh *et al.* (1997a). The system has been analysed in detail by Vennes & Thorstensen (1994a), who confirm that this is a pre-CV system with P=4.2316 days. The red dwarf (M1.5V) mass is $0.028-0.036 M_{\odot}$ and the inclination of the system is $\geq 75°$. Vennes & Thorstensen (1994a) also report a strong, transient HeII 1640Å absorption feature in high resolution IUE SWP spectra, and suggest that the star may be reclassified as a mixed He/H atmosphere DAO. The system is, in any case, very similar to the three slightly shorter period DAO+dM binaries discovered by ROSAT and EUVE, RE J1016−05, RE J2013+40 and RE J0720−31, discussed in Chapter 4.

V471 Tau

The prototype pre-CV, an eclipsing binary consisting of a hot white dwarf and a K2V companion, has been well studied by many authors since its discovery by Nelson & Young (1970). It is a member of the Hyades cluster and thus its age (5×10^8 years) is well determined. The binary period is 0.52 days, and it varies both optically and in the EUV with a period of 554.63s. This modulation is probably due to a dark spot on the surface of the white dwarf, which is accreting from the wind of the active K star companion. The parameters in Table 5.1 are taken from Marsh *et al.* (1997a). The authors subtracted a K2V spectrum from the optical data before the Balmer lines were fitted in their analysis.

HR1608

This hidden white dwarf is analysed in detail by Barstow *et al.* (1994a). The primary is active, with an estimated X-ray luminosity $L_x \approx 3\times10^{29}$ ergs s^{-1}. It is a single-lined spectroscopic binary with a period of 903±5 days.

RE J0534−021

An observation of this hot white dwarf by Jay Holberg (private communication) with the 2.3m Steward Observatory telescope on Kitt Peak in September 1995 revealed small emission lines

in the spectrum, suggesting a binary nature. A further spectrum was therefore obtained with the 1.9m telescope and RPCS spectrograph at SAAO in April 1996 (Figure 5.2, top). This spectrum also shows possible small emission features in the cores of H_ϵ 3970Å and H_δ 4102Å. The temperature and gravity given in Table 5.1 were determined from fitting the four H Balmer lines ($H_\beta - H_\epsilon$), following the prescription of Marsh *et al.* 1997a, using a chemically stratified model supplied by Detlev Koester (these models have been discussed in more detail in Chapters 3 and 4). Further study of this system is required to determine if it is indeed a close pre-CV binary.

KW Aur C

This is a close pre-CV binary, consisting of an F4V star and a hot white dwarf, with a period of 2.99 days (Webbink *et al.* 1992, Hodgkin *et al.* 1993, Barstow *et al.* 1994a).

PG 0824+289

This is the only example of a WD+dwarf Carbon (dC) binary in the ROSAT WFC catalogue. The white dwarf parameters given in Table 5.1 are from Wolff *et al.* (1995). These have been determined from a fit to an IUE SWP spectrum assuming log g=8.0, since the dC star contaminates the optical spectrum to ∼4200Å. This is evident from Figure 5.4. The unidentified features at ∼4300Å and ∼4450Å are almost certainly due to the dC companion. The white dwarf mass ($0.66 M_\odot$) has been estimated using Matt Wood's evolutionary models (Wood 1995). Marsh *et al.* (1997a) calculate T=51,900 and log g=8.00 from modelling the Balmer lines, but they did not allow for the contribution of the dC star.

Less than ten dC stars are known, and only three lie in binaries. Most are thought to be halo (population II) objects. However, this pair are more likely to belong to the young disk population, and the dC star possibly accreted its carbon from the progenitor of the white dwarf, via either a stellar wind or through common envelope evolution. The period of the system has yet to be determined, although Heber *et al.* (1993) report emission lines in the cores of the Balmer absorption dips, indicating that this might be a close binary. An emission line might be present in the core of H_γ 4341Å in Figure 5.4. Further study of this system is required.

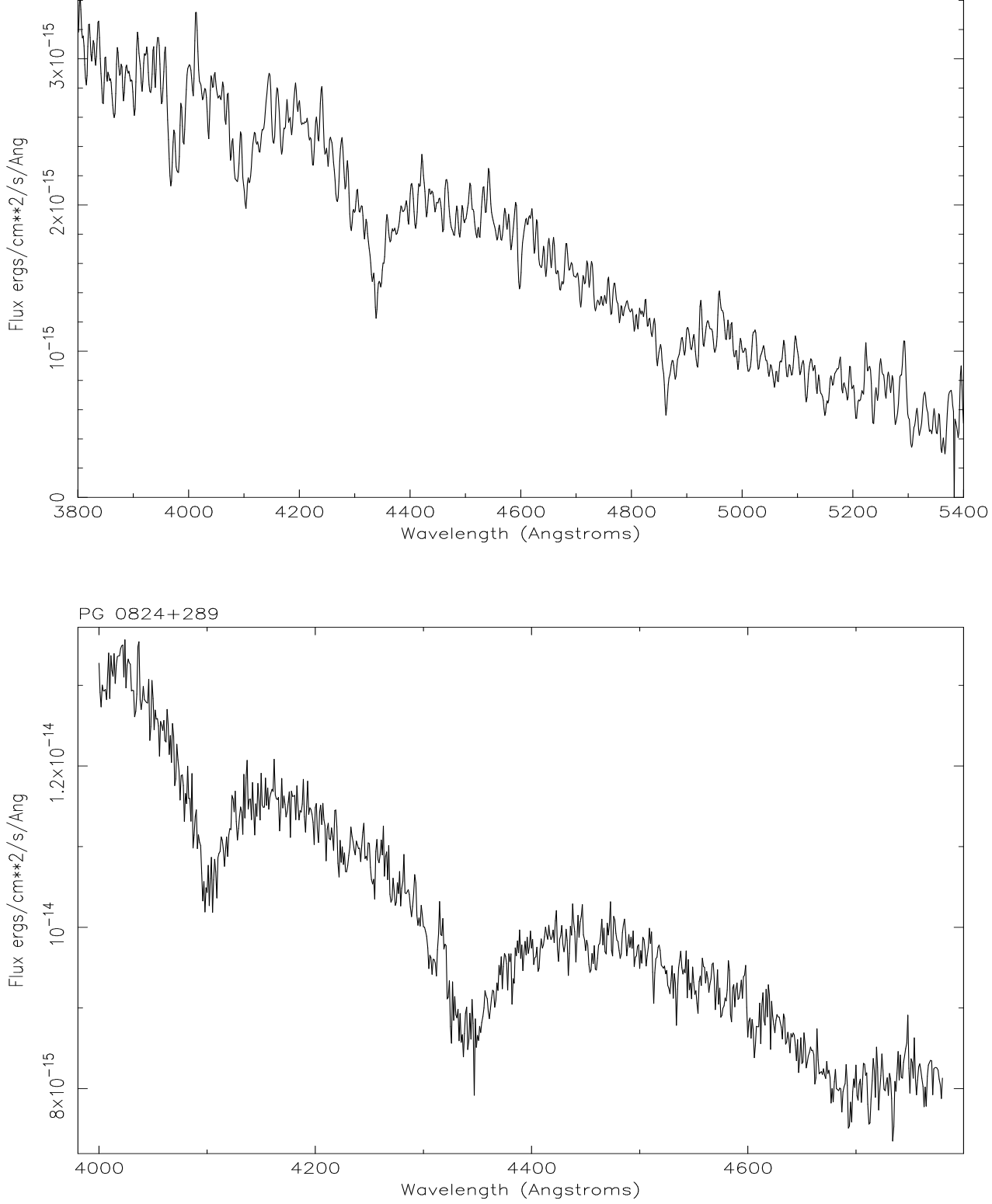

Figure 5.2: Top: Optical spectrum of of RE J0534−02, obtained on 14th April 1996 with the 1.9m telescope at SAAO. Emission lines are visible in the cores of H_ϵ 3970Å and H_δ 4102Å. Bottom: Optical spectrum of PG 0824+289 (DA+dC), taken in 1994 by Jay Holberg on the Steward Observatory 2.3m at Kitt Peak. The absorption features at ∼4450Å and ∼4300Å are probably due to the dwarf carbon star. Note the possible emission feature in the core of H_γ 4341Å.

HD74389

This is a wide resolved binary, with the white dwarf separated from the A0V companion by 20.6 arcsecs. The white dwarf was discovered by Sanduleak & Pesch (1990), and studied in detail by Liebert, Bergeron & Saffer (1990).

GD123

The spectral type of the companion was originally classified K by Green, Schmidt & Liebert (1986), although Schmidt & Smith (1995) report a dM spectral type. Slowly varying radial velocity measurements by Schultz, Zuckerman & Becklin (1996) indicate that this could be a close binary seen at low inclination. However, no emission features are visible in the optical spectrum in Figure 5.3. The white dwarf parameters were computed by Marsh *et al.* (1997a).

β Crateris

The white dwarf parameters are taken from Barstow *et al.* (1994a). Smalley *et al.* (1997) have analysed the atmospheric composition of β Crateris A in detail. They assign it an A2III spectral classification, leading to a distance estimate of 90 ± 10 pc. Radial velocity measurements by Campbell & Moore (1928), taken together with the masses of the two components, led Fleming *et al.* (1991) to suggest that the orbital period was <21 days, in which case this is a candidate pre-CV system. However, Smalley *et al.* (1997) report no radial velocity variations in data taken over several months.

PG 1123+189

A red dwarf companion to this star was first reported by Schmidt & Smith (1995). No radial velocity measurements have been published, and no emission features are visible in Figure 5.3 to indicate that this might be a close binary. The white dwarf parameters are taken from Marsh *et al.* (1997a).

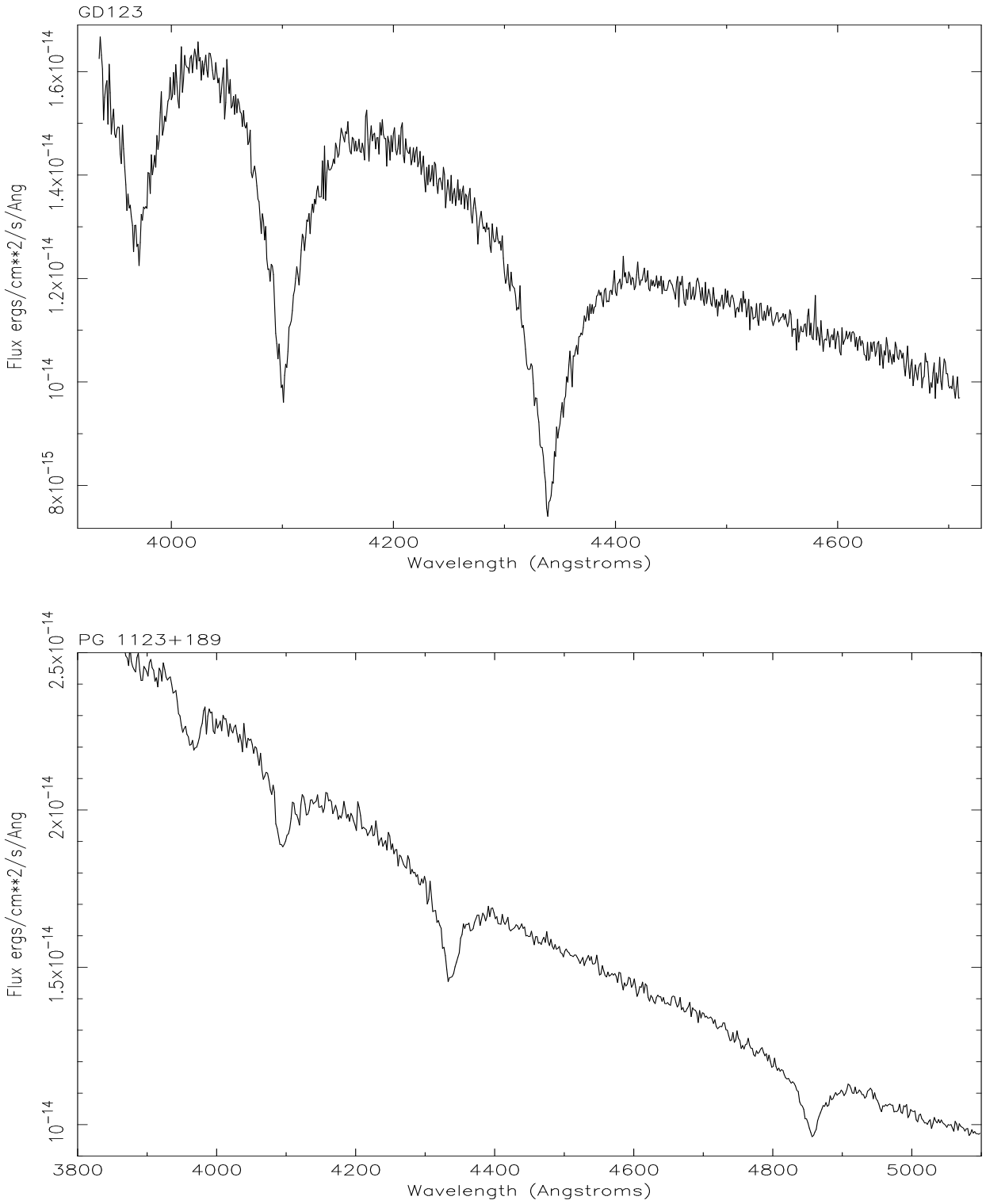

Figure 5.3: Top: Optical spectrum of GD123 (DA+dM), obtained by Jay Holberg with the Steward Observatory 2.3m on Kitt Peak, Arizona, in 1994. There is no evidence for Balmer emission cores in this spectrum. Bottom: Optical spectrum of PG 1123+189, obtained by Jay Holberg with the Steward Observatory 2.3m on Kitt Peak, Arizona, on 24th April 1993. Again, there is no evidence for Balmer emission cores in this spectrum.

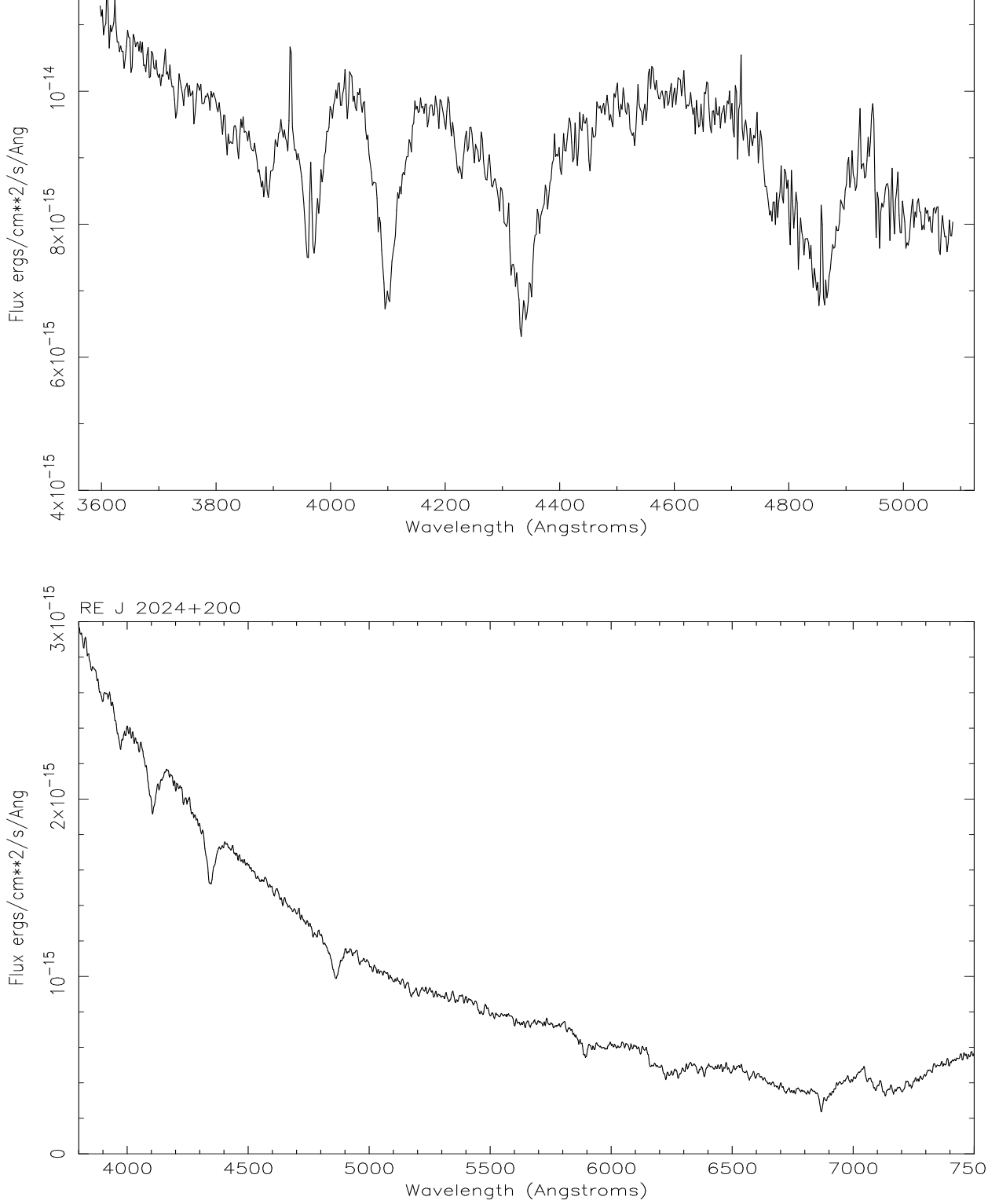

Figure 5.4: Top: Optical spectrum of RE J1426+50, obtained by Tom Fleming with the Steward Observatory 2.3m at Kitt Peak in 1995. The spectrum is contaminated by an M2V companion. It is not clear whether the emission lines in the cores of the H Balmer absorption dips indicate that this is a close binary system, or whether they are due to a nearby active M star which has also fallen within the slit. Bottom: Optical spectrum of RE J2024+20, obtained by Jay Holberg with the Steward Observatory 2.3m on Kitt Peak, Arizona, in 1994. There is no evidence of Balmer emission cores, but the red dwarf companion is clearly visible at longer wavelengths (>5500Å).

RE J1426+50

An optical spectrum (Figure 5.4), taken by Tom Fleming with the 2.3m Steward Observatory telescope at Kitt Peak in 1995, shows narrow emission lines in the cores of the Balmer lines, indicative of a close binary system. The spectrum is clearly contaminated by a late-type companion to at least 3900Å. An analysis of the white dwarf by Martin Barstow (private communication) yields T=26,290 (25,360−27,200) and log g=8.00 (7.85−8.17), assuming a spectral type of dM2 for the companion. Mason *et al.* (1995) report that the hot white dwarf is a member of a visual triple system. The other components are a dM star and a much closer, but resolved, active dMe star. It is plausible that this dMe star has fallen within the slit when the spectrum of the white dwarf was obtained. In that case this may not be a close binary, and should perhaps be better regarded as a common proper motion pair (and, therefore, should be excluded from my catalogue). Further detailed observations of this system are required to determine if this is the case.

RE J1629+78

This binary was the first EUV source detected by the WFC (and christened 'Meaty', Cooke *et al.* 1992). The white dwarf parameters are taken from Sion *et al.* (1995), who found no evidence of radial velocity variations in the narrow Balmer emission lines visible in the optical spectrum. These emission features are probably not due to reprocessing on the surface of the red dwarf but are intrinsic to that star. The period is likely to be between 4 and 6.5 days and the system will not become a CV within the Hubble time (Catalan *et al.* 1995).

RE J2024+20

The white dwarf parameters are taken from Marsh *et al.* (1997a). An optical spectrum taken by Jay Holberg with the 2.3m Steward Observatory telescope at Kitt Peak (Figure 5.2) clearly shows the red dwarf companion. The absence of Balmer emission lines suggests this is not a close binary.

IK Peg (HR8210)

This 21.7 day period pre-CV system, consisting of an A8m star and a hot white dwarf, is discussed in more detail by Landsman, Simon & Bergeron (1993), Barstow *et al.* (1994a), Barstow, Holberg & Koester (1994b), Wonnacott, Kellett & Stickland (1993), and Smalley *et al.* (1996). Re-calculating the mass of the white dwarf with Matt Wood's latest models (Wood 1995) has solved one outstanding problem with the system. Detailed observations to determine the orbit put the minimum mass of the white dwarf at $1.17\,M_{\odot}$ for an inclination of exactly 90° (Landsman, Simon & Bergeron 1995), yet Barstow, Holberg & Koester (1994b) had calculated $M=1.12\,M_{\odot}$, using Wood's earlier 1992 models. Since no eclipse has ever been seen in this system, the inclination must be <88° and therefore the mass even higher than $1.17\,M_{\odot}$. Using the latest evolutionary code and the temperature and gravity determined by Barstow, Holberg & Koester (1994b) from modelling the EUVE spectrum now puts the white dwarf mass at $1.19\,M_{\odot}$, in agreement with the mass derived from the orbital analysis.

5.3 The Mass Distribution

The white dwarf mass distribution is an important tool for constraining theoretical models of the final stages of stellar evolution, since the vast majority of all stars ($M<8\,M_{\odot}$) will end their lives as a white dwarf. Current theories predict that the minimum core mass for reaching the thermally pulsing stage of the AGB is $\approx 0.55\,M_{\odot}$ (Dorman, Rood & O'Connell 1993). White dwarfs less massive than this will have never formed a planetary nebula, since the post-AGB remnant takes too long to become hot enough to ionise the ejected envelope. These stars may have evolved directly from the horizontal branch via O and B subdwarfs. Stars less massive than $\approx 0.45\,M_{\odot}$ could only have evolved through binary interaction, which has brought about a premature end to their normal main sequence evolution. At the other end of the scale, high mass white dwarfs ($M>0.7\,M_{\odot}$) must have evolved from high mass ($M>3\,M_{\odot}$) progenitors.

Constructing and investigating mass and gravity distributions is also an excellent way of comparing a sample of white dwarfs with other studies. The white dwarfs in this study have been selected according to two important criteria: they are all in binary systems, and they are all detected in the EUV with the ROSAT WFC. The second selection effect introduces a bias in that only stars with T$\approx$22,000K or greater are seen. Below this temperature the EUV emission is insignificant. Only $\sim$120 of the $\sim$2,000 known white dwarfs have been observed in the EUV, since the majority are too cool to be detected. Thus, in comparison to most white dwarfs, the stars in this sample can be considered to be young, $<10^8$ years old.

The mass and gravity distributions for the WFC white dwarfs in binary systems are presented in Figures 5.5 and 5.6. Each distribution is compared to the optically-selected sample of Bergeron, Saffer & Liebert (1992) (129 stars, dotted line), and to the sample of 89 mainly isolated WFC white dwarfs of Marsh *et al.* (1997a) (dashed line). Only 12 objects ($\sim$1/3rd) are common to this work and the Marsh *et al.* (1997a) distribution [1]. The Bergeron, Saffer & Liebert (1992) and Marsh *et al.* (1997a) samples have been normalised to the size of the binary sample for easy comparison.

Until the full results of the Palomar-Green survey are published, the Bergeron, Saffer & Liebert

[1] This includes PG 0824+289, but, for reasons outlined earlier in this chapter, different atmospheric parameters have been adopted for this star in the analysis presented in here

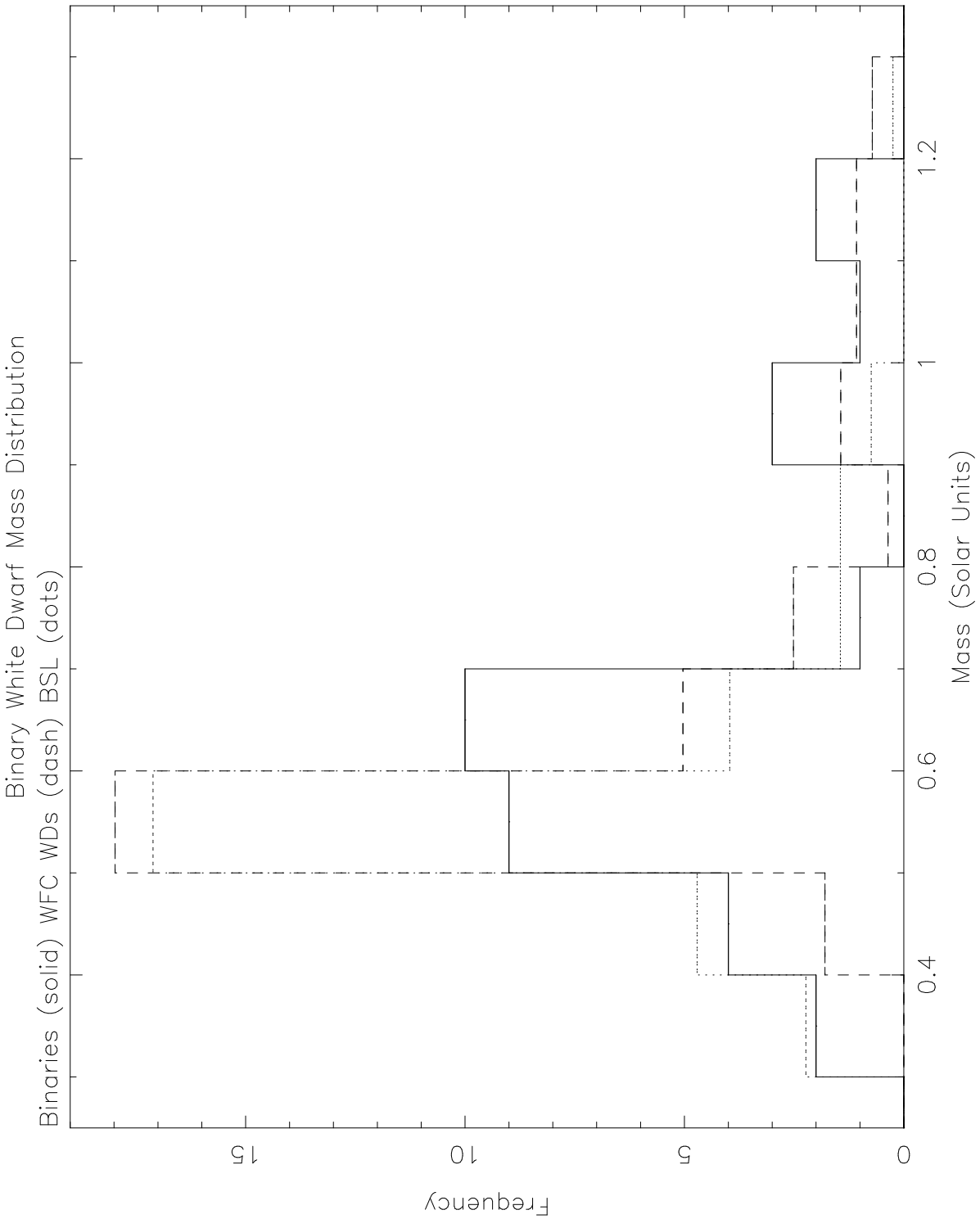

Figure 5.5: The mass distribution for the ROSAT WFC white dwarfs in detached binaries.

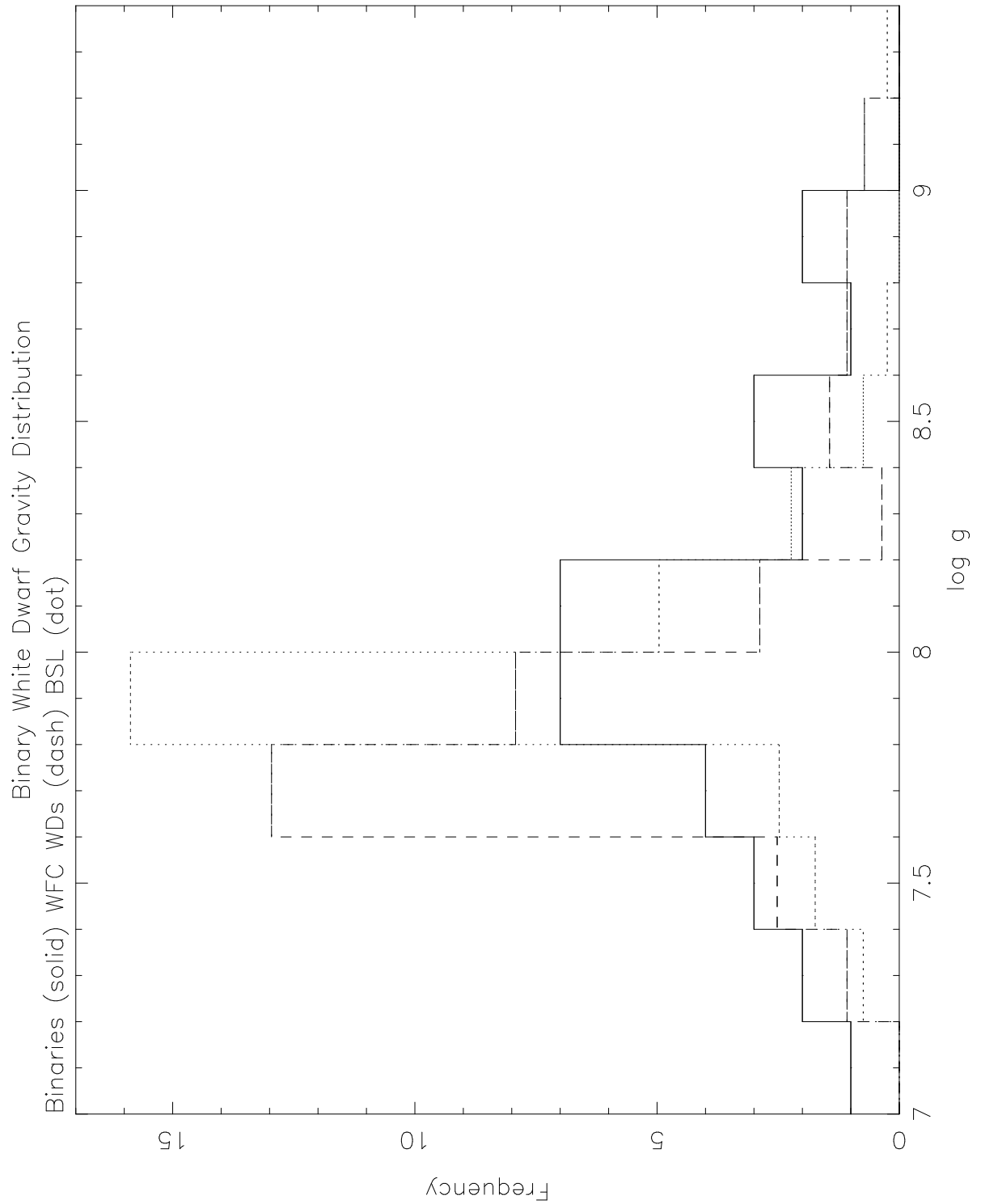

Figure 5.6: The distribution of surface gravities for the ROSAT WFC white dwarfs in detached binaries.

(1992) study is the most complete sample of white dwarfs with which to compare EUV-selected samples. Previous optical studies have been dominated by relatively cool stars with T<15,000K, and their temperatures and gravities were determined by photometric methods. Bergeron, Saffer & Liebert (1992) showed that, for T>15,000K, fitting the optical Balmer lines (where possible) provides a far more accurate method for computing these parameters. Even so, most of the Bergeron, Saffer & Liebert (1992) white dwarfs are still <25,000K, and very few of their objects have been detected by ROSAT. Bergeron, Saffer & Liebert (1992) determined masses using the old models of Wood (1992). These were recalculated by Bergeron, Liebert & Fulbright (1995) using the newer thick H layer models (Wood 1995) and these results have been used here. The mean mass of the Bergeron, Saffer & Liebert (1992) sample is $0.590\pm0.134\,M_{\odot}$, which compares with $0.644\pm0.189\,M_{\odot}$ for the mainly isolated WFC white dwarfs (Marsh *et al.* 1997a) and the mean mass of the WFC binary sample, $0.654\pm0.204\,M_{\odot}$. These are all in good agreement within the errors, which are standard deviations. A further comparison can be made with the gravitational redshift measurements of Reid (1995), which provide an independent check on the spectroscopic mass determinations. These measurements are restricted to white dwarfs with known radial velocities (i.e. white dwarfs in binary systems, common proper motion pairs, or members of open clusters). Using the 10m Keck telescope, and by measuring the velocity of the NLTE-core of the Hα 6563Å line, Reid (1995) derives a mean mass for his sample (34 non-cluster stars) of $0.583\pm0.078\,M_{\odot}$, in good agreement with the spectroscopically determined mass distributions. These results are summarised in Table 5.2.

Table 5.2: Comparison of optical and EUV mean gravities and masses

Sample	log g	σ	M/ $M_{\odot}$	σ	N stars
WFC WD Binaries	7.95	0.44	0.654	0.204	32
Marsh *et al.* (1997a)	7.90	0.38	0.644	0.189	89
Bergeron, Saffer & Liebert (1992)	7.91	0.26	0.590	0.134	129
Reid (1995)	-	-	0.583	0.078	34

The most striking feature of the mass distributions in Figure 5.5 is the apparant excess of high mass objects ($M>0.9\,M_{\odot}$) in the two EUV-selected samples when compared to the optical sample of Bergeron, Saffer & Liebert (1992) (Figure 5.6 also shows a corresponding excess in the EUV gravity distributions). Is this excess statistically significant? Marsh *et al.* (1997a) show that it is in their sample of mainly isolated stars at the 99.7% confidence level. A similar analysis can

be performed for the binary white dwarfs. If the Bergeron, Saffer & Liebert (1992) sample is regarded as a parent distribution of objects from which the EUV-selected groups are drawn, then the number of high mass stars that should have been detected by ROSAT can be calculated. The Bergeron, Saffer & Liebert (1992) sample can be separated into two groups of low mass ($M<0.85\,M_{\odot}$, 124 objects) and high mass ($M>0.85\,M_{\odot}$, 5 objects) stars. The probability that an individual star in this distribution has a high mass is 0.039. None of the WFC white dwarfs in binaries are actually present in the Bergeron, Saffer & Liebert (1992) group, and so, from Poissonian statistics, the prediction is that $1.25 \pm \sqrt{1.25}$ of these stars should have high masses. In fact, 6 stars have $M>0.85\,M_{\odot}$, i.e. an excess of 4.75 objects. Crudely, the significance of this excess is then $4.75/(\sqrt{1.25})=4.25$, equivalent to a confidence level >96%.

Is this high mass excess a feature of binary white dwarfs alone, given that the Bergeron, Saffer & Liebert (1992) and Marsh *et al.* (1997a) sample contain a number of white dwarfs in binaries (like Sirius B at $1.03\,M_{\odot}$) in addition to isolated stars? Figure 5.7 shows the ROSAT WFC binary white dwarf mass distribution plotted against the mass distribution of just the isolated objects (77 stars) from the sample of Marsh *et al.* (1997a). Visually at least, the excess still appears in both distributions. A statistical analysis similar to that performed earlier can also be applied here. If the isolated ROSAT WFC white dwarfs are now assumed to represent the parent population, then, since 11 of the 77 stars have high masses, the probability that any star will have a mass $>0.85\,M_{\odot}$ is found to be 0.143. Thus 4.58 of the binary stars should also have high masses. In fact, 6 binary white dwarfs have $M>0.85\,M_{\odot}$, an excess of 1.42. This is only a significance of $1.42/(\sqrt{4.58})=0.66$, and the conclusion must be that there is no significant difference between the isolated and binary populations, at least in terms of the high mass excess. However, the binary mass distribution does not demonstrate the clear, narrow peak centred at $0.55\,M_{\odot}$ that is visble in the isolated population. This may be partly a statistical effect reflecting the relatively small numbers of objects in the isolated sample, but it may also reflect the uncertainties in determining the properties of the optically invisible white dwarfs. This problem is discussed in more detail below.

This high mass excess implies that the most massive white dwarfs have the largest EUV fluxes, which is surprising since they should have the smallest radii and consequently the lowest luminosity for a given temperature and composition. It would appear, then, that the decrease in flux as a result of a smaller radius is more than offset by an increase in the star's intrinsic luminosity.

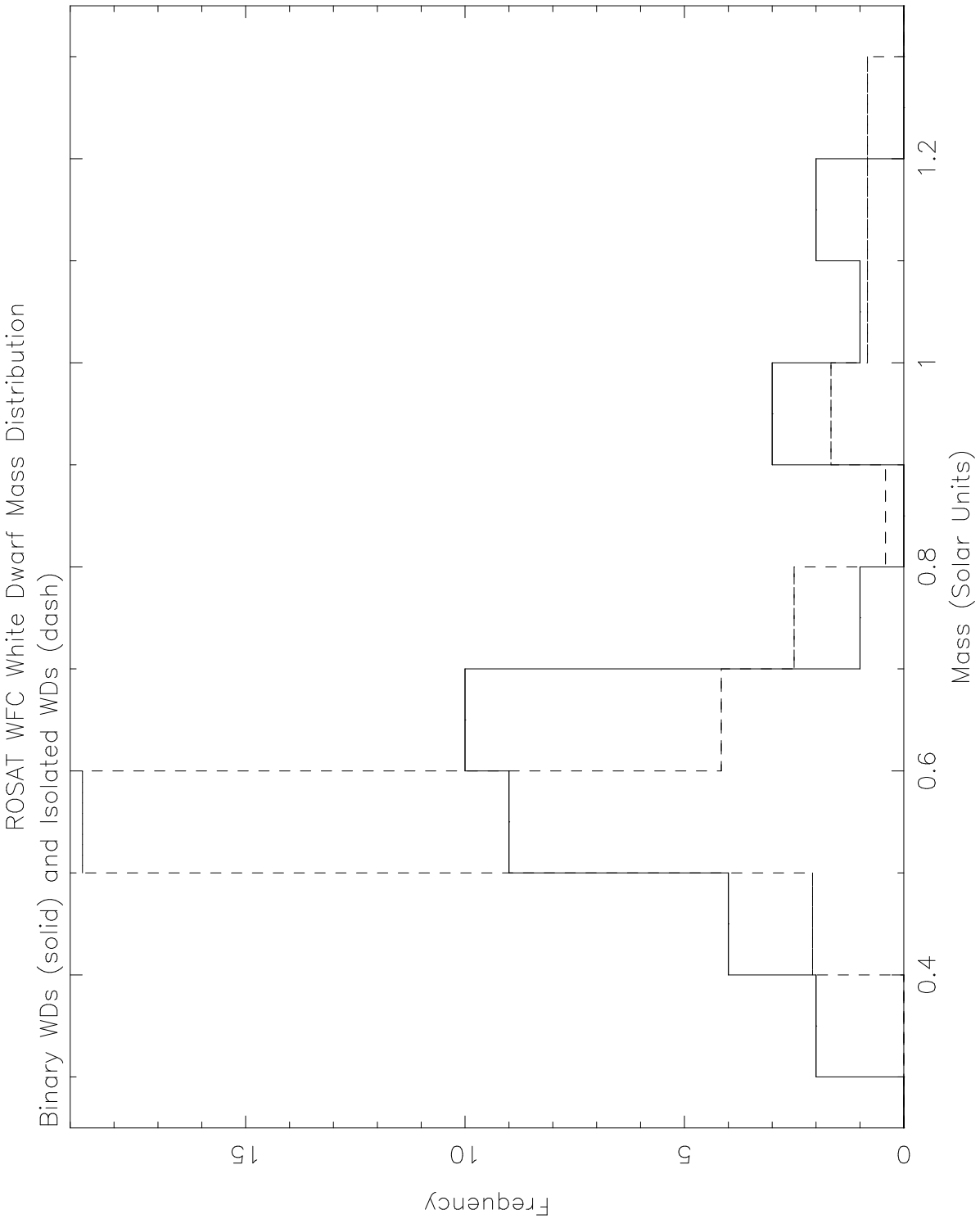

Figure 5.7: Comparison of the mass distributions for the binary white dwarfs and for 77 isolated WFC white dwarfs from Marsh *et al.* (1997a) 151

The photospheric composition of a white dwarf, including trace amounts of elements heavier than He, is determined by a complex balance between the effects of radiative levitation and gravity. Current models assume a strict equilibrium balance between the radiative acceleration on a particular element and the local gravity, although this is insufficient to account for observations in detail (Chayer, Fontaine & Wesemael 1995). For example, at high effective temperatures, radiation flux can overcome gravity to produce a stellar wind (e.g. in hot pre-white dwarfs T>100,000K). However, since the highest mass white dwarfs will also have the highest gravities, it follows that the lowest heavy element abundances should be found among these objects. The heaviest elements will quickly sink out of the atmospheres to leave stars with very low EUV opacities. Hence, they are be more likely to be detected by ROSAT.

It should be remembered, though, that the effects of heavy element opacity in hot white dwarfs only becomes important for stars with temperatures >40,000K (Barstow *et al.* 1993c), and in fact, the more detailed study of Marsh *et al.* (1997b) shows many white dwarfs have an essentially pure H atmosphere up to at least 50,000K. If the masses of the EUV-bright white dwarfs are plotted against temperature (Figure 5.8) it quickly becomes obvious that there are more high mass objects with T<40,000K, where heavy element contamination is unimportant, than with T>40,000K. Indeed, only two high mass white dwarfs in the WFC survey have T>50,000K. It would seem, therefore, that another explanation is required for the EUV high mass excess.

A close study of the predictions of Matt Wood's temperature dependent mass-radius relationships for white dwarfs (Wood 1995) shows that high mass stars cool far more slowly than normal ($M \approx 0.6\,M_{\odot}$) mass objects (Liebert & Bergeron 1995, Finley 1995). For example, there is a sharp decrease in the cooling rate of massive ($M > 1.0\,M_{\odot}$) white dwarfs in the 40,000K−50,000K temperature range in comparison to normal stars. This will have the effect of increasing the numbers of high mass objects expected to be seen in the hot temperature regime, and may be a better explanation for the excess seen in the EUV-selected samples.

Unfortunately, there is as yet no published optically-selected sample of white dwarfs, covering the same distribution of temperatures as the EUV surveys, with which to make a direct comparison. Liebert & Bergeron (1995) point out that optical surveys are biased against high mass white dwarfs because such stars have smaller radii and are therefore less luminous than normal mass objects at the same temperature, but until a suitable survey is completed and published a more

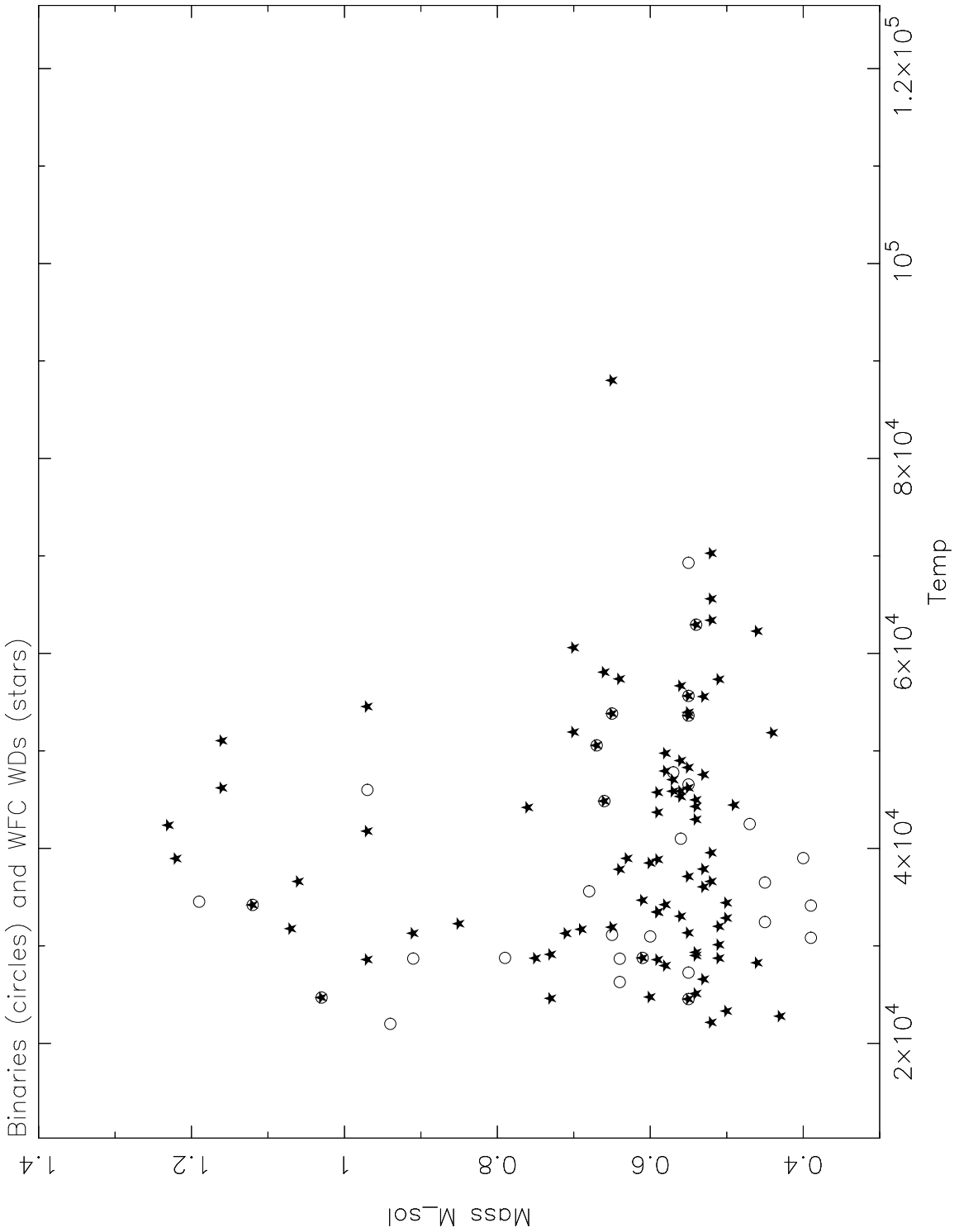

Figure 5.8: White dwarf mass versus effective temperature for the ROSAT WFC white dwarfs in detached binaries (circles) and the 89 mainly isolated WFC white dwarfs of Marsh *et al.* (1997a)

detailed analysis cannot be undertaken.

On the basis of its high mass and rotation rate, it has been suggested that one of the high mass white dwarfs in the Marsh *et al.* (1997a) sample, GD50, may be the result of a double degenerate merger (Vennes, Bowyer & Dupuis 1996. The rapidly rotating (P≈12 minutes) 1.35 $M_\odot$ magnetic white dwarf RE J0317−853 (Barstow *et al.* 1995b), the most massive white dwarf ever found, could also be a coalesced binary (although this object has not been included in the Marsh *et al.* 1997a study). Could the high mass peak in the two EUV-surveys represent a newly discovered population of merged binary stars? Continuing the picture of binary evolution discussed in Chapter 2, Yungelson *et al.* (1994) predict that about 1 in 55 double degenerate systems will have a period short enough for a merger to occur within the Hubble time. Of course, fewer than this will actually have merged to give the high mass objects that are seen, and indeed some pairs may have had a large enough combined mass to push them over the Chandrasekhar limit (1.4 $M_\odot$) and become Type I supernovae. However, if the high mass white dwarfs are indeed all the final results of binary evolution, then, given that there are only 32 binary systems in the ROSAT WFC survey, the number of such massive stars observed is much larger than expected. The theoretical predictions of binary evolution rely heavily on assumptions about the common envelope phase. If the high mass excess in the ROSAT survey is real and represents the products of double degenerate mergers, then these stars could reveal important new information about common envelope evolution, and allow us to place constraints on parameters such as the common envelope ejection efficiency parameter α, which until now has only been constrained to lie somewhere between 0.3 and 1.0 (see Chapter 2).

At the other end of the mass scale, six of the binary white dwarfs have masses $<0.55\,M_\odot$, which would imply they are not the result of normal (post-AGB) evolution. The masses of the two stars with $M<0.4\,M_\odot$ were determined by extending Matt Wood's evolutionary models (for degenerate C cores,Wood 1995) below the $0.4\,M_\odot$ grid limit. However, at these low masses the stars would in reality have He cores. Five of the six stars are from the subset of optically invisible white dwarfs, whose atmospheric parameters have been determined from fitting IUE far-UV spectra and should, therefore, be interpreted with caution. The best fit parameters for these stars were found by assuming the white dwarf lies at the same distance away as the main sequence companion. Since there will always be an uncertainty in the distance estimate, particularly if the spectral type of the companion is not well constrained, then there will also be

a corresponding uncertainty in the white dwarf parameters. For example, the distance to one of these 'low mass' white dwarfs, RE J1925−56 ($0.39\,M_{\odot}$), is very uncertain, between 95 and 160 parsecs. The white dwarf could, therefore, have a mass as high as $\sim 0.6\,M_{\odot}$ (the average mass for white dwarfs), or as low as $0.37\,M_{\odot}$. The quoted mass in Table 5.1 is rather arbitrary, representing a distance estimate ∼midway between the two limits. On the other hand, although the distance to the primary in BD+27°1888 is only constrained to be between 185−218 parsecs, the white dwarf would have to be ∼140 parsecs away for its mass to be as high as $0.55\,M_{\odot}$. In this case the white dwarf may indeed have a low mass and represent a product of common envelope evolution. This should be a motivation for further studies to determine the orbital period. The sixth star, RE J1629+78, is a confirmed close binary (P∼few days, $M=0.47\,M_{\odot}$) and must have passed through a phase of common envelope evolution during which it may have lost mass. These limitations could also be effecting the high mass excess, as four of the six stars with $M>0.85\,M_{\odot}$ also belong to the subclass of hidden white dwarfs.

The gravity distribution (Figure 5.6) also illustrates the limitations of the analysis of the hidden white dwarfs and the effects these could be having on the interpretation of the whole sample. Since 50% of the binaries include an optically invisble white dwarf, the shape of this graph has partly been determined by the fact that, in order to model the hidden star's UV spectrum, a value of log g must be assumed a priori. In fitting the hidden white dwarf spectra the usual procedure has been to step through values of log g from 7.0 to 9.0 with a step size of 0.5. Thus in Figure 5.6 there is a peak of stars with log g=8.0 and another with log g=8.5, although the true gravity of a hidden white dwarf which has been fixed in the analysis at log g=8.0 could be anywhere between log g=7.5 and log g=8.5. Of course, in some cases one can interpolate between these widely spread values of log g, particularly if the distance to the primary is more tightly constrained (e.g. for HD2133, d≈150pc and the best fit white dwarf model giving this distance is for log g=8.25). These uncertainties make it difficult to interpret the binary gravity distribution. For example, Marsh *et al.* (1997a) found that the peak of their gravity distribution was shifted to a lower value in comparison with the optically-selected sample of Bergeron, Saffer & Liebert (1992). The shift occurs because the higher temperature stars found in the EUV survey will have greater radii and lower surface gravities than the cooler stars which dominate the Bergeron, Saffer & Liebert (1992) sample. However, this shift is not evident for the binary white dwarfs.

5.4 Conclusions

Thirty-two of the >120 hot white dwarfs detected in the EUV by the ROSAT WFC have been found to reside in binary systems. Approximately 50% of these stars are in unresolved pairs with bright (spectral type A−K), normal (main sequence or sub-giant) companions. Such objects have never been seen optically and could only have been detected in a satellite survey (although it may be possible for HST to resolve the wide pairs, for example). Thus, this group of objects in particular makes this a unique study with important implications for theoretical models of the white dwarf luminosity function, space density and birthrate (e.g. Fleming, Liebert & Green 1986) which, because of selection effects, are currently dominated by isolated stars.

Between 50% and 80% of all stars are believed to lie in binary or multiple systems. However, in the ROSAT X-ray catalogue of white dwarfs (Fleming *et al.* 1996), only 23% of the 176 objects are detected in binary systems. In addition, 75% of the ∼120 ROSAT WFC white dwarfs appear to be single stars. It is reasonable to believe, then, that there are more white dwarf binaries in the EUV catalogues waiting to be discovered.

However, identifying new systems is becoming increasingly difficult, particularly for the optically undetectable white dwarfs. The searches with IUE have been fairly exhaustive, and, since that observatory has been shut down, it will be almost impossible to conduct similar searches in the future (at least until the competition for HST time decreases). As I completed this thesis, however, I learned of the discovery (in an IUE spectrum) by the Berkeley group of yet another hidden white dwarf binary, RE J0702+129 (K0+DA, Christian, Vennes & Mathioudakis 1997). This discovery is significant in that the main sequence (or slightly evolved) companion has been positively identified in the ROSAT 2RE catalogue (Pye *et al.* 1995), and in the optical identification survey of Mason *et al.* (1995), as an active star. It was not, therefore, included on any target list for our searches with IUE. This raises the question of how many of the >200 'active' stars in the WFC and EUVE catalogues are really the source of the EUV radiation. Until each individual star has been observed and analysed in detail, the suspicion must remain that there are more of these systems in the survey waiting to be discovered.

There are still, though, a couple of excellent known candidates to be targeted. From their WFC count rates and S2/S1 ratios it is likely that two bright EUV sources which appear to be

associated with inactive B stars (HR3665 and HR2875) will have hot white dwarf companions. These white dwarfs, should they exist, will have to be identified spectroscopically with EUVE since the B stars will dominate the far-UV wavelength ranges that are currently only accessible with HST.

At the other end of the spectral range, searches for low mass red dwarf companions may prove more fruitful. Assuming 10% of planetary nebula nuclei are close binaries (Bond 1994) and a birthrate of hot white dwarfs of $\approx 2 \times 10^{-12} \mathrm{pc}^{-3}$ per year, Vennes & Thorstensen (1994b) estimate that between 5−10 new close binary systems with a hot (T>40,000K) white dwarf component should be expected in EUV surveys in addition to those already discovered. Unfortunately, with the current approach (looking for strong Balmer emission due to reprocessing of EUV radiation on the surface of the red dwarf), companions with spectral types later than dM6 are almost undetectable.

None-the-less, programmes are currently being undertaken to obtain R and I photometry of the isolated ROSAT WFC white dwarfs to search for red dwarf companions that may not necessarily be close. Recent results from a week's observing in August 1996 on the 0.75m telescope at SAAO to obtain UBVR and I colours for a sample of southern hemisphere WFC white dwarfs suggest that there are indeed a number of WD+dM pairs awaiting spectroscopic identification. In addition, a future search for very low mass (<dM6) and brown dwarf companions may also add to the number of binary systems in the sample. For example, Gemmo (1997) finds that >25% of a sample of 82 optically selected white dwarfs display a strong infrared excess when observed in the K photometric band.

Appendix A

The Satellite Observatories

A.1 ROSAT

ROSAT (*Röentgensatellit*, Trümper 1984) is an orbiting observatory carrying two major imaging experiments: a German X-ray telescope (XRT, Aschenbach 1988), and the British Wide Field Camera (WFC, Sims *et al.* 1990), designed to explore the Extreme Ultraviolet (EUV) wavelength region. The spacecraft was launched on June 1st 1990 by a Delta II rocket from Cape Canaveral, into a circular orbit with an altitude of about 575km, and an orbital period of approximately 96 minutes. The orbital inclination is around 53° to the equator, and there are 5 or 6 contacts per day with the ground station at Wilheim, near Munich (GSOC - the German Space Operations Centre). Each pass lasts around 10 minutes, and during this time the satellite transmits data to the ground, and new commands are uplinked to the onboard computers.

ROSAT had two major mission objectives. The first was to complete a survey of the entire sky in X-rays and the EUV. The X-ray survey was designed to be 1000 times more sensitive than any previous mission, and the EUV survey was the first to be carried out in that waveband. The survey is discussed in more detail in Chapter 1. The second phase of the mission was to observe selected astronomical targets in pointed observations, in many cases obtaining very deep exposures up to 10 times more sensitive than the previous Einstein mission.

The telescopes and detectors are described in much detail elsewhere, but will be briefly discussed here.

The XRT

The 2.4m focal length XRT (Aschenbach 1988) is a grazing incidence reflecting telescope, consisting of 4 nested Wolter I mirrors (Wolter 1952). The total on axis collecting area of the telescope is 1141cm^2, the aperture is 84cm in diameter, and the field of view is $\approx 2°$. The XRT has three detectors which sit at the focal plane: two German-designed Position Sensitive Proportional Counters (PSPC, Pfeffermann *et al.* 1987), and a High Resolution Imager (HRI), contributed by an American consortium in return for a guaranteed 50% of the pointed observation time. The HRI was not used in the survey phase of the mission. The PSPC is a gas filled proportional counter, and covers the energy range $\approx 6-100$Å (0.1−2.4 keV). It has modest

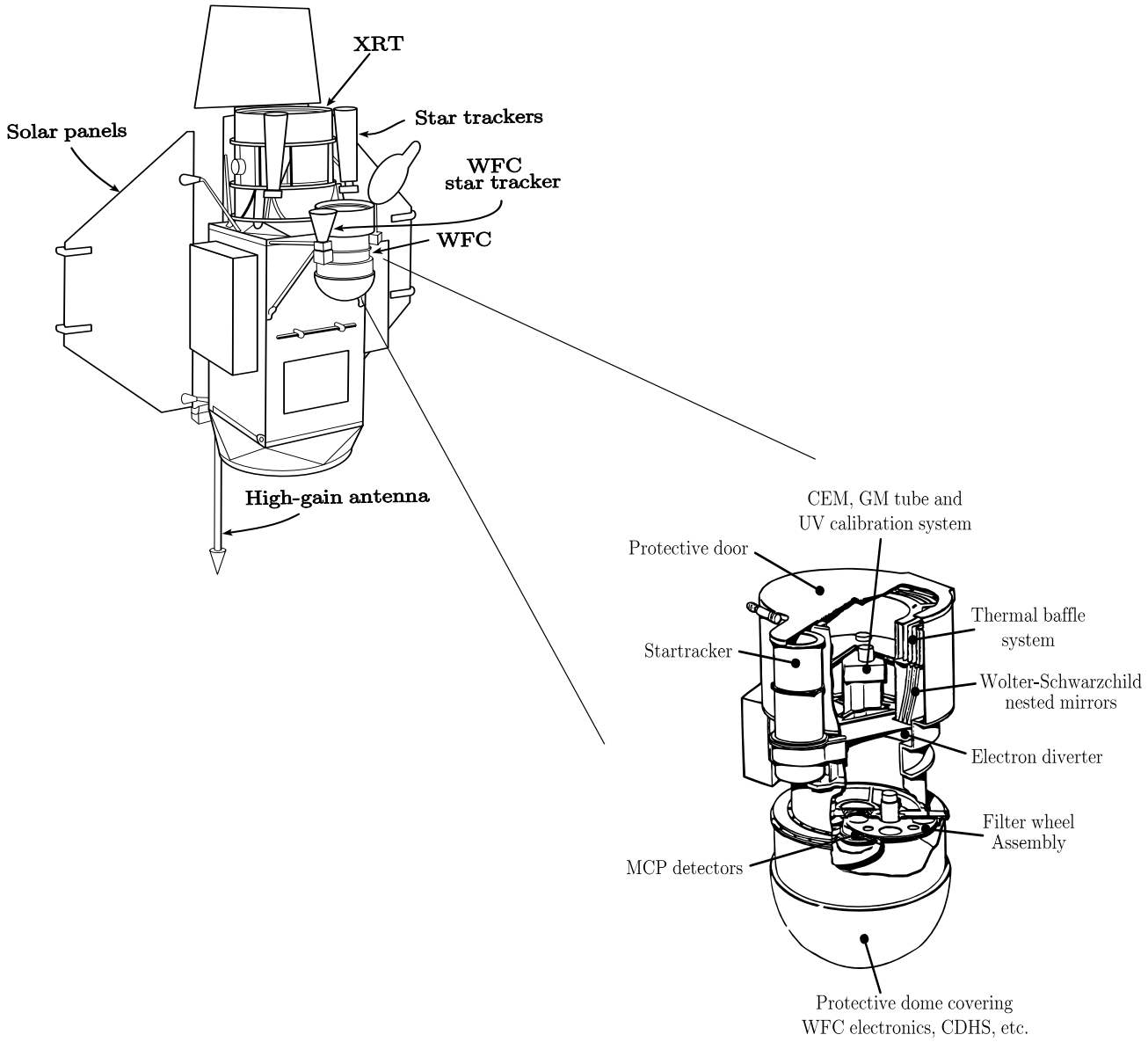

Figure A.1: The ROSAT satellite and an enlarged diagram of the Wide Field Camera

energy resolution, which was exploited in the pointed observation phase, but in this thesis just the integrated count rates are utilised. A boron filter effectively subdivides the PSPC into two energy bands: a hard band (0.4−2.4 keV), and a soft band (0.1−0.4 keV), in which all the X-ray emission of white dwarfs is expected to lie, In fact, the PSPC's polypropylene window has a thin carbon/lexan coating to reduce UV transmission, and this effectively makes the window opaque to energies just above the carbon edge at 0.28 keV. Thus, in reality, the soft band is only sensitive to photons between 0.1−0.28keV.

The WFC

The WFC (Sims *et al.* 1990) covers the EUV waveband in the range ∼60−200Å. The optics consist of 3 nested Wolter-Schwarzchild Type I mirrors, with a focal length of 52.5cm and a collecting area of 456cm^2. The grazing incidence angles have been chosen so that the collecting area is optimised while retaining a large field of view (≈5°).

There are two micro-channel plate detectors in the focal plane, each consisting of ∼10^7 closely packed tubes (Barstow & Sansom 1990). The spatial resolution is around 1 arcminute on axis, but, unlike the PSPC, the WFC has no energy resolution. Instead, two broad band filters were used during the survey: the S1 filter, covering the range 90−200 eV (60−140Å), and the S2 filter, covering the 60−110 eV (112−200Å) band. A number of other filters were available during the pointed phase of the mission. These filters provided a factor 3 better energy resolution than was available with the earlier EXOSAT satellite.

A.2 The Extreme Ultraviolet Explorer (EUVE)

NASA's Extreme Ultraviolet Explorer (Bowyer & Malina 1991) was launched on a Delta II rocket from Cape Canaveral on 7th June 1992, and placed into a circular orbit with an altitude of 550km and an inclination of 28°. The science payload consists of three co-aligned, imaging telescopes, and a deep survey/spectrometer telescope.

The first goal of the mission was to carry out an all sky survey of the EUV sky between 70−760Å. This was completed between 24th July 1992 and 21st January 1993. The three grazing incidence,

Figure A.2: The Extreme Ultraviolet Explorer satellite

imaging telescopes surveyed the entire sky in four band passes centred on ∼100, 200, 400 and 600Å. The A and B telescopes contained filters for both the 100Å and 200Å bands, while the C telescope carried the two longer wavelength filters. At the same time, the deep survey instrument, mounted orthogonally to the three imaging telescopes, was used to carry out a much deeper survey of a $2° \times 180°$ patch of sky along the ecliptic, in order to better determine the faint end of the EUV brightness distribution. The initial survey results were published by Bowyer *et al.* (1994) and Malina *et al.* (1994).

Since the completion of the all sky survey, the primary objective of the EUVE mission has been to make spectroscopic observations of specific targets through a Guest Observer programme, using the deep survey/spectrometer (DS/S) telescope. The DS/S instrument consists of three slitless, imaging spectrometers, each receiving light from one sixth of the telescope collecting area, and the deep survey detector itself which takes 50% of the incoming light. The DS/S telescope utilises grazing incidence reflections, and is a Wolter-Schwarzschild Type II design, with a 40cm diameter. The three spectrometers cover overlapping wavelength ranges. They are: the short wavelength spectrometer (SW, 70−190Å), the medium wavelength spectrometer (MW, 140−380Å), and the long wavelength spectrometer (LW, 280−760Å). Typical spectral resolutions are 0.5Å, 1.0Å and 2.0Å for each of the three spectrometers respectively, although these can vary across each band by a factor of ∼2. Microchannel plate detectors are used to provide photon counting capabilities and high efficiency. The detector electronics produce a 2048×2048 pixel image of the detector plate, containing the spectrum, although the image of the aperture itself covers a smaller circular region roughly 1750Å in diameter.

A.3 The International Ultraviolet Explorer (IUE)

The International Ultraviolet Explorer (IUE) was the most successful astronomy satellite of all time. Launched in January 1978, it remained operational until it was finally shut down, through a lack of funding, in September 1996. IUE was the result of a collaboration between NASA, the European Space Agency (ESA) and the UK Science and Engineering Research Council (SERC). Prior to the launch of HST in 1990, it was the only observatory covering the far-Ultraviolet (far-UV) spectral range. IUE was placed in a 24 hour orbit, and controlled for 16 hours a day from Goddard Space Flight Center (GSFC) near Washington, DC, and for 8 hours a day from the

Villafranca Satellite Tracking Station (Vilspa) near Madrid, Spain. Each day of operations was divided into three shifts of 8 hours, one operated by ESA from Vilspa, and two from Goddard - the US1 shift, characterised by low background, and US2, where the particle background was high and only bright stars could be observed. IUE was unique among modern satellite observatories in that observations were conducted in real time (ROSAT and EUVE are pre-programmed weeks in advance, for example), and Guest Observers were permitted to be present in the control centres at Vilspa and Goddard to oversee and participate in operations. This method of operation allowed a large degree of flexibility for the Guest Observer in his choice of targets and exposure lengths, and decisions to re-observe a specific target on scientific grounds, for example, could be made swiftly to maximise use of the Guest Observer's allocated time.

IUE carried two spectrographs (Boggess *et al.* 1978), integrated with two television cameras to record the image of the detector plate and the spectrum. The Short Wavelength Prime Camera (SWP) covered the range between 1150−1950Å, and a Long Wavelength Prime Camera (LWP) covered the range from 1900−3200Å. IUE could operate in two modes, giving resolutions of either 6Å or 0.1Å. In low dispersion mode, incoming light passed through a normal grating to provide one or two usable spectral orders. In high dispersion mode, an echelle blaze was utilised to split the incoming light into up to 60 orders (in the SWP camera), which were then focussed onto the TV camera. However, due to the long exposure times necessary to obtain a good signal-to-noise spectrum, the high dispersion mode was only useful for the brightest white dwarfs (V$\approx$13 or brighter).

The television cameras were sensitive only to optical light, necessitating use of an ultraviolet-to-optical converter. The incoming signal was then transferred by fibre optics to a secondary electron conduction tube (SEC), where an image was built up over time before being read out at the end of the exposure. Saturation of the SEC occurred above an integration of 10^4 photons per pixel, restricting the signal-to-noise to about 20 per exposure, although this could be improved by co-addition of a number of different observations. Recent refinements in the image extraction and reduction techniques helped to improve the overall quality and signal-to-noise of spectra taken in the last couple of years of opertions, and this extraction technique (called NEWSIPS) is being retrospectively applied to the entire IUE archival database.

Figure A.3: The International Ultraviolet Explorer satellite

References

Aannestad, P. A. & Sion, E. M., 1985. *Astron. J.*, **90**, 1832.

Abt, H. A. & Morrell, N. J., 1995. *Astrophys. J. Suppl.*, **99**, 135.

Abt, H. A., 1961. *Astrophys. J. Suppl.*, **6**, 37.

Alcock, C. & Illarionov, A., 1980. *Astrophys. J.*, **253**, 534.

Allen, C. W., 1964. *Astrophysical Quantities (Second Edition)*, Athlone Press.

Andersson, H. & Edvardsson, B., 1994. *Astr. Astrophys.*, **290**, 590.

Aschenbach, B., 1988. *Applied Optics*, **27**, 1404.

Barstow, M. A. & Sansom, A. E., 1990. *Proc. SPIE Int. Soc. Opt. Eng.,*, **1344**, 244.

Barstow, M. A. *et al.*, 1993a. In: *White Dwarfs: Advances in Theory and Observation*, Barstow, M. A., ed., Kluwer, Dordrecht, p. 433.

Barstow, M. A. *et al.*, 1993b. *Adv. Space Res.*, **13**, 281.

Barstow, M. A. *et al.*, 1993c. *Mon. Not. R. astr. Soc.*, **264**, 16.

Barstow, M. A. *et al.*, 1994a. *Mon. Not. R. astr. Soc.*, **270**, 499.

Barstow, M. A., Holberg, J. B., Marsh, M. C., Tweedy, R. W., Burleigh, M. R., Fleming, T. A., Koester, D., Penny, A. J. & Sansom, A. E., 1994b. *Mon. Not. R. astr. Soc.*, **271**, 175.

Barstow, M. A. *et al.*, 1995a. *Mon. Not. R. astr. Soc.*, **272**, 531.

Barstow, M. A., Jordan, S., O'Donoghue, D., Burleigh, M. R., Napiwotzki, R. & Harrop-Allin, M. K., 1995b. *Mon. Not. R. astr. Soc.*, **277**, 971.

Barstow, M. A., O'Donoghue, D., Kilkenny, D., Burleigh, M. R. & Fleming, T. A., 1995c. *Mon. Not. R. astr. Soc.*, **273**, 711.

Barstow, M. A., Dobbie, P. D., Holberg, J. B., Hubeny, I. & Lanz, T., 1997. *Mon. Not. R. astr. Soc.*, **286**, 58.

Barstow, M. A., Holberg, J. B. & Koester, D., 1994a. *Mon. Not. R. astr. Soc.*, **268**, L35.

Barstow, M. A., Holberg, J. B. & Koester, D., 1994b. *Mon. Not. R. astr. Soc.*, **270**, 516.

Barstow, M. A., Holberg, J. B. & Koester, D., 1995. *Mon. Not. R. astr. Soc.*, **274**, L31.

Barstow, M. A., 1989. In: *White Dwarfs*, Wegner, G., ed., Springer-Verlag, Berlin, p. 156.

Barstow, M. A., 1990. *Mon. Not. R. astr. Soc.*, **243**, 182.

Bergeron, P., Wesemael, F., Beauchamp, A., Wood, M. A., Lamontagne, R., Fontaine, G. & Liebert, J., 1994. *Astrophys. J.*, **432**, 305.

Bergeron, P., Liebert, J. & Fulbright, M. S., 1995. *Astrophys. J.*, **444**, 810.

Bergeron, P., Saffer, R. A. & Liebert, J., 1992. *Astrophys. J.*, **394**, 228.

Boeshaar, P., 1976. *PhD thesis*, Ohio State University.

Boggess, A. *et al.*, 1978. *Nature*, **275**, 372.

Bohlin, R. C. & Grillmair, C. J., 1988. *Astrophys. J. Suppl.*, **66**, 209.

Böhm-Vitense, E., 1980. *Astrophys. J. Letts.*, **239**, 79.

Böhm-Vitense, E., 1993. *Astron. J.*, **106**, 1113.

Böhm-Vitense, E., 1995. *Astron. J.*, **110**, 228.

Bond, H. E., 1994. In: *Interacting Binary Stars*, Shafter, A. W., ed., ASP Conf. Series, p. 179.

Bowyer, S. & Malina, R. F., 1991. In: *Extreme Ultraviolet Astronomy*, Malina, R. F. & Bowyer, S., eds., Pergamon Press, p. 391.

Bowyer, S., Lieu, R., Lampton, M., Lewis, J., Wu, X. & Drake, J. J., 1994. *Astrophys. J. Suppl.*, **93**, 569.

Bowyer, S., Lampton, M., Lewis, J., Wu, X., Jelinsky, P. & Malina, R. F., 1996. *Astrophys. J. Suppl.*, **102**, 129.

Bragaglia, A., Renzini, A. & Bergeron, P., 1995. *Astrophys. J.*, **443**, 735.

Bruhweiler, F. C. & Kondo, Y., 1986. *Astrophys. J.*, **269**, 657.

Bruhweiler, F. C., 1995. In: *Astrophysics in the Extreme Ultraviolet*, Bowyer, S. & Malina,

R. F., eds., Kluwer, p. 261.

Bues, I. & Aslan, T., 1995. In: *White Dwarfs.*, Koester, D. & Werner, K., eds., Springer-Verlag, p. 259.

Campbell, W. W. & Moore, J. H., 1928. *Publ. Lick Obs.*, **16**, 167.

Catalan, M. S., Davey, S. C., Sarna, M. J., Smith, R. C. & Wood, J. H., 1994. *Mon. Not. R. astr. Soc.*, **269**, 879.

Catalan, M. S., Sarna, M. J., Jomaron, C. M. & Smith, R. C., 1995. *Mon. Not. R. astr. Soc.*, **275**, 153.

Chabrier, G., 1997. In: *White Dwarfs*, Isern, J., Hernanz, M. & Garcia-Berro, E., eds., Kluwer, p. 121.

Chandrasekhar, S., 1931. *Astrophys. J.*, **74**, 81.

Chandrasekhar, S., 1939. *An Introduction To The Study Of Stellar Structure*, Cambridge University Press: Cambridge.

Chayer, P. *et al.*, 1995. *Astrophys. J.*, **454**, 429.

Chayer, P., Fontaine, G. & Wesemael, F., 1989. In: *White Dwarfs*, Wegner, G., ed., Springer-Verlag, Berlin, p. 253.

Chayer, P., Fontaine, G. & Wesemael, F., 1995. *Astrophys. J. Suppl.*, **99**, 189.

Christian, D. J., Vennes, S., Thorstensen, J. R. & Mathioudakis, M., 1996. *Astron. J.*, **112**, 258.

Christian, D. J., Vennes, S. & Mathioudakis, M., 1997. *Bull. American Astron. Soc.*, **29**.

Cooke, B. A., Barstow, M. A., Breeveld, E. R. *et al.*, 1992. *Nature*, **355**, 61.

Cruddace, R., Paresce, F., Bowyer, S. & Lampton, M., 1974. *Astrophys. J.*, **187**, 497.

D'Antona, F. & Mazzitelli, I., 1995. In: *White Dwarfs*, Koester, D. & Werner, K., eds., Kluwer, p. 93.

de Kool, M., 1990. *Astrophys. J.*, **358**, 189.

de Kool, M., 1992. *Astr. Astrophys.*, **261**, 188.

de Strobel, G. C., Perrin, M. N., Cayrel, R. & Lebreton, Y., 1989. *Astr. Astrophys.*, **225**, 369.

de Kool, M. & Ritter, H., 1993. *Astr. Astrophys.*, **267**, 397.

Diamond, C. J., Jewell, S. J. & Ponman, T. J., 1995. *Mon. Not. R. astr. Soc.*, **274**, 589.

Dorman, B., Rood, R. T. & O'Connell, W. O., 1993. *Astrophys. J.*, **419**, 596.

Dreizler, S., Heber, U., Napiwotzki, R. & Hagen, H. J., 1995. *Astr. Astrophys. Letts.*, **303**, 53.

Drilling, J. & Schönberner, D., 1985. *Astr. Astrophys. Letts.*, **146**, 23.

Dupuis, J., Vennes, S., Bowyer, S., Pradhan, A. K. & Thejll, P., 1995. *Astrophys. J.*, **455**, 574.

Dupuis, J., Vennes, S. & Bowyer, S., 1997. In: *White Dwarfs*, J.Isern, M.Hernanz & E.Garcia-Berro, eds., Kluwer Academic Publishers, Dordrecht, p. 277.

Finley, D., 1993. In: *Calibrating the Hubble Space Telescope*, STSCI, ed., p. 416.

Finley, D. S., 1995. In: *White Dwarfs.*, Koester, D. & Werner, K., eds., Springer-Verlag, p. 150.

Fleming, T. A., Scmidt, J. H. M. M., Barstow, M. A. & Mittaz, J. P. D., 1991. *Astr. Astrophys.*, **246**, L47.

Fleming, T. A. *et al.*, 1995. *Astrophys. J. Suppl.*, **99**, 701.

Fleming, T. A., Snowden, S. L., Pfefferman, E., Briel, U. & Greiner, J., 1996. *Astr. Astrophys.*, **316**, 147.

Fleming, T. A., Liebert, J. & Green, R. F., 1986. *Astrophys. J.*, **308**, 176.

Fontaine, G. & Wesemael, F., 1987. In: *Proc IAU Colloq. 95: Conference on Faint Blue Stars*, Hayes, D. S., Liebert, J. & Philip, A. G. D., eds., L.davies Press:Schenectady, p. 319.

Frisch, P. & York, D., 1983. *Astrophys. J. Letts.*, **271**, 59.

Fulbright, M. S., Liebert, J., Bergeron, P. & Green, R., 1993. *Astrophys. J.*, **406**, 240.

Garhart, M., 1992. *IUE Newsletter*, **48**, 98.

Gemmo, A., 1997. In: *White Dwarfs*, J. Isern, M. H. & Garcia-Berro, E., eds., Kluwer, p. 315.

Genova, R. *et al.*, 1995. *Astron. J.*, **110**, 788.

Green, R. F., Schmidt, M. & Liebert, J., 1986. *Astrophys. J. Suppl.*, **61**, 305.

Greenstein, J. L. *Stars and Stellar Systems,* Vol 6, *Stellar Atmospheres*, p. 676. Chicago: University of Chicago Press, 1960.

Hamada, T. & Salpeter, E. E., 1961. *Astrophys. J.*, **134**, 683.

Han, Z., Eggleton, P. P., Podsiadlowski, P. & Tout, C. A., 1995. *Mon. Not. R. astr. Soc.*, **277**, 1443.

Heber, U., Dreizler, S. & Hagen, H.-J., 1996. *Astr. Astrophys. Letts.*, **311**, 17.

Heber, U., Bade, N., Jordan, S. & Voges, W., 1993. *Astr. Astrophys. Letts.*, **267**, 31.

Hodgkin, S. T. & Pye, J. P., 1990. *Mon. Not. R. astr. Soc.*, **267**, 840.

Hodgkin, S. T., Barstow, M. A., Fleming, T. A., Monier, R. & Pye, J. P., 1993. *Mon. Not. R. astr. Soc.*, **263**, 229.

Holberg, J. B., Bruhweiler, F. C. & Andersen, J., 1995. *Astrophys. J.*, **443**, 753.

Holberg, J. B., Sandel, B. R., Forrester, W. T., Broadfoot, A. L., Shipman, H. L. & Barry, D. C., 1980. *Astrophys. J. Letts.*, **242**, L119.

Holberg, J. B., Kidder, K., Liebert, J. & Wesemael, F., 1989. In: *IAU Colloq. 114, White Dwarfs*, Wegner, G., ed., New York: Springer, p. 188.

Holberg, J. B. *et al.*, 1993. *Astrophys. J.*, **416**, 806.

Holberg, J. B., Hubeny, I., Barstow, M. A., Lanz, T., Sion, E. M. & Tweedy, R. W., 1994. *Astrophys. J.*, **425**, L105.

Holberg, J. B., Saffer, R. A., Tweedy, R. W. & Barstow, M., 1995. *Astrophys. J. Letts.*, **452**, 133.

Holberg, J. B., 1987. In: *IAU Colloq. 95, The Second Conference on Faint Blue Stars*, Phillip, A. G. D., Hayes, D. S. & Liebert, J., eds., Schenectady: L. Davis Press, p. 285.

Holberg, J. B., 1996. *private communication*, .

Iben, I. & Livio, M., 1993. *Pub. Astr. Soc. Pacific.*, **105**, 1373.

Iben, I. & Macdonald, J., 1985. *Astrophys. J.*, **296**, 540.

Iben, I. & Renzini, A., 1983. *Ann. Rev. Astron. Astrophys.*, **21**, 271.

Iben, I. & Tutukov, A. V., 1984. *Astrophys. J.*, **282**, 615.

Iben, I., 1984. *Astrophys. J.*, **277**, 333.

Jacoby, G. H., Hunter, D. A. & Christian, C. A., 1984. *Astrophys. J. Suppl.*, **56**, 257.

Jeffries, R. D. & Jewell, S. J., 1993. *Mon. Not. R. astr. Soc.*, **264**, 106.

Jeffries, R. D. & Smalley, B., 1996. *Astr. Astrophys. Letts.*, **315**, 19.

Jeffries, R. D. & Stevens, I. R., 1996. *Mon. Not. R. astr. Soc.*, **279**, 180.

Jeffries, R. D., Burleigh, M. R. & Robb, R. M., 1996. *Astr. Astrophys. Letts.*, **305**, 45.

Jeffries, R. D., 1995. *Mon. Not. R. astr. Soc.*, **273**, 559.

Johnson, H. R. & Ake, T. B., 1986. *ESA SP*, **263**, 395.

Jomaron, C. M. *et al.*, 1993. *Mon. Not. R. astr. Soc.*, **264**, 219.

Jordan, S., Koester, D., Wulf-Mathies, C. & Brunner, H., 1987. *Astr. Astrophys.*, **185**, 253.

Jordan, S., Heber, U., Engels, D. & Koester, D., 1993. *Astr. Astrophys. Letts.*, **273**, 27.

Kahn, S., Wesemael, F., Liebert, J., Raymond, J. C., Steiner, J. E. & Shipman, H. L., 1984. *Astrophys. J.*, **278**, 255.

Kellett, B. J. *et al.*, 1995. *Astrophys. J.*, **438**, 364.

King, A. R., Kolb, U., de Kool, M. & Ritter, H., 1994. *Mon. Not. R. astr. Soc.*, **269**, 907.

Koester, D. & Schönberner, D., 1986. *Astr. Astrophys.*, **154**, 125.

Koester, D., Liebert, J. & Saffer, R. A., 1994. *Astrophys. J.*, **422**, 783.

Koester, D., 1989a. In: *Proc. IAU Coll. 114, White Dwarfs.*, Wegner, G., ed., Springer-Verlag, p. 206.

Koester, D., 1989b. *Astrophys. J.*, **342**, 999.

Koester, D., 1991. In: *Proc. IAU Symp. 145, Evolution of Stars: The Photospheric Abundance Connection.*, Michaud, G. & Tutukov, A., eds., Kluwer, Dordrecht, p. 435.

Kuiper, G. P., 1941. *Pub. Astr. Soc. Pacific.*, **53**, 248.

Lampton, M., Margon, B., Paresce, F., Stern, R. & Bowyer, S., 1976. *Astrophys. J. Letts.*, **203**, L71.

Lampton, M., Margon, B. & Bowyer, S., 1976. *Astrophys. J.*, **208**, 177.

Landsman, W., Simon, T. & Bergeron, P., 1993. *Pub. Astr. Soc. Pacific.*, **105**, 841.

Landsman, W., Simon, T. & Bergeron, P., 1995. In: *White Dwarfs*, Koester, D. & Werner, K., eds., Springer, p. 191.

Landsman, W., Simon, T. & Bergeron, P., 1996. *Pub. Astr. Soc. Pacific.*, **108**, 250.

Lanz, T., , Barstow, M. A., Hubeny, I. & Holberg, J. B., 1997. *Astrophys. J.*, **473**, 1089.

Liebert, J. & Bergeron, P., 1995. In: *White Dwarfs.*, Koester, D. & Werner, K., eds., Springer-Verlag, p. 12.

Liebert, J., Bergeron, P. & Saffer, R. A., 1990. *Pub. Astr. Soc. Pacific.*, **102**, 1126.

Liebert, J. *et al.*, 1989. *Astrophys. J.*, **346**, 251.

Luyten, W. J., 1952. *Astrophys. J.*, **116**, 283.

MacDonald, J. & Vennes, S., 1991. *Astrophys. J.*, **371**, 719.

Malaroda, S., 1973. *Pub. Astr. Soc. Pacific.*, **85**, 328.

Malina, R. F. *et al.*, 1994. *Astron. J.*, **107**, 751.

Margon, B., Liebert, J., Gatewood, G., Lampton, M., Sprinrad, H. & Bowyer, S., 1976. *Astrophys. J.*, **209**, 525.

Margoni, R., Munari, U. & Stagni, R., 1992. *Astr. Astrophys. Suppl.*, **93**, 545.

Marsh, T. R. & Duck, S. R., 1996. *Mon. Not. R. astr. Soc.*, **278**, 565.

Marsh, T. R., Dhillon, V. S. & Duck, S., 1995. *Mon. Not. R. astr. Soc.*, **275**, 828.

Marsh, M. C. *et al.*, 1997a. *Mon. Not. R. astr. Soc.*, **286**, 369.

Marsh, M. C. *et al.*, 1997b. *Mon. Not. R. astr. Soc.*, **287**, 705.

Marsh, M. C., 1995a. *PhD thesis*, University of Leicester.

Marsh, T. R., 1995b. *Mon. Not. R. astr. Soc.*, **275**, 1.

Mason, K. O. *et al.*, 1995. *Mon. Not. R. astr. Soc.*, **274**, 1194.

McClure, R. D. & Wordsworth, A. W., 1990. *Astrophys. J.*, **352**, 709.

McClure, R. D., 1997. *Pub. Astr. Soc. Pacific.*, **109**, 536.

McCook, G. & Sion, E. M., 1987. *Astrophys. J. Suppl.*, **65**, 603.

Morrison & McCammon, D., 1993. *Astrophys. J.*, **270**, 119.

Morvan, E., Vauclair, G. & Vauclair, S., 1986. *Astr. Astrophys.*, **163**, 145.

Mullis, C. L. & Bopp, B. W., 1994. *Pub. Astr. Soc. Pacific.*, **106**, 822.

Napiwotzki, R. & Schönberner, D., 1993. In: *White Dwarfs: Advances in Theory and Observation*, Barstow, M. A., ed., Kluwer, Dordrecht, p. 99.

Napiwotzki, R. & Schonberner, D., 1995. *Astr. Astrophys.*, **301**, 545.

Napiwotzki, R., Barstow, M. A., Fleming, T. A., Holweger, H., Jordan, S. & Werner, K., 1993. *Astr. Astrophys.*, **278**, 478.

Napiwotzki, R. *et al.*, 1995. *Astr. Astrophys. Letts.*, **300**, 5.

Napiwotzki, R., 1995. In: *White Dwarfs.*, Koester, D. & Werner, K., eds., Springer-Verlag, p. 132.

Nelson, B. & Young, A., 1970. *Pub. Astr. Soc. Pacific.*, **82**, 699.

Oranje, B. J. & Zwaan, C., 1985. *Astr. Astrophys.*, **147**, 265.

Oswalt, T. D., Hintzen, P. M. & Luyten, W. J., 1988. *Astrophys. J. Suppl.*, **66**, 391.

Paczynski, B., 1976. In: *IAU Symposium 73, Structure and Evolution of Close Binary Systems*,

P. P. Eggleton, S. Mitton, J. W., ed., Riedel, Dordrecht, p. 75.

Page, C. G. *NIPS: New Image Point Search Program.* University of Leicester X-ray Astronomy Group, 1990.

Pallavicini, R., Tagliaferri, G., Pollock, A. M. T., Schmitt, J. H. M. M. & Rosso, C., 1990. *Astr. Astrophys.*, **227**, 483.

Paresce, F., 1984. *Astron. J.*, **89**, 1022.

Pena, M., Ruiz, M. T., Bergeron, P., Torres-Piembert, S. & Heathcote, S., 1997. *Astr. Astrophys.*, **317**, 911.

Petre, R., Shipman, H. L. & Canizares, C. L., 1986. *Astrophys. J.*, **304**, 356.

Pfeffermann, E. *et al.*, 1987. *Proc. SPIE Int. Soc. Opt. Eng.,*, **733**, 519.

Politano, M., 1996. *Astrophys. J.*, **465**, 338.

Popova, E. I., Tutukov, A. V. & Yungelson, L. R., 1982. *Astrophys. and Space. Sci.*, **88**, 55.

Pounds, K. A. *et al.*, 1993. *Mon. Not. R. astr. Soc.*, **260**, 77.

Provencal, J. L., Shipman, H. L., Thejll, P., Vennes, S. & Bradley, P. A., 1996. *Astrophys. J.*, **466**, 1011.

Pye, J. P., McGale, P. A., Allen, D. J., Barber, C. R., Bertram, D., Denby, M., Page, C. G., Ricketts, M. J., Stewart, B. C. & West, R. G., 1995. *Mon. Not. R. astr. Soc.*, **274**, 1165.

Rees, P., Giddings, J., Mills, D. & Clayton, M., 1994. *IUEDR - Reference Manual*, **Starlink Guide 3.4**.

Reid, I. N., 1995. *Astron. J.*, **111**, 2000.

Renzini, A. & Voli, M., 1981. *Astr. Astrophys.*, **94**, 175.

Ritter, H., 1996. *private communication*, .

Saffer, R. A. *et al.*, 1993. *Astron. J.*, **105**, 1945.

Sanduleak, N. & Pesch, P., 1990. *Pub. Astr. Soc. Pacific.*, **102**, 440.

Schafer, R. A. *et al.*, 1991. *ESA*, **TM-09**.

Schatzman, E., 1958. *White Dwarfs*, Amsterdam: North Holland.

Schindler, M., Stencel, R. E., Linsky, J. L., Basri, G. S. & Helfand, D. J., 1982. *Astrophys. J.*, **263**, 269.

Schmidt, G. D. & Smith, P. S., 1995. *Astrophys. J.*, **448**, 305.

Schmidt, G. D., Smith, P. S., Harvey, D. A. & Grauer, A. D., 1995. *Astron. J.*, **110**, 398.

Schmitt, J. H. M. M. *et al.*, 1990. *Astrophys. J.*, **351**, 704.

Schönberg, A. & Chandrasekhar, S., 1942. *Astrophys. J.*, **96**, 161.

Schultz, G., Zuckerman, B. & Becklin, E. E., 1996. *Astrophys. J.*, **460**, 402.

Shipman, H. L. & Geczi, J., 1989. In: *White Dwarfs.*, Wegner, G., ed., Springer-Verlag, Berlin, p. 134.

Shipman, H. L., Thejll, P., Bhatia, S. & Liebert, J., 1991. In: *White Dwarfs.*, Vauclair, G. & Sion, E., eds., Kluwer, Dordrecht, p. 229.

Shipman, H. L., 1976. *Astrophys. J.*, **206**, L67.

Shipman, H., 1997. In: *White Dwarfs*, Isern, J., Hernanz, M. & Garcia-Berro, E., eds., Kluwer, p. in press.

Simon, T. & Landsman, W., 1991. *Astrophys. J.*, **380**, 200.

Simon, T. & Landsman, W., 1997. *Astrophys. J.*, **in press**.

Simon, T., Fekelj, R. F. C. & Gibson, D. M., 1985. *Astrophys. J.*, **295**, 153.

Sims, M. R. *et al.*, 1990. *Opt. Eng.*, **26**, 649.

Sion, E. M., Greenstein, J. L., Landstreet, J., Liebert, J., Shipman, H. L. & Wegner, G., 1983. *Astrophys. J.*, **269**, 253.

Sion, E. M., Holberg, J. B., Barstow, M. A. & Kidder, K. M., 1995. *Pub. Astr. Soc. Pacific.*, **107**, 232.

Sion, E. M., 1986. *Pub. Astr. Soc. Pacific.*, **98**, 821.

Smalley, B., Smith, K. C., Wonnacott, D. & Allen, C. S., 1996. *Mon. Not. R. astr. Soc.*, **278**,

688.

Smalley, B., Kellett, B. J., Wonnacott, D. & Stickland, D. J., 1997. *Mon. Not. R. astr. Soc.*, **284**, 457.

Terman, J. L. & Taam, R. E., 1996. *Astrophys. J.*, **458**, 692.

Thompson, G. I. *et al.*, 1978. *Catalogue of Stellar Ultraviolet Fluxes*, **Science Research Council**.

Thorstensen, J. R., Vennes, S. & Bowyer, S., 1996. *Astrophys. J.*, **457**, 390.

Thorstensen, J. R., Vennes, S. & Shambrouk, A., 1994. *Astron. J.*, **108**, 1924.

Trümper, J., 1984. *Physica Scripta*, **T7**, 209.

Tweedy, R. W. & Kwitter, K., 1994. *Astrophys. J. Letts.*, **433**, 93.

Tweedy, R. W. & Napiwotzki, R., 1992. *Mon. Not. R. astr. Soc.*, **259**, 315.

Tweedy, R. W. & Napiwotzki, R., 1994. *Astron. J.*, **108**, 978.

Tweedy, R. W., Holberg, J. B., Barstow, M. A., Bergeron, P., Grauer, A. D., Liebert, J. & Fleming, T. A., 1993. *Astron. J.*, **105**, 1938.

Vennes, S. & Thorstensen, J. R., 1994a. *Astron. J.*, **108**, 1881.

Vennes, S. & Thorstensen, J. R., 1994b. *Astrophys. J.*, **433**, L29.

Vennes, S. & Thorstensen, J. R., 1996. *Astron. J.*, **112**, 284.

Vennes, S., Bowyer, S. & Dupuis, J., 1996. *Astrophys. J.*, **466**, 1011.

Vennes, S., Pelletier, C., Fontaine, G. & Wesemael, F., 1988. *Astrophys. J.*, **331**, 876.

Vennes, S., Chayer, P., Fontaine, G. & Wesemael, F., 1989. In: *White Dwarfs*, Wegner, G., ed., Springer-Verlag, Berlin, p. 373.

Vennes, S., Chayer, P., Thorstensen, J. R., Bowyer, S. & Shipman, H. L., 1992. *Astrophys. J.*, **392**, L27.

Vennes, S., Mathioudakis, M., Doyle, J. G., Thorstensen, J. R. & Byrne, P. B., 1995. *Astr. Astrophys. Letts.*, **299**, 29.

Voges, W. *et al.*, 1997. *Astr. Astrophys.*, **in press**.

Warwick, R. S., Barber, C., Hodgkin, S. T. & Pye, J. P., 1993. *Mon. Not. R. astr. Soc.*, **262**, 289.

Webbink, R. F. *et al.*, 1992. *Bull. American Astron. Soc.*, **24**, 1127.

Weidemann, V. & Koester, D., 1983. *Astr. Astrophys.*, **121**, 77.

Welsh, B. Y., 1991. *Astrophys. J.*, **373**, 556.

Werner, K., 1991. *Astr. Astrophys.*, **251**, 147.

Werner, K., 1996. *Astr. Astrophys.*, **309**, 861.

Wesemael, F., Auer, L. H., Horn, H. M. V. & Savedoff, M. P., 1980. *Astrophys. J. Suppl.*, **43**, 159.

Wesemael, F. *et al.*, 1994. *Astrophys. J.*, **429**, 369.

Wesemael, F., Green, R. & Liebert, J., 1985. *Astrophys. J. Suppl.*, **58**, 379.

Wesemael, F., Henry, R. C. & Shipman, H. L., 1984. *Astrophys. J.*, **287**, 868.

Wilkinson, E., Green, J. C. & Cash, W., 1992. *Astrophys. J. Letts.*, **397**, L51.

Willingale, R., 1997. *Mon. Not. R. astr. Soc.*, **in preparation**.

Wolff, B., Jordan, S., Bade, N. & Reimers, D., 1995. *Astr. Astrophys.*, **294**, 183.

Wolter, H., 1952. *Opt. Eng.*, **10**, 94.

Wonnacott, D., Kellett, B. J. & Stickland, D. J., 1993. *Mon. Not. R. astr. Soc.*, **262**, 277.

Wood, J. H., Robinson, E. L. & Zang, E. H., 1995. *Mon. Not. R. astr. Soc.*, **277**, 87.

Wood, M. A., 1992. *Astrophys. J.*, **386**, 539.

Wood, M. A., 1995. In: *White Dwarfs*, Koester, D. & Werner, K., eds., Springer, p. 41.

Wu, C. C. *et al.*, 1991. *IUE Ultraviolet Spectral Atlas*, NASA, IUE Newsletter 43.

Yungelson, L. R., Livio, M., Tutukov, A. V. & Saffer, R. A., 1994. *Astrophys. J.*, **420**, 336.